

**IDENTIFICATION OF A MITOGEN-ACTIVATED PROTEIN KINASE,
p56, WHICH MEDIATES THE SELF-INCOMPATIBILITY RESPONSE
IN *PAPAVER RHOEAS* L.**

by

RICHARD LEE TUDOR

**A thesis submitted to The University of Birmingham for the degree of
DOCTOR OF PHILOSOPHY**

**School of Biosciences
College of Life and Environmental Sciences
The University of Birmingham
September 2009**

UNIVERSITY OF
BIRMINGHAM

University of Birmingham Research Archive

e-theses repository

This unpublished thesis/dissertation is copyright of the author and/or third parties. The intellectual property rights of the author or third parties in respect of this work are as defined by The Copyright Designs and Patents Act 1988 or as modified by any successor legislation.

Any use made of information contained in this thesis/dissertation must be in accordance with that legislation and must be properly acknowledged. Further distribution or reproduction in any format is prohibited without the permission of the copyright holder.

Abstract

Self-incompatibility (SI) is the major mechanism used by flowering plants to prevent self-pollination and thus avoid inbreeding. It is a genetically controlled mechanism that encodes a highly specific recognition system that inhibits the growth of incompatible pollen, whereas compatible pollen from an unrelated plant of the same species is able to grow and effect fertilization. In *Papaver rhoeas*, inhibition of incompatible pollen is mediated by a signal transduction pathway that activates a complex network of intracellular events including Ca^{2+} -dependent phosphorylation of p26, an inorganic pyrophosphatase required for pollen tube growth, depolymerisation of the pollen actin cytoskeleton and ultimately programmed cell-death (PCD).

To further understand the mechanisms involved in *Papaver rhoeas* SI it is important to identify and characterize components of the signalling network that mediate the SI response. Recent studies have revealed that p56, a mitogen-activated protein kinase (MAPK), is involved in activation of PCD during SI. MAPKs have been shown to be important signalling components in a range of cellular responses in eukaryotes. In *Arabidopsis thaliana* there are 20 MAPKs with roles including cell division, abiotic stress response, wounding response and hormone signalling.

Preliminary studies suggested an *MPK3*-like gene might encode p56, as an anti-AtMPK3 antibody cross-reacts with a protein corresponding to p56. Experiments carried out here suggest this is not the case. Using a combination of bioinformatics and proteomics data it has been possible to identify and clone a candidate p56 gene from *Papaver rhoeas* pollen. The

putative p56 gene has homology to *AtMPK9* and is a member of the T-D-Y class of MAPKs. It has been designated *PrMPK9-1*. An antibody raised against recombinant PrMAPK9-1 protein is being used to confirm that this gene/protein does indeed correspond to p56.

Dedication

This thesis is dedicated to my mother and father, Julie and Howard, who have shown me continued love and support in whatever I choose to do, and for that I am truly grateful.



Poppy Field - Richard Tudor (15th June 2007)

Acknowledgements

I would like to thank my supervisor Prof. Chris Franklin for his guidance, time, support and helpful advice during my PhD.

I would like to give enormous thanks to Dr. Mike Wheeler, Dr. Kim Osman and Dr. Barend de Graaf for their continued support, helpful discussions and wealth of knowledge.

I would also like to acknowledge Dr. Steve Thomas, Dr. James Higgins, Ruth Perry, Dr. Eugenio Sanchez-Moran, Dr. Maurice Bosch, Dr. Candida Nibau, Dr. Juliet Coates, Dr. Xiao Wang, Prof. Noni Franklin-Tong for general advice and help with methodology.

I would like to thank Antony Jones, Laine Wallace and Cleidi Zampronio for their help with genomic work and FT-ICR MS analysis.

I would like to thank Karen Staples, Mike Robertson, Bill Shotton and Charlie Osgood for their help in the poppy field and providing numerous pots for growing *Arabidopsis* plants.

I would like to mention Natalie Poulter, Nicola Roberts, Daniel Gibbs, Alison Evans, Choon Lin Tiang, Sarah Smith, Sabina Vatovec, Natalie Hadjiosif and Giorgio Perrella for going through the experience with me and for their support and advice.

I would like to thank the BBSRC for their sponsorship of this project.

Finally I would like to thank my family and friends for their continued love and support during my PhD.

Contents

Chapter 1	Introduction	1
1.1	General Introduction	1
1.2	The different mechanisms of self-incompatibility	5
1.2.1	Sporophytic self-incompatibility	5
1.2.2	Gametophytic self-incompatibility	7
1.2.2.1	S-RNase based gametophytic self-incompatibility	8
1.2.2.2	Gametophytic self-incompatibility in <i>Papaver rhoeas</i>	11
1.2.2.2.1	The female component	12
1.2.2.2.2	The male component	14
1.2.2.2.3	The role of calcium	16
1.2.2.2.4	The role of the cytoskeleton	17
1.2.2.2.5	Programmed cell death	18
1.2.2.2.6	Protein phosphorylation during the SI response	19
1.2.2.2.6.1	The role of p26.1, a sPPase	20
1.2.2.2.6.2	The role of p56, a mitogen activated protein kinase	22
1.2.2.2.6.3	Activation of p68	24
1.2.2.2.7	Overview of self-incompatibility in <i>Papaver rhoeas</i>	24
1.3	Mitogen activated protein kinases	26
1.3.1	The roles of MAPK signalling in plants	30
1.3.1.1	MAPK signalling in biotic stress responses	30
1.3.1.2	MAPK signalling in abiotic stress responses	33
1.3.1.2.1	The role of MAPKs in salt and cold stresses	33
1.3.1.2.2	The role of MAPKs in osmotic stresses	34
1.3.1.2.3	The role of MAPKs in oxidative stresses	35
1.3.1.3	MAPK signalling in hormone signalling	36
1.3.1.3.1	The role of MAPKs in ethylene signalling	36
1.3.1.3.2	The role of MAPKs in jasmonic acid signalling	38
1.3.1.3.3	The role of MAPKs in auxin signalling	39
1.3.1.4	MAPK signalling via reactive oxygen species	39
1.3.1.5	MAPK signalling in plant development	40

1.3.1.5.1	The role of MAPKs in embryo development	41
1.3.1.5.2	The role of MAPKs in leaf senescence	41
1.3.1.5.3	The role of MAPKs in stomatal development	42
1.3.1.5.4	The role of MAPKs in the floral abscission	42
1.3.1.5.5	The role of MAPKs in plant cell division and microtubule organisation	43
1.3.1.5.6	The role of MAPKs in the regulation of the actin cytoskeleton	44
1.3.1.6	Summary	45
1.4	General aims and objectives	47
<u>Chapter 2</u>	Methods and Materials	49
2.1	Plant material	49
2.1.1	Plant cultivation	49
2.1.2	Determination of <i>S</i> -genotype in <i>Papaver</i>	49
2.1.3	Production of seed in <i>Papaver</i>	50
2.1.4	Collection of plant tissue	50
2.2	Pollen growth and treatment in <i>Papaver</i>	51
2.2.1	Pollen growth <i>in vitro</i>	51
2.2.2	Induction of SI with recombinant S-proteins	52
2.2.3	Calyculin A treatment of pollen	52
2.3	Nucleic acid manipulations	52
2.3.1	Removal of RNase contamination from equipment	52
2.3.2	Isolation of RNA	52
2.3.2.1	Estimation of RNA concentration	53
2.3.3	DNase treatment of RNA	53
2.3.4	cDNA synthesis	54
2.3.5	Isolation of DNA	54
2.3.5.1	Estimation of nucleic acid concentration	54
2.4	Polymerase Chain Reaction (PCR)	55
2.4.1	Polymerase Chain Reaction (PCR) techniques	55
2.4.1.1	Composition of reactions	55
2.4.1.2	PCR cycling conditions	55

2.4.2	Primer design	56
2.4.2.1	Primers	57
2.4.3	RT-PCR	57
2.4.4	3'RACE	57
2.4.5	5'RACE	58
2.4.6	PCR purification	58
2.5	Agarose gel electrophoresis of DNA and RNA	59
2.5.1	Agarose gel electrophoresis	59
2.5.1.1	DNA ladders	59
2.5.2	Extraction of digested or amplified DNA from agarose gels	60
2.6	Gene cloning	60
2.6.1	Ligation	60
2.6.1.1	Ligation of DNA fragments into vector DNA	60
2.6.1.2	Cloning vectors	60
2.6.2	Transformation of <i>E. coli</i> cells with plasmid DNA	61
2.6.2.1	Transformation of <i>E. coli</i> by heat-shock	61
2.6.2.2	Bacterial strains	62
2.6.2.3	Preparation of competent cells	62
2.6.2.4	Growth media	63
2.6.2.5	Selective media	63
2.6.2.6	Growth conditions	64
2.6.3	Analysis of positive colonies	64
2.6.3.1	Preparation of plasmid DNA from cultures (Mini prep)	64
2.6.3.2	Single colony PCR	65
2.6.3.3	Digestion of DNA with restriction enzymes	65
2.7	DNA sequencing	65
2.7.1	Preparation of plasmid DNA for sequencing	65
2.7.2	DNA Sequencing	66
2.7.3	Sequence analysis and homology searching	67
2.8	Protein manipulations	67
2.8.1	Protein extraction	67
2.8.1.1	Bacterial protein expression and extraction	67

2.8.1.2	Pollen protein extraction	68
2.8.1.3	Leaf protein extraction	69
2.8.1.4	Estimation of protein concentration	69
2.8.2	Protein purification methods	70
2.8.2.1	Bacteria: isolation of His-tagged proteins using Ni-NTA resin	70
2.8.2.2	Removal of small proteins from samples	70
2.8.2.3	Removal of salts from protein samples	71
2.8.2.4	Phosphoprotein purification	71
2.9	Protein analysis methods	71
2.9.1	SDS-Polyacrylamide gel electrophoresis	71
2.9.1.1	Ladders	73
2.9.2	SDS-PAGE gel analysis	74
2.9.2.1	Coomassie staining	74
2.9.2.2	Western blotting	74
2.9.2.2.1	Protein transfer	74
2.9.2.2.2	Ponceau S staining	75
2.9.3	Antibody probing	75
2.9.3.1	Primary antibodies	75
2.9.3.2	Secondary antibodies	76
2.9.4	Antibody detection methods	76
2.9.4.1	Enhanced chemiluminescence (ECL) detection	76
2.9.4.2	Alkaline phosphatase detection	77
2.9.5	Membrane stripping	77
2.10	Antibody purification	77
2.10.1	Antibody clean-up using Immobilised <i>E. coli</i> lysate kit	77
2.10.2	PinPoint™ purification of the anti-PrMPK9-1 antibody	78
2.10.2.1	Preparation of TetraLink™ Tetrameric Avidin Resin	78
2.10.2.2	Columns	79
2.10.2.3	Affinity purification of anti-PrMPK9-1 antibody	79
2.11	Immuno-precipitation	79
2.11.1	Immuno-precipitation using protein A Sepharose	79
2.11.2	Immuno-precipitation of ATP labelled	80

2.11.2.1	Visualisation of ATP labelling	80
2.11.3	Immuno-precipitation with 9B column	81
2.11.3.1	Biotinylation of anti-PrMPK9-1 antibody	81
2.11.3.2	Binding of biotinylated PrMPK9-1 to TetraLink™ Tetrameric Avidin Resin	81
2.11.3.3	Immuno-precipitation of CalA extracts	81
2.12	Immunolocalisation	82
2.13	Analysis of T-DNA insertion lines	82
2.13.1	Isolation of DNA for genotyping experiments	82
2.13.2	Alexander's staining	82
2.13.3	Aniline blue staining	83
2.13.4	Viability test	83
2.14	General Solutions and Buffers	83
2.15	Equipment	84
<u>Chapter 3</u>	Initial attempts to clone a candidate p56 gene	86
3.1	Introduction	86
3.2	Results	90
3.2.1	Cloning of a <i>MPK3</i> orthologue from <i>Papaver rhoeas</i>	90
3.2.1.1	Attempts to clone a <i>MPK3</i> orthologue from <i>P. rhoeas</i> pollen	90
3.2.1.2	Cloning of a <i>MPK3</i> orthologue from <i>P. rhoeas</i> leaf	94
3.2.2	Detection of p56 using the AtMPK3 antibody	100
3.3	Discussion	102
3.3.1	Cloning of a <i>PrMPK3</i> gene from <i>P. rhoeas</i>	102
3.2.2	PrMPK3 detection with the anti-AtMPK3 antibody	105
<u>Chapter 4</u>	A bioinformatics approach to identify p56	106
4.1	Introduction	106
4.2	Results	109
4.2.1	A bioinformatics approach to identify p56	109
4.2.2	A proteomics approach to identify p56	112
4.2.2.1	Analysis of FT-ICR MS data using a Sequest search engine	113

4.2.2.2	Analysis of FT-ICR MS data using a MASCOT search engine	117
4.3	Discussion	120
4.3.1	Bioinformatics analysis	120
4.3.2	Proteomics analysis	122
4.3.2.1	Construction of a plant specific database for MS analysis	125
4.3.3	Summary of bioinformatics and proteomics analysis	125
<u>Chapter 5</u>	Cloning and preliminary characterisation of <i>PrMPK9-1</i>: a putative p56 candidate	127
5.1	Introduction	127
5.2	Results	128
5.2.1	Cloning of candidate T-D-Y MAPKs from <i>Papaver rhoeas</i> pollen using T-D-Y specific primers	128
5.2.2	Cloning of candidate T-D-Y MAPKs from <i>Papaver rhoeas</i> pollen using gene specific primers	131
5.2.2.1	Cloning of a <i>Papaver rhoeas</i> MPK9-like gene	134
5.2.2.2	Cloning of a second <i>Papaver rhoeas</i> MPK9-like gene	135
5.2.2.3	Attempts to clone <i>Papaver rhoeas</i> MPK8-like, MPK19-like and MPK17-like genes	136
5.2.3	Re-analysis of the FT-ICR MS data	137
5.2.4	Expression analysis of <i>Papaver rhoeas</i> MAPKs using semi-quantitative RT-PCR	138
5.2.4.1	Cloning of a <i>Papaver rhoeas</i> GAPDH	139
5.2.4.2	Expression analysis of <i>Papaver rhoeas</i> MAPKs	142
5.3	Discussion	148
5.3.1	Cloning of candidate T-D-Y MAPK genes from <i>P. rhoeas</i>	148
5.3.2	Re-analysis of the FT-ICR MS data	151
5.3.3	Expression analysis of the <i>P. rhoeas</i> MAPKs	151
5.3.4	Summary	153
<u>Chapter 6</u>	Studies to confirm <i>PrMPK9-1</i> encodes p56	154
6.1	Introduction	154

6.2	Results	156
6.2.1	Expression of full-length PrMPK9-1 recombinant protein	156
6.2.2	Detection of recombinant PrMPK9-1 protein with the AtMPK3 antibody	163
6.2.3	Production of an anti-PrMPK9-1 antibody	165
6.2.3.1	Production of an anti-PrMPK9-1 peptide antibody	165
6.2.3.2	Construction of a PrMPK9-1 recombinant protein for antibody production	166
6.2.4	The anti-PrMPK9-1 antibody can detect a ~56kDa protein in pollen	175
6.2.5	The anti-PrMPK9-1 antibody cross-reacts with a 56kDa phospho-protein	177
6.2.6	PinPoint™ purification of the anti-PrMPK9-1 antibody	180
6.2.6.1	PinPoint™ purified anti-PrMPK9-1 antibody can detect PrMPK9-1C recombinant protein	185
6.2.7	The PinPoint™ purified anti-PrMPK9-1 antibody can detect a ~56kDa protein from <i>P. rhoeas</i> pollen	187
6.2.8	Detection of p56 during compatible and incompatible SI reactions	189
6.2.8.1	The anti-PrMPK9-1 antibody can detect proteins present in recombinant S-protein samples used to initiate SI <i>in vitro</i>	191
6.2.9	Immuno-precipitation experiments using the anti-PrMPK9-1 antibody	193
6.2.9.1	Immuno-precipitation using Protein A sepharose beads	193
6.2.9.2	Immuno-precipitation of radio-labelled proteins	198
6.2.9.3	Immuno-precipitation using affinity-purified, biotinylated anti-PrMPK9-1 antibody	200
6.2.10	Immuno-localisation of PrMPK9-1	208
6.3	Discussion	210
6.3.1	The anti-AtMPK3 antibody can detect recombinant PrMPK9-1	210
6.3.2	Production of an anti-PrMPK9-1 antibody	210
6.3.3	Detection of pollen proteins using the anti-PrMPK9-1 antibody	212
6.3.4	Immuno-precipitation of p56 with the anti-PrMPK9-1 antibody	213
6.3.5	Immuno-localisation	215

6.3.6	Summary	216
<u>Chapter 7</u>	Preliminary studies to define a role for MPK9 in <i>Arabidopsis thaliana</i>	217
7.1	Introduction	217
7.2	Results	220
7.2.1	Determination of MAPK homozygous T-DNA knockout lines	220
7.2.2	Phenotypic analysis of T-DNA insertion lines	223
7.2.2.1	Pollen viability test using Alexander's stain	223
7.2.2.2	<i>In vivo</i> pollen growth using aniline blue staining	224
7.2.2.3	Effects on fertility	225
7.2.3	Construction of double T-DNA knockout lines	226
7.2.3.1	Pollen viability test using Alexander's stain	227
7.2.3.2	<i>In vivo</i> pollen growth using aniline blue staining	227
7.2.3.3	Effects on fertility	228
7.3	Discussion	229
<u>Chapter 8</u>	General Discussion	231
<u>References</u>		241
<u>Appendixes</u>		278

List of figures and tables

Figures

Figure 1.1a	Genetic control of self-incompatibility	4
Figure 1.2.1.2.7a	An overview of the events during an incompatible reaction in <i>Pavaver rhoeas</i> SI	13
Figure 1.2.1.2.7b	Time-line of events during an incompatible reaction in <i>Pavaver rhoeas</i> SI	13
Figure 1.3a	Simplified MAPK cascade	29
Figure 3.1a	An anti-AtMPK3 antibody cross-reacts with a ~56kDa <i>Papaver rhoeas</i> pollen protein	89
Figure 3.2.1.1a	Degenerate PCR products obtained using MPK3-like primers on pollen cDNA	92
Figure 3.2.1.2a	Relative expression of <i>AtMPK3</i> (top) and <i>AtMPK6</i> (bottom) in pollen and leaf tissues from Affymetrix chip data	95
Figure 3.2.1.2b	Degenerate PCR products obtained using <i>MPK3</i> -like primers on leaf cDNA	97
Figure 3.2.1.2c	Amplification of a larger region of the <i>PrMPK3</i> gene	97
Figure 3.2.1.2d	Predicted protein sequence of <i>PrMPK3</i> from leaf mRNA	99
Figure 3.2.2a	The anti-AtMPK3 antibody can detect AtMPK3 in <i>Arabidopsis thaliana</i> leaf and a ~56kDa protein in <i>Papaver rhoeas</i> pollen	101
Figure 3.3.1a	Phylogenetic tree of <i>Arabidopsis thaliana</i> and <i>Papaver rhoeas</i> MAPK proteins	104
Figure 4.3.2a	MAPK phylogenetic tree showing proteins that contained peptides found in p56	124
Figure 5.2.1a	Amplification products from leaf cDNA using T-D-Y specific primers	129
Figure 5.2.1b	Predicted protein sequence of <i>PrMPK20</i> from pollen mRNA	131
Figure 5.2.2.1a	Predicted protein sequence of <i>PrMPK9-2</i> from pollen mRNA	135
Figure 5.2.2.2a	Predicted protein sequence of <i>PrMPK9-1</i> from pollen mRNA	136
Figure 5.2.4.1a	Amplification of <i>PrGAPC-2</i>	140
Figure 5.2.4.1b	Predicted protein sequence of <i>PrGAPD-C</i>	142

Figure 5.2.4.2a	Semi-quantitative RT-PCR expression analysis of PrMPK9-1	144
Figure 5.2.4.2b	Semi-quantitative RT-PCR expression analysis of <i>P. rhoeas</i> MAPKs	147
Figure 5.3.1a	Phylogenetic tree of PrMPK9-1, PrMPK9-2 and the T-D-Y AtMPKs	149
Figure 5.3.1b	Phylogenetic tree of the <i>A. thaliana</i> , <i>P. trichocarpa</i> and <i>P. rhoeas</i> MAPK proteins	150
Figure 6.2.1a	Amplification of full-length PrMPK9-1 for protein expression	158
Figure 6.2.1b	Expression of the full-length PrMPK9-1 recombinant protein	158
Figure 6.2.1c	Full-length PrMPK9-1 recombinant protein expression can be detected with the anti-6xHis antibody	160
Figure 6.2.1d	Full-length PrMPK9-1 recombinant protein is expressed in the soluble and insoluble cell fractions	160
Figure 6.2.1e	Purification of the PrMPK9-1 recombinant protein with Ni-NTA Agarose resin	162
Figure 6.2.1f	Purification of the PrMPK9-1 recombinant protein with Ni-NTA Agarose resin	162
Figure 6.2.2a	The anti-AtMPK3 antibody cross-reacts with the PrMPK9-1 recombinant protein	164
Figure 6.2.3.2a	Expression of the PrMPK9-1C recombinant protein	168
Figure 6.2.3.2b	Purification of the PrMPK9-1C recombinant protein with Ni-NTA Agarose resin	168
Figure 6.2.3.2c	Purification of PrMPK9-1C using the PD-10 desalting columns	170
Figure 6.2.3.2d	The anti-PrMPK9-1 antibody detects recombinant PrMPK9-1C	172
Figure 6.2.3.2e	The purified anti-PrMPK9-1 antisera can detect PrMPK9-1C	174
Figure 6.2.3.2f	Detection of the full-length PrMPK9-1 recombinant protein with the anti-PrMPK9-1 antibody	174
Figure 6.2.4a	The anti-PrMPK9-1 antibody detects a ~56kDa protein in <i>Papaver rhoeas</i> pollen	176
Figure 6.2.5a	A ~56kDa phospho-proteins cross-reacts with the anti-PrMPK9-1 antibody	179

Figure 6.2.5b	A ~56kDa phospho-protein can be detected by the anti-pTXpY antibody that specifically detects activated MAPKs	179
Figure 6.2.6a	Expression of the PrMPK9-1CPP recombinant protein	182
Figure 6.2.6b	PrMPK9-1CPP cross-reacts with the anti-PrMPK9-1 antibody	183
Figure 6.2.6c	PrMPK9-1CPP cross-reacts with the NeutrAvidin Protein	183
Figure 6.2.6.1a	PrMPK9-1C recombinant protein cross-reacts with PinPoint™ affinity purified anti-PrMPK9-1 antibody	186
Figure 6.2.7a	PinPoint purified anti-PrMPK9-1 antibody compared to unpurified anti-PrMPK9-1 antibody	188
Figure 6.2.8a	The anti-PrMPK9-1 and anti-pTXpY antibodies detect the same ~56kDa protein band in an incompatible SI reaction	190
Figure 6.2.8.1a	Recombinant S-proteins used to stimulate an incompatible SI reaction are detected by anti-PrMPK9-1 antibody	192
Figure 6.2.9.1a	Proteins immuno-precipitated with the anti-PrMPK9-1 antibody and detected with the anti-pTEpY antibody	194
Figure 6.2.9.1b	Proteins immuno-precipitated with the anti-PrMPK9-1 antibody and detected with a light-chain-specific secondary antibody	197
Figure 6.2.9.1c	Proteins immuno-precipitated with the anti-pTXpY antibody and detected with the anti-PrMPK9-1 antibody	197
Figure 6.2.9.2a	Phosphor-image of ³² P labelled proteins immuno-precipitated using the anti-PrMPK9-1 antibody	199
Figure 6.2.9.3a	Biotinylation of anti-PrMPK9-1	203
Figure 6.2.9.3b	Anti-PrMPK9-1 antibody binds to the avidin resin	203
Figure 6.2.9.3c	Anti-PrMPK9-1 successfully binds to the avidin resin	204
Figure 6.2.9.3d	Calyculin A treated and untreated pollen protein input for immuno-precipitation experiments	206
Figure 6.2.9.3e	Immuno-precipitation of calyculin A treated and untreated pollen with the anti-PrMPK9-1 antibody, detected by western blotting with the anti-pTXpY antibody	206
Figure 6.2.10a	Immuno-localisation of PrMPK9-1	209
Figure 7.1a	Alexander's stain showing viable and non-viable pollen grains	219
Figure 7.1b	Aniline blue staining of growing pollen tubes	219

Figure 7.2.1a	Expression analysis of mRNA in the MAPK T-DNA knockout lines	222
<u>Tables</u>		
Table 3.2.1.1a	Primer combinations and annealing temperatures used to amplify a <i>MPK3</i> orthologue from <i>Papaver rhoeas</i> pollen	91
Table 3.2.1.1b	Comparison of the homology between <i>AtMPK3</i> , <i>AtMPK6</i> and <i>PrMPKB</i> at the nucleotide level	93
Table 3.2.1.1c	Combinations of <i>MPK3</i> -specific primers used to amplify a <i>Papaver rhoeas</i> <i>MPK3</i> -like gene	94
Table 3.3.1a	Comparison of homology between <i>AtMPK3</i> , <i>AtMPK6</i> , <i>PrMPK3</i> and <i>PrMPKB</i>	102
Table 4.2.1a	Expression of <i>Arabidopsis thaliana</i> MAPKs in pollen	110
Table 4.2.1b	Expression of <i>Populus trichocarpa</i> MAPKs in male floral buds	111
Table 4.2.1c	Predicted protein size of the <i>Oryza sativa</i> MAPKs	112
Table 4.2.2.1a	Sequest search of the FT-ICR MS data against an ‘ <i>Arabidopsis/Brassica</i> ’ database	115
Table 4.2.2.1b	List of plant species whose proteins were added to the ‘Plant’ database	116
Table 4.2.2.1c	Sequest search of the mass spectrometry data using the ‘Plant’ database	117
Table 4.2.2.2a	A MASCOT search of the FT-ICR MS data against a ‘Viridiplantae’ database	119
Table 5.2.2a	Primer and annealing temperatures used to clone specific T-D-Y MAPKs from <i>Papaver rhoeas</i> pollen	133
Table 5.2.3a	Reanalysis of the mass spectrometry data using the ‘Plant’ database	138
Table 6.2.9.3a	PrMPK9-1 peptides identified from the ~56kDa protein band	207
Table 7.2.1a	Primers used to amplify gene and insert sequences from MAPK T-DNA knockout lines	221
Table 7.2.2.1a	Pollen viability in the MAPK T-DNA knockout lines	224
Table 7.2.2.2a	Pollen growth rates in the MAPK T-DNA knockout lines	225
Table 7.2.2.3a	Fertility in the MAPK T-DNA knockout lines	226

Table 7.2.3.1a	Pollen viability in the MAPK double T-DNA knockout lines	227
Table 7.2.3.2a	Pollen growth rates in the MAPK double T-DNA knockout lines	228
Table 7.2.3.3a	Fertility in the MAPK double T-DNA knockout lines	228

List of Abbreviations

5'RACE	5' rapid amplification of complimentary ends
3'RACE	3' rapid amplification of complimentary ends
ABA	abscisic acid
ABP	actin binding protein
ACC	aminocyclopropane-1-carboxylic
ARC1	armadillo repeat-containing protein 1
bp	base pairs
[Ca ²⁺] _i	cytosolic free calcium
DNA	deoxyribonucleic acid
FT-ICR	Fourier transform-ion cyclotron resonance
GAPDH	glyceraldehyde-3-phosphate dehydrogenase
GM	growth media
GSI	gametophytic self-incompatibility
HRP	horseradish peroxidase
HT-B	H-top band
JA	jasmonic acid
kDa	kilodalton
MBP	myelin basic protein
MPK	mitogen-activated protein kinase
MAPK	mitogen-activated protein kinase
MAPKK	mitogen-activated protein kinase kinase
MAPKKK	mitogen-activated protein kinase kinase kinase
MLPK	M-locus protein kinase
MS	mass spectrometry
ORF	open reading frame
PAGE	poly-acrylamide gel electrophoresis
PAGE-IEF	poly-acrylamide gel electrophoresis-isoelectric focusing
PAMP	pathogen associated molecular pattern
PARP	poly (ADP-ribose) polymerase
PCD	programmed cell death

PCR	polymerase chain reaction
PrpS	<i>Papaver rhoeas</i> pollen-S
PrsS	<i>Papaver rhoeas</i> stigma-S
RNA	ribonucleic acid
ROS	reactive oxygen species
RT-PCR	reverse-transcription PCR
SA	salicylic acid
SAR	systemic acquired resistance
SCR	S-locus cysteine-rich protein
SDS	sodium dodecyl sulfate
SDW	sterile distilled water
SI	self-incompatibility
SLF	S-locus F-box
SP11	S-locus protein 11
SBP	S-protein binding protein
SBP1	S-RNase binding protein 1
SRK	S-locus receptor kinase
SSI	sporophytic self-incompatibility
SSK1	SLF-interacting SKP-like 1
UTR	un-translated region

CHAPTER 1

Introduction

CHAPTER 1 - INTRODUCTION

1.1 General Introduction

In angiosperms successful sexual reproduction is dependent on a series of contingent events. These include the delivery of pollen to the stigma, pollen adherence, hydration and germination of pollen on the stigma surface, growth of the pollen through the pistil to the ovary and, finally, fertilization of the egg. In flowering plants there is a large diversity in floral morphology and reproductive mechanisms that involve species-specific pollen-pistil interactions (for a review see Hiscock and Allen, 2008). Self-incompatibility (SI) is a very important mechanism in angiosperms that prevents self-fertilization (inbreeding) and therefore promotes out-breeding in order to maintain the genetic diversity within a single species. There are over 250,000 species of angiosperms and it is estimated more than half of these have evolved a form of SI (Igic and Kohn, 2006).

There are two major classes of SI based on floral morphology, heteromorphic and homomorphic. Heteromorphic SI involves a species having morphologically different flowers, which produces a physical barrier for self-fertilization and therefore promotes out-breeding (for a review see Weller, 2009). Examples of heteromorphic SI include distyly and tristly in which flowers of a species contain styles and stamens of different lengths (morphs). These differences prevent self-fertilization and cross-fertilization by the same morph, and promote out-crossing between different morphs. Heteromorphic SI is widely distributed and has been described in 24 plant families, covering 164 genera, including *Primula* and *Linum* (Ganders, 1979).

In homomorphic SI the flowers are morphologically the same and there is no physical barrier to self-pollination. Homomorphic SI involves a recognition event between the pollen and the pistil, which results in rejection of self-pollen and acceptance of non-self pollen. In homomorphic self-incompatibility, if genetically unrelated pollen ('non-self') from the same species lands on the stigma, then germination, penetration of the stigmatic papilla cells and normal growth of the pollen tube occurs, with the pollen finally reaching the ovule and fertilizing the egg. If pollen from the same plant ('self'), or a genetically related plant ('cross'), lands on the stigma, its growth is halted, either on the stigma or during growth through the pistil (depending on the species) where pollen growth is terminated.

In most species homomorphic SI is a genetically controlled mechanism that involves genes at a single polymorphic 'S-locus' and is responsible for the plant being able to recognise and reject self pollen, while still being able to accept non-self pollen (for a review see Takayama and Isogai, 2005). The S-locus encodes genes that are expressed in both the male (pollen) and female (pistil) parts of the reproductive organs. The pollen and pistil genes at this S-locus are linked, and it has been proposed that in different species the number of S-alleles can range from around 20 (in *Nicotiana sanderae*) to an estimated 193 (in *Trifolium pratense*) (Lawrence, 2000). The number of alleles depends on population size and the rate of new alleles formed by mutation. Frequency dependent selection induced by self-incompatibility systems tends to increase rare S-alleles in a population to a point of equilibrium and therefore a large number of S-alleles are maintained at the S-locus (Wright, 1939).

Current opinion is that homomorphic SI mechanisms have evolved independently at least six times during the evolution of dicotyledonous land plants (Hiscock and McInnis, 2003; for a

review see Hunter, 2009) and to date two major subgroups of homomorphic self-incompatibility have been described; gametophytic self-incompatibility and sporophytic self-incompatibility (see Figure 1.1a). In gametophytic self-incompatibility (GSI), the pollen SI phenotype is determined by its own haploid (gametophytic) genome. GSI is widespread and has been found to be present in the *Solanaceae*, *Rosaceae*, *Plantaginaceae* (formerly *Scrophulariaceae* (Albach *et al.*, 2005)), *Ranunculaceae*, *Leguminosae*, *Onagraceae* and *Papaveraceae*. By comparison, in sporophytic self-incompatibility (SSI) the pollen SI phenotype is determined by the diploid parent (sporophytic) genome. SSI is less common but has been described in the *Brassicaceae*, *Asteraceae* and *Convolvulaceae*. The three most well characterised forms of homomorphic SI will be discussed; sporophytic self-incompatibility in *Brassica*, S-RNase based gametophytic self-incompatibility and gametophytic self-incompatibility in *Papaver rhoeas*.

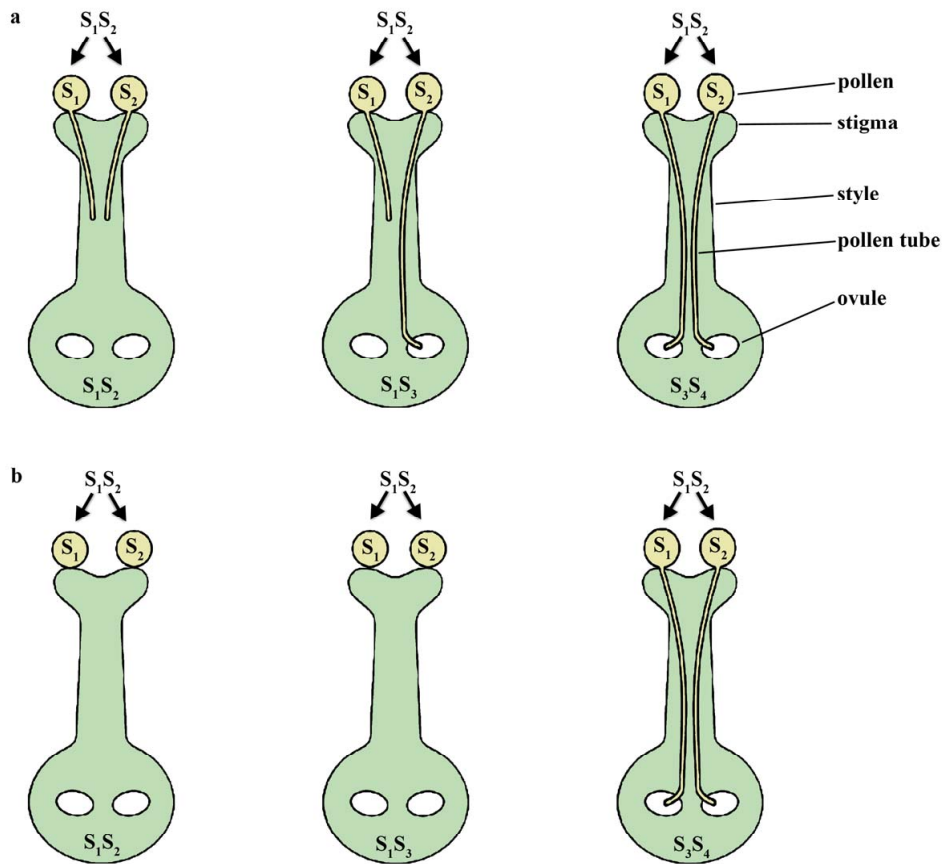


Figure 1.1a Genetic control of self-incompatibility. When alleles at the *S*-locus are matched in the pollen (male component) and pistil (female component) an incompatible reaction occurs. The *S*-alleles of the male and female parent plants and the haplotype of the pollen are indicated. The *S*-alleles are expressed co-dominantly in the pistil. **(a)** In gametophytic self-incompatibility (GSI), the pollen SI phenotype is determined by its own haploid (gametophytic) genome. In a cross between an S_1S_3 plant (pistil) and a S_1S_2 plant (pollen) half of pollen is compatible, as half the pollen grains express the S_1 allele and half the S_2 allele. In GSI pollen tube inhibition generally occurs in the style. **(b)** In sporophytic self-incompatibility (SSI) the pollen SI phenotype is determined by the diploid parent (sporophytic) genome and the parental *S*-alleles are expressed co-dominantly in the pollen. In SSI the pollen *S*-alleles are expressed sporophytically in diploid cells of the anther tapetum that supplies the *S*-proteins to the pollen coating. Therefore in a cross between S_1S_3 plant (pistil) and an S_1S_2 plant (pollen) all the pollen will be inhibited. In SSI pollen tube inhibition generally occurs on the stigma surface.

1.2 The different mechanisms of self-incompatibility

1.2.1 Sporophytic self-incompatibility

In *Brassica*, sporophytic self-incompatibility involves a receptor-ligand interaction on the stigma surface between a pollen grain and a stigmatal epidermal cell. *Brassica* SSI is extremely rapid, occurring within minutes of the pollen-stigma interaction. This interaction has been shown to be very localised, with a single stigmatal papillae cell being able to differentiate between two genetically different pollen grains (Dickinson, 1995). Unlike GSI, pollen inhibition in *Brassica* SSI does not involve cell death, as pollen has been shown to be viable on compatible stigmas after spending time on incompatible stigmas (Geitmann, 1999). In *Brassica* two highly polymorphic genes control SSI and are located at an *S*-locus. The male component is SCR (*S*-locus cysteine-rich protein, or SP11, *S*-locus protein 11), a small peptide expressed in the pollen coat, which acts as a ligand for the female component (Schopfer *et al.*, 1999; Suzuki *et al.*, 1999; Takayama *et al.*, 2000; Shiba *et al.*, 2001). The female component is SRK (*S*-locus receptor kinase), which encodes a single pass trans-membrane serine/threonine kinase in the plasma membrane of the stigmatal epidermal cells (Stein *et al.*, 1991, Stein *et al.*, 1996, Takasaki *et al.*, 2000). When pollen lands on the stigma SCR and other pollen coat proteins are transferred to the stigma surface, where SCR interacts with SRK in a *S*-haplotype specific manner (Kachroo *et al.*, 2001; Takasaki *et al.*, 2000; Shimosato *et al.*, 2007). It has been shown that SCR and SRK are both essential and sufficient for SSI in *Brassica* and expression of SCR and SRK in the self-compatible *Arabidopsis thaliana* is enough to induce self-incompatibility (Nasrallah *et al.*, 2002). The interaction of

SCR with SRK is thought to initiate downstream signalling events that result in the rejection of self-pollen, but to date these mechanisms are poorly understood.

It was shown that two thioredoxin h-like proteins, THL1 and THL2, were able to interact with SRK (Bower *et al.*, 1996). Haffani *et al.* (2004) demonstrated that THL1 and THL2-deficient plants resulted in the low level constitutive rejection of all pollen. In addition, phosphorylation of SRK is prevented by THL1, and this inhibition can be reversed by the addition of pollen coat proteins (Cabrillac *et al.*, 2001). SRK has been shown to form dimers via domains located in the extracellular region of the protein (Giranton *et al.*, 2000; Naithani *et al.*, 2007). It is proposed that THL1 and THL2 are involved in the negative regulation of SSI and keep SRK dimers inactive in the absence of SCR. When SCR is present, THL1 and THL2 are removed and SRK is activated.

MLPK (M-locus protein kinase) has been shown to play a role in SSI, as the stigmas in MLPK-deficient plants are unable to inhibit self-pollen (Murase *et al.*, 2004). MLPK encodes a cytosolic serine/threonine protein kinase. This kinase contains an N-terminal myristoylation signal that anchors the protein to the membrane. It has been shown that MLPK encodes two isoforms that both locate to the plasma membrane and can be phosphorylated by SRK (Kakita *et al.*, 2007).

ARC1 (armadillo repeat-containing protein 1) is a protein with a U-box domain and an Arm repeat region, which possesses E3-ubiquitin ligase activity (Gu *et al.*, 1998; Stone *et al.*, 2003), and down-regulation of ARC1 was shown to induce a partial breakdown of SSI. ARC1 was shown to interact with the phosphorylated kinase domain of SRK via the C-terminal

Arm-repeat domain and can be phosphorylated by SRK (Gu *et al.*, 1998). In addition, SRK is required for the localisation of ARC1 with the proteasome and the COP9 signalosome (Stone *et al.*, 2003). As MLPK was also shown to phosphorylate ARC1, it was proposed that an MLPK/SRK complex might activate ARC1 (Samuel *et al.*, 2008). In transgenic *Arabidopsis thaliana* plants that can undergo SSI, AtPUB8 was identified which is thought to regulate SRK in stigma development (Liu *et al.*, 2007). AtPUB8 encodes a protein with a putative U-box domain and an Arm repeat region, like ARC1, and it is likely to show E3-ubiquitin ligase activity. However, AtPUB8 is not considered to be the orthologue of ARC1.

Although the targets of these proteins are not known it is thought that they may ubiquitinate, and therefore degrade, downstream targets that may be inhibitors of SSI or proteins required for pollen tube growth. One proposed target of ARC1 is Exo70A1. Exo70A1 is expressed in stigmas and is thought to be required in compatible pollen for hydration, germination and growth (Samuel *et al.*, 2008). Exo70A1 has been shown to interact with the N-terminus of ARC1 and can be ubiquitinated by ARC1, and it is proposed to play a role in regulating targeted secretion.

1.2.2 Gametophytic self-incompatibility

Gametophytic self-incompatibility occurs later than SSI, during growth of the pollen tube through the style. The two forms of gametophytic self-incompatibility, the S-RNase based gametophytic self-incompatibility and gametophytic self-incompatibility in *Papaver rhoeas*, will be discussed. Both these forms are associated with pollen tube death but the mechanism by which this occurs is very different.

1.2.2.1 S-RNase based gametophytic self-incompatibility

S-RNase based GSI is the most common type of SI found in plants. The majority of work on S-RNase based GSI has been carried out in the *Solanaceae*, *Rosaceae* and *Plantaginaceae* families. GSI in these species involves S-RNases within the stigma that differentiate between compatible and incompatible pollen. In S-RNase based GSI the female components are glycoproteins that encode pistil-specific S-RNases, nucleases that catalyse the degradation of RNA (McClure *et al.*, 1989; Anderson *et al.*, 1986; Ioerger *et al.*, 1991; Ishimizu *et al.*, 1998; Xue *et al.*, 1996; Sassa *et al.*, 1996; Singh and Kao, 1991). The S-RNases give the plants *S*-haplotype specificity and they are highly polymorphic (McCubbin and Kao, 2000). Their ribonuclease activity is essential for their function and it was shown that the S-RNases were sufficient and necessary for this type of GSI (Huang *et al.*, 1994; Lee *et al.*, 1994; Murfett *et al.*, 1994). The S-RNases are secreted into the pistil's extra-cellular matrix of the transmitting tract, where they are taken up by growing pollen tubes in a non-specific manner (Luu *et al.*, 2000). The S-RNases are non-specific in their degradation of RNA but only act in incompatible pollen (McClure *et al.*, 1990).

The male component of S-RNase based GSI was identified as SLF (*S*-locus F-box) (Lai *et al.*, 2002; Wang *et al.* 2004; Qiao 2004a; Sijacic *et al.*, 2004) (SFB (*S*-haplotype-specific F-box) in *Rosaceae* (Ushijima *et al.*, 2003; Entani *et al.*, 2003)). SLF is a cytoplasmic F-box protein, whose family members function as part of the E3 ubiquitin ligase complex, which ubiquitinates proteins and marks them for degradation by the proteasome, and is essential for inhibiting S-RNase activity (Golz *et al.*, 1999; Golz *et al.*, 2000). SLF has been shown to interact with E3 ubiquitination complex components, and proteasomal inhibitors inhibit

compatible pollen tubes, but not incompatible pollen tubes (Qiao *et al.*, 2004b; Hua and Kao, 2006). In addition, Qiao *et al.* (2004b) have shown that SLF and the S-RNases interact, but this is in a non-specific manner. It is proposed that SLF is involved in the ubiquitin-mediated proteolysis of the pistil S-RNases.

In addition to SLF and S-RNase there are other pollen and stilar factors that are required for or involved in S-RNase based gametophytic self-incompatibility. Stilar factors include HT-B (H-top band) and 120K glycoprotein. HT-B is a small asparagine-rich protein that is expressed in the style (McClure *et al.*, 1999; Kondo *et al.*, 2002a; Kondo *et al.*, 2002b; O'Brien *et al.*, 2002). HT-B is needed for SI and without it the ability to reject incompatible pollen is lost. Goldraij *et al.* (2006) have shown that HT-B is at lower levels in incompatible pollen tubes, where it prevents disintegration of S-RNase compartments. No interaction has been described between HT-B and S-RNase or SLF, but it is thought that HT-B is required for SI and it might be involved in transporting S-RNases from the endomembrane to the cytoplasm where the S-RNases perform their function. The 120K glycoprotein is expressed in the stilar extracellular matrix and has been shown to be taken up by pollen tubes (Lind *et al.*, 1994; Lind *et al.*, 1996; Hancock *et al.*, 2005). Loss of the 120K glycoprotein results in the loss of SI and it has been shown to prevent disintegration of S-RNase compartments (Goldraij *et al.*, 2006; Hancock *et al.*, 2005). In addition, it has been shown to bind to S-RNases *in vitro*, but its role in SI is still not clear (Cruz-Garcia *et al.*, 2005). Pollen factors include SSK1 and SBP1. SSK1 (SLF-interacting SKP-like 1) is a SKP1 orthologue that is a core component of the SCF-type E3 ubiquitin ligase complex, which mediate protein degradation by the 26S proteasome (Huang *et al.*, 2006). SSK1 is thought to function as an adapter to connect SLF to CUL1 (a crucial component of the SCF-type E3 ubiquitin ligase complex), and SLF and

SSK1 are recruited to a canonical SCF complex. It is thought this complex may be involved in the ubiquitination and degradation of S-RNases. SBP1 (S-RNase binding protein 1) is a protein that contains a RING-finger domain that is found in E3 ubiquitin ligases (O'Brien *et al.*, 2004; Sims and Ordanic, 2001). SBP1 interacts with SLF and CUL1 and it is proposed that SLF and CUL1 are part of an E3 ubiquitin ligase complex that ubiquitinates S-RNases (Hua and Kao, 2006).

There are currently two proposed models explaining how S-RNase based GSI functions. In the first model, S-RNases are taken up by the pollen tube where they interact with SLF, in a non-specific manner. However, only non-self S-RNases are recognized and ubiquitinated leading to degradation, whereas self S-RNases are protected and can degrade RNA by haplotype-specific interaction with SLF, or with other unknown molecules. It is proposed that there is an unknown general inhibitor of RNases that inhibits all RNases by binding to the active site, therefore inactivating them, either by sequestering them, or by degradation. Allele-specific binding of SLF to S-RNase prevents binding of the inhibitor and the S-RNase can therefore degrade the pollen tube RNA and inhibit its growth. In addition, a modification of this first model was proposed that involves SBP1 and CUL1 (Hua and Kao, 2006). S-RNases are taken up by the pollen tube in a non-specific manner where they bind to an SBP1-CUL1 complex, which results in their degradation. Non-self S-RNases are bound to an SBP1-CUL1 complex including SLF, which preferentially bind to non-self S-RNases and results in their degradation. In self-pollen, SLF binds to S-RNase in an allele-specific manner but this is not degraded and can initiate RNA degradation.

The second model is much more complex and involves the pistil factors (Goldraij *et al.*, 2006). The S-RNases, HT-B and 120K glycoprotein are all taken up by the growing pollen tubes non-specifically, where they are sequestered by endocytosis in membrane-bound endosomes. In non-self pollen tubes the S-RNases remain in the endosomes, but a general RNase inhibitor degrades any that escape. In self-pollen tubes, allele-specific binding of SLF protects these escaped S-RNases, which are therefore not degraded. This interaction is proposed to lead to stabilization of HT-B, potentially by degradation of an unknown HT-B inhibitor, via ubiquitination by SLF. HT-B then breaks down the endosomes that contain the S-RNases and the S-RNases are released into the cytoplasm where they degrade the RNA. The amount of S-RNases released is thought to be too abundant for the general RNase inhibitor and therefore pollen RNA is degraded. In non-self pollen, S-RNases do not interact with SLF and HT-B is inhibited and/or degraded or sequestered in the endosomes.

1.2.2.2 Gametophytic self-incompatibility in *Papaver rhoeas*

The molecular and biochemical basis for the recognition, discrimination and rejection of incompatible pollen observed during the SI response in *Papaver rhoeas* (field poppy) has been investigated for over twenty years. The ability to mimic the SI response in *P. rhoeas* pollen *in vitro* (Franklin-Tong *et al.*, 1988) and major advances in recent years have allowed detailed studies of the signalling cascades triggered by SI. Because of this *Papaver* SI is considered one of the most well characterised cell-cell signalling pathways in flowering plants. SI in *P. rhoeas* is governed by a single multi-allelic *S*-locus containing both pollen and pistil components (Lawrence *et al.*, 1978), but the mechanism used to inhibit pollen is dramatically different to that of the S-RNase mediated self-incompatibility system.

The known components involved in *Papaver rhoeas* SI are discussed in detail below. Figure 1.2.2.2a/b provides a summary of these events and the timings at which they occur.

1.2.2.2.1 The female component

The female component of *P. rhoeas* SI, PrsS, comprises small (~15kDa) extra-cellular signalling molecules (S-proteins), which are secreted by stigmatic papillae cells and are specifically expressed in the stigma. There are estimated to be ~66 alleles present in *P. rhoeas* (Lane and Lawrence, 1993) and several S-proteins have been cloned (S₁, S₃, S₈) (Foote *et al.*, 1994; Walker *et al.*, 1996; Kurup *et al.*, 1998). Separation of S₁ and S₃-linked stigmatic proteins by PAGE-IEF allowed identification of specific allele related proteins, which allowed their sequence to be partially determined by a protein micro-sequencer. This sequence was then used to design oligonucleotides to identify the gene encoding S₁ and S₃ by screening a cDNA library (Foote *et al.*, 1994; Walker *et al.*, 1996). The S₈ allele was identified by immuno-detection and PCR screening using an antibody and oligonucleotides based on the conserved region of S₁ and S₃ (Kurup *et al.*, 1998). The S-proteins have been shown to be highly polymorphic and share between 51% and 63% homology at the protein level, but show no homology to other proteins with known function (Foote *et al.*, 1994). The proteins share four conserved cysteine residues and a predicted conserved secondary structure with 6 β -strands and 2 α -helices linked by 7 hydrophilic surface loops (Walker *et al.*, 1996). It has also been shown that certain residues in hydrophilic loop six are crucial for pollen recognition, as proteins mutated at these residues have been shown to lose their biological activity (Kakeda *et al.*, 1998).

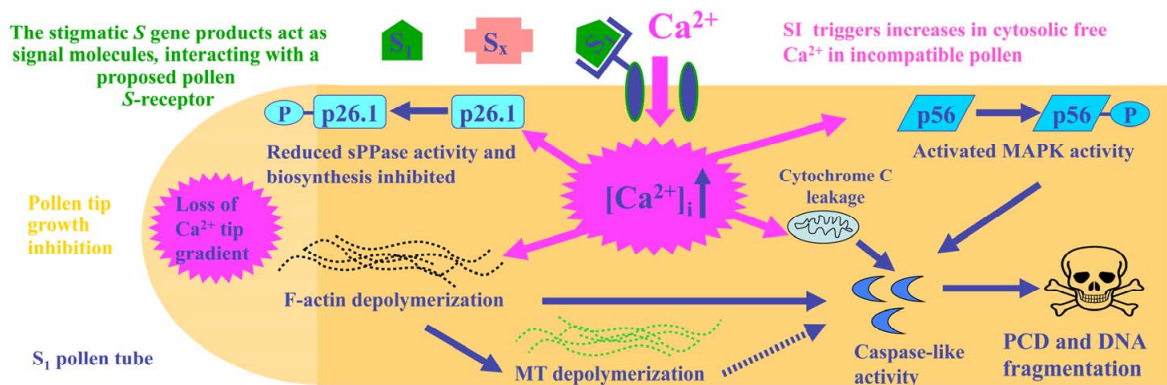


Figure 1.2.2.2a An overview of the events during an incompatible reaction in *Papaver rhoeas* SI. See text (and 1.2.2.2.7) for description of events.

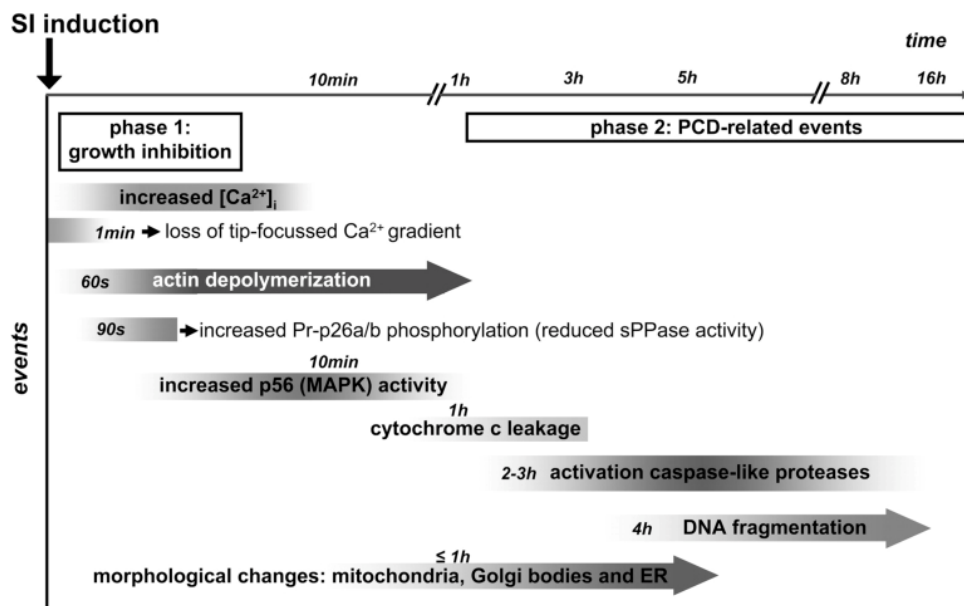


Figure 1.2.2.2b Time-line of events during an incompatible reaction in *Papaver rhoeas* SI. On induction of SI there is an influx of extracellular calcium into the shank of the pollen tube, causing an increase in $[Ca^{2+}]_i$ within seconds. Within 1-2 minutes there is actin depolymerisation and phosphorylation of the sPPase, p26.1. These early events are likely to be involved in pollen tube inhibition. By 10 minutes there is a peak in activation of the MAPK, p56. This is thought to trigger the later PCD-related events. By 1h there is cytochrome-c leakage, by 2-3h activation of caspase-like activity and finally, by 4h DNA fragmentation. See text (and 1.2.2.2.7) for description of events (from Bosch *et al.*, 2008).

1.2.2.2.2 The male component

As *P. rhoeas* SI stimulates an initial increase in intracellular free calcium ($[Ca^{2+}]_i$) induced by a Ca^{2+} influx (see below, Franklin-Tong *et al.*, 2002) it was thought that the pollen-S component was likely to be a plasma membrane receptor that was involved with transducing the Ca^{2+} signal. One candidate for this role was S-protein binding protein (SBP). SBP is a pollen specific plasma membrane glycoprotein with a molecular weight of 70-120kDa. SBP binds specifically to S-proteins, but it was shown that this binding was not allele-specific (Hearn *et al.*, 1996). Biochemical analysis of SBP was carried out using site-directed mutagenesis of S-proteins. All S-protein mutants that showed reduced ability to inhibit incompatible pollen also showed a reduced SBP binding activity (Jordan *et al.*, 1999). These results suggest that if SBP is not the pollen receptor, then it is still likely to have a role as an accessory receptor. Recent work (Wheeler *et al.*, 2009) suggests that SBP is unlikely to be the pollen-S component as a pollen gene linked to the *S*-locus has been identified. This gene shows properties expected of the elusive pollen-S component.

The cloning and sequencing of a region of the *P. rhoeas* genome, containing the stigmatic *S_I* gene, allowed the *S_I* locus to be characterised (Wheeler *et al.*, 2003). As both stigma and pollen genes are encoded at the *S*-locus it was hoped that identifying the sequence around the *S*-locus might help to identify the pollen-*S* gene. This approach had proved successful in identifying the pollen-*S* gene (*SCR*) in *Brassica* (Schopfer *et al.*, 1999; Suzuki *et al.*, 1999). Analysis of a *P. rhoeas* λS_I clone revealed that the *P. rhoeas* *S_I* locus did share some structural similarities with the *S*-loci of *Solanaceae* and *Brassicaceae*, although there was no evidence of genes transcribed in pollen and no part of the clone exhibited any homology with

known plant receptor genes, suggesting there was no candidate for the pollen *S*-gene. Examination of the *S*-locus confirmed the presence of a leaf-specific transcript 10kb downstream of stigma *S₁*. Because in *Brassica* the pollen and pistil genes are adjacent and, as the *P. rhoeas* *S*-locus contained a leaf-specific gene downstream of the stigma *S₁* gene, it was thought the pollen *S*-gene might lie upstream of this region (Wheeler *et al.*, 2003). Probing a *S₁S₃* genomic library with the *S₁* pistil gene identified a 42kb cosmid clone containing the *S₁* locus. Sub-clones from the *S₁* cosmid that corresponded to the region upstream of the stigmatic *S*-gene were sequenced and revealed the presence of an ORF, the 3' end of which is located 450bp upstream of the stigmatic *S₁* gene (Wheeler *et al.*, 2009). RT-PCR was used to show that this gene was expressed specifically in pollen. The gene has been designated *PrpS* (*Papaver rhoeas* pollen S) (Wheeler *et al.*, 2009). *PrpS₁* is predicted to encode a 20.5kDa protein that contains between three and five membrane spanning regions, and it was found that PrpS₁ does not show homology to any known protein suggesting that it could represent a novel trans-membrane protein. The localisation of PrpS₁-GFP fusion protein under the control of the NTP303 promoter was used to determine the localisation of the protein. Evidence suggests that the protein localises to the pollen plasma membrane but not in the tip region of pollen tubes. During an SI response there is an influx of extracellular Ca²⁺ into the pollen tube shank and influx at the tip is inhibited. This result is therefore consistent with the proposition that PrpS is involved with transducing the Ca²⁺ signal. In addition, *PrpS* has been shown to be polymorphic which is required of the pollen *S*-gene. Finally, the extra-cellular loop of PrpS has been shown to interact with PrsS, and PrpS-deficient plants show that PrpS is involved in the S-specific inhibition of self-pollen (Wheeler *et al.*, 2009).

1.2.2.2.3 The role of calcium

Investigations were carried out to see if there were any changes in cytosolic free calcium ($[Ca^{2+}]_i$) during an incompatible SI reaction, as $[Ca^{2+}]_i$ is a key second messenger in intracellular signalling (for a review see Hetherington and Brownlee, 2004). Ca^{2+} is essential for pollen tube growth (Brewbaker and Kwack, 1963; Iwano *et al.*, 2009) and it has been shown that there is an oscillating apical high $[Ca^{2+}]_i$ gradient present in growing pollen tubes, and not in pollen tubes that are not growing, but its role is unclear (Franklin-Tong *et al.*, 1993). The localised apical $[Ca^{2+}]_i$ gradient has been shown to be caused by a Ca^{2+} influx in the extreme apex of the pollen tube (Pierson *et al.*, 1996; Franklin-Tong *et al.*, 1997). Calcium imaging was used to show that after the S-specific induction of SI there was a rapid increase in $[Ca^{2+}]_i$ in pollen tubes (Franklin-Tong *et al.*, 1993) and it was revealed that the stigmatic-S proteins were enough to induce this Ca^{2+} influx (Franklin-Tong *et al.*, 1995). The Ca^{2+} influx was shown to occur only in the sub-apical 'shank' region of the pollen tubes seconds after challenge, continuing for several minutes, and not in the tip region of the pollen tubes (Franklin-Tong *et al.*, 2002). It was demonstrated that the influx of Ca^{2+} during an incompatible reaction coincided with a loss of the oscillating high $[Ca^{2+}]_i$ gradient at the pollen tube tip. This loss of oscillating high $[Ca^{2+}]_i$ gradient is likely to play a role in the inhibition of pollen tube growth as low apical $[Ca^{2+}]_i$ levels are associated with loss of growth. It was thought that the inhibition of pollen tube growth may be mediated by inositol triphosphate-induced Ca^{2+} release (Franklin-Tong *et al.*, 1996), but there is no evidence of an inositide signalling pathway in *P. rhoeas* SI (Straatman *et al.*, 2001).

1.2.2.2.4 The role of the cytoskeleton

The actin cytoskeleton is known to be a target of many signals in both plants and animals. In plants, the actin cytoskeleton has been shown to rearrange in response to a number of stimuli (Staiger, 2000). In pollen the actin cytoskeleton is highly dynamic and is essential for pollen tube growth, involved with the delivery of vesicles at the growing tip. Because of this role, experiments were carried out to distinguish if SI had any effect on the actin organisation during an incompatible reaction. It was shown that there were rapid and dramatic alterations in F-actin organisation, but these changes were not seen in compatible reactions. After just 1 minute longitudinal F-actin bundles were lost, while cortical F-actin remained. By 5 to 10 minutes the remaining F-actin had a fine speckled appearance. Later punctate foci of F-actin were seen in the cortex, and these remained for several hours after challenge (Geitmann *et al.*, 2000). Quantification of the F-actin content revealed a rapid large-scale depolymerisation of the F-actin (Snowman *et al.*, 2002). By 1 minute a 30% loss in actin was seen, and by 1 hour this was as high as 75%. Artificially increased levels of $[Ca^{2+}]_i$ showed a rapid depolymerisation and reorganisation of actin after 1 minute, which suggests that the actin cytoskeleton is a very early target of SI and is downstream of the Ca^{2+} signalling cascade (Snowman *et al.*, 2002).

The dynamics of actin are dependant upon the activity of actin binding proteins (ABPs). PrABP80 is a Ca^{2+} regulated ABP that was identified as a gelsolin, and exhibits a potent Ca^{2+} -dependent severing activity. Evidence suggests that PrABP80 and profilin (another ABP) have a role in Ca^{2+} -dependant F-actin depolymerisation during an incompatible SI reaction (Huang *et al.*, 2004). This data implies a link between calcium increases and actin

depolymerisation, and suggests a mechanism for rapid actin depolymerisation and inhibition of pollen tube growth by directly affecting the transport of vesicles to the growing pollen tube tip.

The roles of microtubules were also investigated in SI. Microtubules, like actin, are highly dynamic and interact with microtubule-associated proteins (Erhardt and Shaw, 2006) that help to determine cell shape and growth (Smith and Oppenheimer, 2005). It has been shown that during an incompatible reaction there is rapid depolymerisation of the cortical microtubules after just 1 minute (Poulter *et al.*, 2008). Evidence also illustrated that while actin depolymerisation can trigger depolymerisation of the microtubules, the reverse is not true (Poulter *et al.*, 2008). It has been shown that although disruption of the microtubule dynamics does not trigger programmed cell death (PCD, see below), evidence suggests there may be a role for microtubule depolymerisation in mediating PCD.

1.2.2.2.5 Programmed cell death

Apoptosis and programmed cell death (PCD) have been shown in both plants and animals to be an efficient way of removing cells in response to both developmental and defence response signals and involve several hallmark features such as caspase-like activity, cytochrome-c release from the mitochondria, and DNA fragmentation (for a review see Reape *et al.*, 2008). Studies were carried out to see if PCD was involved during SI as a mechanism for killing self-pollen. Experiments showed that DNA fragmentation was induced in pollen 4 hours after an incompatible reaction, and is still seen at least 20 hours after SI (Jordan *et al.*, 2000). More recently this DNA fragmentation was shown to be inhibited by Ac-DEVD-CHO (a caspase-3

inhibitor) (Thomas and Franklin-Tong, 2004). Pre-treatment with DEVD was also able to overcome SI-induced pollen tube inhibition. These results suggested that a caspase-3-like activity might also be involved. Caspases are cysteine proteases involved in apoptosis, although to date no plant caspases have been identified (Bonneau *et al.*, 2008). To confirm this caspase-3-like activity, pollen extracts were tested using PARP (poly (ADP-ribose) polymerase) a substrate for caspase-3. Evidence showed that there was cleavage of PARP 2 hours after induction of an incompatible reaction, suggesting that this caspase-like activity is downstream of cytoskeletal changes, but upstream of DNA fragmentation.

Another feature of PCD in many species is leakage of cytochrome-c from the mitochondria where it triggers caspase activation (Green and Reed, 1998). It was demonstrated that there was cytochrome-c leakage as early as 10 minutes after an incompatible reaction and this increase was maintained until 120 minutes after induction (Thomas and Franklin-Tong, 2004)

It was also shown that all of the above markers of PCD could be induced by artificially increasing $[Ca^{2+}]_i$ (Thomas and Franklin-Tong, 2004). This suggests that these features are all stimulated by the SI-specific Ca^{2+} signalling cascade and provide a mechanism for ensuring the pollen tubes do not resume growth.

1.2.2.2.6 Protein phosphorylation during the SI response

It is well documented that reversible protein phosphorylation is an important post-translational mechanism for the transfer of information within and between cells. This is achieved via the phosphorylation of proteins by kinases and their dephosphorylation by

phosphatases (see below). An investigation was carried out in order to determine if there were any changes in protein phosphorylation during the SI response (Rudd *et al.*, 1996). *P. rhoeas* pollen proteins were extracted and incubated in the presence of ^{32}P -labelled orthophosphate. ^{32}P in the cell is incorporated into any proteins that become phosphorylated and these proteins can be visualised by autoradiography. Pollen was then treated with compatible, incompatible or heat-denatured incompatible S-proteins to stimulate the SI response and the proteins were then analysed by 2-dimensional SDS-PAGE and autoradiography. A number of proteins showed varying degrees of phosphorylation when challenged with incompatible S-proteins, but not with compatible or heat-denatured incompatible S-proteins, suggesting a SI-specific increase in phosphorylation. The role of two sPPases (Pr-p26.1a/b), a MAPK (p56) and an unidentified protein (p68) are discussed below.

1.2.2.2.6.1 The role of p26.1, a sPPase

During the SI response it was shown there was SI-specific phosphorylation of a 26kDa protein with a pI of 6.2 (Rudd *et al.*, 1996). Phosphorylation of this 26kDa protein (p26) was shown to increase by 21.9% by 90 seconds after an incompatible reaction and by 40.1% by 400 seconds. Experiments were carried out to determine the sub-cellular localization of p26 and showed that it actually consisted of two proteins, one soluble (p26.1) and one in the microsomal fraction (p26.2). To confirm these proteins were different, phospho-peptide mapping was carried out and suggested that these were in fact two different proteins. As SI involves a rise in $[\text{Ca}^{2+}]_i$ it was tested whether the presence of Ca^{2+} and calmodulin (to test the activities of the kinase responsible for phosphorylating the protein) were necessary for the phosphorylation of p26.1 and p26.2. Results showed that while phosphorylation of both

proteins was Ca^{2+} -dependant, only p26.1 phosphorylation was calmodulin-dependant. Experiments were carried out to determine if both proteins were involved in the SI response. A huge increase in the phosphorylation of p26.1 after SI stimulation suggested that this protein was involved with the SI response. Evidence suggested that p26.2 was not involved in the SI response.

Further work was carried out to try and determine the identity of p26.1. Purification of the Pr-p26.1 protein from pollen, amino acid sequencing and cloning of the complementary DNA showed that p26.1 itself consisted of two proteins, p26.1a and p26.1b (Rudd and Franklin-Tong, 2003). p26.1a was a 24.4kDa protein with a pI of 6.11 and p26.1b was 26.5kDa with a pI of 6.03 and they shared 78% identity with each other. The two proteins showed high homology to Family 1 sPPases, which are highly conserved enzymes that hydrolyse inorganic pyrophosphate (PPi) to orthophosphate (2Pi) and their activity is essential for making biosynthetic processes thermodynamically favourable (Cooperman *et al.*, 1992). p26.1a and p26.1b also contained the sPPase signature sequence needed for catalytic activity, 14 conserved sPPase residues and putative phosphorylation sites. It was also shown that the proteins have classic Mg^{2+} -dependant sPPase activity, which is inhibited by Ca^{2+} . Expression analysis showed that p26.1a and p26.1b were specific to mature pollen, which suggested a role in pollen germination or growth and not in pollen development (de Graaf *et al.*, 2006). Fractionation, immuno-localisation and GFP fusion proteins of both p26.1a and p26.1b confirmed the cytosolic location of the proteins (de Graaf *et al.*, 2006).

Although a few cytosolic sPPases have been cloned they are still rare in plants (Rojas-Beltran *et al.*, 1999; Visser *et al.*, 1998; Dujardin *et al.*, 1995). de Graaf *et al.* (2006) suggest this

unusual cytosolic localisation of the sPPase could be due to the fact that they are present in highly metabolically active pollen cells. It was tested whether phosphorylation of these sPPases could modify their activity, as evidence had previously shown that there was SI-induced Ca^{2+} -dependant phosphorylation of p26.1. Results showed that both Ca^{2+} and phosphorylation reduced their activity suggesting a novel mechanism for the regulation of sPPases in eukaryotes.

1.2.2.2.6.2 The role of p56, a mitogen activated protein kinase

Another protein that showed SI-specific phosphorylation was a 56kDa protein, named p56 (Rudd *et al.*, 2003). As mitogen activated protein kinase (MAPK) cascades have been implicated in a wide range of stress responses (Innes, 2001), and as the response of pollen to signals from the stigma could be considered a stress response, investigations were made to see if there was any involvement of MAPKs in the SI response. Myelin basic protein (MBP) is a substrate for MAPKs and MBP in-gel kinase assays can be used to identify MAPK activity. Assays showed that p56 extracted from pollen undergoing an SI response could phosphorylate MBP. The phosphorylation of MBP was detectable 5 minutes after treatment with incompatible S-proteins, peaked after 10 minutes, but remained at high levels for over 30 minutes. This change was not detected in pollen tubes challenged with compatible S-proteins or heat-denatured incompatible S-proteins. When the MBP in-gel kinase assay was repeated using apigenin (a MAPK inhibitor), p56 activity was abolished. Further evidence that p56 is a MAPK came from the discovery that p56 can be immuno-precipitated with an anti-phosphotyrosine antibody, as a diagnostic feature of MAPKs is phosphorylation on their tyrosine and threonine residues. An anti-pT-X-pY antibody that binds to the phosphorylated

MAPK activation domain was also used to detect p56. All this evidence suggests that p56 is a MAPK.

As the SI response involves an influx of $[Ca^{2+}]_i$, experiments were carried out to see if this influx was necessary for p56 activation. Mastoparan, a peptide toxin from wasp venom, can induce an intracellular influx in calcium (Takahashi *et al.*, 1998; Franklin-Tong *et al.*, 1996) and has also been shown to induce many of the SI-induced responses (Snowman *et al.*, 2002; Jordan *et al.*, 2000). Mastoparan was shown to cause an increase in phosphorylation just 2 minutes after treatment, which suggests that the calcium influx is upstream of p56 activation. Lanthanum is a calcium ion channel blocker and can be used to inhibit the SI induced influx of Ca^{2+} . Pollen pre-treated with lanthanum and then treated with S-proteins showed a reduced activation of p56 compared to untreated controls, and suggests the Ca^{2+} influx is necessary for the activation of p56.

In plants MAPKs have been shown to be functionally involved in regulating PCD (Ligterink *et al.*, 1997; Yang *et al.*, 2001; Kroj *et al.*, 2003). As the activity of p56 peaks after the arrest of pollen tube growth it is thought that p56 may not play a role in the initial inhibition of pollen tube growth but have a role in a signalling cascade to PCD in incompatible pollen to allow irreversible inhibition of pollen tube growth. Li *et al.* (2007) have shown that U0126, a MAPK inhibitor, can inhibit pollen tube growth and p56 activity, while not affecting the viability of the pollen, which is rapidly reduced during the SI response. U0126 was shown to 'rescue' incompatible pollen, while its negative analogue, U0124, did not (Li *et al.*, 2007). DNA fragmentation can be used as a hallmark feature of PCD. To investigate whether p56 is involved in signalling to PCD, pollen was pre-treated with U0126 with the result that DNA fragmentation could be inhibited, compared to controls (Li *et al.*, 2007). SI has been shown to

involve a caspase-3-like (DEVDase-like) activity (Thomas and Franklin-Tong, 2004). Evidence showed that the SI-induced caspase-like activity could also be inhibited by pre-treatment with U0126, which suggests that p56 may signal to PCD via this caspase-3-like activity.

1.2.2.2.6.3 Activation of p68

Rudd *et al.* (1997) demonstrated that during the SI reaction there is also SI-specific phosphorylation of a 68kDa protein (p68, pI 6.1-6.45). p68 showed slightly increased phosphorylation levels after 240 seconds after an SI challenge, with a 127% increase by 400 seconds. SI is mediated by an increase of $[Ca^{2+}]_i$ and experiments have shown that, unlike p26, p68 phosphorylation is unexpectedly independent of these $[Ca^{2+}]_i$ changes. As p68 phosphorylation occurs later than that of p26.1 it is thought that the enzymes responsible for the phosphorylation of p68 are likely to be downstream of those involved in p26.1 phosphorylation.

1.2.2.2.7 Overview of self-incompatibility in *Papaver rhoeas*

The above studies describe the many events that take place in an incompatible interaction. These are shown in Figure 1.2.2.2a/b. To summarise, in an incompatible reaction PrsS interacts with the receptor PrpS in an S-haplotype specific manner. This results in an influx of extracellular calcium into the shank of the pollen tube, causing an increase in $[Ca^{2+}]_i$ within seconds of an incompatible reaction. This leads to the rapid depolymerisation of actin. In addition, phosphorylation of p26.1, via $[Ca^{2+}]_i$, results in inhibition of its sPPase activity,

resulting in loss of calcium at the pollen tube tip required for growth. Taken together these early events are thought to result in the inhibition of pollen tube tip growth. The later events are thought to involve a commitment phase by which the pollen tube enters into PCD and the pollen tube is actively killed. It is thought that the MAPK, p56, may be involved in triggering this commitment phase that passes it into a point of no return, which leads to hallmark features of PCD, such as cytochrome-c release, caspase-like activities and DNA fragmentation.

1.3 Mitogen-activated protein kinases

As plants are sessile they need to continuously respond to changes in the environment. This is achieved by the transmission of extra-cellular signals into the cell that results in a variety of responses. Research has identified and characterised several signalling molecules and proteins that play roles in different signalling cascades. Protein phosphorylation is one of the most widespread post-transcription modifications in all organisms and plays a major role in these signalling cascades. In eukaryotic cells, it is thought ~30% of proteins are phosphorylated, and this phosphorylation is regulated by protein kinases and phosphatases. Protein phosphorylation generally occurs at serine, threonine and tyrosine residues. The addition of a phosphate group to one of these amino acid residues can turn a hydrophobic portion of the protein into an extremely hydrophilic region. Interaction of this hydrophilic region with other residues results in a conformational change in the protein, which causes it to become activated or deactivated.

One of the major groups of kinases involved in signal transduction pathways is the highly conserved mitogen-activated protein kinase (MAPK) super-family. The MAPK family are conserved between humans, yeast and plants (Widmann *et al.*, 1999), and can efficiently multiply and integrate information from a cell's environment to initiate gene transcription and metabolomic responses. A MAPK cascade generally consists of three protein kinases; a mitogen-activated protein kinase kinase kinase (MAPKKK), a mitogen-activated protein kinase kinase (MAPKK) and a mitogen-activated protein kinase (MAPK) (Widmann *et al.*, 1999). As the MAPK modules are highly conserved at each level, the structure of each gene

family is very similar, although members generally show distinct roles. However there is some functional redundancy within the families (Jonak *et al.*, 2002).

Receptor-mediated activation of a MAPKKK can occur by physical interaction with the receptor and/or by phosphorylation by the receptor itself, by bridging factors, or by MAPKKK-kinases (MAPKKKK). MAPKKKs are serine/threonine kinases that activate MAPKKs by phosphorylation on two serine/threonine residues at a conserved S/T-X₃₋₅-S/T motif. MAPKKs are dual-specificity kinases, which phosphorylate MAPKs on threonine and tyrosine residues and contain a conserved motif in the N-terminal domain, which acts as a kinase interaction motif and is important for activation (Bardwell and Thorner, 1996; Ichimura *et al.*, 2002). MAPKs are phosphorylated at a T-X-Y motif (where X represents aspartate, glutamate, glycine or proline) in its activation loop (or T-loop). For activation, phosphorylation of both threonine and tyrosine residues is required. MAPKs are serine/threonine kinases that phosphorylate a variety of substrates including transcription factors, other protein kinases and cytoskeletal proteins. It has been shown that, although MAPKKs are specific to certain MAPKs, they are capable of activating multiple MAPKs (Pearson *et al.*, 2001). The MAPK signalling pathway is complex, with a number of upstream stimuli being able to activate a number of kinases at one level, and act upon more than one downstream target (Cardinale *et al.*, 2002; Garrington and Johnson, 1999). Upon activation, MAPKs have been shown to relocate to the nucleus where they can phosphorylate transcription factors and initiate gene transcription, or they can phosphorylate other kinases or other membrane and cytosolic proteins. The specificity of each MAPK cascade can be determined by specific MAPK docking domains (Tanoue and Nishida, 2003) and scaffold proteins (Levchenko *et al.*, 2000; Whitmarsh and Davis, 1998), or the spatio-temporal

localisation of the signalling components. This specificity is also increased by the dephosphorylation of MAPKs by specific phosphatases (Keyse, 2000). To date a number of *Arabidopsis thaliana* MAPK-specific phosphatases have been identified; PHS1, IBR5, AtMKP1, AtMKP2 and DsPTP1 (Lee and Ellis, 2007; Gupta *et al.*, 1998; Ulm *et al.*, 2001; Ulm *et al.*, 2002; Monroe-Augustus *et al.*, 2003). Figure 1.3a provides an overview of a simplified MAPK signalling pathway.

Evidence has shown that there are more MAPK family genes in plants than in other metazoans (Hamel *et al.*, 2006). In *A. thaliana* there are 60 MAPKKKs that are organised into three groups based on mammalian homologues; MEKK-like, Raf-like and ZIK-like protein kinases, but only the MEKK-like protein kinases have been shown to function *in planta* (Ichimura *et al.*, 2002; Champion *et al.*, 2004). In *A. thaliana* there are 10 MAPKKs that are organised into four groups (Ichimura *et al.*, 2002) and 20 MAPKs, all of which show highest similarity to the mammalian ERK MAPK sub-family (Hirt, 2000) and are organised into 4 different sub-groups (A, B, C and D) (Ichimura *et al.*, 2002). MAPKs contain 11 domains that are highly conserved and N- and C-terminal domains that are more divergent between each MAPK. Group A, B and C MAPKs contain a T-E-Y motif, whereas the group D MAPKs contain a T-D-Y motif and generally contain long C-terminal domains. To date, no plant MAPKs have been found that contain a T-P-Y or T-G-Y domains, which are found in other species.

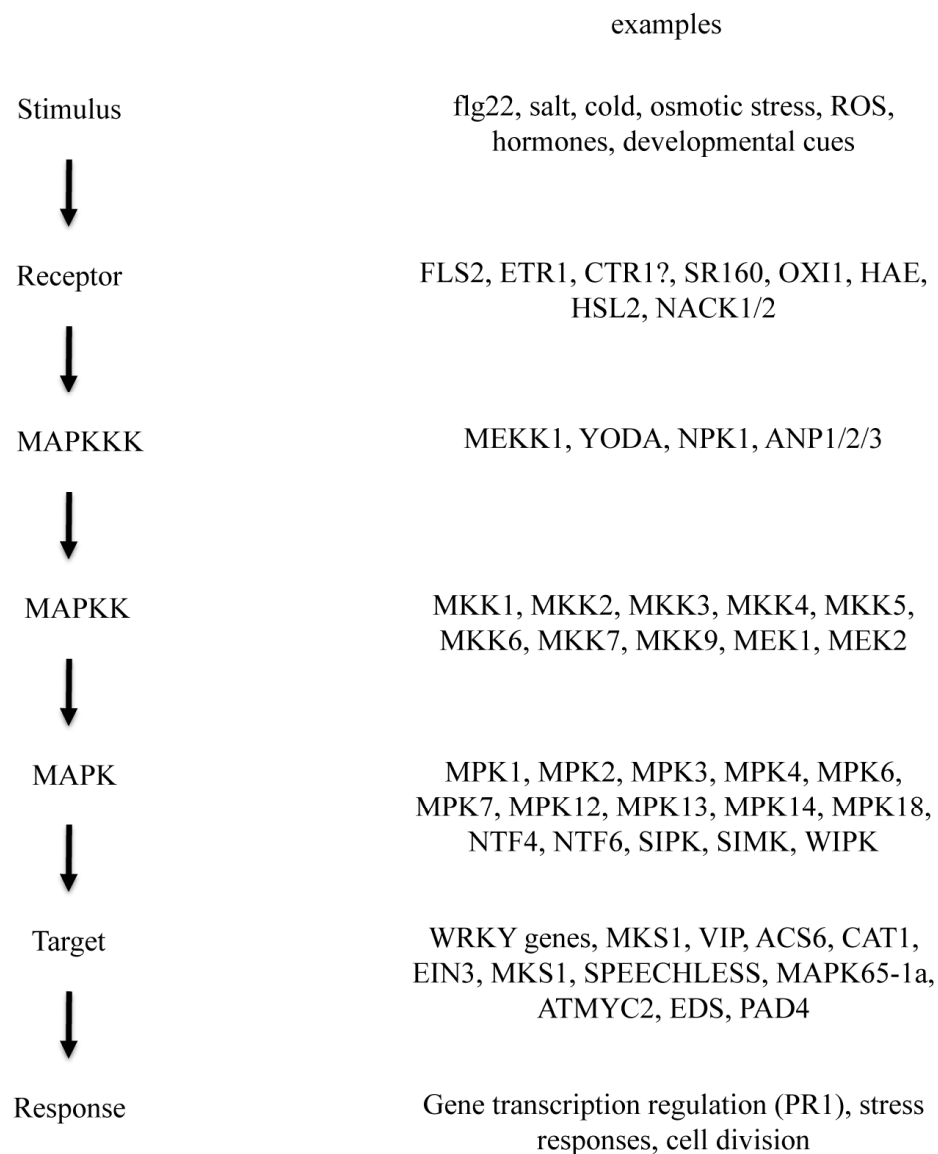


Figure 1.3a Simplified MAPK cascade. On the left is a simplified MAPK cascade showing the 3 MAPK modules (MAPKKK, MAPKK and MAPK). On the right are examples of proteins/genes, stimuli and responses at each 'stage' of the signalling cascade. The protein/genes examples are taken from signalling pathways described in the text below.

1.3.1 The roles of MAPK signalling in plants

The MAPKs have been shown to regulate cell growth and death, the cell cycle and cell differentiation and are activated by both abiotic and biotic stress, hormones and wounding (Mishra *et al.*, 2006). It is beyond the scope of this review to cover all aspects of MAPK signalling pathways. Therefore, there will be an emphasis on the role of MAPK cascades in *Arabidopsis thaliana*, focusing mainly on the MAPK components, although other important cascades from other species will be discussed.

1.3.1.1 MAPK signalling in biotic stress responses

Plants have developed methods for coping with pathogen attack via an innate immune system (for a review see Jones and Dangl, 2006). Plants have developed mechanisms to recognise molecules common to microbes (pathogen associated molecular patterns (PAMPs)) that result in the production of anti-microbial agents and cell wall modifications. In response, pathogens developed virulence factors to allow them to thrive in the host. However, some plants have evolved to recognise these specific virulence factors, either directly, or as a consequence of the effects these factors have on the host, and to respond via defence-related signalling pathways. Resistance often involves changes in hormones in the plant, which can result in a hypersensitive response, the local cell death that prevents the spread of infection. In addition, hormones can also function in systemic acquired resistance (SAR), which ‘primes’ the plant for future pathogen attack.

It has been shown that defence responses in plants can be activated by flg22, a 22 amino acid peptide from flagellin, a structural protein that makes up filaments in bacterial flagella (Felix

et al., 1999). flg22 is a PAMP, which interacts with a FLS2/BAK1 receptor-like kinase complex (Chinchilla *et al.*, 2007). Once activated, this complex initiates a signalling cascade that results in the phosphorylation of kinases and other proteins, gene activation and an oxidative burst (Gómez-Gómez *et al.*, 1999; Nuhse *et al.*, 2007; Zipfel *et al.*, 2004). flg22 signalling has been shown to activate two individual MAPK signalling cascades that act antagonistically to control flg22-induced signalling.

To date, the most complete MAPK signalling cascade identified is that of FLS2-MEKK1-MKK4/MKK5-MPK3/MPK6-WRKY29/FRK1 (receptor-MAPKKK-MAPKK-MAPK-target respectively) from protoplast transient expression experiments (Asai *et al.*, 2002). It was shown that constitutively active MEKK1 activates MKK4/MKK5, which induces the activation of WRKY29/FRK1. Constitutive expression of MKK4/MKK5 results in the activation of MPK3/6 and bypasses flg22-induced activation of WRKY29/FRK1. In addition, a dominant-negative form of MKK4/MKK5 alleviates flg22-induced gene expression. Taken together, it suggests a role for this MAPK cascade in flg22-mediated signalling. However, it was also shown that in MEKK1-deficient plants, flg22 could still activate MPK3/6, suggesting functional redundancy in this pathway (Ichimura *et al.*, 2006; Suarez-Rodriguez *et al.*, 2007). Downstream of this MAPK signalling pathway there is flg22-induced activation of ACS6 (a 1-aminocyclopropane-1-carboxylic acid synthase, which converts S-adenosyl-methionine to ACC) by MPK6, and ethylene production (Liu and Zhang, 2004). MPK3 has been shown to activate VIP, a bZIP transcription factor, which, upon activation, relocates from the cytoplasm to the nucleus where it initiates transcription of defence-related genes, such as PR1 (Djamei *et al.*, 2007). It is not yet known which of these two pathways involves WRKY29/FRK1.

Phytoalexins are antibiotics that are used by plants as a defence against infection, and Ren *et al.* (2008) have shown that MPK3/MPK6 activation by a fungus result in phytoalexin biosynthesis. Although the upstream MAPKs are not known, this pathway activates PAD2 and PAD3 that are involved in biosynthesis and regulation of phytoalexin production (Glazebrook and Ausubel, 1994).

A second cascade activated by flg22 is the MEKK1-MKK1/MKK2-MPK4 cascade, which negatively regulates PAMP-induced cell death. MPK4 has been shown to be a negative regulator in systemic acquired resistance (SAR). MPK4-deficient plants are dwarfed and upon challenge by pathogens show enhanced resistance and disease resistance genes are constitutively induced (Petersen *et al.*, 2000). Salicylic acid (SA) is required for SAR and in MPK4-deficient plants levels of SA are increased. NahG (which converts SA to catechol) and MPK4 double mutant plants rescue the phenotype seen in MPK4-deficient plants. It has also been shown that MPK4 has a role in the positive regulation of the jasmonic acid (JA) response (Petersen *et al.*, 2000). MPK4 and MEKK1-deficient plants show related phenotypes, suggesting a role in the same pathway (Ichimura *et al.*, 2006). It was shown that MPK4 activation is increased by flg22 (Droillard *et al.*, 2004) and that in MEKK1-deficient plants there is no activation of MPK4 (Ichimura *et al.*, 2006; Suarez-Rodriguez *et al.*, 2007). In addition, MEKK1 and MPK4 show constitutive expression of pathogenesis-related genes and spontaneous cell death in leaves. These data suggest a role in the negative regulation of PAMP-induced cell death. It has been shown that MKK1/MKK2 are likely to be upstream of MPK4. In MKK1-deficient plants flg22 cannot activate MPK4 (Mészáros *et al.*, 2006) and over-expression of MKK2 results in increased MPK4 activation (Brader *et al.*, 2007). More

recently, Qiu *et al.*, (2008) have shown that MKK1/MKK2-deficient plants show a similar phenotype to MEKK1 and MPK4-deficient plants suggesting these MAPKKs do play a role in this signalling pathway. Downstream of this pathway, MPK4 has been shown to activate the WRKY transcription factors WRK25 and WRK23, and MKS1 (MAP kinase 4 substrate 1) (Andreasson *et al.*, 2005; Qiu *et al.*, 2008). In addition, it was shown that MKK1/MKK2 were involved in SA and JA-dependent defence signalling mediated by MKS1 activation by MPK4 (Qiu *et al.*, 2008).

In *A. thaliana* AP2C1, a serine/threonine phosphatase, has been shown by Schweighofer *et al.* (2007) to negatively regulate MPK4 and MPK6. This reduction of MAPK activation is involved in reduced ethylene and JA production and innate immunity against a necrotrophic pathogen.

1.3.1.2 MAPK signalling in abiotic stress responses

In addition to biotic stress responses, MAPK cascades have also been implicated in abiotic stress signalling. This includes responses to cold and heat, salt, touch, wind, wounding, UV and osmotic stresses.

1.3.1.2.1 The role of MAPKs in salt and cold stresses

Work by Teige *et al.* (2004), has shown that a MEKK1-MKK2-MPK4/MPK6 signalling cascade plays a role in salt and cold stresses in *A. thaliana*. During salt and cold stress MEKK1 activates MKK2, which in turn activates MPK4/MPK6. This pathway initiates the

altered gene expression of 152 genes involved in transcriptional regulation and stress-responses that allow the plant to tolerate freezing and salt stress.

1.3.1.2.2 The role of MAPKs in osmotic stresses

Abscisic acid (ABA) is a phytohormone that is involved in seed dormancy and germination and responses to water stress. Gudesblat *et al.* (2007) have shown that *A. thaliana* MPK3 is activated by ABA and H₂O₂ in guard cells, which control stomatal movements. Stomata are special epidermal structures that regulate gas and water vapour exchange in plants. MPK3-deficient plants suggested that this gene was involved in ABA-dependant inhibition of stomatal opening, but not in ABA-induced stomatal closure. MPK3-deficient plants also showed more sensitivity to H₂O₂, which acts as a secondary messenger of ABA-signalling in plants, in both stomatal opening and closure. As ABA-induced H₂O₂ synthesis was normal in this MPK3-deficient line, it suggests that MPK3 signalling is downstream of H₂O₂. It has been proposed that the MAPK phosphatase PHS1 may be involved in the negative regulation of ABA-signalling, as PHS1-deficient lines show ABA hypersensitivity in stomatal opening and it is thought that PHS1 is likely to initiate a MAPK cascade (Quettier *et al.*, 2006). In addition to MPK3, MPK6 is also thought to be involved in ABA-signalling. MPK6-deficient lines are hypersensitive to ABA and, like MPK3, have been shown to interact with a protein phosphatase, ABI1, which negatively regulates ABA-dependant signalling (Leung *et al.*, 2006). More recently, Xing *et al.* (2008) have shown that MKK1 and MPK6 are involved in the ABA-dependent activation of CAT1, a catalyse gene that leads to the production of H₂O₂.

Although the function of MPK1 and MPK2 have yet to be fully investigated Ortiz-Masia *et al.*, (2007) have shown the two proteins are activated by ABA and may mediate ABA-signalling. Evidence has shown that the MAPKK, MKK3, can activate MPK1 and MPK2 (Doczi *et al.*, 2007).

Osmotic shock is the sudden change in osmotic pressure that causes a rapid change in the movement of water across the cell membrane. MPK3 and MPK6 in *A. thaliana* (Droillard *et al.*, 2002; Droillard *et al.*, 2004) and SIPK in tobacco (Hoyos and Zhang, 2000) are activated by hyper- and hypo-osmotic shock, although this has only been shown in cell culture. *A. thaliana* MPK4 is activated by hypo-osmotic shock, but not by hyper-osmotic shock. However, MPK4-deficient plants show resistance to hyper-osmotic stress, suggesting that it may have a role in negatively regulating hyper-osmotic stress (Droillard *et al.*, 2004). Early evidence implies that MKK1 may activate MPK4 in osmotic stress signalling (Matsuoka *et al.*, 2002).

1.3.1.2.3 The role of MAPKs in oxidative stresses

Environmental pollutants, such as ozone, and pathogens can induce MAPK signalling cascades by the action of reactive oxygen species (ROS), which generally result in the accumulation of hormones such as JA, ethylene and SA, and can result in hypersensitive response-like cell death. ROS production is thought to be an early response to biotic and abiotic stresses, which not only signals to MAPK cascades, but also can be induced by MAPK signalling pathways.

Ahlfors *et al.* (2004) have shown that ozone generates ROS, which activate MPK3 and MPK6. It was shown that ozone also results in transcriptional activation of MPK3. Results suggested that MAPK activation was independent of ethylene or JA signalling. Although ozone-induced activation of MPK6 did not require SA, it was required for the full activation of MPK3. These results suggest a mechanism for the hormone-independent signalling by ROS in plants. In addition MPK3 and MPK6-deficient plants show hypersensitivity to ozone (Miles *et al.*, 2005). More recently, Lee and Ellis (2007) have suggested a role for the MAPK phosphatase, MKP2, in the positive regulation of MPK3/MPK6 response to ozone. In tobacco ROS have been shown to induce activation of SIPK and WIPK the AtMPK6 and AtMPK3 orthologues, respectively (Kumar and Klessig, 2000; Samuel *et al.*, 2000).

1.3.1.3 MAPK signalling in hormone signalling

1.3.1.3.1 The role of MAPKs in ethylene signalling

Ethylene is a phytohormone that plays a role in many plant development processes such as response to stresses, the ripening of fruit, abscission and senescence. Recently, Yoo *et al.* (2008) have proposed a CTR1-MKK9-MPK3/6 signalling cascade, which regulates gene transcription in ethylene signalling in *A. thaliana*. Upon treatment with 1-aminocyclopropane-1-carboxylic acid (ACC, the ethylene precursor) MKK9 relocates from the cytoplasm to the nucleus and activates MPK3/6. MPK3/6 phosphorylates and stabilises the nuclear transcription factor EIN3, which goes on to induce transcription of genes in ethylene signalling. It was previously shown that the ethylene receptor ETR1 can target the Raf-like protein kinase CTR1 (Kieber *et al.*, 1993) and that ethylene activates MPK6, and this

ethylene-dependent action of MPK6 requires ETR1, but not EIN2 (Ouaked *et al.*, 2003). In other species Raf-like protein kinases act as MAPKK activators, but as data suggest CTR1 is a negative regulator of ethylene signalling, it was proposed that ethylene signalling was involved in a cascade connecting ETR1-CTR1-MKK9-MPK3/6-EIN3, in which ethylene inactivates the negative regulator CTR1 in order to activate the positive MKK9-MPK3/6 cascade (Yoo *et al.*, 2008). Yoo *et al.* (2008) have also shown that there is a MKK9-MPK3/6-independent, EIN2-dependent signalling pathway involved in ethylene-dependent gene transcription.

More recently it has been suggested that the MKK9-MPK3/6 is involved in the biosynthesis of ethylene, but is not part of the ethylene-signalling pathway (Xu *et al.*, 2008). ACS6 has been described as the first substrate for a MAPK (Liu and Zhang, 2004; Joo *et al.*, 2008), which interacts with MPK6. MPK3/6 are thought to phosphorylate and stabilise ACS6, which prevents it from being degraded by the 26S proteasome. This results in activation of the ethylene signalling pathway and the production of ethylene. It is proposed this signals in a cascade involving MKK4/MKK5 and MPK3/MPK6 (Liu and Zhang, 2004). It has not been described how these two cascades function independently and use the same kinases and there is also still much debate as to whether the MPK9-MPK3/6 pathway acts in ethylene biosynthesis, an ethylene signalling pathway or both (for a review see Hahn and Harter, 2009).

1.3.1.3.2 The role of MAPKs in jasmonic acid signalling

Jasmonic acid (JA) is involved in biotic and abiotic stresses, SAR, growth inhibition, senescence, and leaf abscission (Balbi and Devoto, 2008). It has been proposed that MKK3 activation of MPK6 is involved in the negative regulation of JA-signalling and ATMYC2/JIN1 expression, a transcription factor that represses defence-related genes and is involved in JA cross-talk with ethylene (Takahashi *et al.*, 2007, Lorenzo *et al.*, 2004). It has also been shown that JA-signalling activates MPK1/MPK2 (Ortiz-Masia *et al.*, 2007). Together with other group C MAPKs, MPK7 and MPK14, these MAPKs have been shown to interact with or act downstream of MKK3 (Dóczi *et al.*, 2007). As MPK6 was shown not to directly interact with MKK3 it was proposed the activation of MPK6 by MKK3 might be downstream of the MKK3-MPK1/2/7/14 cascade.

MPK4 is thought to play a role in the hormone balance of SA and JA/ethylene by the regulation of EDS and PAD4 (Brodersen *et al.*, 2006) and MPK4 has been shown to interact with MEKK1 *in vitro* (Ichimura *et al.*, 1998). Qiu *et al.* (2008) have shown that MKK1/MKK2 are involved in SA and JA-dependent defence signalling, mediated by MKS1 activation by MPK4. Whether this represents a full MAPK cascade remains to be determined.

Systemin is a hormone involved in wound-response. In tomato, after wounding by herbivorous insects, systemin is detected by the receptor SR160. This signalling has been shown to involve activation of MPK1 and MPK2 (AtMPK6 orthologues), which is thought to be upstream of JA-signalling and wound-response gene expression (Kandoth *et al.*, 2007).

1.3.1.3.3 The role of MAPKs in auxin signalling

Auxin plays crucial roles in the regulation of many aspects of plant growth and development. MPK12 has been shown to be a negative regulator of auxin signalling (Lee *et al.*, 2009). MPK12 interacts with the MAPK phosphatase, IBR5, which confers reduced sensitivity to auxin and ABA in roots (Monroe-Augustus *et al.*, 2003). MPK12-deficient plants showed the same sensitivity to auxin in roots, resulting in an increase in auxin-responsive genes and auxin-hypersensitive root growth, but its sensitivity to ABA was normal. MKK7 has also been shown to negatively regulate polar auxin transport (Dai *et al.*, 2006b). Whether the two proteins are linked in a cascade is yet to be determined. In tobacco NPK1 (a MAPKKK) activates a MAPK cascade that results in the suppression of early auxin response gene transcription (Kovtun *et al.*, 1998).

1.3.1.4 MAPK signalling via reactive oxygen species

Reactive oxygen species (ROS) have been shown to act in the early response to biotic and abiotic stress responses and also in response to hormones. MAPKs are not only induced by ROS, but can also regulate ROS production.

It has been shown in *A. thaliana* that MPK3 and MPK6 are activated by H₂O₂-dependent activation of ANP1, a MAPKKK (Kovtun *et al.*, 2000). MKK4 and MKK5 are thought to initiate ROS activation and result in hypersensitive response-like cell death (Ren *et al.*, 2002), as overactive MKK4/MKK5 initiate in the increase of MPK3/6 activation and the increase of

H₂O₂, resulting in cell death. In addition, MKK4 has been shown to be involved in the H₂O₂-dependent activation of MPK6 (Doczi *et al.*, 2007).

NDP2, an NDP kinase thought to be involved in regulation of nucleotide triphosphates (NTPs), has shown to be induced by H₂O₂ and specifically interacts with MPK3 and MPK6 (Moon *et al.*, 2003). OXI1, a serine/threonine kinase, is induced by H₂O₂ and wounding, and OXI1 deficient plants are susceptible to pathogens and show reduced MPK3/MPK6 activation upon treatment with H₂O₂ and elicitors (Rentel *et al.*, 2004). Whether this represents a full cascade in ROS signalling remains to be determined.

A MEKK1-MPK4 pathway is also activated by H₂O₂ (Nakagami *et al.*, 2006). H₂O₂ has been shown to activate MEKK1 and in MEKK1-deficient plants H₂O₂-dependent activation of MPK4 is inhibited. In addition, there is MKK3-dependent activation of MPK7 in H₂O₂-induced signalling (Dóczi *et al.*, 2007). All group C MAPKs are activated by MKK3 (Dóczi *et al.*, 2007) and it has been shown that MPK1/MPK2 are activated by H₂O₂ (Ortiz-Masia *et al.*, 2007), but this pathway has yet to be fully investigated.

1.3.1.5 MAPK signalling in plant development

MAPKs have more recently been shown to play roles in plant development as well as in response to stresses, including roles in the cell cycle, senescence and abscission, and the development of the embryo, stomata and floral organs. These roles are discussed below.

1.3.1.5.1 The role of MAPKs in embryo development

YODA, a MAPKKK, was identified by Lukowitz *et al.*, (2004) and was shown to be required for partitioning extra-embryonic cell fates in *A. thaliana*. YODA acts as a molecular switch that promotes extra-embryonic cell fate in the basal lineage. YODA-deficient plants fail to develop a normal suspensor cell and often the embryo is trapped between the developing seed coat cell walls and is forced out of the seed coat. MPK6 also plays a role in embryo development and MPK6-deficient plants show the embryo protrusion phenotype seen in YODA-deficient lines (Bush and Krysan, 2007). This suggests that MPK6 acts downstream of YODA in embryo development. In addition, MPK3/MPK6-deficient lines have also been shown to be embryo lethal (Wang *et al.*, 2007). Previously, MPK3 and MPK6 have been shown to act redundantly in various signalling pathways (Mishra *et al.*, 2006), but as MPK3-deficient lines do not show the embryo protrusion phenotype it is proposed that it plays no role in embryo development. In addition to its role in embryo development, MPK6 has also been shown to be involved in anther and inflorescence development (Bush and Krysan, 2007).

1.3.1.5.2 The role of MAPKs in leaf senescence

Leaf senescence is a developmental process whereby leaves undergo an active degenerative phase that allows the redistribution of nutrients to new leaf growth and seed and fruit development and can be induced by a number of environmental cues. Leaf senescence involves changes in cell structure, gene expression and metabolism, which result in a programmed cell death (for a review see Lim *et al.*, 2007). *A. thaliana* MKK9 and MPK6-deficient lines have been shown to cause a delay in leaf senescence and over-expression of the

genes results in early leaf senescence (Zhou *et al.*, 2009). This suggests that MKK9 and MPK6 are involved in the regulation of leaf senescence.

1.3.1.5.3 The role of MAPKs in stomatal development

It has been shown that a MAPK signalling cascade is involved in the negative regulation of non-random "one cell spacing" stomatal patterning in *A. thaliana*. Initial experiments demonstrated that the MAPKKK, YODA, was required for the correct distribution of stomata (Bergmann *et al.*, 2004). Further evidence showed that YODA was part of a YODA-MKK4/MKK5-MPK3/MPK6 signalling cascade and phosphorylation by these MAPKs was essential for stomatal development (Wang *et al.*, 2007). More recently, it has been shown that the transcription factor SPEECHLESS is a substrate for MPK3/MPK6 (Lampard *et al.*, 2008). SPEECHLESS is needed for the formation of stomata and its phosphorylation by MPK3/MPK6 limits the patterning of stomata.

1.3.1.5.4 The role of MAPKs in the floral abscission

Abscission is a developmental process that results in the active shedding of non-functional or infected organs, such as leaves, petals and fruit (for a review see Lewis *et al.*, 2006). In floral abscission this involves the hydrolysis of the middle lamella of the abscission zone, an anatomically specialized cell layer, by cell wall modifying and hydrolysing enzymes. Evidence has shown that a MAPK signalling cascade, involving the MAPKKs MKK4/5 and the MAPKs MPK3/6, can regulate floral organ abscission in *A. thaliana* (Cho *et al.*, 2008). This MAPK signalling cascade is thought to be downstream of ligand-receptor interaction, in

which IDA, a predicted small-secreted protein, acts as a ligand for the receptor-like kinases HAE and HSL2, which then initiate the MAPK signalling cascade, resulting in cell separation during floral abscission.

1.3.1.5.5 The role of MAPKs in plant cell division and microtubule organisation

A few MAPKs have been shown to play a role in the cell cycle and microtubule organisation. During late cytokinesis there is the formation of a phragmoplast, a complex structure composed mainly of microtubules, which is required for the creation of a new cell wall, to form two daughter cells. In tobacco, the NPK1-MEK1-NTF6 cascade is involved in the lateral expansion of the cell plate that follows the phragmoplast at cytokinesis. NPK1 was identified as a MAPKKK that is cell cycle-dependent, and localises at the equatorial regions of the phragmoplast during cytokinesis (Nishihama *et al.*, 2001). NPK1 activation is regulated by kinesin-like proteins NACK1 and NACK2, which determine its activation and localisation at late M phase (Nishihama *et al.*, 2002). This activation has been shown to be upstream of MEK1 (a MAPKK) (Soyano *et al.*, 2003). MEK1 has been shown to interact with and phosphorylate NTF6 (a MAPK) and both are co-expressed at the cell plate during cytokinesis (Calderini *et al.*, 2001; Nishihama *et al.*, 2001). MAP65-1a, a microtubule-associated protein, is phosphorylated by NTF6 at the phragmoplast, which down-regulates its microtubule bundling activity and in turn increases destabilisation and turnover of microtubules at the phragmoplast, allowing progression of cytokinesis (Sasabe *et al.*, 2006).

In alfalfa MMK3 is likely to play a role in the regulation of the cell cycle. MMK3 was activated only in cells showing phragmoplast formation (Bögge *et al.*, 1999). It was also

shown that activation of MMK3 requires intact microtubules, but they are not required for the localisation of MKK3. It was proposed that MMK3 might be involved in the construction of the phragmoplast by regulating microtubule stability.

In *A. thaliana* a family of three MAKKK genes (ANP1/2/3) have been shown to play a role in the regulation of cytokinesis (Krysan *et al.*, 2002). A mutation in the NtMEK1 (tobacco) orthologue AtMKK6 (ANQ1) has been shown to affect cytokinesis (Soyano *et al.*, 2003) and Melikant *et al.* (2004) have provided evidence that ANP1/2/3, AtMKK6 and AtMPK13 are involved in the same MAPK cascade, although, to date, no function of this *A. thaliana* cascade has been described.

In *A. thaliana* the only T-D-Y MAPK with an assigned role is AtMPK18, which has been shown to mediate cortical microtubule function (Walia *et al.*, 2009). PHS1 is a MAPK-specific phosphatase and had previously been shown to play a role in microtubule organisation (Naoi and Hashimoto, 2004). Walia *et al.* (2009) have shown that AtMPK18 is a substrate for PHS1 and that MPK18-deficient seedlings show defects in microtubule functions and have hyper-stabilised microtubules.

1.3.1.5.6 The role of MAPKs in the regulation of the actin cytoskeleton

In alfalfa, SIMK has been shown to play a role in the formation of root hairs, by signalling from the actin cytoskeleton to the tip growth machinery (Samaj *et al.*, 2002). SIMK localises to the root hair tip and its activation requires vesicle trafficking and an intact actin cytoskeleton. Evidence suggests that SIMK is not only associated with the actin cytoskeleton, but changing actin dynamics directly affects its activity. To date it is not known how SIMK

interacts with actin, but Limmongkon *et al.* (2004) have shown the SIMK orthologue in tobacco, SIPK, can phosphorylate profilin. Profilin is an actin binding protein and regulates actin dynamics where it binds to monomeric actin preventing the polymerization of actin into filaments and also under certain circumstances promotes actin polymerization (for a review see McCurdy *et al.*, 2001). It was shown that SIPK (and NTF4), when activated by the MAPKK MEK2, can phosphorylate profilin *in vitro*, and that SIPK and profilin co-localise in the pollen cytosol (Limmongkon *et al.*, 2004). The MEK2-SIPK-profilin cascade is thought to play a role in the reorganisation of the actin cytoskeleton during pollen germination and growth. It is likely, as pollen and roots have been shown to grow by similar mechanisms of tip growth, that alfalfa SIMK functions by a similar mechanism.

1.3.1.6 Summary

Evidence suggests that certain MAPKs (such as AtMPK3, AtMPK4 and AtMPK6) play roles in a wide variety of biological processes. Although the functions of some other MAPKs have been described, many remain uncharacterised. It may be that certain plant MAPK orthologues no longer have any function. For example, AtMPK10 belongs to the same family as AtMPK3 and AtMPK6 which have been well characterised, but to date has no known function. In plants some MAPK paralogues show similar expression patterns (such as *PtMPK16-1* and *PtMPK16-2*, *PtMPK20-1* and *PtMPK20-2* from poplar), while others (*PtMPK9-1* and *PtMPK9-2*, *PtMPK3-2* and *PtMPK3-1*) show different patterns of expression suggesting they may have developed possible sub-functions. It may be that the specific localisation and function of certain MAPKs mean that it is not possible to easily study their function. This can be seen by AtMPK3 and AtMPK6, in which only AtMPK6 is thought to be involved in embryo

development, but function redundantly in other processes such as biotic stress response. At the MAPKK level, AtMKK3 can target AtMPK6 and AtMPK7, but this is under different environmental conditions (Dóczi *et al.*, 2007).

Future work should help unravel the complexity of MAPK signalling; both at the level of single signalling cascades and other levels. Microarray data and high throughput technologies are already helping in disentangling MAPK cascades and their downstream targets (Feilner *et al.*, 2005; Lee *et al.*, 2008a; Popescu *et al.*, 2009).

1.4 General aims and objectives

The aim of this project is to clone and characterise the gene (and protein) that encodes p56, the MAPK involved in the self-incompatibility signal transduction pathway in *Papaver rhoeas*. Due to the timing of p56 activation and the fact that PCD-related features require p56 activation, it is proposed that p56 may be involved in linking early events that inhibit pollen tube growth (such as actin and microtubule depolymerisation and p26.1 sPPase activity) and processes that actively terminate the pollen tube via PCD. It is thought that p56 may be involved in a so-called “commitment phase” between these events.

Previously cloning experiments have been carried out to identify the gene that encodes p56, but so far these have failed to identify a strong candidate gene. Candidates will be selected using a variety of methods including bioinformatic and proteomic analysis. Degenerate PCR will then be used to clone candidate MAPK genes. Once a suitable candidate is identified, a specific antibody will be raised against the predicted protein sequence of the candidate gene and used to confirm that this gene encodes p56, and to further characterise its role in SI. Various methods, including western blotting, immuno-precipitation and immuno-localisation will be utilised.

The use of reverse genetics is an important tool in understanding the role of known genes. Because poppy is not amenable to traditional transformation techniques, attempts will be made to use other species to try and determine the possible role of candidate MAPKs. *Arabidopsis thaliana* is a model plant species and a large number of T-DNA insertion

knockout lines are available for many genes. A number of MAPK knockout lines will be obtained and their phenotypes will be investigated.

CHAPTER 2

Methods and Materials

CHAPTER 2 - METHODS AND MATERIALS

2.1 Plant material

2.1.1 Plant cultivation

Arabidopsis thaliana: Seeds were sown in John Innes No. 1 potting compost, which were then covered with a thin layer of perlite to retain moisture. Seeds were grown at 15°C, with 16 hours white light per day, and watered twice daily by immersion.

Papaver rhoeas; Seeds of *Papaver rhoeas* L. (Shirley) of known pedigree were first allowed to germinate in humidified Petri dishes for ~2 days. Germinated seeds were then planted, three per pot, in John Innes No.1 potting compost. Seeds were then covered with a thin layer of vermiculite to retain moisture and kept in a greenhouse at 15°C. After growing to a height of around 5-10cm, plants were thinned to one per pot. At ~8 weeks plants were allowed to harden outside for ~4 weeks and were then transplanted into a field in rows with approximately 50cm between plants and approximately 90cm between rows.

2.1.2 Determination of *S*-genotype in *Papaver*

S-genotype was determined by pollinating each plant with pollen of known *S*-genotype. Once plants were in flower, two flowers, 1-2 days prior to anthesis were emasculated by removal of all anthers using forceps. Emasculated flowers were then covered with a cellophane bag wired at the base to prevent entrance of insect pollinators. Emasculated flowers were pollinated the

following day by application of pollen with a fine paintbrush directly onto the stigmatic rays. After pollination, cellophane bags were replaced over the flower and stigmas were harvested one day after pollination. The pollinated portion of the stigma was removed with a scalpel, placed in aniline blue and left overnight to allow the stigmas to soften. A sample of the stigma was then removed and placed on a microscope slide and viewed under a microscope using UV illumination. All families grown were two-class families and thus were pollinated with two classes of pollen, one to provide a fully incompatible pollination and one to provide half-compatible pollination. Those stigmas exhibiting fully incompatible pollination had easily identifiable callose in the pollen grains and few, if any, pollen tubes. Those exhibiting half-compatible pollinations had 50% reacting as above whilst the remainder has no callose in the grain and long pollen tubes with callose plugs at intervals along the length of the tube.

2.1.3 Production of seed in *Papaver*

Seed that would produce plants of a two-class family were produced following a similar method to that already described in 2.1.2. Emasculated flowers were pollinated with pollen of known *S*-genotype and left for approximately 6 weeks. After approximately 6 weeks seed was collected from seed pods and stored in paper bags at 4°C.

2.1.4 Collection of plant tissue

Material was collected from *Arabidopsis thaliana* (Col-0) or *Papaver rhoeas* (Shirley).

Arabidopsis: Leaf material was harvested from plants using a scalpel or by trapping the leaf in an Eppendorf tube with the cap and flange, depending upon the amount of material required.

Papaver: All tissues were harvested from plants grown in the field or from young plants in the greenhouse where appropriate, snap frozen in liquid nitrogen and immediately placed at -70°C for long-term storage. For pollen collection flowers at 1 day prior to anthesis were harvested approximately 15cm below the flower. The sepals and petals were removed and the remaining stems were placed in a cellophane bag and hung upside-down overnight. Pollen was released by vigorous shaking, and collected by tipping into gelatine capsules. Capsules were then dried over silica gel at room temperature before freezing at -20°C.

2.2 Pollen growth and treatment in *Papaver*

2.2.1 Pollen growth *in vitro*

Pollen was hydrated for at least 30 minutes in a moist chamber at 25°C. The shape of pollen grains was used to assess the state of hydration. When desiccated, pollen grains take an elliptical form, when hydrated pollen grains appear spherical (Franklin-Tong *et al.*, 1988). Following hydration, pollen was resuspended in 1ml liquid germination medium (GM) and then sown on to solid GM in 9cm plates, or 2ml on 14cm plates. Liquid GM comprised 0.01% (w/v) H₃BO₃, 0.01% (w/v) KNO₃, 0.01% (w/v) Mg(NO₃)₂·6H₂O, 0.036% (w/v) CaCl₂·2H₂O, 13.5% (w/v) sucrose. Solid GM was the same as liquid GM but supplemented with 1.0% (w/v) agarose. Pollen was grown for at least 45 minutes and assessed for percentage germination prior to experimentation.

2.2.2 Induction of SI with recombinant S-proteins

Pollen was hydrated and grown as described in 2.2.1. S-proteins were expressed and purified as described in Kakeda *et al.* (1998). SI was induced for the required time (generally 10 minutes) by adding S-proteins (final concentration 10µl/ml) to invoke a compatible or incompatible reaction as described in Snowman *et al.* (2002).

2.2.3 Calyculin A treatment of pollen

Pollen was hydrated and grown as described in 2.2.1. After growth, pollen was treated with a 0.25mM (final concentration) Calyculin A (Sigma) for 10 minutes.

2.3 Nucleic acid manipulations

2.3.1 Removal of RNase contamination from equipment

RNases were removed from equipment by standing for 16 hours in $1/1000$ diethyl pyrocarbonate (DEPC, Sigma) before rinsing in DEPC SDW and autoclaving. Glassware used for RNA preparation was double-baked prior to use.

2.3.2 Isolation of RNA

RNA was extracted using an 'RNeasy Plant Mini Kit' (Qiagen) following the 'RNeasy Mini Protocol for Isolation of Total RNA from Plant Cells and Tissues and Filamentous Fungi'.

Buffer RLT was used. For pollen RNA extraction, tissue was ground in a 5ml glass grinder with 450µl Buffer RLT, and then transferred to the QIAshredder (step 4). Other tissues were placed in a 1.5ml tube and broken open using a DEPC treated blue plastic pestle or using a pestle and mortar. The amount of RNase-free water used in the elution step was dependant upon the concentration of RNA needed, but generally 30µl. Finally, to check for the presence of RNA, 5µl of RNA was added to 5µl of RNA sample loading buffer (Sigma) and 10µl of SDW (both DEPC). This solution was placed at 65°C for 5 minutes then run on a 1% agarose gel.

2.3.2.1 Estimation of RNA concentration

RNA concentration was estimated by measuring absorbance of 200-fold diluted samples at OD260. Absorbance readings were converted to RNA concentrations given that an RNA solution of concentration 40µg/ml has absorbance (OD260) of 1.0.

2.3.3 DNase treatment of RNA

RNA (<500ng) was treated in following solution: 1.1µl 10X buffer, 0.9 µl RNasein (Promega), 1µl DNase I (Invitrogen), and made up to 11µl with DEPC water, and kept at RT for 15 minutes EDTA (2mM) was added and the solution and incubated at 65°C for 10 minutes An equal volume of phenol was added, the solution mixed, spun (13,000 rpm, 10 seconds), and the upper phase collected. An equal volume of chloroform was added, and after mixing and spinning, the upper phase was collected. RNA was precipitated by adding 2.5 volumes ethanol and 0.1 volumes NaAc and left at -20°C for at least 30 minutes The solution

was mixed thoroughly by inversion before centrifugation (13,000 rpm, 3 minutes), to pellet the RNA. The supernatant was removed by inversion of the tube and the pellet washed in 70% ethanol. The pellet was then vacuum-dried for 20 minutes and resuspended in 100µl RNase free water (Qiagen).

2.3.4 cDNA synthesis

cDNA was synthesised using 'Invitrogen™ SuperScript™ II Reverse Transcriptase' kit according to manufacturer's instructions. For total cDNA synthesis an oligo dT primer was used.

2.3.5 Isolation of DNA

For the isolation of genomic DNA a 'Nucleon PhytoPure Plant DNA Extraction Kit' (Amersham Biosciences) or the 'Sigma Plant Extract'n'Amp PCR' kit was used, following manufacturer's instructions.

2.3.5.1 Estimation of nucleic acid concentration

DNA concentration was estimated by measuring absorbance of 100-fold diluted samples at 260nm. Absorbance readings were converted to DNA concentrations given that a DNA solution of concentration 50µg/ml has absorbance (OD260) of 1.0. Alternatively, the concentration of nucleic acid samples was estimated by comparison with DNA of known concentration (Bioline HyperLadder I), following manufacturer's instructions.

2.4 Polymerase Chain Reaction (PCR)

2.4.1 Polymerase Chain Reaction (PCR) techniques

All PCR based reactions were performed in a Hybaid Omni-E, PCR sprint or Techne TC-412 cycler.

2.4.1.1 Composition of reactions

PCR was routinely carried out to amplify products from plasmid DNA, cDNA, or gDNA. '2x ReddyMix™ PCR Master Mix' (1.5mM MgCl₂) (Abgene) or 'REDTaq® ReadyMix™ PCR Reaction Mix' (Sigma) was used routinely to produce PCR products with an overhang. These were the polymerases of choice in all PCR reactions performed, unless otherwise stated. 'KOD Hot Start DNA Polymerase' (Novagen) was used to produce blunt ended PCR products. KOD polymerase has proof reading activity and therefore is less prone to errors in the amplification process. All reactions were composed following manufacturer's instructions.

2.4.1.2 PCR cycling conditions

The number of cycles used in a given reaction was dependent on the procedure being carried out but was routinely 30 cycles. For PCR reactions using ReddyMix (Abgene) or ReadyMix (Sigma) initial denaturation stages were carried out at 94°C for 2 minutes. This was followed by cycles (generally 30) of the following steps. Template denaturation stage was carried out at 94°C for 1 minute. Annealing was carried out for 1 minute and the temperature depended on

the melting temperature of the primers being used. Temperature was calculated according to the formula devised by Freier *et al.* (1986):

$$T_m = 64.9 + 0.41(\%C + \%G) - 600/n$$

where n = the length in bases of the primer in question. The length of time allowed for the annealing stage was 1 minute. The extension phase of amplification was carried out at 72°C, the optimum temperature for the activity of Taq polymerase derived from the thermophilic bacteria *Thermus aquaticus*. Time allowed for completion of the extension phase was calculated at 1 minute per kb of DNA to be amplified. A final extension phase of 5 minutes at 72°C was used to ensure completion of amplification.

For PCR reactions using KOD Hot Start polymerase an initial template melting stage was carried out at 95°C for 2 minutes. 30 cycles of the following were then carried out. Template denaturation stage was carried out at 95°C for 20 seconds, followed by an annealing stage of 10 seconds (temperature was dependant on the primers used), and finally an extension phase at 70°C allowing 20 seconds per kb of DNA to be amplified.

2.4.2 Primer design

For amplification of insert DNA from plasmid vectors, common sequencing primers were generally used (M13 forward, M13 reverse and T7 promoter). For PCR amplification primers were designed and supplied by MWG Biotech. All primer sequences used are shown below. All primers were diluted to a working concentration of 10µM.

2.4.2.1 Primers

Name	Sequence
Lba1	5'-TGGTTCACGTAGTGGGCCATCG-3'
M13F-20	5'-GTAAAACGACGGCCAG-3'
M13R	5'-CAGGAAACAGCTATGACC-3'
3'RACE17AP	5'-GACTCGAGTCGACATCGATTTTTTTTTTTTTTTTTTTT-3'
3'RACEUAP	5'-GACTCGAGTCGACATCGA-3'
5'RACE17AP	5'-GGCCACGCGTCGACTAGTACGGGNNGGGNNGGGNNG-3'
5'RACEUAP	5'-GGCCACGCGTCGACTAGTAC-3'

For other primers see appendix ii.i.

2.4.3 RT-PCR

RT-PCR was carried out using a 'QIAGEN OneStep RT-PCR' kit, following manufacturer's instructions.

2.4.4 3'RACE

Amplification was carried out on cDNA using a 3'RACE17AP and 5' gene specific primer. The product was PCR purified and then re-amplified with a 3'RACE17UAP primer and nested gene specific 5' primer.

2.4.5 5'RACE

cDNA was synthesised as described in cDNA synthesis (2.3.4) but a primer specific to the 3' end of the gene of interest was used rather than the oligo dT primer. This change meant that only cDNA from the gene of interest was synthesised rather than from all transcripts. The cDNA was then cleaned-up using a 'QIAquick PCR Purification Kit' (Qiagen). A tailing reaction was then performed as follows to add a poly-C tail at the 5' end of the gene of interest. A solution containing 10µl cDNA (after clean up using Qiagen columns), 2.5µl dCTP (2mM), 5µl 5x tailing buffer (Roche), and 6.5µl H₂O was incubated at 94°C for 2 minutes and then cooled on ice for 1 minute. Terminal transferase (1µl (Roche)) was added to the solution and incubated at 37°C for 10 minutes, followed by 10 minutes at 65°C. PCR amplification was then carried out with a 5'RACE Abridged primer and a second gene specific 3' primer. This amplification product was PCR purified and then re-amplified with a 5'RACE unabridged and third nested gene specific 3' primer.

2.4.6 PCR purification

PCR purification of PCR amplification products was carried out using a 'QIAquick PCR Purification Kit' (Qiagen) following manufacturer's instructions. Products were eluted in 30µl H₂O.

2.5 Agarose gel electrophoresis of DNA and RNA

2.5.1 Agarose gel electrophoresis

Visualisation of nucleic acid samples was accomplished by electrophoresis in 1x DNA/RNA loading buffer on agarose gels. An estimation of size was achieved by electrophoresis of an aliquot of 1kb ladder (Invitrogen). Agarose gels were constructed, depending on the size of nucleic acid of interest, between 0.8% (w/v) for a large molecular weight to 3% (w/v) for visualisation nucleic acids <300bp. Agarose was made up in 0.5x TBE and heated in a microwave until all agarose had dissolved. To allow visualisation of nucleic acids, 0.5µg/ml ethidium bromide was added to molten agarose prior to setting the gel. 0.5x TBE was used as a buffer for resolving the gel. Gels were poured and electrophoresed using Hybaid or Biorad electrophoresis kits. Images of gels were captured using a FluorS Multi-imager and analysed using Quantity One[®] software (Biorad) if necessary. The method described above can also be used for visualising RNA.

2.5.1.1 DNA ladders

For estimation of DNA fragments on agarose gels a 1kb DNA ladder (Invitrogen) was used.

2.5.2 Extraction of digested or amplified DNA from agarose gels

Bands were excised from the gel following minimal UV exposure to reduce the incidence of single-stranded nicking. Gel extraction was then carried out using 'QIAquick Gel Extraction Kit' (Qiagen) and following manufacturer's instruction. For elution 30µl of H₂O was used.

2.6 Gene cloning

2.6.1 Ligation

2.6.1.1 Ligation of DNA fragments into vector DNA

Ligation reactions varied according to the vector being used and the concentration of DNA fragments to be cloned. Ligation reactions were carried out according to manufacturer's instructions. All ligations were left overnight at 14°C.

2.6.1.2 Cloning vectors

pZErO™-2 (Invitrogen)

A 3.3kb plasmid that has multiple cloning sites within the lacZ gene for blue/white selection. Downstream of the cloning site is a ccdB gene encoding a lethal protein that acts by inhibiting the action of topoisomerase II. Cloning into the multiple cloning sites (MCS) disrupts ccdB expression so only recombinants can grow. The plasmid also contains the kanamycin resistance gene and priming sites for sequencing.

pDrive (Qiagen)

A 3.85kb plasmid with a number of useful features designed to facilitate analysis of cloned PCR products. These include a large number of unique restriction enzyme recognition sites, universal sequencing primer sites, and promoters for in vitro transcription. In addition, the vector allows both ampicillin and kanamycin selection as well as blue/white screening of recombinant colonies.

pET21-b (Novagen)

A 5.4kb plasmid with a multiple cloning site downstream of a T7 promoter, under the regulation of the Lac operator (*lacI*). Immediately downstream of the MCS are six repeats of the CAC codon, which adds hexahistidine tag to a protein translated from the expressed insert. Also includes ampicillin resistance.

2.6.2 Transformation of *E. coli* cells with plasmid DNA

2.6.2.1 Transformation of *E. coli* by heat-shock

Ligation reaction (4µl) was added to a 50µl aliquot of competent cells, gently mixed and incubated on ice for 30 minutes. The mixture was transferred to a water bath at 42°C for 45 seconds prior to the addition of 200µl LBB and subsequent incubation at 37°C for 45 minutes. The cells were pipetted onto an 8cm LB plate with appropriate selective agents and grown overnight at 37°C.

2.6.2.2 Bacterial strains

E. coli DH5 α (Invitrogen): *supE44*, Δ *lacU169* (ϕ 80*lacZ* Δ M15), *hsdR17*, *recA1*, *endA1*, *gyrA96*, *thi-1*, *relA1*

E. coli BL21 (Invitrogen): F- *ompT hsdSB*(rB-mB-) *gal dcm araB::T7RNAP-tetA*

E. coli JM109 (Promega): *endA1*, *recA1*, *gyrA96*, *thi*, *hsdR17* (r_k^- , m_k^+), *relA1*, *supE44*, Δ (*lac-proAB*), [F' *traD36, proAB, laqIqZ* Δ M15].

2.6.2.3 Preparation of competent cells

A 5ml aliquot of LB medium was inoculated with a single, fresh colony of *E. coli* DH5 α and grown at 37°C for 16 hours. 200 μ l of this culture was added to 100ml of fresh LB medium in a 1 litre conical flask and grown for a further 2.5 hours at 37°C. Optical density of the culture was taken OD₅₅₀ (optimum required 0.35-0.45). The culture was chilled on ice for 5 minutes and then centrifuged at 1300 g for 5 minutes at 4°C. The supernatant was discarded and the cells were resuspended in 40ml TfbI (30mM potassium acetate, 10mM rubidium chloride, 10mM calcium chloride, 50mM manganese chloride, 15% (v/v) glycerol, pH5.8). Cells were then left on ice for 3 hours and then centrifuged once more at 1300 g for 5 minutes at 4°C. Once again the supernatant was discarded. Following this the cells were resuspended in 4ml TfbII (10mM MOPS, 75mM calcium chloride, 10mM rubidium chloride, 15% (v/v) glycerol, pH6.5) and left on ice for 16 hours in a refrigerator. The cells were then pipetted into microfuge tubes and snap frozen in liquid nitrogen. Cells were stored at -70°C until used.

For JM109 cells, a 5ml aliquot of LB medium was inoculated with a single, fresh colony of *E.coli* JM109 and grown at 37°C for 16 hours. 400µl of this culture was added to 20ml of fresh LB medium in a 250ml conical flask and grown for a further 2 hours at 37°C. Optical density of the culture was taken OD550 (optimum required 0.3-0.5). The culture was chilled on ice for 5 minutes and then centrifuged at 1300 g for 5 minutes at 4°C. The supernatant was discarded and the cells were resuspended in 4ml 10mM NaCl then centrifuged at 1300 g for 5 minutes at 4°C. The supernatant was removed and the cells were gently resuspended in 4ml 100mM CaCl₂ and incubated on ice for 20 minutes then centrifuged at 1300 g for 5mins at 4°C. The supernatant was removed and the cells were gently resuspended in 1ml 100mM CaCl₂ and aliquoted into Eppendorf tubes (20µl each).

2.6.2.4 Growth media

All media was prepared in distilled water and sterilised at 15 psi at 121°C for 20 minutes. LB medium: 10g l⁻¹ bacto-tryptone, 5g l⁻¹ bacto-yeast extract, 10g l⁻¹ NaCl. LB agar: 10g l⁻¹ bacto-tryptone, 5g l⁻¹ bacto-yeast extract, 10g l⁻¹ NaCl, 15g l⁻¹ bacto-agar.

2.6.2.5 Selective media

Antibiotic resistance was selected for by the addition of kanamycin (50µg/ml) or ampicillin (50µg/ml). For blue/white selection, using the vector pDrive, 40mg/ml 5-bromo-4-chloro-3-indolyl-β-D-galactosidase (X-gal) 40µl was added to plates.

2.6.2.6 Growth conditions

Liquid cultures were grown for ~16 hours at 37°C on a rotary shaker at ~200 rpm. Agar plates were grown inverted for ~16 hours at 37°C. Inoculations of liquid culture and agar plates were carried out under aseptic conditions.

2.6.3 Analysis of positive colonies

2.6.3.1 Preparation of plasmid DNA from cultures (Mini prep)

Amplification of some cloned fragments was achieved using a boil prep method. 1ml of cells from an overnight culture was centrifuged at full speed for 30 seconds. The supernatant was removed and cells resuspended by thoroughly vortexing with 100µl of STET buffer. 10µl of chilled 10mg/ml lysozyme was added, mixed, placed in a boiling bath for 45 seconds, and then immediately centrifuged at top speed for 10 minutes. The viscous white pellet that formed was removed with a pipette tip, and then 10µl sodium acetate (NaOAc) and 500µl ethanol (100%, -20°C) were added. The sample was then placed at -20°C to precipitate the DNA. The mixture was centrifuged at top speed for 10 minutes to recover the nucleic acids. The ethanol was removed and the DNA was washed by addition of 500µl of 70% ethanol, vortexing, and centrifugation (13,000 rpm, 2 minutes). The ethanol was then removed with a pipette and the DNA vacuum dried. Finally the nucleic acids were resuspended in SDW, the amount depending upon the concentration required (generally 100µl was added).

2.6.3.2 Single colony PCR

For some applications DNA fragments were amplified directly from bacterial colonies. Colonies were brushed with the end of a sterile pipette tip and the end of the tip briefly placed in the reaction mix. Cycles were then programmed dependent on the fragment to be amplified as described above.

2.6.3.3 Digestion of DNA with restriction enzymes

Restriction enzymes were obtained from either Invitrogen or New England Biolabs. Digests were carried out in appropriate buffers supplied with the enzymes, and following manufacturer's instructions. Plasmid DNA was digested at 37°C for approximately 2 hours. Unless otherwise stated restriction enzymes were removed by heat denaturation or phenol/chloroform extraction.

2.7 DNA sequencing

2.7.1 Preparation of plasmid DNA for sequencing

DNA at a suitable level of purity for sequencing and cloning was produced using a silica column method (Wizard Plus SV (Promega)), following manufacturer's instructions.

2.7.2 DNA Sequencing

The DNA template and primer is supplied to The Functional Genomics Laboratory as an aqueous 10 μ l aliquot:

200-600ng	Plasmid DNA template
4 μ l	Primer (0.8 μ mol μ l ⁻¹)
x μ l	SDW (to 10 μ l total)

Sequencing reagents are added robotically by the Roboseq 4204S (MWG Biotech), before undergoing thermal cycling in the PrimusHT 96-well plate thermal cycler (MWG Biotech).

Thermal Profile:

Initial heating	96°C for 10 seconds	1 cycle
Sequencing*	96°C for 10 seconds	
	50°C for 5 seconds	
	60°C for 4 minutes	25 cycles
Final stage	35°C for 30 minutes	1 cycle
Hold	4°C	

*Alteration between the temperatures is done by ramping at 1°C/s.

The residual sequencing is then removed using a silica column method (Edge BioSystem). DNA is eluted in Hi-diformaide (Applied Biosystems) and loaded onto the AB13700. Any

manual steps are carried out by the members of The Functional Genomics Laboratory (The University of Birmingham).

2.7.3 Sequence analysis and homology searching

DNA sequences were analysed using Chromas software (Technelysium Pty Ltd). Homology searches were undertaken using the website provided by the National Centre for Biotechnology Information. Searches utilized the Entrez and BLAST (Altschul *et al.*, 1997) functions of the site. DNA and amino acid sequence alignments were made using ClustalW 1.7 available via the Internet (<http://www.ebi.ac.uk/Tools/clustalw2/index.html>)

2.8 Protein manipulations

2.8.1 Protein extraction

2.8.1.1 Bacterial protein expression and extraction

E. coli protein extracts were made for the analysis of recombinant protein. A 25ml liquid culture of recombinant *E. coli* was incubated at 37°C overnight in the presence of the appropriate selection. The culture was then diluted 1:10 with L-broth (5ml overnight culture added to 45ml L-broth) in two separate flasks. The cultures were allowed to grow further for between 1 and 4 hours. After this time, one of the cultures was supplemented with between 0.5mM and 1.0mM isopropylthio- β -D-galactosidase (IPTG) (Sigma). Both cultures were then incubated for a further 1-4 hours at 37°C to allow expression of the recombinant protein.

Culture was then transferred to a falcon tube and centrifuged at 3,000 g for 10 minutes. The supernatant was discarded and the cell pellet resuspended in either 500µl (varied according to size of pellet) Bugbuster (Novagen) containing benzonase (Novagen) at 1µl/ml or 1.5ml lysis buffer (50mM Tris, 300mM NaCl (pH 8)) with 1.0mM (final concentration) lysozyme (fresh stock). Cells were incubated on a rotor at either room temperature for 20 minutes (Bugbuster) or 30 minutes on ice (NaCl buffer), and then sonicated on ice (6 times for 5 seconds at 10 microns), with 30 seconds rest between each pulse to allow for cooling. Cells were centrifuged (13,000 rpm, 10 minutes) at 4°C. The supernatant (soluble fraction) was transferred to a fresh tube, and the pellet (insoluble fraction) was resuspended in 100µl NaCl buffer. Protein loading dye (5x) was added to each sample before being analysed by SDS-PAGE. The pellet represents membrane proteins, and the supernatant represents soluble proteins.

2.8.1.2 Pollen protein extraction

30µg pollen was hydrated and germinated (and/or treated) as described in 2.2.1. Pollen was collected from plates in 15ml Falcon tubes by pouring off the mixture of pollen and liquid GM. An additional 5ml liquid GM was added to each plate and collected in order to collect the maximum amount of pollen. If a pipette was required for collection, cut blue tips (1ml) were used in order to prevent breaking the tubes. Pollen was centrifuged (1,000 rpm, 5 minutes) and the supernatant removed, leaving a residual of ~500µl above the pollen pellet. To the pollen, 500µl 2x IP buffer was added (to make a final 1X concentration), the mixture pipetted up and down and transferred to a pre-cooled 3ml glass grinder. Pollen was ground for at least 70 strokes and then checked under the microscope to check that a majority of pollen

grains/tubes were disrupted. Ground pollen was then transferred to a 1.5ml microfuge tube (on ice), and sonicated on ice (6 times for 5 seconds at 10 microns), with 30 seconds rest between each pulse to allow for cooling and then centrifuged (13,000 rpm, 10 minutes, 4°C). The pellet (membrane enriched fraction) contains the pollen cell wall, plasma membrane and microsomes. The supernatant (soluble fraction) contains soluble proteins from the pollen.

2.8.1.3 Leaf protein extraction

Leaf proteins were extracted by grinding pollen with a pestle and mortar in the presence of liquid nitrogen. The material was transferred to an Eppendorf tube and 500µl 2x IP buffer was added (to make a final 1X concentration). The sample was vortexed and then treated as described in 2.8.1.3 from the sonication step.

2.8.1.4 Estimation of protein concentration

Protein concentration was estimated using the Biorad assay according to the manufacturer's instructions. The protein assay reagent (which contains Coomassie Brilliant Blue G-250) was added to diluted protein samples and the absorbance was measured at 595nm using a spectrophotometer. BSA (5µg/µl) was used as a standard.

2.8.2 Protein purification methods

2.8.2.1 Bacteria: isolation of His-tagged proteins using Ni-NTA resin

Proteins were isolated as described in 2.8.1.1 using the NaCl buffer. A small aliquot of extract was transferred to a separate tube for SDS-PAGE analysis: sample 'before binding'. 1ml Ni-NTA slurry (Qiagen) was added per 4.0ml of lysate and incubated on a rotor for 60 minutes at room temperature to allow binding of the His-tag to the resin. Cells were centrifuged (13,000 rpm, 2 minutes) and the supernatant discarded. A small aliquot of supernatant was saved for SDS-PAGE analysis for a sample 'after binding'. The resin was washed by addition of 1ml wash buffer (50mM TRIS, 300mM NaCl (pH8)) placing on a rotor at 4°C for 15 minutes and centrifuging at 13,000 rpm for 2 minutes. The supernatant was removed and kept for analysis. The wash step was repeated with increasing volumes of imidazole (20mM, 50mM, 100mM, 150mM, 200mM, 250mM) in the wash buffer to elute the proteins from the beads. Washes were analysed by SDS-PAGE to determine what concentration of imidazole eluted the protein of interest.

2.8.2.2 Removal of small proteins from samples

Small proteins (<10kDa) were removed from samples using Amicon[®] Ultra-4 Centrifugal Filter Units (Millipore). Samples were added to the column and spun to remove the small proteins. Samples were washed by adding the relevant buffer and spinning. The final sample was removed from the unit and transferred to Eppendorf tubes.

2.8.2.3 Removal of salts from protein samples

Salts were removed from samples using a PD-10 Desalting column (Amersham Biosciences) following manufacturer's instructions.

2.8.2.4 Phosphoprotein purification

Phosphoprotein purification from samples was achieved using a PhosphoProtein Purification Kit (QIAGEN) and following manufacturer's instructions.

2.9 Protein analysis methods

2.9.1 SDS-Polyacrylamide gel electrophoresis

Proteins were analysed using the Biorad self-assembly kits. Gels were cast as follows:

The resolving gel is cast first and the stacking gel is cast on top of the resolving gel.

12% resolving gel:

3.3ml SDW

4.0ml 30% Protogel (37.5 acrylamide:1 methylene bisacrylamide)

2.5ml resolving buffer (1.5M Tris, pH8.8)

100µl 10% (w/v) sodium dodecyl sulphate (SDS)

100µl 10% (w/v) ammonium per sulphate (APS)

4µl N,N,N',N'-tetramethylethylenediamine (TEMED) (Sigma)

15% resolving gel:

2.3ml SDW

5.0ml 30% Protogel (37.5 acrylamide:1 methylene bisacrylamide)

2.5ml resolving buffer (1.5M Tris, pH8.8)

100µl 10% (w/v) SDS

100µl 10% (w/v) APS

4µl TEMED (Sigma)

18% resolving gel:

1.3ml SDW

6.0ml 30% Protogel (37.5 acrylamide:1 methylene bisacrylamide)

2.5ml resolving buffer (1.5M Tris, pH8.8)

100µl 10% (w/v) SDS

100µl 10% (w/v) APS

4µl TEMED (Sigma)

N.B APS and TEMED are added immediately prior to pouring.

The resolving gel was covered (before setting) with butanol to level the top of the gel. Once polymerisation has taken place and the gel was set the butanol was washed off the gel with SDW.

Stacking gel:

3.4ml SDW

0.83ml 30% Protogel (37.5 acrylamide:1 methylene bisacrylamide)

0.63ml stacking buffer (1.0M Tris, pH6.6)

50µl 10% (w/v) SDS

50µl 10% (w/v) APS

5µl TEMED (Sigma)

N.B APS and TEMED are added immediately prior to pouring.

A medium size toothed comb is inserted before polymerisation of the stacking gel to form the wells. Following the polymerisation, the comb is removed, the wells rinsed with SDW and the kit assembled in to the electrophoresis apparatus. Proteins to be loaded were mixed with 5x protein loading buffer, boiled for 5 minutes and centrifuged for 5 minutes at 13,000 rpm prior to loading. Gels were run in 1x reservoir buffer (25mM Tris, 192mM glycine, 0.1% (w/v) SDS, pH8.3) according to the manufacturer's instructions.

2.9.1.1 Ladders

SeeBlue[®] Plus2 Pre-Stained Standard (Invitrogen)

PageRuler[™] Plus Prestained Protein Ladder (Fermentas)

2.9.2 SDS-PAGE gel analysis

2.9.2.1 Coomassie staining

Gels were stained for between 1 hour and 20 hours at room temperature in Coomassie stain (0.1% Coomassie Blue R-250, 45% (v/v) SDW, 45% (v/v) methanol, 10% glacial acetic acid) and de-stained for ~2 hours in de-stain solution (30% (v/v) methanol, 10% (v/v) glacial acetic acid). Gels were washed in SDW and preserved between cellophane sheets.

2.9.2.2 Western blotting

2.9.2.2.1 Protein transfer

After the proteins had been resolved by SDS-PAGE the stacking gel was removed. The gel was then transferred onto two sheets of Whatman paper soaked in 1x protein transfer buffer and cut to size. A nylon membrane (Hybaid-C extra (Amersham)) was cut to size, soaked in protein transfer buffer and laid over the gel and a glass rod used to remove any air bubbles. Two more sheets of Whatman paper were soaked in protein transfer buffer and laid on top of the membrane. The layered arrangement was then sandwiched between two electro-blotting pads (Biorad). This was then inserted into the electro-blotting tank (Biorad), which was filled with 1x protein transfer buffer. An ice block was also placed in the tank to prevent the solution overheating. Biorad power packs were used to blot the gel at 400mA for 1.5 hours. Following transfer, the nylon membrane was removed and stored in 1x TBS at 4°C.

2.9.2.2.2 Ponceau S staining

This is a rapid and reversible staining method for locating protein bands on western blots. Ponceau S Staining Solution (0.1% (w/v) Ponceau S in 5% (v/v) acetic acid) was incubated with the filter for ~30 seconds and then removed. After detection the stain was removed by a number of washes in 1x TBS.

2.9.3 Antibody probing

The blot was incubated with primary antibodies, diluted at varying concentrations depending on the antibody being used, in blocking solution (1xTBS, 5% milk) for 2 hours at room temperature or 14°C overnight. Following the initial probing the blot was washed 3x for 10 minutes in blocking solution and then incubated with the secondary antibody in blocking solution for 1 hour. The blot was then washed 1x for 10 minutes in blocking solution and 3x for 10 minutes in 1x TBS.

2.9.3.1 Primary antibodies

Phospho-p44/42 MAPK (Erk1/2) (Thr202/Tyr204) (D13.14.4E) Rabbit mAb (4370P; New England Biolabs). Titre: 1:2000.

Anti-PrMAPK9B rabbit antibody (Biogenes). Titre: 1:1,000.

Anti-AtMPK3 antibody produced in rabbit (M8318; Sigma). Titre: 1:1000.

2.9.3.2 Secondary antibodies

Anti-Mouse IgG (Fab specific)–Alkaline Phosphatase antibody produced in goat (Sigma).

Titre: 1:5000.

Anti-Rabbit IgG (whole molecule)–Alkaline Phosphatase antibody produced in goat (Sigma).

Titre: 1:5000.

Peroxidase-conjugated IgG Fraction Monoclonal Mouse Anti-Rabbit IgG, Light Chain Specific Antibody (Jackson ImmunoResearch). Titre 1:10,000.

Anti-Rabbit IgG (whole molecule)–Peroxidase antibody produced in goat (Sigma). Titre: 1:5000.

2.9.4 Antibody detection methods

2.9.4.1 Enhanced chemiluminescence (ECL) detection

ECL western blotting reagents (Amersham) or homemade solutions (Solution 1: 100 mM glycine (pH10 with NaOH), 0.4 mM luminol (Sigma) and 8mM 4-iodophenol (Aldridge); Solution 2: 0.12 % (w/w) hydrogen peroxide in water) were used to detect the secondary antibody. Reagents 1 and 2 were mixed 1:1 and poured over the blot. Excess reagents were removed and the blot was wrapped in cling film. Blots were analysed using an Agfa Curix 60 xograph.

2.9.4.2 Alkaline phosphatase detection

NBT (66 μ l) (NBT, 70% (v/v) DMF) and 33 μ l BCIP (BCIP, 100% (v/v) DMF) was added to 9.9ml alkaline phosphatase detection buffer (100mM NaCl, 5mM MgCl₂, 100mM Tris, pH9.5). The solution was poured over the blot and a colour change observed where the secondary antibody was present.

2.9.5 Membrane stripping

To strip antibodies from membranes, the membrane was washed in 100ml 0.05M NaPhosphate (pH6.5), 10M Urea and 0.1M B-mercaptoethanol for 30 minutes at 60°C. The membrane was then thoroughly washed three times in 400ml 1x TBS for 10 minutes on a shaker.

2.10 Antibody purification

2.10.1 Antibody clean-up using Immobilised *E. coli* lysate kit

The removal of contaminating *E. coli* antibodies from their primary antibody preparations was accomplished by applying primary antibody preparations onto a column containing immobilised bacterial proteins (Immobilised *E. coli* lysate kit, Pierce, Rockford). After the Immobilised *E. coli* Lysate column was brought to room temperature and the storage solution removed, the column was equilibrated with 10ml TBS buffer (BupHTM Tris buffered saline dissolved in 500ml distilled water). Eight microfuge tubes were prepared, the column placed

above the first tube and 1ml of sample (crude antibody) added to the column. Once the entire sample had entered the gel, an extra 100µl TBS buffer was added, and the exudates collected. Additional 1ml fractions of TBS were added to the column, and the column moved to the next tube with each additional fraction added. Each fraction was diluted 1:100 in TBS and the Bioread assay used to estimate the protein concentration. The fractions with the highest protein concentration were pooled. Following protein separation, the column was washed with at least 10ml of Regeneration Buffer, followed by 10ml of TBS containing 0.02% sodium azide.

2.10.2 PinPoint™ purification of the anti-PrMPK9-1 antibody

PinPoint™ purification of the anti-PrMPK9-1 antibody was carried out using the PinPoint™ Xa Protein Purification System (Promega) following manufacturer's instructions. In order to irreversibly bind the recombinant protein to resin TetraLink™ Tetrameric Avidin Resin (Promega) was used in place of the SoftLink™ Resin. To make the column Disposable Plastic Columns (Pierce) were constructed using manufacturer's instructions and 1ml of TetraLink™ Tetrameric Avidin Resin was used.

2.10.2.1 Preparation of TetraLink™ Tetrameric Avidin Resin

TetraLink™ Tetrameric Avidin Resin (Promega) was prepared by washing in 1ml 1xPBS (+1mM PMSF), which was allowed to settle and the supernatant was removed. This was repeated five times, to leave 1ml resin.

2.10.2.2 Columns

Columns were constructed using Disposable Plastic Columns (Pierce) following manufacturer's instructions.

2.10.2.3 Affinity purification of anti-PrMPK9-1 antibody

The resin, in the (what) column, was washed with 10ml 1x PBS (+1mM PMSF). 5ml of antiserum was passed over the column in 1ml aliquots, and each aliquot was passed over the column 4 times. The resin was then washed with 10ml 1x PBS (+1mM PMSF). The antiserum was eluted from the resin in 500µl aliquots of 100mM citric acid (pH3), into 1.5ml Eppendorf tubes containing 200µl 2M TRIS-HCl (pH8). The resin was washed with at least 8ml 1x PBS (+1mM PMSF) containing 0.02% sodium azide, and the column was stored, in this buffer, at 4°C.

2.11 Immuno-precipitation

2.11.1 Immuno-precipitation using protein A Sepharose

For immuno-precipitation using protein A Sepharose, Protein A Sepharose CL-4B (GE Healthcare) beads were used. The protein A Sepharose was prepared according to manufacturer's instructions. Protein samples were incubated with 25µl antibody at 4°C for 3 hours, on a rotor. 50ul of the Protein A Sepharose slurry (25µl beads) was added to protein/antibody mixture, and incubated for 1.5-2 hours at 4°C on a rotor. To remove

unbound protein the sample was spun at 3,000 rcm at 4°C for 1 minute and the supernatant removed. The sample was washed by adding 500µl relevant extraction buffer and spinning at 3,000 rcm at 4°C for 1 minute and the supernatant was removed. 50-150µl 1x FSB was added to the beads. The beads were boiled to remove proteins, spun to separate the beads and separated on an SDS-PAGE gel for analysis.

2.11.2 Immuno-precipitation of ATP labelled

The required amount of protein was incubated at 30°C for 30 seconds. 0.5µl of ³²P-gammaATP (4000 Ci/mmol) check the conc (PerkinElmer) was added, and the sample was incubated for 10-15 minutes at 30°C. 300µl of 1x IP buffer was added to the sample. Immuno-precipitation was then carried out as described above.

2.11.2.1 Visualisation of ATP labelling

SDS-PAGE gels were washed in destain (40% methanol, 10% HAc) for 40 minutes on a shaker. The gels were then dried onto Whatman paper in a vacuum dryer for 1 hour 30 minutes at 80°C. Gels were then exposed to either film or a phosphor-screen. Signal on the phosphorscreen were visualised on a FX imager using Quantity One[®] software (Biorad).

2.11.3 Immuno-precipitation with 9-1 column

2.11.3.1 Biotinylation of anti-PrMPK9-1 antibody

For biotin labelling the EZ-Link[®] Sulfo-NHS-LC-Biotinylation Kit (Pierce) was used, following manufacturer's instructions. For biotin incorporation the Cuvette Format was used. <http://www.piercenet.com/aba/habacalc.cfm>

2.11.3.2 Binding of biotinylated PrMPK9-1 to TetraLink[™] Tetrameric Avidin Resin

1ml of resin was added to the biotinylated anti-PrMPK9-1 (2.11.3.1), made up to 5ml with 1xPBS (+1mM PMSF), and incubated at 4°C overnight. This resin, with bound antibody, was spun (7,000 rpm, 1 minute) and the supernatant was removed. The resin was washed 3x with 1ml 1xPBS (+1mM PMSF). The PrMPK9-1-avidin resin was stored in 1ml 1xPBS (+1mM PMSF) and 0.02% sodium azide.

2.11.3.3 Immuno-precipitation of CalA extracts

For immuno-precipitation, 100µl PrMPK9-1-avidin resin was added to pollen extracts, and made to a final volume of 1ml with 1xIP buffer. This was incubated overnight at 4°C. The resin was washed for 2 minutes with 500µl 1xIP buffer, spun (7,000 rpm, 1 minute), and the supernatant removed. This step was repeated twice. The resin was then incubated for 5 min. with 100µl 100mM citric acid (pH3) to elute the proteins. The resin was spun (7,000 rpm, 1

minute) at the supernatant, containing eluted proteins was collected into 40µl 2M TRIS (pH8).

2.12 Immunolocalisation

Immuno-localisation was carried out as described in Poulter *et al.*, 2008, but using the PinPoint purified anti-PrMPK9-1 antibody as the primary antibody. For detection of the anti-PrMPK9-1 antibody an anti-rabbit fluorescein isothiocyanate antibody was used.

2.13 Analysis of T-DNA insertion lines

2.13.1 Isolation of DNA for genotyping experiments

For this a 'Sigma Plant Extract'n'Amp PCR' kit was used. 40µl extraction buffer was added to a young leaf (between 0.5 and 1cm in length) and incubated at 95°C for 10 minutes in a PCR machine. After the addition of 40µl Dilution solution, the tube was flicked several times in order to break the tissue up and then spun at 13,000 rpm for 15 seconds 1µl of DNA was used in PCR reactions (final volume 25µl).

2.13.2 Alexander's staining

Pollen was collected from newly open flowers and fixed in 3:1 ethanol:acetic acid for 3 hours. Pollen was then washed and transferred to microscope slide. A drop of Alexander's stain

(Alexander, 1969) was added, a cover slip was placed over the pollen and sealed with nail varnish. Pollen viability was visualised under a light microscope.

2.13.3 Aniline blue staining

Aniline blue staining of pollen tubes in pistils was carried out as described in Jiang *et al.*, 2005. Pollinated pistils were collected after 2, 4, 6 and 12 hours after pollination.

2.13.4 Viability test

Plants were analysed when the siliques had reached maturity. Siliques were measured and then opened with a paintbrush and the seeds were counted.

2.14 General Solutions and Buffers

5x TBE: 0.45M Tris, 0.45M Orthoboric acid, 12.5mM EDTA

10x TBS (pH7.4): 80g/l NaCl, 2g/l KCl, 30g/l Tris

1x protein transfer buffer: 14.4g Glycine, 3.03g TRIS, 200ml methanol, up to 1000ml with SDW.

DNA loading buffer: 40% (v/v) glycerol, 0.25% bromophenol blue

5x Protein loading dye: 12.5% (v/v) Tris-HCl (2M, pH6.8), 2% (w/v) SDS, 10% (v/v) Glycerol, 5% (v/v) B-mercaptoethanol, 0.001% (w/v) Bromophenol blue

Alkaline phosphatase detection buffer (pH9.5): 100mM NaCl, 5mM MgCl₂, 100mM Tris. Add 66µl NBT (Sigma; 70%) and 33µl BCIP (Sigma) to 9.9ml Buffer before use.

STET buffer: 8% (w/v) Sucrose, 0.5% Triton X-100, 50mM N₂EDTA (pH 8.0), 10mM TRIS-HCl (pH 8.0).

DNA loading buffer: (40% (v/v) glycerol, 0.25% (w/v) bromophenol blue, 0.25% (w/v) xylene cyanol).

RNA Loading Buffer: (Sigma): 62.5% (v/v) de-ionised formamide, 1.14M formaldehyde, 1.25x MOPS buffer, 200µg/ml bromophenol blue, 200µg/ml xylene cyanol, 50µg/ml ethidium bromide.

5x IP buffer: 125mM Tris-Cl pH7.8, 375mM NaCl, 75mM EGTA (pH8 with NaOH), 75mM β-Glycerophosphate, 75mM p-nitrophenylphosphate, 50mM MgCl₂, 5mM DTT, 5mM NaF, 2.5mM Na vanadate, 2.5mM PMSF, 5x PI tablet (Sigma), 0.5% v/v Tween 20.

5x NaCl buffer: 50mM TRIS, 300mM NaCl.

2.15 Equipment

Bench top centrifuges: Micro Centaur (MSE[®]), MICRO 20 (Hettich Zentrifugen[®]).

Large centrifuge: SORVALL[®] RC26 plus (values in g).

Spectrophotometer: Jenway[®] 6305.

Microscopes: Nikon Eclipse Tε300, BioRad Radiance 2000 laser scanning system, Nikon SMZ645.

CHAPTER 3

Initial attempts to clone a candidate p56 gene

CHAPTER 3 - INITIAL ATTEMPTS TO CLONE A CANDIDATE p56 GENE

3.1 INTRODUCTION

Previously attempts have been made to isolate the gene that encodes p56 from *Papaver rhoeas* pollen by degenerate PCR (Whittaker, 2001). Primers were designed based on a highly conserved region found in all plant MAPKs, near to the activation motif, and used to amplify a ~480bp gene fragment from pollen cDNA. Sequencing reactions confirmed that this fragment actually represented three independent clones of 481bp, 482bp and 485bp, designated *PrMPKA*, *PrMPKB* and *PrMPKC*, respectively. These shared between 74% and 80% homology at the nucleotide level. The three PCR fragments were subsequently used to screen a *P. rhoeas* pollen cDNA library to identify full-length cDNA sequences of the three genes (Osman, unpublished). This resulted in the isolation of a 1488bp clone that corresponded to *PrMPKB*. Based on DNA sequence analysis *PrMPKB* was predicted to encode a 403 amino acid protein with a predicted molecular weight of 45.4kDa and a pI of 5.33. Based on the classification system of Ichimura *et al.* (2002), the predicted PrMPKB protein belongs to the group A class of MAPKs, and contains an N-terminal extension like other members of this group. PrMPKB shared the highest homology with the *Arabidopsis thaliana* AtMPK6 protein.

Clones corresponding to the other two PCR fragments could not be identified from the cDNA library, so 5'RACE and 3'RACE (*Rapid Amplification of Complimentary Ends*) were used to clone the full-length genes. Based on DNA sequence analysis *PrMPKC* was predicted to

encode a 368 amino acid protein, with a molecular weight of 42.0kDa and a pI 6.60. The predicted PrMPKC protein belongs to the group C class of MAPKs and was most similar to *A. thaliana* AtMPK1. It was also found that there was a probable *PrMPKC* variant, with 25 nucleotide differences, which resulted in two amino acid changes at the protein level. It was only possible to obtain a partial *PrMPKA* clone, including the C-terminal. The partial 328 amino acid protein represents a group B MAPK, and shows most similarity to *A. thaliana* AtMPK4.

In general the N-terminal and C-terminal regions of MAPK proteins are more variable than the central catalytic domains, and are therefore routinely used to generate specific antibodies (Droillard *et al.*, 2004; Mészáros *et al.*, 2006). Octomeric Multiple Antigenic Peptides (MAP) were synthesised based on the N-terminal region of PrMPKB (amino acids 9-23), and the C-terminal regions of PrMPKA (amino acids 314-328) and PrMPKC (amino acids 354-368). These were used to raise polyclonal antibodies in rabbit. The antibodies were used in immuno-blotting experiments on proteins extracted from pollen that had undergone an incompatible SI reaction and proteins from an untreated control sample, to determine if they could detect p56. In immuno-blotting experiments p56 could be identified in an incompatible SI-stimulated pollen sample at the 56kDa position, using an anti-pTXpY antibody, which specifically cross-reacted with the phosphorylated T-X-Y motif of activated MAPKs. The anti-PrMPKC antibody specifically detected a single protein of the expected size of ~42kDa. The anti-PrMPKB antibody detected an expected protein of ~45kDa, but also cross-reacted with an unidentified ~65kDa protein. The anti-PrMPKA antibody detected several proteins, and it was uncertain which of these, if any, corresponded to PrMPKA (due to only obtaining a partial sequence). The detection patterns for both incompatible SI-stimulated and control

treatments were identical. Based on these experiments, and also the distance the full-length recombinant PrMPKB and PrMPKC proteins migrated (compared to p56 which is shown to migrate to ~56kDa), it was unlikely that any of the above *P. rhoeas* MAPKs corresponded to p56.

It is known that MAPKs are highly conserved between plant species (Hamel *et al.*, 2006). Experiments were therefore carried out to determine if antisera, raised against known plant MAPKs from other species, could be used to specifically detect the ~56kDa MAPK from *P. rhoeas* pollen (Li *et al.*, 2007). The results showed that an *A. thaliana* MPK3 polyclonal peptide antibody, raised against the specific C-terminal part of AtMPK3 (and not found in the other *A. thaliana* MAPKs) cross-reacted with a ~56kDa protein from *P. rhoeas* pollen (Figure 3.1a). *A. thaliana* MPK4 and *Nicotiana tabacum* SIPK (an *A. thaliana* MPK6 orthologue) antibodies cross-reacted with *P. rhoeas* pollen proteins of ~43kDa and ~48kDa respectively, and did not cross-react with a ~56kDa protein (Figure 3.1a). It was proposed that, as the anti-AtMPK3 antibody specifically cross-reacted with a ~56kDa pollen protein, p56 might be encoded by a *P. rhoeas* orthologue of the *A. thaliana* AtMPK3 gene (Li *et al.*, 2007).

In order to clone a *MPK3*-like gene from *P. rhoeas* degenerate PCR will be used. Degenerate PCR is a method of PCR that uses degenerate primers to amplify unknown sequences of DNA, and is useful to amplify unknown members of a gene family or orthologues of genes from other organisms (Wang *et al.*, 2003). This chapter describes attempts to clone a *P. rhoeas* *MPK3*-like gene from pollen, by degenerate PCR.

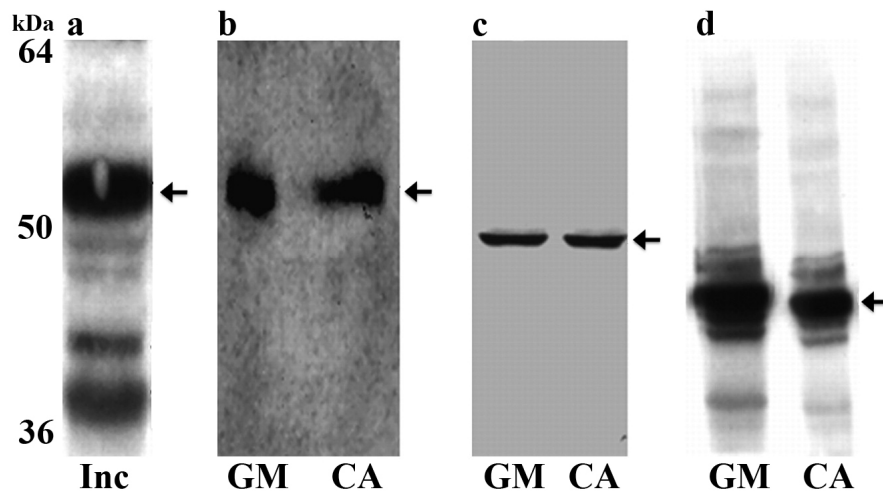


Figure 3.1a An anti-AtMPK3 antibody cross-reacts with a ~56kDa *Papaver rhoeas* pollen protein. p56 can be detected by an anti-pTXpY antibody, that detects activated MAPKs, in an incompatible SI reaction (**a**, arrowed). Protein extracts from control (**GM**) and calyculin A treated (**CA**) pollen contain a protein of ~56kDa (that corresponds to p56) that cross-reacts strongly with an anti-AtMPK3 antibody (**b**, arrowed). Calyculin A is a serine/threonine protein phosphatase inhibitor that can be used to prevent dephosphorylation of MAPKs (Honkanen *et al.*, 1994) and can therefore be used to increase levels of phosphorylated phospho-proteins above their basal level (such as p56) in the absence of a stimulus. An anti-NtSIPK antibody detects a protein migrating to ~48kDa, that does not correspond to p56 (**c**, arrowed). An anti-AtMPK4 antibody detects a protein migrating to ~43kDa, that does not correspond to p56 (**d**, arrowed). **Inc**: incompatible pollen sample. Modified from Li *et al.* (2007).

3.2 RESULTS

3.2.1 Cloning of a *MPK3* orthologue from *Papaver rhoeas*

3.2.1.1 Attempts to clone a *MPK3* orthologue from *Papaver rhoeas* pollen

A number of primers were designed to amplify various regions of a potential *MPK3* orthologue from *P. rhoeas* pollen. The primers were based on sequences from ~15 plant species including both monocotyledonous and dicotyledonous plants. Alignments were made between all the *A. thaliana* MAPKs and the *MPK3* orthologues from other species to try and identify a region that was conserved between the *MPK3* orthologues, but differed from all the other *A. thaliana* MAPKs. From this sequence data, five primers were designed (Table 3.2.1.1a, for primer sequences see Appendix ii.i). For some of the primer sequences a degenerate primer was designed based on the amino acid degeneracy of the *MPK3* proteins. In addition, specific primers were designed based on the specific base pair sequences that occur in the *MPK3* orthologues.

Total RNA was extracted from hydrated *P. rhoeas* pollen and from this, total cDNA was synthesised. Unless otherwise stated hydrated pollen cDNA was used for all the PCR amplifications below, using ReadyMix™ Taq PCR Reaction Mix. For initial attempts at PCR amplification specific primers were used (*MPK3spe1_5'* vs. *MPK3spe1_3'* and *MPK3spe2_5'* vs. *MPK3spe1_3'*) with an annealing temperature of 50°C. Products were visualised by separation on agarose gels. These PCR amplifications yielded no products. In

case this was due to low gene expression, 1µl of the above amplification reactions were re-amplified (30 cycles). Again this yielded no amplification products.

In order to reduce the specificity of the primers, in case there were sequence differences between a potential *P. rhoeas* *MPK3*-like sequence and the primer sequences, the annealing temperature of the PCR was reduced by various increments. Table 3.2.1.1a summarises the various annealing temperatures and combinations of primers that were used, including specific *AtMPK3* primers (*AtMPK3_5'* vs. *AtMPK3_3'*). As a result of these modifications four PCR products were obtained. For primer combinations 1 and 2, products were amplified using an annealing temperature of 37°C. For primer combinations 3 and 4, products were amplified using an annealing temperature of 40°C. Figure 3.2.1.1a shows the amplification products obtained.

Combination #	5' Primer	3' Primer	A.t. Size (bp)
1	MPK3spe1_5'	MPK3spe1_3'	708
2	MPK3spe2_5'	MPK3spe1_3'	396
3	MPK3deg1_5'	MPK3deg1_3'	708
4	AtMPK3_5'	AtMPK3_3'	466

	50°C (Re)	42°C (Re)	40°C (Re)	37°C (Re)
1	x (x)	x (x)	x (y)	x (y)
2	x (x)	x (x)	x (y)	x (y)
3		x (y)	x (y)	
4		x (y)	x (y)	

Table 3.2.1.1a Primer combinations and annealing temperatures used to amplify a *MPK3* orthologue from *Papaver rhoeas* pollen. Top: Primer combinations used to amplify a potential *P. rhoeas* *MPK3* orthologue. **A.t. Size:** predicted size of product based on *A. thaliana* sequence. Bottom: Annealing temperatures used for PCR amplification with each primer combination. **(Re):** re-amplification (30 cycles); **x:** no fragment amplified; **y:** fragment amplified.

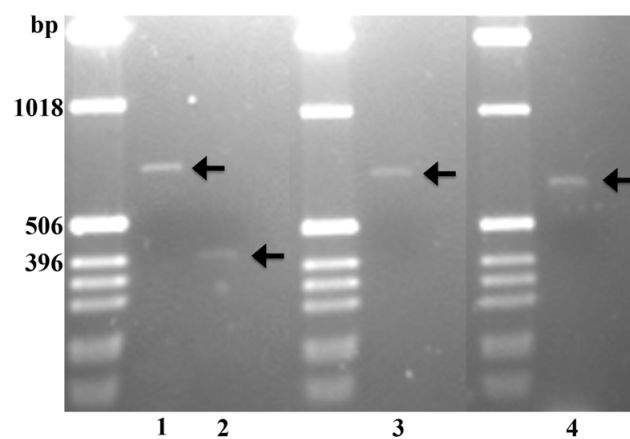


Figure 3.2.1.1a Degenerate PCR products obtained using MPK3-like primers on pollen cDNA. PCR products amplified with the primer combinations listed in table 3.2.1.1a. Products from primer combinations **1**, **2**, **3** and **4** are shown from left to right (arrowed). The predicted fragment sizes for each amplification product based on *A. thaliana* sequence are 708bp, 396bp, 708bp and 466bp, respectively.

All of the amplified fragments were gel purified, ligated into the pDrive cloning vector, and *Escherichia coli* DH5 α competent cells were transformed with the construct. Colonies were grown on selective media, positive colonies were identified by selection with X-gal, and the presence of an insert was confirmed by digestion of crude DNA extracts. From recombinant clones that contained inserts of the predicted size, purified plasmid preparations were prepared and used in nucleotide sequencing reactions. In total, 30 clones were sequenced that covered all combinations of primers used, to confirm that each band did not contain different products of the same size. Of these 30 sequenced clones, 16 were either unsuccessful or contained poor sequence, or had cloned genes that were un-related to MAPKs. Of the sequences that resembled MAPKs, all 14 were 99-100% identical to the *PrMPKB* gene previously cloned (Osman, unpublished).

After comparing the primers with the *PrMPKB*, *AtMPK3* and *AtMPK6* sequences it could be seen that there was the potential for the primers to preferentially amplify *PrMPKB* due to sequence similarity, especially as the lower PCR annealing temperatures reduced primer specificity. Table 3.2.1.1b shows the high level of homology between the three genes.

	<i>AtMPK3</i>	<i>AtMPK6</i>	<i>PrMPKB</i>
<i>AtMPK3</i>	-	63.80%	63.04%
<i>AtMPK6</i>	63.80%	-	75.41%
<i>PrMPKB</i>	63.04%	75.41%	-

Table 3.2.1.1b Comparison of the homology between *AtMPK3*, *AtMPK6* and *PrMPKB* at the nucleotide level.

An attempt was made to design new, more specific primers. This proved difficult as wherever a region was found that diverged between *MPK3*-like and *MPK6*-like genes, it also diverged

between the *MPK3*-like orthologues themselves. However, several suitable regions were identified and primers were designed. Based on the position of these primers, various combinations of primers were once again used, with annealing temperatures of both 45°C and 40°C. Table 3.2.1.1c summarises the combinations of primers used. Unfortunately, it was not possible to amplify any products with any of the combinations of primers.

5' Primer	3' Primer	45°C	40°C
MPK3deg2_5'	MPK3 spe1_3'	x	x
MPK3 spe2_5'	MPK3deg2_3'	x	x
MPK3B_3'	MPK3A_3'	x	x
MPK3A_5'	MPK3A_3'	x	x
MPK3B_3'	MPK3B_3'	x	x
MPK3A_5'	MPK3B_3'	x	x
MPK3A_5'	MPK3deg2_3'	x	x
MPK3B_3'	MPK3deg2_3'	x	x
MPK3deg2_5'	MPK3B_3'	x	x
MPK3deg2_5'	MPK3A_3'	x	x

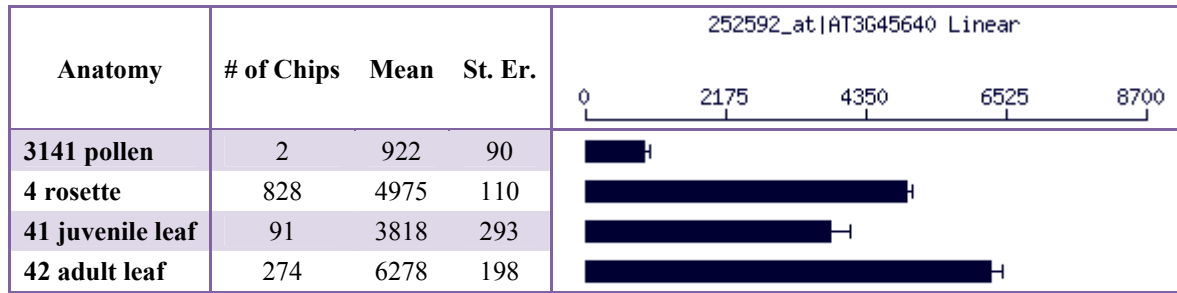
Table 3.2.1.1c Combinations of *MPK3*-specific primers used to amplify a *Papaver rhoeas* *MPK3*-like gene.

Annealing temperatures used for PCR amplification with each primer set are shown. x: no fragment amplified; y: fragment amplified.

3.2.1.2 Cloning of a *MPK3* orthologue from *Papaver rhoeas* leaf

As it was not possible to clone a *PrMPK3*-like gene from *P. rhoeas* pollen, the relative expression of the *A. thaliana* homologues, *AtMPK3* and *AtMPK6*, were investigated in pollen and other tissues. Figure 3.2.1.2a shows the relative expression of the two *A. thaliana* genes from Affymetrix chip experiments (Genevestigator; <https://www.genevestigator.com>; Hruz *et al.*, 2008) in pollen and leaf-related tissues. The expression profiles indicate that *AtMPK3* expression is much higher in leaf tissues relative to pollen, whereas *AtMPK6* showed the reverse pattern.

AtMPK3



AtMPK6

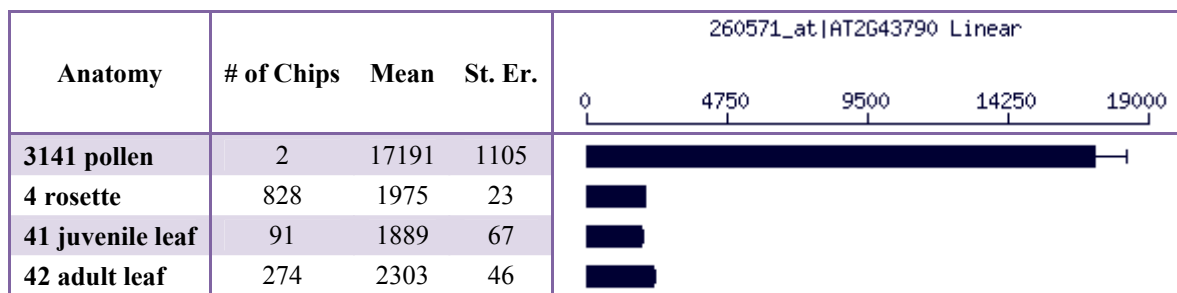


Figure 3.2.1.2a Relative expression of *AtMPK3* (top) and *AtMPK6* (bottom) in pollen and leaf tissues from Affymetrix chip data. The data shows that *AtMPK6* is nearly 17 times more highly expressed in pollen than *AtMPK3*. By contrast, *AtMPK3* is around 2.5 times more highly expressed than *AtMPK6* in leaf tissues. **St. Er.:** standard error. Data from Genevestigator (Hruz *et al.*, 2008).

In terms of expression in pollen, *AtMPK6* was 17 times more highly expressed in pollen tissues than *AtMPK3* (17,191 units compared to 922). This suggested that primers that detected both genes would, in theory, be 17 times more likely to amplify *PrMPKB* than a *MPK3*-like gene from pollen, assuming expression was similar between the species. As *AtMPK3* was more highly expressed in leaf tissues than *AtMPK6* (4,975 units compared to 1,975), an attempt was made to clone a *MPK3* homologue from *P. rhoeas* leaf tissue, as expression of a *MPK3*-like gene was potentially higher in this tissue.

Total leaf RNA was extracted and from this, total cDNA was synthesised. PCR amplification was carried out on leaf cDNA using combinations of the previously designed primers (MPK3deg2_5' vs. MPK3deg2_3' and MPK3A_5' vs. MPK3A_3'). The annealing temperature used was 40°C. The amplification with MPK3deg2_5' vs. MPK3deg2_3' primers gave a product of ~700bp (Figure 3.2.1.2b) which was as expected based on the *A. thaliana* gene sequence (703bp). The ~700bp fragment was cloned and its sequence determined. Of 6 clones sequenced, 3 showed 99-100% identity to *PrMPKB*. The other 3 clones were identical to each other and, in a Basic Local Alignment Search Tool search (BLAST; <http://blast.ncbi.nlm.nih.gov/Blast.cgi>; Altschul *et al.*, 1990) showed 74.85% (497/664bp) homology to *AtMPK3*, the most similar of the *A. thaliana* MAPKs. This suggested it was likely to be a *MPK3* orthologue.

To obtain the full-length gene sequence, 5'RACE and 3'RACE were carried out. For 3'RACE, PCR was carried out on leaf cDNA using a gene-specific primer (PrMPK3_3'R) and an abridged oligo-dT primer (3'RACE17AP). The resultant ~500bp fragment was cloned and sequenced. The resultant 453bp fragment contained a 105bp coding sequence followed by a 348bp downstream untranslated region (UTR). The coding sequence shared 82.17% (553/673bp) identity with the *AtMPK3* gene.

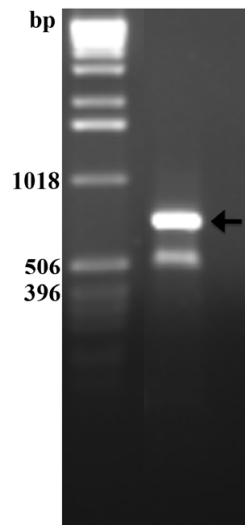


Figure 3.2.1.2b Degenerate PCR products obtained using *MPK3*-like primers on leaf cDNA. The gel shows a product amplified using the MPK3deg2_5' and MPK3deg2_3' primers on leaf cDNA (arrowed). Based on the *A. thaliana* sequence the product should be 703bp.

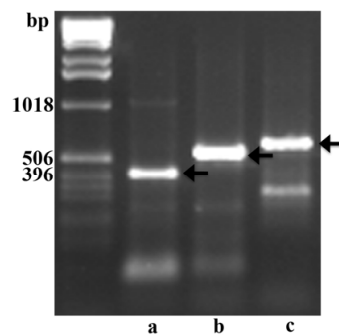


Figure 3.2.1.2c Amplification of a larger region of the *PrMPK3* gene. The gel image shows amplification products obtained using MPK3A_5' as the 5' primer. From left to right: MPK3A_5' vs. PrMPK3_5'R1A (**a**, arrowed), MPK3A_5' vs. PrMPK3_5'R2A (**b**, arrowed), MPK3A_5' vs. PrMPK3_5'R3A (**c**, arrowed). All the arrowed bands were of an expected size based on *A. thaliana* sequence.

For 5'RACE, leaf cDNA was prepared in the standard way but the 5'RACE17AP primer was replaced with a gene-specific primer (PrMPK3_5'R3A). Nested primers (PrMPK3_5'R2A and PrMPK3_5'R1A) were then used in subsequent PCR reactions along with 5'RACEAAP and 5'RACEUAP primers, respectively. Attempts to amplify a product failed.

It was known from previous experiments using 5'RACE that there is often difficulty in amplifying fragments greater than ~800bp. As the potential 5'RACE product was expected to be around this size, an attempt was made to clone a larger part of the gene first using specific 3' primers based on the sequence already acquired (PrMPK3_5'R3A, PrMPK3_5'R2A and PrMPK3_5'R1A) and a non-specific 5' primer based on the *AtMPK3* sequence (MPK3A_5' and MPK3B_5'). The PCR was carried out with an annealing temperature of 40°C. Each of the 6 amplification reactions gave a product but the products using the MPK3A_5' primer (as the 5' primer) gave 3 successively larger fragments with each of the 3' primers, which would be expected due to the positions of the primers (Figure 3.2.1.2c). The largest of these bands (MPK3A_5' vs. PrMPK3_5'R3A) was cloned and sequenced. The sequence provided an extra 325bp of *PrMPK3*-like sequence. This new sequence was used to design new primers (PrMPK3_5'R3B, PrMPK3_5'R2B and PrMPK3_5'R1B) for 5'RACE, as above. A fragment of ~450bp was amplified, cloned and sequenced. In a BLAST search this fragment showed most similarity to the *AtMPK3* gene.

In order to check that the full-length sequence obtained by PCR, 3'RACE and 5'RACE was correct, amplification of the full-length gene was carried out using primers designed in the upstream and downstream UTRs of the *PrMPK3*-like gene (PrMPK3_5'A and PrMPK3_3'A). A ~1.6kb fragment was amplified using a proof-reading polymerase (KOD

Hot Start DNA Polymerase), cloned and sequenced. The open reading frame (ORF) was 1140bp in length, and the predicted protein was 379 amino acids. The predicted protein had a molecular weight of 43.53kDa and a pI of 5.38. The full-length sequence shared 72.19% (823/1140bp) identity at the nucleotide level and 76.78% (291/379 amino acids) identity and 92.35% (350/379 amino acids) similarity at the amino acid level with the *AtMPK3* gene. Figure 3.2.1.2d shows the predicted protein sequence of the gene (see Appendix iii.i for the gene sequence).

>PrMPK3 leaf protein

```
MADIPQNPDNANNPPADFPAILLTHGGRFVQYNI FGNLFEITIKYRPPIMPPIGRGAYGIVCSVLNSETNEMVAIKK
IANAFDNYMDAKRTLREIKLLQHLDHENVIGIRDVI PPPIPGAFSDVYIATELMDSLHQI IRSNQGLSEEHSQY
FLYQILRGLKYIHSANVIHRDLKPSNLLLNNANCDLKICDFGLARPTSENEFMTEYV VVTRWYRAPELLLNSSDYTA
AIDVWSVGCIFMELMNRRLPLFAGRDHVHQLRLLTELLGTPTEADLGFVRSDDARRYLQQLPPHPRQPFAMVFPHV
NPVAIDLIEKMLTFDPTRRITVVEEALAHPLYLERLHDIADPEVCSVPFSEFEFEQQVLTEEQIKEMIYRESVAFNPE
YLHR*
```

Figure 3.2.1.2d Predicted protein sequence of *PrMPK3* from leaf mRNA. The T-X-Y motif is indicated in grey. *: stop codon.

To sequence the genomic copy of the gene several primer sets were used to clone the genomic copy in a number of overlapping fragments, to ease the cloning and sequencing process (PrMPK5'Rcont vs. PrMPK3_5'R3A, PrMPK3u/s1 vs. PrMPK3_5'R3A, PrMPK3_5'C vs. PrMPK3d/s1, PrMPK3_5'C vs. PrMPK3_3'C, PrMPK3_5' vs. PrMPK3d/s2, PrMPK3_5'C vs. PrMPK3d/s2, PrMPK3_5' vs. PrMPK3d/s1). Fragments were amplified from all primer combinations, and fragments that represented the entire length of the gene were cloned and sequenced. The genomic copy of the gene was 3330bp (from start to stop codon) and contained 6 exons and 5 introns (see Appendix iii.i).

Once the full-length mRNA sequence was obtained from leaf, an attempt was made to clone the gene from pollen. Using the specific PrMPK3_5'A and PrMPK3_3'A primers, a product was amplified, cloned and sequenced. This pollen cDNA was identical to the leaf cDNA.

3.2.2 Detection of p56 using the AtMPK3 antibody

To determine whether the anti-AtMPK3 antibody could detect the PrMPK3 protein in leaf and pollen, western blotting was carried out. Previous experiments had shown that the anti-AtMPK3 antibody could detect the ~42kDa AtMPK3 protein in leaf (Sigma-Aldrich, product number M8318), and also a ~56kDa protein from *P. rhoeas* pollen, corresponding to p56 (Li *et al.*, 2007). Protein extracts were prepared from *A. thaliana* leaf and *P. rhoeas* leaf and pollen, and the protein concentration of each extract determined. Approximately 50µg of protein was separated on a 12% SDS-PAGE gel, transferred to a nitrocellulose membrane and probed with the anti-AtMPK3 antibody. For detection of the bound antibody, an anti-rabbit alkaline phosphatase conjugated antibody was used. Figure 3.2.2a shows that in *A. thaliana* leaf and *P. rhoeas* pollen proteins of ~42kDa and ~56kDa respectively, were detected, as expected. However, it was not possible to detect PrMPK3 in leaf which was expected to be ~43kDa based on the predicted protein sequence from DNA sequence analysis.

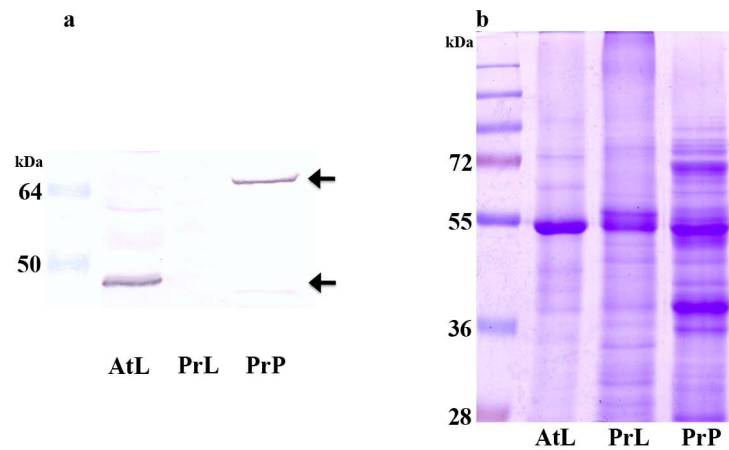


Figure 3.2.2a The anti-AtMPK3 antibody can detect AtMPK3 in *Arabidopsis thaliana* leaf and a ~56kDa protein in *Papaver rhoeas* pollen. In *A. thaliana* leaf a protein of ~42kDa is detected as expected (**a**, **AtL**, lower arrow). In *P. rhoeas* leaf (**a**, **PrL**) it was not possible to detect PrMPK3 which was predicted to be ~43kDa. As shown previously, there is no detection of a ~43kDa protein in *P. rhoeas* pollen, but a protein of ~56kDa can be detected, that corresponds to p56 (**a**, **PrP**, upper arrow). The Coomassie Blue stained gel shows protein loading (**b**). **AtL**: *A. thaliana* leaf protein; **PrL**: *P. rhoeas* leaf protein; **PrP**: *P. rhoeas* pollen protein.

3.3 DISCUSSION

3.3.1 Cloning of a *PrMPK3* gene from *P. rhoeas*

Evidence suggested that p56 might be encoded by a *MPK3* orthologue. This chapter describes the successful cloning and sequencing of a *PrMPK3* gene from both *P. rhoeas* leaf and pollen. The gene encoding p56 is expected to be expressed in pollen, so initial attempts were made to clone the gene from this tissue. Due to the high homology of *AtMPK3*, *AtMPK6* and *PrMPKB*, and the fact that wherever these genes diverged in sequence, the *MPK3* orthologues also diverged in sequence, it was difficult to design specific primers to amplify a *P. rhoeas* *MPK3*-like gene. Table 3.3.1a shows the homology between the genes at the nucleotide and protein level. It can be seen that differences between the *AtMPK3* and *PrMPK3* genes were almost as great as the differences between *AtMPK3* and *AtMPK6* (or *PrMPKB* and *PrMPK3*) (i.e. the difference between homologues is almost as great as the difference between orthologues) and it was these differences that were likely to make primer design difficult.

	<i>AtMPK3</i>	<i>AtMPK6</i>	<i>PrMPKB</i>	<i>PrMPK3</i>
<i>AtMPK3</i>	-	63.80%	63.04%	72.19%
<i>AtMPK6</i>	87.34%	-	75.41%	67.09%
<i>PrMPKB</i>	86.35%	91.87%	-	67.33%
<i>PrMPK3</i>	92.35%	89.91%	87.59%	-

Table 3.3.1a Comparison of homology between *AtMPK3*, *AtMPK6*, *PrMPK3* and *PrMPKB*. The table shows homology at the nucleotide level (top right) and similarity at the amino acid level (bottom left).

Due to considerable difficulty in primer design specificity, the failure to amplify products with a large number of primer sets, and the inability to clone anything other than the *PrMPKB* gene, it was decided that a different approach was required. It was realised that there may be a

problem due to the expression level of a potential *P. rhoeas* *MPK3* orthologue in comparison to that of the *PrMPKB* gene in pollen, as previous experiments had shown that *PrMPKB* was potentially highly expressed in pollen (Osman, unpublished). As the *AtMPK3* gene was much more highly expressed in leaf than in pollen, compared to *AtMPK6*, it was argued that the expression might be similar in *P. rhoeas*. Attempts were therefore made to amplify a *MPK3*-like gene from leaf tissue. This resulted in the cloning and sequencing of a *PrMPK3* gene.

Figure 3.3.1a shows the phylogeny of the *A. thaliana* and *P. rhoeas* MAPKs and shows, due to the similarity to *AtMPK3* and its clustering with this gene, why the gene cloned was designated *PrMPK3*. *PrMPK3* was predicted to encode a protein of 43.53kDa. Due to the predicted molecular weight of the PrMPK3 protein it was unlikely to encode p56 (~56kDa). Koo *et al.* (2007) have provided evidence of MAPK splice variants, but to date this is the only published evidence in plants. They show that the *OsBWMK1* gene encodes 3 splice variants (L, M and S), which encode 65.9kDa, 58.5kDa and 57.9kDa proteins respectively. Although it is possible that *PrMPK3* does encode splice variants, which may include p56, there is no evidence to suggest that this is the case.

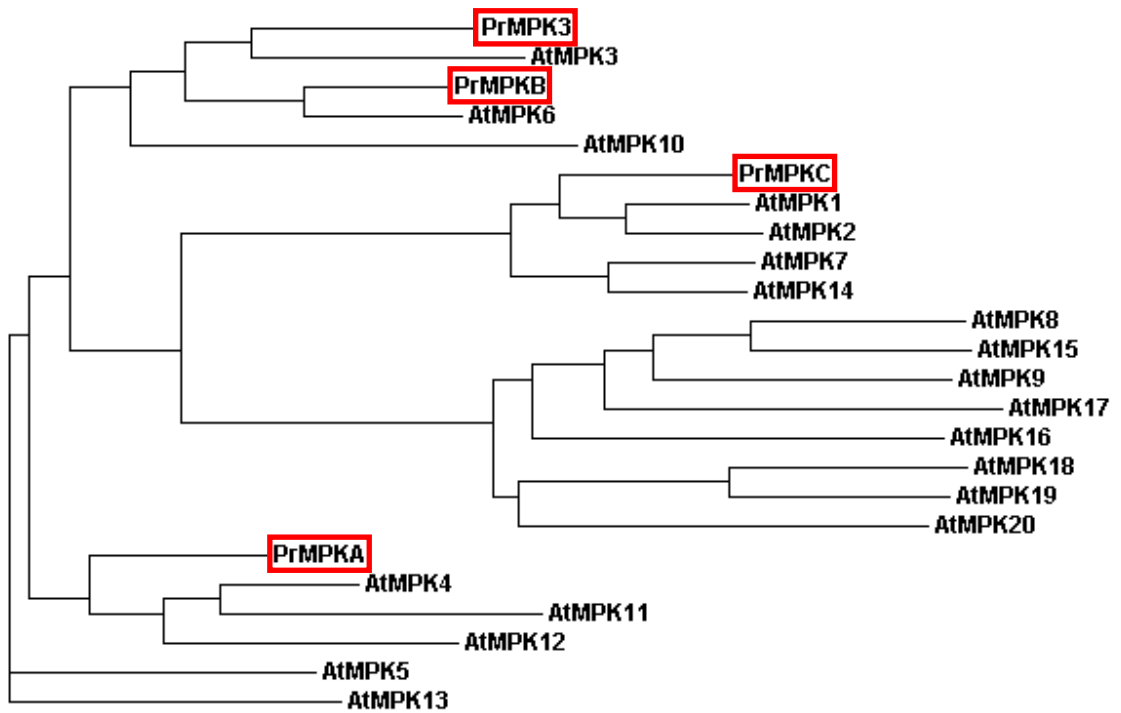


Figure 3.3.1a Phylogenetic tree of *Arabidopsis thaliana* and *Papaver rhoeas* MAPK proteins. PrMPK3 shows the highest homology to AtMPK3. The *P. rhoeas* MAPKs are shown boxed. To identify the origin of species an acronym is included before the protein name: At, *Arabidopsis thaliana*; Pr, *Papaver rhoeas*. The tree was constructed using Clustal W (<http://www.ebi.ac.uk/Tools/clustalw2/index.html>; Larkin *et al.*, 2007).

3.2.2 PrMPK3 detection with the anti-AtMPK3 antibody

Western blot analysis showed that it was not possible to detect PrMPK3 in *P. rhoeas* leaf and pollen, although a protein of ~56kDa was detected in pollen (corresponding to p56). Although the anti-AtMPK3 antibody bound specifically to AtMPK3 (and not to the other 19 MAPKs found in *A. thaliana*) this binding is not specific in *P. rhoeas*. Cloning experiments showed that it was possible to detect the leaf mRNA in *P. rhoeas*, but the protein was not detected. Whether the protein is only expressed at low levels, and therefore not detected by immunoblotting, remains to be determined. PrMPK3 and AtMPK3 show 50% identity and 83% similarity in the region used to raise the anti-AtMPK3 antibody (amino acids 359-370), and there was a possibility the antibody would detect the PrMPK3 protein, but no evidence of this was found. It has been shown that the anti-AtMPK3 antibody detects a ~56kDa band in *P. rhoeas* pollen (Figure 3.2.3a, see also Li *et al.*, 2007). Whether the binding of the anti-AtMPK3 antibody to the ~56kDa protein is due to non-specific binding, or whether it is detecting another *P. rhoeas* MAPK of the same size which shows homology to AtMPK3, remains to be determined. It has been established that the smallest antigenic determinant can be between just 3 and 6 amino acids (Lydyard *et al.*, 2004). As the MAPKs are highly conserved it is possible that although the anti-AtMPK3 antibody is specific to AtMPK3 in *A. thaliana*, it may detect a different MAPK in *P. rhoeas*, as the MAPK family in this species has yet to be sequenced.

CHAPTER 4

A bioinformatics approach to identify p56

CHAPTER 4 - A BIOINFORMATICS APPROACH TO IDENTIFY p56

4.1 INTRODUCTION

Previous results suggested that, despite the cross-reactivity of p56 with the anti-AtMPK3 antibody, *PrMPK3* was unlikely to encode p56. As there were no other potential candidates, analysis was carried out to investigate which orthologues of MAPK genes might encode the p56 protein. This chapter describes how a combination of bioinformatics and proteomics approaches led to the identification of new p56 candidates. There were three main criteria used to identify candidates: i) the predicted size of the protein is ~56kDa; ii) the tissue specificity of the gene and its expression in pollen; iii) identification of peptides present in the p56 protein.

Bioinformatics is a useful tool in studying gene characterisation and function using information technology. Bioinformatics covers a wide range of applications including sequence analysis, genome annotation, gene and protein expression analysis, protein structure prediction and many modelling techniques. Databases allow access to readily available data and also the opportunity to submit new data as it becomes available. GenBank[®] (Benson *et al.*, 2008) is a DNA sequence database that contains sequences submitted from individual laboratories and from data exchange from other international sequence databases, from many different species. Information from this database will be used to identify MAPK genes that have been cloned from various plant species. As MAPKs are highly conserved between species we can use information from other plant species to identify candidate genes that show characteristics expected of p56.

High-throughput technologies such as microarrays and expressed sequence tag (EST) analysis are allowing a revolution in the understanding of the mechanisms underlying biological processes. These technologies allow gene-expression profiling which can be used to measure the expression of thousands of genes from a single sample. Gene expression can be investigated at various development stages or in response to diverse stimuli and drug treatments. *Arabidopsis thaliana* is a model plant species and its genome has been fully sequenced. Many of its genes have been characterised and numerous gene-expression experiments have been carried out, the results of which are available in an online database (Genevestigator; <http://www.genevestigator.com>; Hruz *et al.*, 2008). This database will be used to select MAPK candidates based on their expression profiles.

Proteomics is the large-scale analysis of proteins in living cells. Proteomics can be used to identify proteins and to characterise protein expression, localisation, activity, regulation and post-transcriptional modification. One of the major techniques utilised for proteomics analysis is mass spectrometry (MS). MS techniques are used to measure the mass of ions, and can be used to determine the composition of a molecule or mixture of molecules (including peptides), by determining the mass of its component ions. FT-ICR MS (Fourier Transform-Ion Cyclotron Resonance mass spectrometry; Comisarow and Marshall, 1974; for a review see Marshall *et al.*, 1998) is the highest resolution mass spectrometry technique available and can measure mass, to high accuracy, of a molecule from complex mixtures of molecules. Conventional MS techniques are not always perfect at measuring the mass of ions. These techniques often group together several molecules of a similar mass and give a weighted average of the molecules present and therefore, do not truly represent all the molecules present. Because FT-ICR has a much higher resolution it can be used to determine the mass of

molecules to 10^{-5} Daltons, and can also simultaneously separate and recognise more than 10,000 separate constituents from a single sample.

How does FT-ICR MS determine the mass of molecules from a mixture of molecules? Initially, samples are ionised to give the molecules a charge. These charged molecules are then passed to an analyser cell at the centre of a super-conducting magnet, where the ions circle in the magnetic field. Ions of different mass circle the magnet with the same radius, but the speed of each ion is determined by its mass. This speed is defined as the ion's cyclotron frequency. As the power of the cyclotrons magnet increases, the difference between ion's cyclotron frequency increases and this is the main principle behind FT-ICR MS's high powers of resolution. On the outside of the analyser cell there are excitation plates, which contain electrodes. The electrodes are part of a circuit that pass oscillating radio frequency pulses to the excitation plates, which cause like ions in the analyser cell to respond to the same frequency and group together. These grouped ions take energy from the radio frequency and their orbit increases in the magnetic field. The orbiting ions are detected at a detector plate by electrodes that are linked to a second circuit. When ions get close to the electrodes they induce negatively charged electrons in this circuit, which are measured by a resistor, which measures the voltage of the ions. When the radio frequency pulses are turned off the ions return to their original orbit and the resistor records this subsidence. Each voltage reading is then converted by the Fourier Transform (FT) algorithm to show the amplitude of each of the different frequencies, which corresponds to the number of ions associated with that frequency. The FT results are translated to a mass-spectrum, which gives the mass to charge ratio (m/z) of each of the molecules. The mass to charge ratio refers to the molecules atomic mass. The height of a peak in the mass-spectrum represents the abundance of that molecule. This data

can be used to deduce the molecules present in a mixture of molecules and the amount of each of those molecules.

Mass spectrometry techniques have been used in a number of plant species (including *A. thaliana*, pea and tobacco) to investigate the proteomes of mitochondria (Brugiere *et al.*, 2004, Millar *et al.*, 2005, Bardel *et al.*, 2002), chloroplasts (Gomez *et al.*, 2002, Salvi *et al.*, 2003), cell walls (Feiz *et al.*, 2006), vacuoles (Carter *et al.*, 2004), nuclei (Pendle *et al.*, 2005) and specifically in pollen (Dai *et al.*, 2006a, Noir *et al.*, 2005, Holmes-Davis *et al.*, 2005, Zou *et al.*, 2009). Here, FT-ICR will be used to identify the MAPK that corresponds to p56.

4.2 RESULTS

4.2.1 A bioinformatics approach to identify p56

As p56 is expressed and functions in pollen it was predicted that the gene that encodes p56 would be strongly expressed in pollen and possibly specific to that tissue. The expression profiles of the *A. thaliana* MAPKs in pollen were analysed using data from Geneinvestigator, which summarises gene expression from hundreds of microarray experiments (<https://geneinvestigator.ethz.ch/>; Hruz *et al.*, 2008). Table 4.2.1a shows the expression profiles of *AtMPKs* in pollen. *AtMPK17* is the most highly expressed MAPK (96,375 units), with *AtMPK8* also showing a very high expression range (22,943 units). *AtMPK6* (17,191 units), *AtMPK19* (11,423 units), *AtMPK9* (7,655 units) show high expression ranges, and *AtMPK20* shows a moderate expression range (2,104 units). The remainder of the *AtMPKs* show only moderate or low expression. The next criterion that was applied was to identify which *AtMPK*

family members encoded proteins in the size range of p56. Table 4.2.1a shows that *AtMPK8*, *AtMPK9*, and *AtMPK17* are in the region of the predicted size of p56 (~56kDa).

MAPK	Pollen expression	MW (kDa)	T-loop
<i>AtMPK17</i>	96375	59.0	TDY
<i>AtMPK8</i>	22943	61.5	TDY
<i>AtMPK6</i>	17191	45.0	TEY
<i>AtMPK19</i>	11423	65.9	TDY
<i>AtMPK9</i>	7655	58.4	TDY
<i>AtMPK20</i>	2104	68.8	TDY
<i>AtMPK3</i>	922	42.7	TEY
<i>AtMPK10</i>	893	45.2	TEY
<i>AtMPK11</i>	893	31.6	TEY
<i>AtMPK15</i>	781	49.4	TDY
<i>AtMPK18</i>	604	69.4	TDY
<i>AtMPK12</i>	388	42.3	TEY
<i>AtMPK5</i>	346	28.9	TEY
<i>AtMPK4</i>	254	42.9	TEY
<i>AtMPK14</i>	187	42.0	TEY
<i>AtMPK13</i>	166	42.2	TEY
<i>AtMPK2</i>	152	43.1	TEY
<i>AtMPK7</i>	125	42.3	TEY
<i>AtMPK16</i>	104	64.9	TDY
<i>AtMPK1</i>	88	42.7	TEY

Table 4.2.1a Expression of *Arabidopsis thaliana* MAPKs in pollen. The expression levels are based on Affymetrix chip expression data. The genes are listed in descending order of pollen expression. Relative expression values from Affymetrix probe sets are shown (**Pollen expression**), along with the molecular weight of the protein (**MW**) and the T-loop activation sequence (**T-loop**). Expression is scored as follows: <500, very low expression; 500-1000, low expression; 1000-5,000, moderate expression; 5,000-20,000, high expression; >20,000, very high expression.

MAPK gene families have also been cloned from *Populus trichocarpa* and their expression profiles have been investigated (Nicole *et al.*, 2006). Although expression in pollen was not investigated directly, expression of MAPKs in male floral buds was studied. Table 4.2.1b shows that *PtMPK17*, *PtMPK19*, *PtMPK20-1*, *PtMPK18*, *PtMPK11*, *PtMPK7*, *PtMPK5-2* and *PtMPK16-1* were all highly expressed in male floral buds. In terms of protein size, only *PtMPK17* was predicted to encode a protein in the region of p56.

MAPK	MFB expression	MW (kDa)	T-loop
<i>PtMPK17</i>	2485.94	57.1	TDY
<i>PtMPK19</i>	2430.96	69.3	TDY
<i>PtMPK20-1</i>	1468.88	70.9	TDY
<i>PtMPK18</i>	1370.3	68.1	TDY
<i>PtMPK11</i>	1183.42	42.6	TEY
<i>PtMPK7</i>	1111.58	42.5	TEY
<i>PtMPK5-2</i>	1051.38	44.3	TEY
<i>PtMPK16-1</i>	1009.02	64.1	TDY
<i>PtMPK20-2</i>	926.16	70.6	TDY
<i>PtMPK6-1</i>	784.64	45.2	TEY
<i>PtMPK1</i>	652.24	42.7	TEY
<i>PtMPK4</i>	519.29	42.8	TEY
<i>PtMPK9-1</i>	367.78	67.1	TDY
<i>PtMPK5-1</i>	316.44	43.2	TEY
<i>PtMPK6-2</i>	284.22	42.9	TEY
<i>PtMPK9-2</i>	267.88	68.4	TDY
<i>PtMPK3-2</i>	201.74	42.5	TEY
<i>PtMPK14</i>	169.74	42.7	TEY
<i>PtMPK2</i>	57.56	43.1	TEY
<i>PtMPK3-1</i>	56.52	42.7	TEY
<i>PtMPK16-2</i>	47.52	64.1	TDY

Table 4.2.1b Expression of *Populus trichocarpa* MAPKs in male floral buds. The expression levels are based on experiments carried out by Nicole *et al.* (2006). The genes are listed in descending order of mature floral bud expression. The table shows number of transcripts per ng total RNA in male floral buds (**MFB expression**) along with the molecular weight of the protein (**MW**) and the T-loop activation sequence (**T-loop**). Expression is scored as follows: <100, very low; 100-400, moderate; 400-1000, high; >1000, very high.

A family of *Oryza sativa* MAPKs have also been cloned (Liu and Xue, 2007) but to date there is little expression data available for this group of MAPKs. Table 4.2.1c shows these MAPKs along with their predicted protein sizes. Although no comment can be made on the expression of these genes in pollen, *OsMPK12*, *OsMPK13*, *OsMPK15* encode proteins in the size region of p56.

MAPK	MW (kDa)	T-loop
OsMPK9	79.1	TDY
OsMPK10	69.4	TDY
OsMPK7	67.0	TDY
OsMPK17	66.4	TDY
OsMPK8	65.2	TDY
OsMPK16	64.8	TDY
OsMPK11	64.5	TDY
OsMPK14	61.8	TDY
OsMPK13	58.3	TDY
OsMPK12	58.0	TDY
OsMPK15	57.0	TDY
OsMPK1	44.9	TEY
OsMPK2	44.6	TEY
OsMPK5	43.0	TEY
OsMPK6	42.8	TEY
OsMPK3	42.5	TEY
OsMPK4	42.2	TEY

Table 4.2.1c Predicted protein size of the *Oryza sativa* MAPKs. The genes are listed in descending order of size. The table shows the molecular weight of the protein (MW) and the T-loop motif sequence (T-loop).

These bioinformatics data suggest that *A. thaliana* MPK8, MPK9, and MPK17, *P. trichocarpa* MPK17, and *O. sativa* MPK12, MPK13 and MPK15 were good candidate p56 orthologues.

4.2.2 A proteomics approach to identify p56

In conjunction with the bioinformatics analysis, attempts were made to gain additional information as to the identity of the p56 protein directly, using a proteomics approach. A total protein extract from hydrated poppy pollen was prepared and fractionated on a 12% SDS-PAGE gel. Coomassie Blue staining was used to detect the separated proteins and a protein band corresponding to p56 was excised. The protein band was digested with trypsin, a serine endopeptidase that catalyzes the hydrolysis of peptide bonds on the carboxyl side of arginine and lysine residues, to digest the proteins into smaller fragments for analysis. These peptide

fragments were then sent for analysis via FT-ICR tandem MS (MS/MS) to determine the amino acids present, from the mass of the peptides.

Although the mass-spectrum can determine which amino acids are present in a peptide, it cannot determine in which order these amino acids are present (e.g. if amino acids A, B and C are present in the peptide they could be arranged A-B-C, A-C-B, B-C-A etc.). In order to determine actual peptides (and therefore proteins) that were represented, the mass spectrum of peptides was used to search a protein database to link the individual peptides to the original proteins. The mass-spectrum was used to search databases by two different methods. One using a Sequest search engine from Xcalibur[®], and the other using a MASCOT search engine from Matrix Science.

4.2.2.1 Analysis of FT-ICR MS data using a Sequest search engine

Sequest (BioWorks, Xcalibur[®]) is a MS data analysis tool used for the identification of peptides and proteins. Sequest uses indexed and non-indexed FASTA protein databases, to cross-correlate MS data of peptides and proteins from a sample to these databases. The BioWorks program provides various species specific databases for comparing the MS data, but to date no specific plant database is available. For an initial search, the MS data was compared to an '*Arabidopsis/Brassica*' database, that was compiled from *Arabidopsis* and *Brassica* proteins that had been submitted to the NCBI protein database (<ftp://ftp.ncbi.nih.gov/blast/db/FASTA/>). The search also allows for protein modifications that may be incorporated into the peptides during treatment prior to FT-ICR MS analysis. Trypsin digestion often induces artificial modifications to peptides, due to changes in buffer pH and

temperature, and these have to be accounted for during database searching. Oxidation, disulphate bonds reduction, deamination and phosphorylation modifications were accounted for. Table 4.2.2.1a shows the predicted MAPK peptides that were found in the protein sample (the results have been collated from all samples sent for analysis and the best probability and score is shown for each protein/peptide. For the raw data see Appendix iv.i). Each peptide has a significance value, which determines if it is likely to be real. This P (pro) value is defined as:

“P (pro): This entry displays the probability of finding a match as good or better than the observed match by chance. The value displayed for the protein is the probability of the best peptide match (the peptide with the lowest score)” (Bioworks, Xcalibur[®]).

Generally the significance cut-off point is determined by a peptide that has a P(pro) value of <0.001. Each protein/peptide is also given a score, which determines how good the peptide matches are to a particular protein. This is defined as:

“Score (XC): Score displays a score for the Sequest results; the higher the score, the better the match to the searched sequence. The unified score is calculated by:

$$\text{Score} = (10,000 \times ((\Delta C_n^2) + S_p)) \times X\text{Corr}$$

If you have not selected a Unified Score filter in the Search Results Options dialog box, this score is calculated by multiplying the first entry in the Hits column by 10, the second entry by 8, the third by 6, the fourth by 4, and the fifth

by 2, and then summing these values” (Bioworks, Xcalibur[®]) (see Appendix iv.ii for equation values).

The search shows that two peptides (KINDVFDHISDATRI and RLLAFDPKD) occurred in nearly all of the MAPKs detected. AtMPK9 had two specific peptides matches (KGSYGVVASAIIDTHSGEKV and RNGTHSQTGYSARS) and AtMPK8 had one (KLEFDFERK). The probabilities of all these peptides however, were non-significant.

Reference Scan(s)	Peptide	P (pro) P (pep)	Score XC
AtMPK9		1	28.13
	K.INDVFEHVSDATR.I	1	3.08
	K.GSYGVVASAIIDTHSGEK.V	1	2.59
	R.LLAFDPK.D	1	2.28
	R.NGTSQTGYSAR.S	1	1.58
AtMPK8		1	18.15
	K.INDVFEHVSDATR.I	1	3.08
	R.LLAFDPK.D	1	2.28
	K.LEFDFER.K	1	1.61
BnMPK9		1	10.15
	K.INDVFEHVSDATR.I	1	3.08
	R.LLAFDPK.D	1	2.28
AtMPK19		1	10.11
	R.LLAFDPK.D	1	2.28
AtMPK15		1	8.13
	K.INDVFDHISDATRI.I	1	2.57
	R.LIAFDPK.D	1	2.28

Table 4.2.2.1a Sequest search of the FT-ICR MS data against an ‘*Arabidopsis/Brassica*’ database. Peptides found from the ‘*Arabidopsis/Brassica*’ database in descending order of score, showing peptide/protein scores (XC) and probability (P (pro)/P (pep)). To identify the origin of species an acronym is included before the protein name: At: *Arabidopsis thaliana*; Bn: *Brassica napus*.

Because the above database did not represent all the plant proteins available (and no dedicated plant database was available), a new specific plant database was created using proteins stored in the NCBI protein database (the database included protein sequences from SwissProt, PIR,

PRF, PDB, and translations from annotated coding regions in GenBank and RefSeq; ftp://ftp.ncbi.nih.gov/blast/db/FASTA/). To create the new ‘Plant’ protein database, proteins from a large number of plant species were included in the database. In order to add proteins to the 'Plant' database they had to be identified in the NCBI database. Proteins in the database were not ‘tagged’ in any way (i.e. proteins in a certain kingdom e.g. Viridiplantae) so proteins from each genus of plant had to be searched for individually by using word specific search terms (i.e. searching for ‘Papaver’ would select all the proteins that contained the word ‘Papaver’ in the protein name). Table 4.2.2.1b shows the species that were included in the database. In addition to these proteins, a group of *Populus trichocarpa* MAPKs (Nicole *et al.*, 2006) and the PrMPK3 predicted protein were added as they were not currently in the NCBI database. The final database contained 335,107 proteins from 50 plant species.

Arabidopsis	Citrus	Lilium	Petunia	Securigera
Arachis	Cucumis	Litchi	Phaseolus	Solanum
Arthrophyllum	Cucurbita	Lotus	Physcomitrella	Sorghum
Asparagus	Drosera	Lycopersicon	Pinus	Spinacia
Astragalus	Dubautia	Malus	Pisum	Striga
Avena	Elaeagnus	Medicago	Populus	Triphysaria
Brassica	Glycine	Nicotiana	Prunus	Triticum
Brugmansia	Gossypium	Nitella	Raphanus	Vicia
Carica	Helianthus	Oryza	Rheum	Vitis
Chara	Hordeum	Papaver	Secale	Zea

Table 4.2.2.1b List of plant species whose proteins were added to the ‘Plant’ database. In total the database contained 335,107 proteins from 50 plant species.

The FT-ICR MS data was cross-correlated with the new ‘Plant’ database. The results (Table 4.2.2.1c; for raw data see Appendix iv.i) showed two peptides from *Oryza sativa* MPK8 and AtMPK9 and one peptide from AtMPK8 and AtMPK15, *Brassica napus* MPK9, and *Populus trichocarpa* MPK9-1, MPK9-2 and MPK17. All of the peptide matches were non-significant.

Reference Scan(s)	Peptide	P (pro) P (pep)	Score XC
OsMPK8		0.9995207498558	14.06
	K.IHNIFEHLSDAAR.I	1	1.27
	K.VSTVQYGVSR.M	0.9995207498558	0.73
AtMPK8		1	10.11
	K.INDVFEHVSDATR.I	1	2.23
PtMPK9-2		1	10.10
	R.RTNHNNHDHINNINKTTSSNVSSSGCPQSSVNVKEGIK.G	1	1.95
PtMPK9-1		1	10.10
	K.GSYGVVGS AIDTHTGEK.V	1	1.91
BnMPK9		1	10.07
	R.QFAHLEEHY GK.G	1	1.37
PtMPK17		1	10.06
	K.YIHTGNVFHR.D	1	1.26
OsMPK7		0.9999302959035	10.05
	R.QFAILEENG GK.S	0.9999302959035	1.04
AtMPK15		1	8.11
	K.INDVFDHISDATR.I	1	2.19
AtMPK9		1	10.09
	K.GSYGVVAS AIDTHS GEK.V	1	2.22
	K.ICDFGLAR.V	1	1.16
OsMPK11		1	10.06
	K.IHNIFEHISDAAR.I	1	1.27
Zm MAPK		1	8.07
	I.KKIANVFDNRVDALR.V	1	1.37

Table 4.2.2.1c Sequest search of the mass spectrometry data using the ‘Plant’ database. Peptides found from the ‘Plant’ database in descending order of score, showing peptide/protein scores (XC) and probability (P (pro)/P (pep)). At: *Arabidopsis thaliana*; Bn: *Brassica napus*; Os: *Oryza sativa*; Pt: *Populus trichocarpa*; Zm: *Zea mays*.

4.2.2.2 Analysis of FT-ICR MS data using a MASCOT search engine

In addition to the Sequest search, the FT-ICR MS data was also analysed by a MASCOT search engine (Matrix Science; <http://www.matrixscience.com/>) using the ‘MS/MS Ion Search’. The MASCOT search is a powerful search engine that is distinctive from other search methods as it integrates various proven methods of searching. For the search there was an automatic limit put on the results in order to display only the protein hits that had a protein score exceeding a significance threshold, plus one extra hit. The data was run against a ‘Viridiplantae’ database, which contained proteins from green plants. To account for

artificially induced trypsin modifications, potential carbamidomethyl and oxidation modifications were included. In the results each protein/peptide is given a score, which is defined as:

“The score for an MS/MS match is based on the absolute probability (P) that the observed match between the experimental data and the database sequence is a random event. The reported score is $-10\log(P)$ ” (Matrix Science).

Each protein also has an emPAI value, which is defined as follows:

“The Exponentially Modified Protein Abundance Index (emPAI) offers approximate, label-free, relative quantitation of the proteins in a mixture based on protein coverage by the peptide matches in a database search result” (Matrix Science).

Table 4.2.2.2a shows the collated results from the MASCOT search (for the raw data see Appendix iv.iii). Peptide matches that are both bold and red are the most likely assignments. This suggested that the best matches were OsMPK13 and AtMPK9.

Prot.	em	Peptide	Sc.
Os MPK 13	0.12		36
		R.LLAFDPK.D	9
		K.ICDFGLAR.V	3
		K.FEFEFER.R	8
		K.YIHSANVFHR.D	36
		K.NRASAYPNGIINLNSNPK.I	8
At MPK 9	0.06		35
		K.ICDFGLAR.V	35
		R.NGTSQTGY SAR.S	8
		K.INDVFEHVSDATR.I	21
		K.GSYGVVASAIDTHSGEK.V	13
		R.GGEQTSFMYPGVD RFR.K	2
At MPK 8	0.05		35
		R.HPDVVEIK.H	5
		K.ICDFGLAR.V	35
		K.LEDFER.K	10
		M.GGGNLDV DGV.R	6
		K.NILANADCK.L	2
		K.INDVFEHVSDATR.I	21
Os MPK 12	0.05		35
		K.CVAVKDNK.E	10
		K.ICDFGLAR.A	35
		K.GERGSPLQRK.H	5
		K.INDVFEHVSDATR.I	21
Os MPK 9	0.04		35
		K.ICDFGLAR.V	35
		K.VTADVALDMR.G	10
		R.KLEFEFEQK.K	5
		R.MVTQTDIYTR.S	6
		R.GALWELVW GERSVRER.N	2
At MPK 15	0.05		35
		K.ICDFGLAR.V	35
		M.GGGNLDV DGV.R	6
		K.NILANADCK.L	2
		K.INDVFDHISDATR.I	8
At MPK 16	0.05		35
		R.NAQMPMSR.I	7
		K.ICDFGLAR.V	35
		K.NILANADCK.L	2
		R.RMVRNPAAASQY PK.R	2
		K.GLAKVEREPSAQPVTK.L	5
Os MPK 8	0.05		35
		K.ICDFGLAR.V	35
		K.ADPAALKLLQR.L	0
		R.QFANLEENG GK.N	4
		R.YQPSEHFMDAK.V	8
		K.IHNIFEHLSDAAR.I	1

Prot.	em	Peptide	Sc.
Os MPK 14	0.05		35
		K.ICDFGLAR.V	35
		R.RYLNSMR.R	5
		K.NILANADCK.L	2
		R.DNNLKSQDSASV GASR.I	7
At MPK 20	0.05		35
		K.ICDFGLAR.V	35
		R.FKVQEVIGK.G	2
		K.GLAKVEREPSCQPITK.M	2
		R.NLSAAKPSTFMGPVAPFDNGR.I	6
At MPK 1	0.08		35
		K.ICDFGLAR.A	35
		M.ATLVDP PNGIRNEGK.H	5
Os MPK 11	0.05		35
		K.HIMLPPSK.M	3
		K.ICDFGLAR.V	35
		R.KYLTCMR.K	3
		K.IHNIFEHLSDAAR.I	1

Table 4.2.2.2a A MASCOT search of the FT-ICR

MS data against a 'Viridiplantae' database. The

use of red and bold typefaces highlights the most

logical assignment of peptides to proteins. The first

time a peptide match to a query appears in the results,

it is shown in bold face. Whenever the top ranking

peptide match appears, it is shown in red. This means

that protein hits with peptide matches that are both

bold and red are the most likely assignments. These

hits represent the highest scoring protein that contains

one or more top ranking peptide matches. **Prot:**

protein, **em:** emPAI, exponentially modified protein

abundance index; **Sc:** Score; At: *Arabidopsis thaliana*;

Os: *Oryza sativa*.

4.3 DISCUSSION

Combined bioinformatics and proteomics based approaches were used to identify genes that could encode p56. For this, three main criteria were investigated: i) the predicted size of the protein is ~56kDa; ii) the tissue specificity of the gene and its expression in pollen; iii) identification of peptides present in the p56 protein.

4.3.1 Bioinformatics analysis

Although MAPKs are highly conserved between plant species (Hamel *et al.*, 2006), analysis was carried out on data available from *A. thaliana*, *O. sativa* and *P. trichocarpa* (three highly diversified species representing monocots and eudicots). Analysis of the MAPK group showed that in general the T-D-Y group of MAPKs (group D) are generally in the molecular weight range of 55-79kDa, compared to the T-E-Y groups of MAPKs (A, B and C), which are generally smaller, between 42kDa and 45kDa. This suggested that p56 might be a member of the T-D-Y group of MAPKs, as its predicted protein size falls into this group.

Analysis of the *A. thaliana* and *P. trichocarpa* MAPK expression (Table 4.2.1a and Table 4.2.1b) suggested that the T-D-Y group of MAPKs were generally the most highly expressed of the MAPKs in pollen and male floral buds. Of the *AtMPK* genes, *AtMPK17*, *AtMPK8*, *AtMPK6*, *AtMPK19* and *AtMPK9* orthologues were suitable candidates based on expression in pollen. An *AtMPK6* orthologue (*PrMPKB*) had already been cloned from poppy pollen and evidence suggested that this gene was unlikely to encode p56. However, combining the predicted molecular weights of the *AtMPK* genes and expression data suggested that *AtMPK8*, *AtMPK9* and *AtMPK17* orthologues were good candidates for p56. Expression analysis of

PtMPK genes suggested that there were a number of suitable candidates although expression data was obtained using male floral buds, and not derived directly from pollen. Taking into account the molecular weight of the proteins, a *PtMPK17* orthologue was a good candidate to encode p56. Although there was no expression data available for the *OsMPK* genes, candidates were chosen based on the molecular weight of the proteins. *OsMPK12*, *OsMPK13* and *OsMPK15* encoded genes that were a similar size to p56. In a phylogenetic analysis (see Figure 4.3.2a) the *OsMPK12* and *OsMPK13* proteins clustered with the *AtMPK8*, *AtMPK9* and *AtMPK15* MAPKs, and *OsMPK15* clustered with *AtMPK16* suggesting that a protein in these groups may encode p56.

Although there have been a large number of studies to elucidate the MAPK signalling pathways, this work has focused on a small number of MAPK genes. In *A. thaliana* the majority of previous research has focused on *AtMPK4*, *AtMPK3* and *AtMPK6* and these genes are well characterised. These genes have been shown to play a variety of roles in response to biotic and abiotic stresses, response to hormones, in stomatal patterning, cell division, and floral abscission (see Introduction). To date, the only evidence of a role of an *A. thaliana* T-D-Y MAPK is that of *AtMPK18*, which has been shown to play a role in mediating cortical microtubule functions (Walia *et al.*, 2009). In monocotyledonous species there seem to be a higher number of T-D-Y MAPKs, compared to T-E-Y MAPKs, in each species. Even so, there is not a wealth of information on the function of these T-D-Y MAPKs. In rice several T-D-Y MAPKs have been characterised and have been shown to respond to a variety of stimuli including, abiotic and biotic stresses (including bacterial infection) and hormones (Lee *et al.*, 2008b; Yuan *et al.*, 2007; Reyna and Yang, 2006; Agrawal *et al.*, 2003a; Agrawal *et al.*, 2003b; Agrawal *et al.*, 2002; Fu *et al.*, 2002; He *et al.*, 1999; Cheong *et al.*, 2003; Huang *et*

al., 2002; Jeong *et al.*, 2006; Song and Goodman, 2002; Wen *et al.*, 2002). Because the MAPK genes described in the literature respond to such varied stimuli it is difficult to select candidates that could be orthologues of p56 based on the functional characteristics of these MAPKs.

4.3.2 Proteomics analysis

The data from the Sequest '*Arabidopsis/Brassica*' search (Table 4.2.2.1a) showed that two peptides occurred in nearly all of the MAPKs detected (AtMPK9, AtMPK8, AtMPK15, AtMPK19 and BnMPK9). AtMPK9 also had two specific peptide matches and AtMPK8 had one. The MAPKs that contained matches are all members of the T-D-Y group of MAPKs and AtMPK9, AtMPK8 and AtMPK15 also form a small cluster within the T-D-Y group. It was likely that the AtMPK15 peptides were identified due to the similarity of this protein to AtMPK9 and AtMPK8, rather than representing a true match. Although matches fell below the significance threshold, AtMPK9 had the greatest number of matches from this search. From the Sequest 'Plant' search there were two peptide matches from OsMPK8 and AtMPK9 and one from AtMPK8, PtMPK9-2, PtMPK9-1, BnMPK9, PtMPK17, OsMPK7 and AtMPK15. Although most of these matches were specific to each MAPK they were non-significant. These peptides were all from proteins that represented T-D-Y MAPKs. From the MASCOT search the best matches were with OsMPK13 and AtMPK9. AtMPK8 and OsMPK12 were also good matches. All of these proteins are grouped around the same AtMPK8, AtMPK9 and AtMPK15 cluster as mentioned before.

Although most of the peptides identified had non-significant probability values or low emPAI values, their presence was still an indicator of the identity of the gene that encodes p56. Figure 4.3.2a shows a phylogenetic tree including the *A. thaliana*, *O. sativa* and *P. trichocarpa* MAPKs and all the MAPKs from other species that contained peptides predicted to be found in p56. It is interesting to note that all the MAPK proteins that contained predicted peptides from p56 all fell into the group D category of MAPKs (with the T-D-Y activation domain) which, as alluded to before, suggests p56 could be encoded by a T-D-Y MAPK. Although the data obtained was non-significant, it was interesting that AtMPK9 and its closely related proteins from other species (BnMPK9, PtMPK9-1, PtMPK9-2, OsMPK13 and OsMPK12) had the most significant and most numerous peptides, predicted to be present in p56. Based on this, the proteomics data suggested that p56 was likely to be encoded by an *AtMPK9* orthologue.

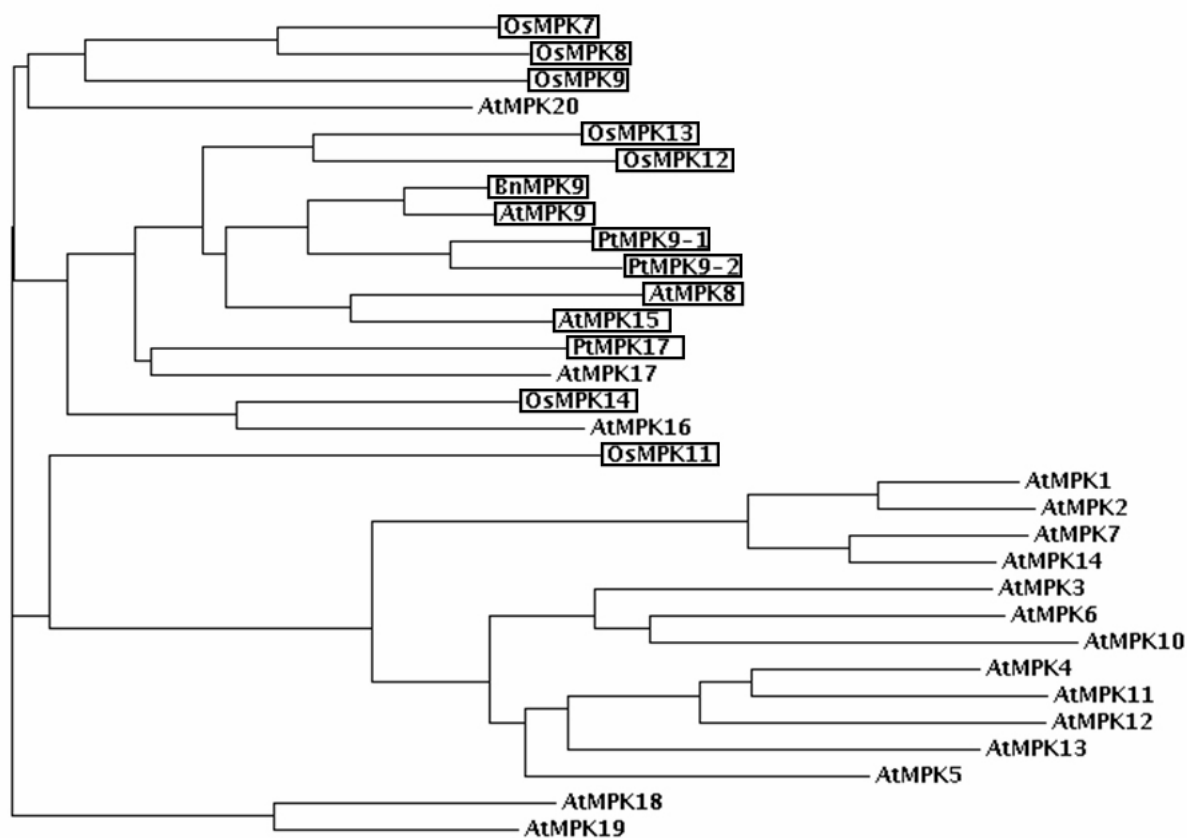


Figure 4.3.2a MAPK phylogenetic tree showing proteins that contained peptides found in p56. All the AtMPK, PtMPK and OsMPK genes are shown together with all other proteins that showed peptide matches with the p56 protein. All proteins that were identified from the FT-ICR MS analysis are shown in boxes. All the proteins that contained predicted matches to p56 fall into the group D MAPKs that contain the T-D-Y motif. At: *Arabidopsis thaliana*, Bn: *Brassica napus*, Os: *Oryza sativa*, Pt: *Populus trichocarpa*. The tree was constructed using ClustalW (Larkin *et al.*, 2007).

4.3.2.1 Construction of a plant-specific database for MS analysis

A plant database was created using protein sequences available from the NCBI database. Proteins from each genus of plant were searched for individually by using word-specific search terms (i.e. searching for 'Papaver' would select all the proteins that contained the word 'Papaver' in the protein name). One problem with this method of creating the database was that species that contained names of other species would also be included in the database (e.g. for the plant species *Chara*; *Characidium* (a fish) and *Charaxes* (a butterfly) proteins would also be included). Proteins were only collated from 50 plant species (most of them model species) but this is not an exhaustive collection of all the plant proteins (and species) existing in the NCBI database. A comprehensive plant database would greatly facilitate the Sequest method of analysing mass spectrometry spectra.

An additional problem with the 'Plant' database created is that it is also confined to a single time point. Although proteins are constantly being added to the NCBI database, there is no way to automate their inclusion into the specific 'Plant' database. In order to update the 'Plant' database a new search would have to be carried out periodically in order to add new proteins.

4.3.3 Summary of bioinformatics and proteomics analysis

Candidate genes were selected based on the following criteria: i) the predicted size of the protein is ~56kDa; ii) the tissue specificity of the gene and its expression in pollen; iii) identification of peptides present in the p56 protein. The bioinformatic analysis suggested that p56 was likely to be encoded by a T-D-Y MAPK and could be an *AtMPK9*, *AtMPK8* or

AtMPK17/PtMPK17 orthologue based on the size of the predicted proteins being ~56kDa and their expression in pollen. The proteomics analysis suggested that an *AtMPK9* orthologue was likely to encode p56, due to p56 containing the most numerous and most significant matches with *AtMPK9* orthologues (BnMPK9, PtMPK9-1, PtMPK9-2, OsMPK13 and OsMPK12). Therefore, based on the selection criteria, the combined bioinformatics and proteomics analysis suggested that a *MPK9* orthologue was the strongest candidate to encode p56.

CHAPTER 5

**Cloning and preliminary characterisation of *PrMPK9-1*: a
putative p56 candidate**

CHAPTER 5 - CLONING AND PRELIMINARY CHARACTERISATION OF *PrMPK9-1*: A PUTATIVE p56 CANDIDATE

5.1 INTRODUCTION

The bioinformatics and proteomics analyses suggested that it was highly probable p56 was encoded by a T-D-Y MAPK and was very likely to be a MPK9 orthologue. This chapter is concerned with cloning and the preliminary characterisation of candidate T-D-Y MAPKs from *P. rhoeas*. Degenerate PCR was used to clone genes from poppy pollen. By using predicted protein sequences from cloned poppy MAPKs the FT-ICR MS data was reanalysed, with the poppy MAPK protein sequences added to the 'Plant' database, to see if the cloned poppy MAPK genes showed any similarity to p56.

Reverse-transcription PCR (RT-PCR) provides a highly sensitive technique that can be used to semi-quantitatively measure RNA expression levels, thus allowing comparison of levels of specific transcripts in different cells or tissues (Wang *et al.*, 1989). One method of quantifying transcripts by RT-PCR is to compare them against levels of transcripts of a control, housekeeping gene (such as actin or glyceraldehyde-3-phosphate dehydrogenase (GAPDH)). Expression analysis of cloned poppy MAPKs will be investigated using RT-PCR to look at the expression of each gene in a variety of tissues. As there is little sequence data available for the *Papaver rhoeas* genome, it will be necessary to find a control gene that can be used to normalise nucleic acid loading for expression analysis experiments. Housekeeping genes are genes that are involved in basic cellular functions in order to sustain the cell and are generally constitutively expressed at the same level in all cells. For this reason they are good genes to

use as controls. Glyceraldehyde-3-phosphate dehydrogenase (GAPDH) is a housekeeping gene that has been used in both mammals and plants (Higgins *et al.*, 2004, Eisenberg and Levanon, 2003). GAPDH is a classical glycolytic enzyme, which converts glyceraldehyde-3-phosphate to 1,3-bisphosphoglycerate in a NAD⁺-dependent manner in order to provide the cell with energy and carbon molecules. It is now thought that as well as this glycolytic role GAPDH is also involved in membrane fusion, microtubule bundling, phosphotransferase activity, nuclear RNA export, DNA replication and DNA repair (for a review see Sirover, 1999). Therefore a GAPDH gene will be cloned from *P. rhoeas* to use as a control gene.

5.2 RESULTS

5.2.1 Cloning of candidate T-D-Y MAPKs from *Papaver rhoeas* pollen using T-D-Y specific primers

Attempts were made to clone and sequence T-D-Y MAPKs from poppy pollen. Degenerate primers were designed based on conserved regions of the T-D-Y group of *A. thaliana* MAPKs, that did not appear in the T-E-Y MAPKs (TDYdeg5'1, TDYdeg5'2, TDYdeg3'1 and TDYdeg3'2). For all the following amplifications ReddyMix PCR Master Mix was used to amplify cDNA from hydrated pollen, unless otherwise stated. The primers were used in all combinations in PCR amplifications, with annealing temperatures of 45°C, 40°C, or a round of seven cycles at 37°C followed by twenty-three cycles at 45°C. Amplification using leaf cDNA, with an annealing temperature of 40°C, was also carried out.

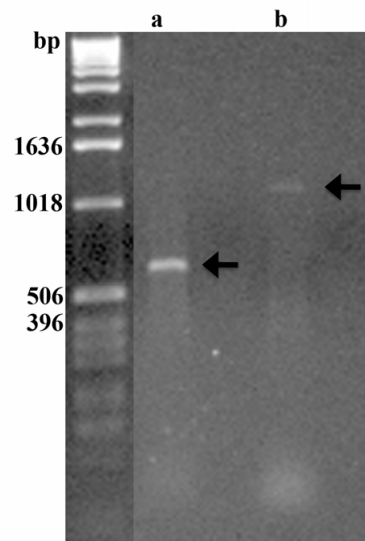


Figure 5.2.1a Amplification products from leaf cDNA using T-D-Y specific primers. Primers TDYdeg5'1 vs. TDYdeg3'1 (**a**, arrowed) and TDYdeg5'1 vs. TDYdeg3'2 (**b**, arrowed) amplified products from leaf cDNA. The predicted sizes of these fragment based on *A. thaliana* sequence were 536bp and 1003bp respectively.

Figure 5.2.1a shows that two products of 536bp and 1003bp were amplified from leaf cDNA using the TDYdeg5'1 vs. TDYdeg3'1 and TDYdeg5'1 vs. TDYdeg3'2 primer combinations. No products were obtained from other primer combinations. These two products were cloned and sequenced. The TDYdeg5'1 vs. TDYdeg3'1 amplification product shared the highest identity with *AtMPK20* (81.29%, 404/497bp) in a BLAST search.

To obtain the full-length gene sequence, 5'RACE and 3'RACE were carried out. For 3'RACE, PCR was carried out on leaf and pollen cDNA using a gene specific PrMPK20-3RACE1 primer and an abridged oligo-dT primer (3'RACE17AP). Nested PCR with a PrMPK20-3RACE2 and an unabridged oligo-dT primer (3'RACEAP) was then used to increase specificity. A fragment of ~1.1kb was amplified from pollen cDNA, which was subsequently cloned and sequenced. For 5'RACE, pollen cDNA was made in the standard way but the 5'RACE17AP primer was replaced with a gene-specific primer (PrMPK20-5R1). Nested primers (PrMPK20-5R2 and PrMPK20-5R3) were then used in subsequent PCR reactions along with 5'RACE17AP and 5'RACEUAP primers, respectively. A product of ~1.1kb was amplified, which was cloned and sequenced.

In order to check that the full-length sequence obtained was correct and to clone the genomic copy of the gene, primers were designed in the upstream UTR and downstream UTR regions of the gene (PrMPK20gen5' and PrMPK20gen3'). Also, an internal set of primers was designed (PrMPK20gen5'int and PrMPK20gen3'int) to aid cloning of the genomic copy, due to the predicted large size of the genomic DNA. PCR was carried out using a proofreading polymerase (KOD Hot Start polymerase). A ~1.9kb mRNA product from both pollen and leaf cDNA and two genomic fragments (~1.6kb and ~1.8kb) were amplified, cloned and

sequenced. The ORF was 1839bp in length, with the protein predicted to be 613 amino acids, with a molecular weight of 69.70kDa and a pI of 9.18. Figure 5.2.1b shows the predicted protein sequence of the gene (for the mRNA and genomic sequence see Appendix v.i). The ORF shared 68.08% (1254/1842bp) identity at the nucleotide level and 71.78% (440/613 amino acids) identity and 88.09% (540/613 amino acids) similarity at the amino acid level with *AtMPK20*, the most similar *AtMPK*, and was therefore designated *PrMPK20*.

>PrMPK20 pollen protein

```

MDFFTDYGDANRYKIQEVVVGKGSYGVVCSAIDTHTGKVAIKKIHDIFEHISDAARILREIKLLRLLRHDPDIVEI
KHIMLPPSRDFKDIYVVFELMESDLHQVIKANDDLTKDHYQFFLYQLLRALKYIHTANVFHRDLKPKNILANAN
CKLKICDFGLARVAFNDTPTTIFWTDYVATRWRAPELCGSFFFSKYTPAIDIWSIGCIFAELVTGKPLFPGKNVV
HQLDLMTDLLGTPLSLDTISRVRNEKARKYLTSMRKKQPVSFQAQKFPNADPFAVKLLERLLAFDPKDRPTAEEALA
DPYFKSLSRAREPSCQPI TKLEFEFERRRVTKDDIKELIFREILEYHPQLLKDYISGAERTNFLYPSAVDQFRK
QFAHLEDNGGKSAPVIPLERKHSVSLPRSTIVHSNTIPPKEQPDLRERQIQDTGYKYNPRDANGISGSLSRIQPV
AQQRNSMAKPGKVAGPVVPEYENTSGIRDAYDPRTYIRNAVLPQPI PPSYGI RRTNVMVNQEKGSGSEIERDLSLA
RQSQLSQCNMMAKLAPDVAIDINSSQFYLRAGVTSKIDQTDNNNQIAIDTNLLQAKSQFGEMGVAAAAAARR
KVSTVQYGM SRMY*

```

Figure 5.2.1b Predicted protein sequence of *PrMPK20* from pollen mRNA. The T-X-Y motif is indicated in grey. *: stop codon.

5.2.2 Cloning of candidate T-D-Y MAPKs from *Papaver rhoeas* pollen using gene specific primers

In addition to using degenerate primers, primers were also designed to amplify each *P. rhoeas* TDY gene specifically, with primers based on *A. thaliana* sequences (*AtMPK8*, *9*, *17*, *18*, *19* and *20*) and their orthologues from other species. In all cases the PCR amplifications were conducted using cDNA synthesised from RNA from hydrated pollen. Each primer set was used with various annealing temperatures. Table 5.2.2a shows the combinations of primers, and the annealing temperatures used during the PCR amplification. Where products approximated in size to their respective *A. thaliana* orthologue, they were cloned and

sequenced. Some primer sets gave no amplification product and some products, when sequenced, shared no homology with MAPK genes. Where no amplification product was obtained, 1 μ l of the PCR product was re-amplified. This further amplification was to ensure that each MAPK was not expressed at low levels in pollen and could therefore not be detected by a single amplification cycle.

	5' Primer	3' Primer	55°C	52°C	50°C	47°C
MAPK9	MPK9-5'1	MPK9-3'1		y		
	MPK9-5'2	MPK9-3'2		y		
	MPK9-5'2	MPK9-3'3	x	y	y	
	MPK9-5'2	MPK9-3'4	x	y	y	
	MPK9-5'3	MPK9-3'3	x		y	
	MPK9-5'3	MPK9-3'4	x		y	
	MPK9-5'2	MPK9-3'1			x	
	MPK9-5'3	MPK9-3'1			x	
	MPK9-5'4	MPK9-3'5			x	
	MPK9-5'4	MPK9-3'6			x	
	MPK9-5'5	MPK9-3'5			y	
	MPK9-5'5	MPK9-3'6			y	
	MAPK8	MPK8-5'1	MPK8-3'1		y	
MPK8-5'1		MPK8-3'2		x		
MPK8-5'2		MPK8-3'3				y
MPK8-5'2		MPK8-3'2				x
MPK8-5'1		MPK8-3'3				x
MPK8-5'1		MPK8-3'2				x
MAPK17	MPK17-5'1	MPK17-3'1		x		
	MPK17-5'1	MPK17-3'2	x	x	x	
	MPK17-5'1	MPK17-3'3	x		x	y
	MPK17-5'2	MPK17-3'2	x		x	x
	MPK17-5'2	MPK17-3'3	x		x	y
	MPK17-5'2	MPK17-3'4				y
	MPK17-5'3	MPK17-3'3				x
	MPK17-5'3	MPK17-3'4				x
	MPK17-5'3	MPK17-3'2				x
	MPK17-5'1	MPK17-3'4				x
	MPK17-5'1	MPK17-3'2				x
	MPK17-5'4	MPK17-3'5			y	
	MPK17-5'4	MPK17-3'6			y	
	MPK17-5'5	MPK17-3'5			y	
MPK17-5'5	MPK17-3'6			x		
MAPK19	MPK19-5'1	MPK19-3'1		x		
	MPK19-5'1	MPK19-3'2		y		
	MPK19-5'2	MPK19-3'3			x	
MAPK20	MPK20-5'1	MPK20-3'1		x		
	MPK20-5'1	MPK20-3'2		y		

Table 5.2.2a Primer and annealing temperatures used to clone specific T-D-Y MAPKs from *Papaver rhoeas* pollen. Boxes highlighted in grey represent successful MAPK genes sequenced. x: no fragment amplified; y: fragment amplified.

5.2.2.1 Cloning of a *Papaver rhoeas* MPK9-like gene

The MPK9-5'5 and MPK9-3'5 primers amplified a ~950bp fragment. This fragment was cloned and its nucleotide sequence determined. This gene shared highest identity (79.09%, 715/904bp) with *AtMPK9* at the nucleotide level. To obtain the full-length gene sequence, 5'RACE and 3'RACE were carried out. For 3'RACE, PCR was carried out on pollen cDNA using a gene specific PrMPK9-3R1 primer and an abridged oligo-dT primer (3'RACE17AP). Nested PCR with a PrMPK9-3R2 and an unabridged oligo-dT primer (3'RACEAP) was then used to increase specificity. A fragment of ~800bp was amplified, which was subsequently cloned and sequenced. For 5'RACE, pollen cDNA was made in the standard way but the 5'RACE17AP primer was replaced with a gene specific primer (PrMPK9-5R1). Nested primers (PrMPK9-5R2 and PrMPK9-5R3) were then used in subsequent PCR reactions along with 5'RACE17AP and 5'RACEUAP primers, respectively. A product of ~1kb was amplified, cloned and sequenced.

To confirm the full-length gene sequence was correct, primers were designed in the upstream UTR and downstream UTR regions of the gene (PrMPK9A5'NdeI and PrMPK9A3'NotI) and PCR was carried out using a proofreading polymerase (KOD Hot Start polymerase). A ~1.8kb mRNA product was amplified, cloned, and sequenced. The pollen ORF was 1818bp in length, and the predicted protein was 606 amino acids, with a molecular weight of 68.95kDa and pI of 6.32. The gene showed highest homology to *AtMPK8* and *AtMPK9*. The gene shared 68.09% (1240/1821bp) identity at the nucleotide level and 70.46% (427/606 amino acids) identity and 89.27% (541/606 amino acids) similarity at the amino acid level with *AtMPK8* and 62.00% (1129/1821bp) identity at the nucleotide level and 65.02% (394/606 amino acids) identity and 79.54% (482/606 amino acids) similarity at the amino acid level with *AtMPK9*.

This gene was designated *PrMPK9-2*. Figure 5.2.2.1a shows the predicted protein sequence of *PrMPK9-2* (for the mRNA sequence see Appendix v.ii).

>PrMPK9-2 pollen protein

```
MGGGGTLVDGVRWFQRRSSSTSSSSTSHRKLNSDDNKNDDNEETGQITLPATVPEEDEQQQEELTIIEDFDLS
GLKSIKVPKRQNWVTFDSQNKKGTVDEFFTEYGEASRYQIQEVIGKGSYGIVGSAVDHTTGEKVAIKKINDVF
GHVSDAMRILREIKLLRLLRHPDVVEIKHIMLPPSRREFKDIYVVFELMESDLHQVIKVNDDL TREHHQFFLFQL
LRALKYIHTANVFHRDIKPKNILVNADCKLKICDFGLARVSFNDAPSAIFWTDYVATRWRAPELCGSFFSKYTP
AIDIWSIGCIFAEMLSGKPLFPGKNVHVQLDLMTDLLGTPSTESITRIRNEKARRYLSNMRKKTVPVFSQKFPDA
DPLALQLLERLLAFDPKDRPSAEDALTDPYFRGLSTADRESSAQPI SKLEFEFEKRKLAKEDVRELIYREILEYH
PQMLQEYLRGADQASFMYPGVDRFKRQFAHLEENYGRGEKGTPLHRKHDSLPRERVCAPKDE TAYLKNNGFEKH
GAALVPSTIENLPRSHLEMDASLIQNGPSKGNYS PNSSLLKSASISGSQCVVVKGMKDSEEEPIMEQNGEVVDDLS
TKLRAL*
```

Figure 5.2.2.1a Predicted protein sequence of *PrMPK9-2* from pollen mRNA. The T-X-Y motif is indicated in grey. *: stop codon.

5.2.2.2 Cloning of a second *Papaver rhoeas* MPK9-like gene

The MPK17-5'4 and MPK17-3'5 primers amplified a fragment that was cloned and sequenced. This gene shared highest identity with *AtMPK8* (80.23%, 706/880bp) and *AtMPK9* (79.77%, 702/880bp) at the nucleotide level. To obtain the full-length gene sequence, 5'RACE and 3'RACE were carried out. For 3'RACE, PCR was conducted on pollen cDNA using a gene specific PrMPK8-3R1 primer and an abridged oligo-dT primer (3'RACE17AP). Nested PCR with a PrMPK8-3R2 and an unabridged oligo-dT primer (3'RACEAP) was then used to increase specificity. A fragment of ~700bp was amplified, which was subsequently cloned and sequenced. For 5'RACE, pollen cDNA was made in the standard way, but the 5'RACE17AP primer was replaced with a gene specific primer (PrMPK8_5RACE3). Nested primers (PrMPK8-5R2, PrMPK8-5R3) were then used in subsequent PCR reactions along with 5'RACE17AP and 5'RACEUAP primers, respectively. A product of ~500bp was amplified, cloned and sequenced.

To confirm the full-length gene sequence was correct, primers were designed in the upstream UTR and downstream UTR regions of the gene (PrMPK9₁gen5' and PrMPK8₃gen3'). PCR was carried out using a proofreading polymerase (KOD Hot Start polymerase). A ~1.6kb mRNA product was amplified, cloned, and sequenced. The pollen ORF was 1479bp in length and the predicted protein was 493 amino acids, with a molecular weight of 56.26kDa and pI of 6.49. The gene showed highest homology to *AtMPK8* and *AtMPK9*. The full-length sequence shared 63.05% (1116/1770bp) identity at the nucleotide level and 65.53% (386/589 amino acids) identity and 78.44% (462/589 amino acids) similarity at the amino acid level to the *AtMPK8* gene and 72.73% (1115/1533bp) identity at the nucleotide level and 79.41% (405/510 amino acids) identity and 92.16% (470/510 amino acids) similarity at the amino acid level with *AtMPK9*. This gene was designated *PrMPK9-1*. Figure 5.2.2.2a shows the predicted protein sequence of *PrMPK9-1* (for the mRNA sequence see Appendix v.iii).

>PrMPK9-1 pollen protein

```

MGETEFFTEYGEASRYQILEVIGKGSYGVVASAVDTHTEKVAIKKINDVFEHVSDATRILREIKLLRLLRHPDV
VEIKHIMLPPSRREFKDIYVVFELMESDLHQVIKANDDLTPEHYQFFLYQLLRSLKYIHSANVFHRDLKPKNILA
NADCKLKICDFGLARVSFNDAPSAIFWTDYVATRWRAPELCGSFFSKYTPAIDIWSIGCIFAELLTGKPLFPKG
NVVHQLDLMTDLLGTPSTESVARIRNEKARRYLSGMWKKPPVPFTQKFPKVDPLALNLLERLLAFDPKDRPSAEE
ALADPYFHGLANVDREPSTQPI SKFEFEFERRKLSKEDVRELIYREILEYHPQMLQEYLNQADQTSFLYPSGVDR
FKRQFAHLEEHYKSGEKSTPPLQRQHASLPRERVCAPKEESADQHDNSENRSAA SVVHKTLQSP TKANSATRSL
MKSESISASQCVVNGKKNLTGEPIDEQSEVDDLSQKISQLGS*

```

Figure 5.2.2.2a Predicted protein sequence of *PrMPK9-1* from pollen mRNA. The T-X-Y motif is indicated in grey. *: stop codon.

5.2.2.3 Attempts to clone *Papaver rhoeas* *MPK8*-like, *MPK19*-like and *MPK17*-like genes

Several primer sets were designed to amplify and clone *MPK8*, *MPK19* and *MPK17* orthologues from pollen cDNA (Table 5.2.2a), but all attempts were unsuccessful. In addition,

PCR amplification was attempted on leaf cDNA, but it was not possible to obtain products from these genes.

5.2.3 Re-analysis of the FT-ICR MS data

To determine if any of the recently cloned *P. rhoeas* MAPK showed any similarity to the p56 protein, the FT-ICR MS data, from a protein sample corresponding to p56 (see Chapter 4), was reanalysed. The predicted proteins of the *PrMPK3*, *PrMPK20*, *PrMPK9-1* and *PrMPK9-2* genes were added to the 'Plant' database created for analysis with the Sequest search engine. The FT-ICR MS data was then cross-correlated with the 'Plant' database with these new proteins added. In theory, if p56 were one of these recently cloned MAPKs, more peptides matches would be expected, with a greater significance. Table 5.2.3a shows the results of the reanalysis of the FT-ICR MS data. Some of the peptides from the previous analysis (Figure 4.2.2.1c) were still present but, as before, were not significant (as would be expected). The highest scoring of the *P. rhoeas* MAPK genes was PrMPK9-1. PrMPK9-1 had two peptides matches that were highly significant (KGSYGVVASAVDTHHTGEKV and KVDPLALNLLERL), one peptide that was non-significant, just below the significance threshold (RYQILEVIGKG) and one peptide that, although non-significant, had a higher score than all the other previous MAPK peptide matches (KKPPVPFTQKF). The only other *P. rhoeas* MAPK that was present was PrMPK9-2 with two matches (KGNYSPLNSLLKS and KGSYGIVGSAVDTHHTGEKV), but both were non-significant.

Reference Scan(s)	Peptide	P (pro) P (pep)	Score XC
PrMPK9-1		0.000075250920647	40.22
	K.GSYGVVASAVDTHHTGEK.V	0.000075250920647	4.41
	R.YQILEVIGK.G	0.0018111587421	2.79
	K.VDPLALNLLER.L	0.0003717292925217	3.06
	K.KPPVPFTQK.F	0.6772105976899	1.54
AtMPK8		0.9680661595954	20.15
	K.INDVFEHVSDATR.I	0.9680661595954	3.08
	K.HIMLPPSR.R	1	1.74
PrMPK9-2		0.9999757996385	18.18
	K.GNYSPNSLLK.S	1	1.90
	K.GSYGIVGSAVDTHHTGEK.V	0.9999757996385	3.53
AtMPK15		1	18.13
	R.LIAFDPK.D	1	2.06
	K.INDVFDHISDATR.I	1	2.57
BnMPK9		1	10.09
	R.QFAHLEEHYK.G	1	1.84
OsMPK7		0.9996027803257	10.05
	R.QFAILEENGK.S	0.9996027803257	1.04
PtMPK17		1	8.14
	K.YIHTGNVFHR.D	1	2.77
AtMPK19		1	8.10
	R.LLAFDPK.D	1	1.94

Table 5.2.3a Reanalysis of the mass spectrometry data using the ‘Plant’ database. MAPK peptide matches from the 'Plant' database with the newly cloned *Papaver rhoeas* MAPKs added (*PrMPK3*, *PrMPK20*, *PrMPK9-1* and *PrMPK9-2*). *PrMPK9-1* is the highest scoring MAPK with the most significant peptide matches. Peptides with a probability (**P (pep)**) of less than 0.001 are considered significant.

5.2.4 Expression analysis of *Papaver rhoeas* MAPKs using semi-quantitative RT-PCR

RT-PCR can be used to semi-quantitatively measure levels of gene expression. To determine where the *P. rhoeas* MAPK genes were expressed, RT-PCR was carried out on each of the cloned MAPK genes in a range of tissues. As p56 is expressed in pollen, it was argued that the gene encoding p56 would also be expressed in pollen, and possibly specific to this tissue. In order to quantify transcripts by RT-PCR they need to be compared against transcript levels of a control, housekeeping gene (e.g. GAPDH). As there is little sequence data available for

P. rhoeas, a suitable control gene had to be identified. Therefore attempts were made to clone and sequence GAPDH from *Papaver rhoeas* to use as a control.

5.2.4.1 Cloning of a *Papaver rhoeas* GAPDH

Previously, a potential fragment of a *GAPDH-C* subunit had been cloned using primers based on conserved regions of the same gene from other plant species (GAPDN and GAPDC). This corresponded to base pairs 345 to 885 of the ORF in *Arabidopsis thaliana* (*GAPC-1*, At3g04120) (Wheeler, unpublished). In order to clone a full-length *Papaver rhoeas* *GAPDH-C* orthologue, the above clone was sequenced, giving a 541bp fragment that showed highest homology to the *A. thaliana* *GAPC-2* gene (At1g13440). Based on this sequence, new specific poppy primers were designed (PrGAPD5' and PrGAPD3'). To check these primers could amplify the poppy GAPDH gene, RNA was extracted from both leaf and hydrated pollen and used to synthesise cDNA. PCR amplification of the cDNA was carried out using ReddyMix PCR buffer and a fragment of ~400bp was cloned and sequenced (Figure 5.2.4.1a). The sequence was 423bp in length and was most similar to the *A. thaliana* *GAPC-2* gene (At1g13440) sharing 81% identity.

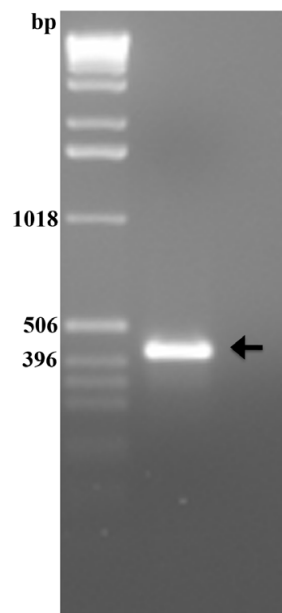


Figure 5.2.4.1a Amplification of *PrGAPC-2*. PCR amplification of the ~400bp GAPDH fragment from *P. rhoeas* (arrowed). Based on *A. thaliana* sequence the fragment was predicted to be 423bp.

In order to determine the full-length gene sequence 5'RACE and 3'RACE were used. For 3'RACE, PCR was carried out on leaf cDNA using the above PrGAPD5' primer and the abridged oligo dT primer (3'RACE17AP). The ~950bp fragment was cloned, and sequenced. The resultant 969bp fragment contained a 673bp coding sequence followed by a 296bp downstream UTR. The coding sequence shared 82.17% (553/673) identity with *AtGAPC-2*. For 5'RACE, cDNA was made in the normal way but the 5'RACE17AP primer was replaced with a gene specific primer (PrGAPD-5R1). Nested primers (PrGAPD-5R2 and PrGAPD-5R3) were then used in subsequent PCR reactions along with 5'RACEAAP primer and 5'RACEUAP primers, respectively. The ~600bp fragment was cloned, and sequenced. The 5'RACE product was 570bp.

To confirm that the sequence obtained was correct, the full gene was re-amplified from leaf cDNA using a proofreading polymerase (KOD Hot Start DNA polymerase (Novagen)), and also from genomic DNA in order to obtain the full-length genomic copy of the gene. PrGAPDCu/s and PrGAPDCd/s primers were used, located in the up-stream and down-stream UTR regions of the gene, respectively. The resultant ~1.2kb (mRNA) and ~2.9kb (genomic) fragments cloned, and sequenced. The leaf mRNA had a 1020bp ORF and showed 82.35% (840/1020bp) identity with *AtGAPC-2* (AT1G13440). The protein was predicted to be 339 amino acids in length, with a molecular weight of 36.93kDa and a pI of 6.34. This shared 87.32% (296/339) identity and 97.35% (330/339) similarity with *AtGAPC-2*. The genomic copy was 2725bp in length (from start to stop codon), and contained 10 exons (9 introns). The predicted protein is shown in figure 5.2.4.1b (for the mRNA and genomic sequence see Appendix v.iv)

>PrGAPC-2 protein

```
MAPAKIKIGINGFGRIGRLVARVALQRDDVELVAVNDPFIITTDYMTYMFKYDTVHGQWKHHELKVKDTKTLFGE  
KEVAVFGCRNPEEIPWAETGAEYIVESTGVFTDKDKAAAHLKGGAKKVIISAPSKDAPMFVVGVNEKEYTSDINI  
LSNASCTTNCLAPLAKVINDRFGIVEGLMTTVHAMTATQKTVDGPSSKDWRGGRAASFNIIPSSTGAAKAVGKVL  
PALNGKLTGMAFRVPTVDVSVVDLTVRLEKKATYEEIKAAIKEESEGGKMGILGYVDEDLVSTDFLGDNRSSIFD  
AKAGIALNDNFVKLVSWYDNEWGYSRVIDLIVHVANTQ*
```

Figure 5.2.4.1b Predicted protein sequence of *PrGAPD-C*. *: stop codon.

5.2.4.2 Expression analysis of *Papaver rhoeas* MAPKs

In order to look at the expression profiles of the cloned poppy MAPKs (*PrMPKA*, *B*, *C*, *20*, *3*, *9-1* and *9-2*), semi-quantitative RT-PCR was used to examine expression in a variety of tissues. Primers were designed to amplify each gene (GAPD: PrGAPD5' vs. PrGAPD3', GAPDN vs. GAPDC; MPK9-2: PrMPK91gen5' vs. PrMPK8gen3'; MPK9-1: PrMPK92gen5' vs. PrMPK92gen3'; MPK3: PrMPK3_5'A vs. PrMPK3_3'C, PrMPK3-5' vs. PrMPK3-3'; MPK20: PrMPK20-5' vs. PrMPK20-3'; MPKB: PrMPKB-5'1 vs. PrMPKB-3'1, PrMPKB-5'2 vs. PrMPKB-3'2; MPKC: PrMPKC-5'1 vs. PrMPKC-3'1, PrMPKC-5'2 vs. PrMPKC-3'2) and *PrGAPC-2* (see above) was used as a control to normalise loading. Expression was examined in the following tissues: immature anthers; an anther series with -3, -2, -1 and +1 stages of anther development (numbers denote days from anthesis); hydrated pollen; root; leaf and stigma.

RNA was extracted from 100mg of each of the tissues (maximum 100µg total RNA) and from this cDNA was synthesised. PCR was then carried out on this cDNA. The semi-quantitative RT-PCR was carried out at least three times, on at least two different RNA samples, and often with several primer sets.

The GAPDH controls were separated on 1% agarose gels and the peak densities of each DNA band were calculated using Quantity One[®] software. A second gel was then run with roughly equal levels of GAPDH and relative amounts of the MAPK gene of interest, compared to the GAPDH control. Figure 5.2.4.2 shows an example of the PrMPK9-1 expression levels. In order to analyse the data accurately, each sample had to be normalized to the GAPDH control. QuantityOne software was used to measure the peak density of each of the DNA bands for each tissue sample. To standardize the data, the GAPDH control peak density was measured and adjusted to an arbitrary value of 100,000 units. The value for each MAPK gene tissue sample was then calculated relative to this GAPDH value. The results are shown in Figure 5.2.4.2b.

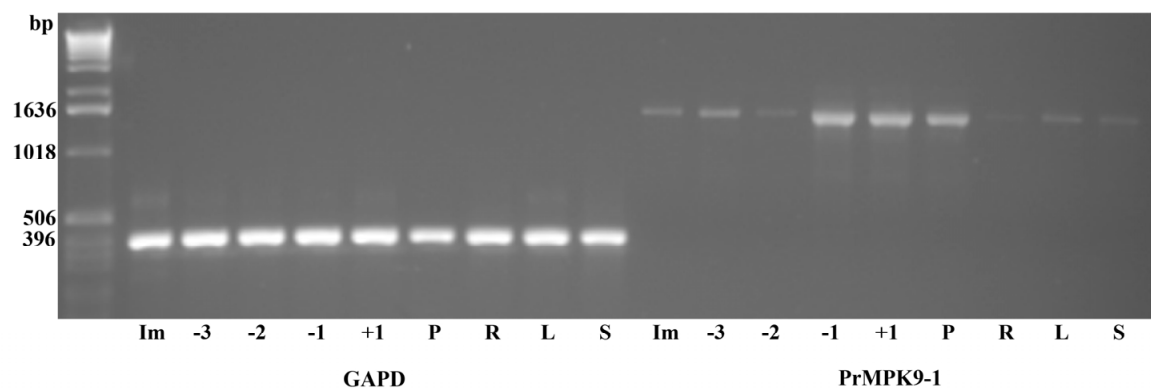


Figure 5.2.4.2a Semi-quantitative RT-PCR expression analysis of PrMPK9-1. **Im:** immature anthers; **-3/-2/-1/+1:** stages of anther development (days from anthesis); **P:** hydrated pollen; **R:** root; **L:** leaf; **S:** stigma.

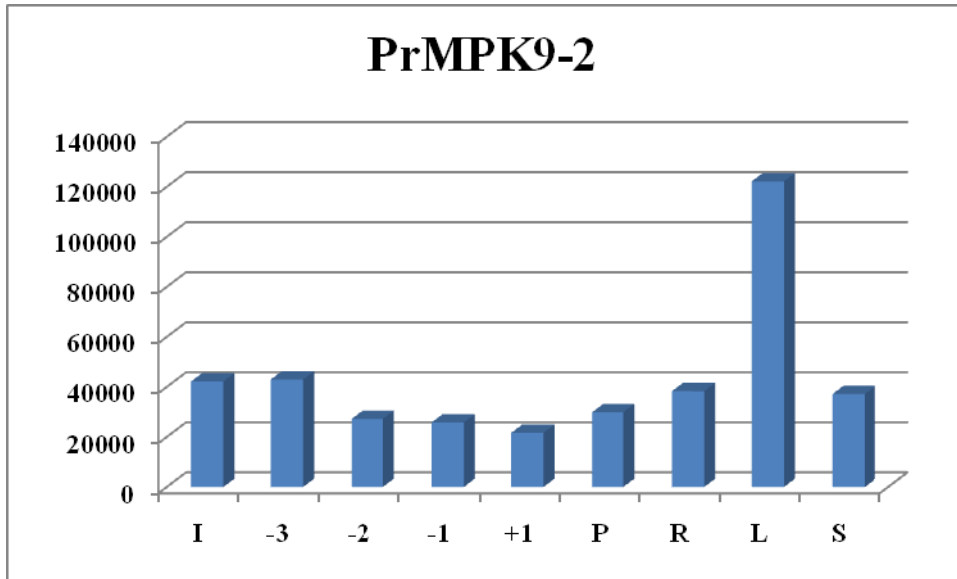
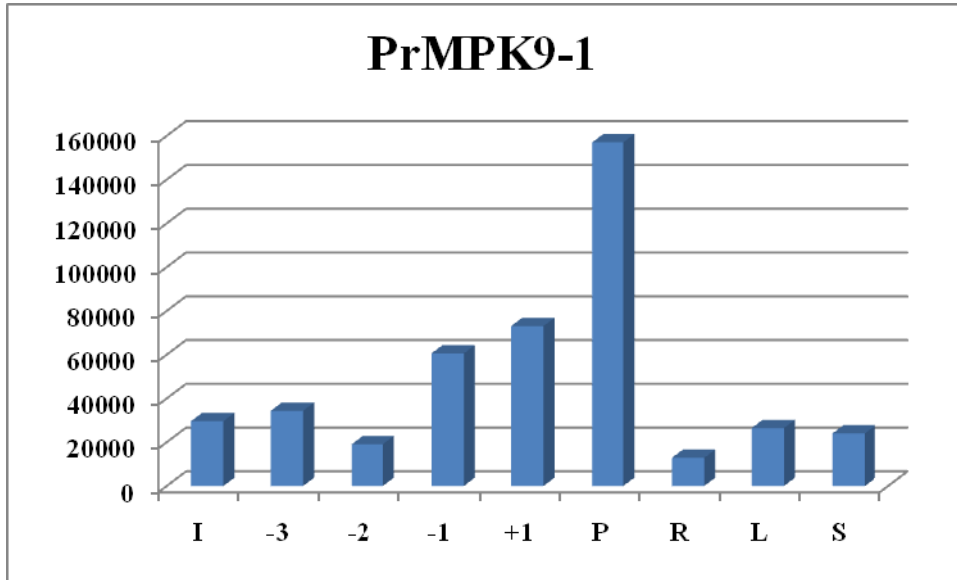


Figure 5.2.4.2b (see below)

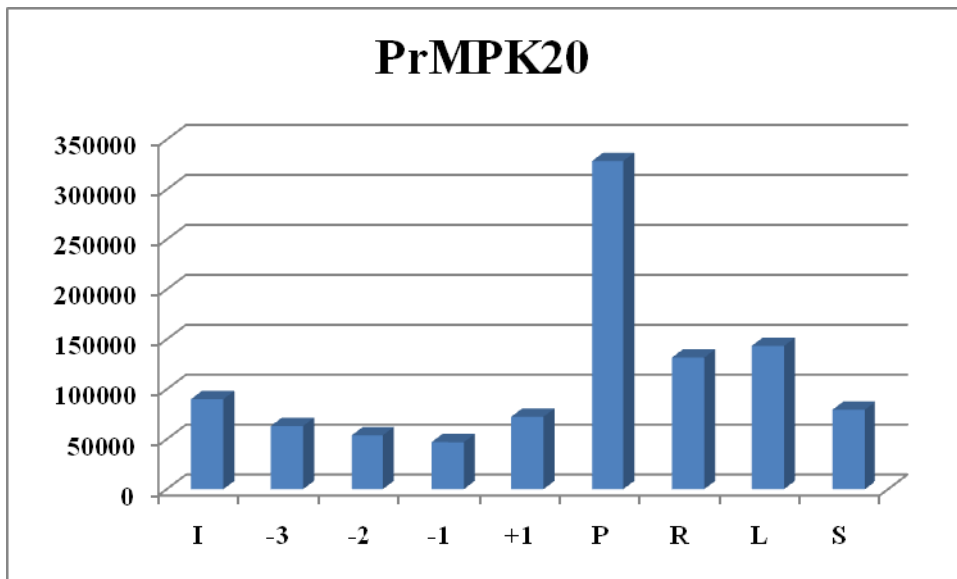
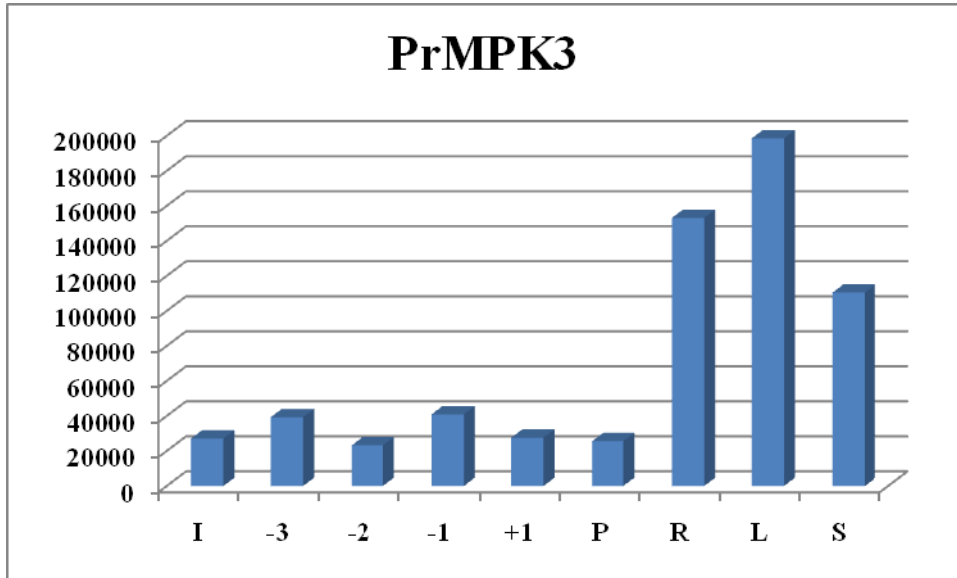


Figure 5.2.4.2b (see below)

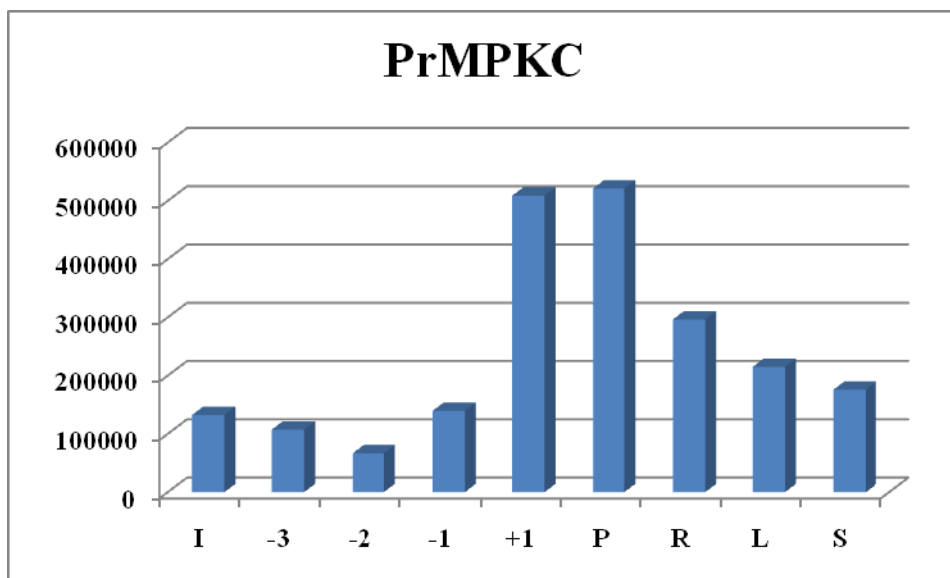
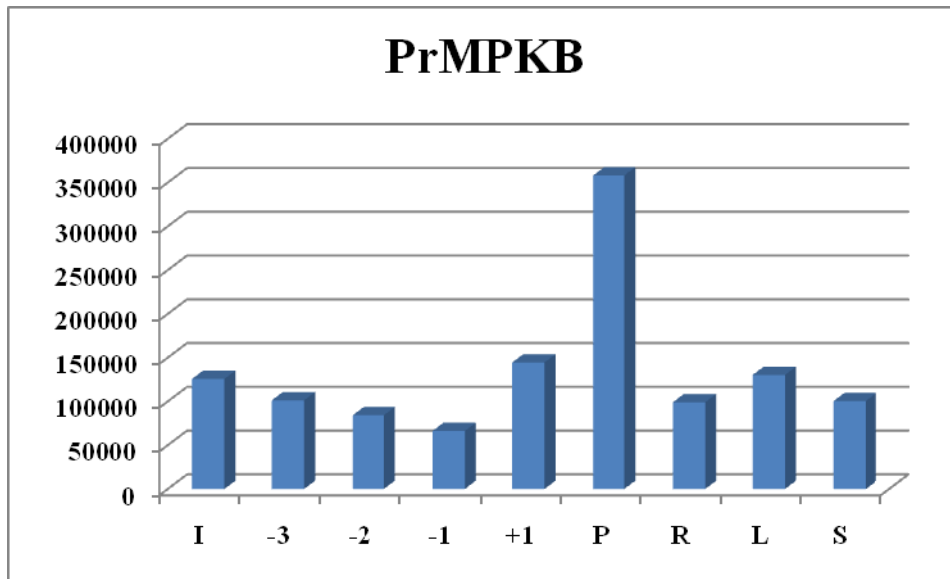


Figure 5.2.4.2b Semi-quantitative RT-PCR expression analysis of *P. rhoeas* MAPKs. Relative levels of expression are shown compared to a normalised GAPD control gene. **Im**: immature anthers; **-3/-2/-1/+1**: stages of anther development (days from anthesis); **P**: hydrated pollen; **R**: root; **L**: leaf; **S**: stigma.

5.3 DISCUSSION

5.3.1 Cloning of candidate T-D-Y MAPK genes from *P. rhoeas*

Attempts were made to clone candidate T-D-Y MAPKs from *Papaver rhoeas* pollen. To date, potential *AtMPK3*, *AtMPK20* and two *AtMPK9/AtMPK8* orthologues have been cloned. Cloning experiments led to the sequencing of two genes that shared high homology to *AtMPK9* and *AtMPK8*. Although initial homology searches suggested an *AtMPK8* and an *AtMPK9* orthologue had been cloned, phylogenetic analysis suggested this might not be the case. Both *P. rhoeas* DNA and protein sequences were introduced into a phylogenetic tree prediction program (ClustalW, <http://www.ebi.ac.uk/Tools/clustalw2/index.html>) along with *A. thaliana* T-D-Y MAPKs. The trees are shown in Figure 5.3.1a.

Phylogenetic analysis suggested that both *PrMPK9-1* and *PrMPK9-2* were both most closely related to *AtMPK9* at both the nucleotide and amino acid level. Although *AtMPK8* and *AtMPK9* share high homology, one difference is that *AtMPK8* contains a 249bp 5' extension compared to *AtMPK9* (or 83 amino acids at the N terminus). *PrMPK9-2* shows a similar 5' extension, but *PrMPK9-1* does not. The original homologies were calculated over the whole length of the genes/proteins and therefore do not take into account that *PrMPK9-1* is shorter. If we compare the genes with the 5' (or N terminus) removed, *PrMPK9-2* shows higher homology with *AtMPK9* than with *AtMPK8* (*PrMPK9-2*; 72.98% (1129/1547bp) identity at the nucleotide level, and 76.65% (394/514 amino acids) identity and 93.77% (482/514 amino acids) similarity at the amino acid level with *AtMPK9*, compared to 68.09%, 70.46% and 89.27% with *AtMPK8*, respectively).

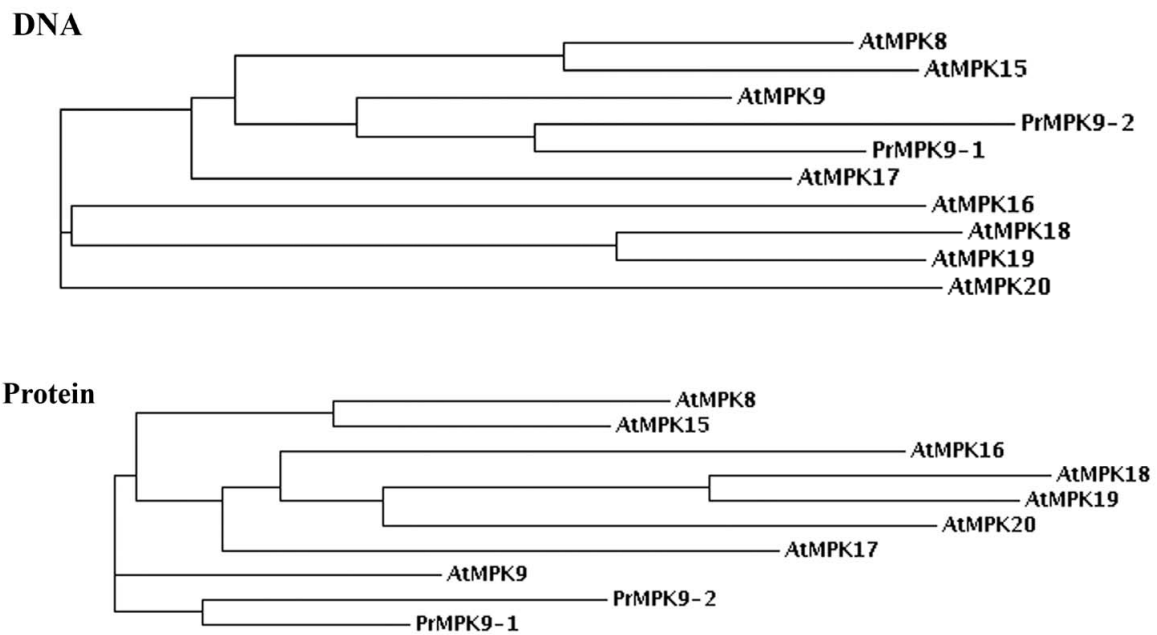


Figure 5.3.1a. Phylogenetic tree of PrMPK9-1, PrMPK9-2 and the T-D-Y AtMPKs. DNA (above) and protein (below) phylogenetic trees of PrMPK9-1, PrMPK9-2 and the T-D-Y AtMPKs. At: *Arabidopsis thaliana*; Pr: *Papaver rhoeas*. The tree was constructed using Clustal W (<http://www.ebi.ac.uk/Tools/clustalw/>; Larkin *et al.*, 2007).

The identification of two *MPK9* orthologues in a single species has also been demonstrated in the Poplar (*Populus trichocarpa*) MAPKs (Nicole *et al.*, 2006). Here, Nicole *et al.* showed that there were two *AtMPK9* orthologues, *PtMPK9-1* and *PtMPK9-2* (Figure 5.3.1b). In a number of cases in Poplar, two paralogues were identified for a single *A. thaliana* MAPK sequence (*PtMPK3-1* and *PtMPK3-2*, *PtMPK6-1* and *PtMPK6-2* etc.). It is also worth mentioning that of the 21 Poplar genes cloned, there were no orthologues of *AtMPK8*, which may explain why it has not been possible to clone an *AtMPK8* orthologue from poppy.

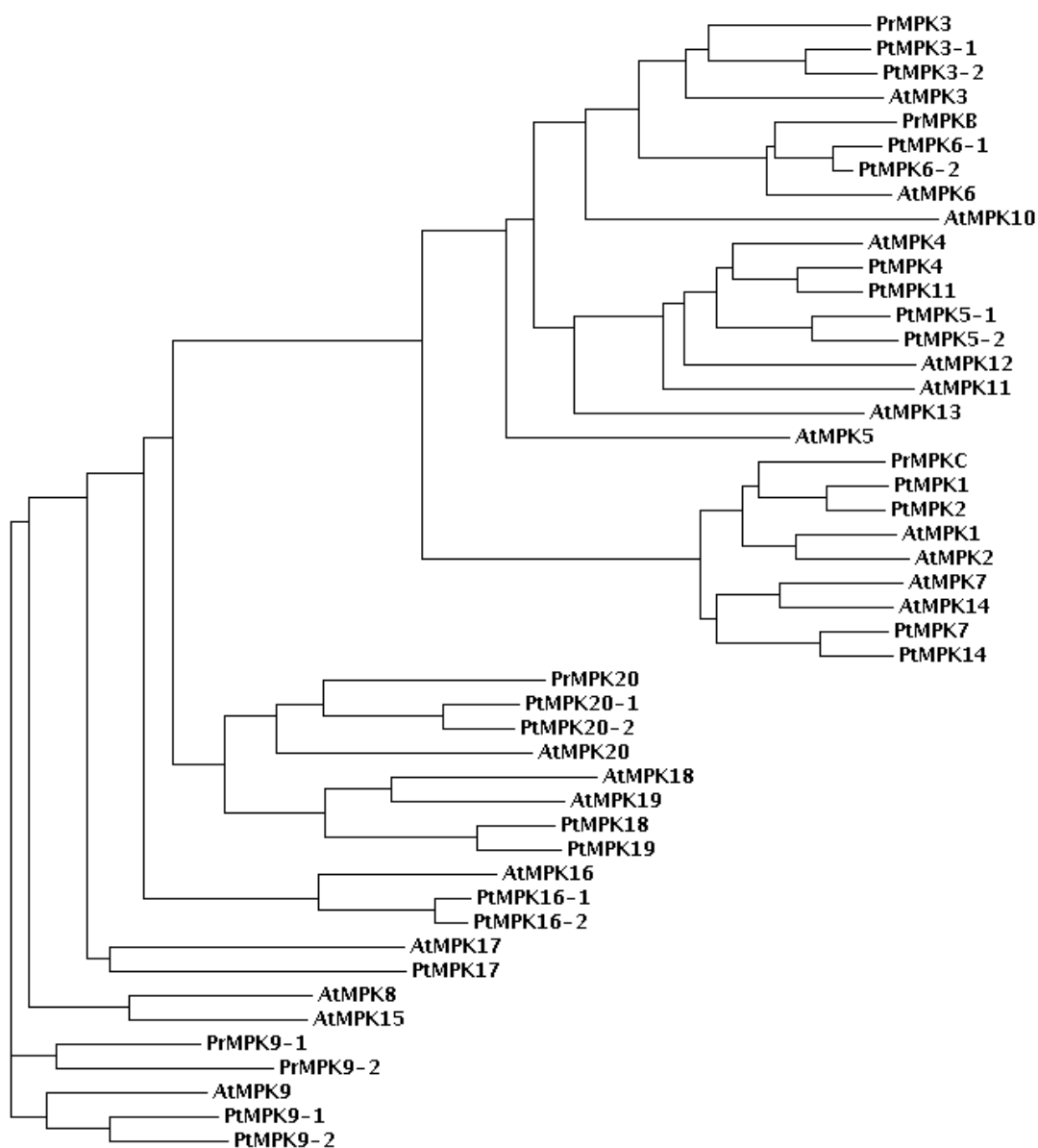


Figure 5.3.1b Phylogenetic tree of the *A. thaliana*, *P. trichocarpa* and *P. rhoeas* MAPK proteins. *P. rhoeas* and *P. trichocarpa* both have two *MPK9*-like genes, and no *MPK8*-like genes. PrMPK20 clusters with PtMPK20-1, PtMPK20-2 and AtMPK20. At: *Arabidopsis thaliana*; Pr: *Papaver rhoeas*; Pt: *Populus trichocarpa*. The tree was constructed using Clustal W (<http://www.ebi.ac.uk/Tools/clustalw2/index.html>; Larkin *et al.*, 2007).

Figure 5.3.1b also shows the relationship of *PrMPK20* to the other MAPKs. Due to the fact it clusters with other *MPK20* orthologues it was supposed that this gene was a *MPK20* orthologue.

5.3.2 Re-analysis of the FT-ICR MS data

The re-analysis of the FT-ICR MS data showed that the p56 protein shared highly significant peptide matches with PrMPK9-1. Although the data showed matches to other MAPKs, these were non-significant. This was very good evidence that p56 could be encoded by *PrMPK9-1*. It was not possible to re-analyse the MS data using a MASCOT search. MASCOT relies on proteins that are presently submitted to one of the databases it uses for searching (MSDB, NCBIInr, SwissProt or dbEST). As the poppy predicted proteins are not currently submitted to any of these databases it was not possible to re-analyse the MS using a MASCOT search.

5.3.3 Expression analysis of the *Papaver rhoeas* MAPKs

PrMPK9-1 showed increasing expression during pollen development and relatively low expression in root, leaf and stigma. This expression mirrors the pollen *S*-gene (*PrpS*) expression (Wheeler *et al.*, 2009), which would be expected if both these genes were involved in SI. The closely related *PrMPK9-2* seemed to show a low and potentially decreasing level of expression during pollen development. In contrast to *PrMPK9-1*, its expression was highest in leaf, which potentially suggests different roles for these genes. In *A. thaliana* *AtMPK9* is highly expressed exclusively in mature pollen, and late stages of stamen maturation (data

from NASC and AtGen expression data). This pattern of expression is similar to that seen in *PrMPK9-1*, but shows no similarity to *PrMPK9-2* expression.

PrMPK3 expression was low in pollen related tissues, high in root and leaf and moderate in stigma. This result helps to explain why there was difficulty in amplifying *PrMPK3* from pollen, especially when compared to the expression of its closest *P. rhoeas* homologue *PrMPKB*. *PrMPKB* shows high expression in hydrated pollen and relatively low expression in other tissues. The *A. thaliana* *AtMPK3* is highly expressed in various leaf related tissues and this is comparable with *PrMPK3*. Although *AtMPK3* shows moderate expression in roots, there is no evidence the gene is expressed in the stigma. *AtMPK6* shows high exclusive expression in mature pollen and late stages of stamen maturation, which is similar to *PrMPKB*.

PrMPKC showed highest expression in pollen and mature anthers. In comparison, its closest orthologues in *A. thaliana*, *AtMPK1* and *AtMPK2*, show a low level of expression in all tissues and no obvious tissue specificity.

PrMPK20 showed high expression in mature pollen and relatively low expression in all other tissues. In *A. thaliana* *AtMPK20* shows a moderate level of expression in most of the tissues studied, suggesting no tissue specificity.

Semi-quantitative RT-PCR is useful to give an indication of which tissues express a particular gene. However, in order to accurately measure the expression levels of the *PrMPKs*, real-time RT-PCR (qRT-PCR) will need to be used. Traditional RT-PCR uses agarose gels for

detection of PCR amplification at the final phase or end-point of the PCR reaction. In comparison, real-time RT-PCR allows for the detection of PCR amplification during the early phases of the reaction, in the exponential growth phase. Measuring the kinetics of PCR in the early phases of the reaction provides a distinct advantage over traditional RT-PCR detection. In real-time RT-PCR each amplicon generated incorporates fluorescent reporter signal, which is measured and this is directly proportional to the number of amplicons generated. This allows real-time RT-PCR to detect two-fold differences in gene expression, compared to ten-fold in traditional RT-PCR techniques. In addition to this, real-time RT-PCR requires no post-PCR processing.

5.3.4 Summary

In summary, this chapter has provided convincing evidence that p56 is likely to be encoded by *PrMPK9-1*. In the previous chapter (Chapter 4), criteria were stated which the gene that encodes p56 should satisfy: i) the predicted size of the protein is ~56kDa; ii) the tissue specificity of the gene and its expression in pollen; iii) identification of peptides present in the p56 protein. *PrMPK9-1* is predicted to encode a protein of 56.26kDa, it is highly expressed in pollen compared to other tissues, and peptides found in p56 show high homology to those found in the PrMPK9-1 predicted protein.

CHAPTER 6

Studies to confirm *PrMPK9-1* encodes p56

CHAPTER 6 - STUDIES TO CONFIRM *PrMPK9-1* ENCODES p56

6.1 INTRODUCTION

This chapter describes the production of an anti-PrMPK9-1 antibody and other techniques used to confirm that p56 is encoded by *PrMPK9-1*. The production of antibodies to specific proteins is a powerful tool in molecular biology and may be used to confirm the identity of specific proteins, by immuno-precipitation and western blotting experiments and to further characterise genes using immuno-localisation. Previous results suggested that *PrMPK9-1* was a very strong candidate to encode p56. In order to confirm the identity of p56, a specific antibody will be raised against PrMPK9-1. Western-blotting experiments will be carried out to determine if the anti-PrMPK9-1 antibody can detect p56.

Phospho-protein purification systems can be used which separate the phosphorylated and un-phosphorylated proteins from cell lysates and can be used to investigate the phosphorylation state of specific proteins (Meimoun *et al.*, 2007). As approximately 10% of the protein mass in the cell is phosphorylated, purification allows isolation of phospho-proteins, which reduces the complexity of the cell lysate and allows for more sensitive detection. As p56 is predicted to be a MAPK, it becomes phosphorylated when activated by a stimulus, for example in an incompatible SI reaction. In addition, serine/threonine protein phosphatase inhibitors can artificially activate MAPKs. This phosphorylation allows them to be selected by phospho-protein purification. In order to enrich for phosphorylated proteins, phospho-proteins will be selected using a column and western blotting will be carried out to determine if the anti-

PrMPK9-1 antibody can cross-react with a ~56kDa phosphorylated protein, as would be expected if p56 is encoded by *PrMPK9-1*.

Specific antibodies can be used for immuno-precipitation, which allows isolation of specific proteins, or groups of proteins, from a solution. Immuno-precipitation can be used to identify antigens, concentrate or enrich for specific proteins, or to establish protein-protein interactions (Trieu *et al.*, 2009; Elion, 2006; Kaboord and Perr, 2008). To determine if p56 is encoded by *PrMPK9-1*, experiments will be carried out to see if p56 could be immuno-precipitated with a PrMPK9-1 antibody. Previous evidence had shown that p56 could cross-react with an antibody that specifically detects activated MAPKs (anti-pTXpY antibody), by cross-reacting with the dually phosphorylated activation motif (Rudd *et al.*, 2003). Once proteins are immuno-precipitated with the anti-PrMPK9-1 antibody, experiments will be carried out to determine whether the anti-pTXpY antibody can identify these proteins.

The anti-PrMPK9-1 antibody can also be used in immuno-localisation experiments, to determine the localisation of the PrMPK9-1 protein. In plants, various studies have provided evidence for the localisation of MAPKs in various tissues, in both the cytoplasm and nucleus (Préstamo *et al.*, 1999, Cheong *et al.*, 2003). Immuno-localisation has also provided evidence of the translocation of MAPKs from the cytoplasm to the nucleus, in response to changing cell conditions, such as pollen maturation and germination, or stress responses, such as wounding or pathogen attack (Ligterink *et al.*, 1997, Coronado *et al.*, 2002, Koo *et al.*, 2007). The localisation of PrMPK9-1 will be investigated in growing pollen and also in response to an incompatible SI response.

In an attempt to understand and characterize the functions of proteins it is useful to express these proteins recombinantly in a controlled environment. Therefore, expression of a PrMPK9-1 recombinant protein will be carried out, in order to further characterise the protein.

6.2 RESULTS

6.2.1 Expression of full-length PrMPK9-1 recombinant protein

To allow further analysis of *PrMPK9-1*, attempts were made to express the full-length recombinant protein. Primers were designed to amplify the full-length coding region of *PrMPK9-1* (PrMPK9-1_5'NdeI and PrMPK9-1_3'XhoI). The primers contained *NdeI* and *XhoI* restriction sites to allow directional ligation of *PrMPK9-1* into the pET-21b expression vector. A 1482bp cDNA fragment, corresponding to the predicted ORF, was amplified using a proofreading polymerase (KOD Hot Start DNA Polymerase) and is shown in Figure 6.2.1a.

The *PrMPK9-1* amplification product was cloned in the pDrive cloning vector, and recombinant plasmid DNA was sequenced to verify the construct. *PrMPK9-1* was digested from the pDrive cloning vector using the *NdeI* and *XhoI* restriction sites and ligated into the pET-21b expression vector (which was also digested using the same restriction sites). The pET-21b(+) vector is a protein expression vector that contains a tag, consisting of six histidine residues (6xHis-tag), downstream of the multiple cloning site. Expression of the 6xHis-tag downstream of the recombinant protein allows identification and purification of the protein of interest. The vector also contains a *lac* promoter and operator that allow induction of gene

expression using IPTG (Isopropyl β -D-1-thiogalactopyranoside). The PrMPK9-1-pET-21b construct was cloned and recombinant plasmid DNA was sequenced to verify the construct.

For protein expression, plasmid DNA containing the PrMPK9-1-pET-21b construct was used to transform *E. coli* BL21 competent cells, which are highly efficient in high-level expression of a variety of recombinant proteins (Terpe *et al.*, 2006). Pilot experiments were carried out to test protein expression levels. *E. coli* was grown and expression was either induced or not induced for either 2 or 4 hours with 1mM IPTG. Protein was extracted from 1.5ml samples using 100 μ l BugBuster Protein Extraction Reagent. 10 μ l of each sample was separated on a 12% SDS-PAGE gel and stained with Coomassie Blue stain.

The Coomassie Blue stained gel (Figure 6.2.1b) suggested that there was induction of PrMPK9-1 recombinant protein (~57kDa) after 2 and 4 hours of induction with 1mM IPTG. Protein expression could not be detected in the un-induced samples, or in the control samples containing empty vector. Visual inspection suggested that expression seemed to be stronger after 4 hours of induction, compared to 2 hours of induction.

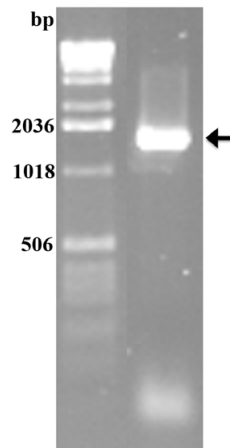


Figure 6.2.1a Amplification of full-length PrMPK9-1 for protein expression. The full-length coding region was 1482bp (arrowed). The gene contained *NdeI* and *XhoI* restriction sites upstream and downstream, respectively, to allow ligation into the pET-21b vector.

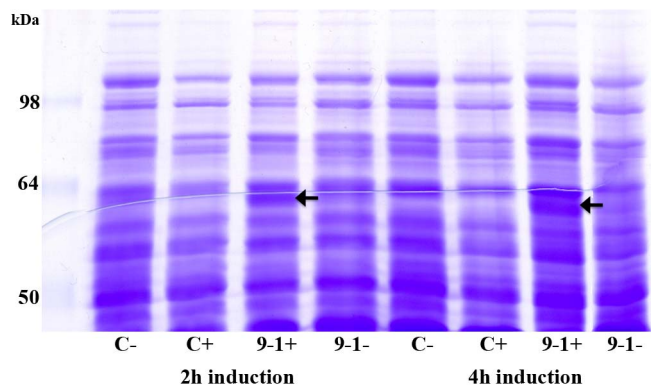


Figure 6.2.1b Expression of the full-length PrMPK9-1 recombinant protein. Expression was induced for 2 hours (**2h**) or 4 hours (**4h**) with 1mM IPTG. The gel shows expression of PrMPK9-1 recombinant protein (~57kDa, ~56kDa plus 6xHis-tag, arrowed) after both 2 and 4 hours in samples that were induced with 1mM IPTG (**9-1+**), but this could not be detected in un-induced extracts and control extracts, containing empty vector (**9-1-** and **C+/C-**, respectively).

To confirm the ~57kDa protein corresponded to PrMPK9-1, western blotting was carried out using the anti-6xHis antibody, which specifically detects His-tagged proteins. The samples were separated on a 12% SDS-PAGE gel, transferred to nitrocellulose membrane and probed with an anti-6xHis antibody. For detection, an anti-mouse IgG alkaline phosphatase conjugated antibody was used. Western blotting (Figure 6.2.1c) confirmed that there was expression after both 2 and 4 hours and there was no expression in control samples. However, the results suggested that there was expression of the recombinant protein in un-induced samples. This suggested that protein expression might be 'leaky', being expressed in the absence of induction with IPTG.

Furthermore, experiments were carried out to determine whether the PrMPK9-1 recombinant protein was present in the soluble or insoluble cell fraction. Protein expression was carried out by induction of protein expression for 4 hours with 1mM IPTG. Proteins were extracted using a TRIS-NaCl buffer and separated into the two fractions by centrifugation. 30µl of sample was separated on a 12% SDS-PAGE gel, transferred to nitrocellulose filter, and probed with the anti-6xHis antibody. Figure 6.2.1d shows the majority of the protein was expressed in the insoluble fraction, although there was some expression in the soluble fraction.

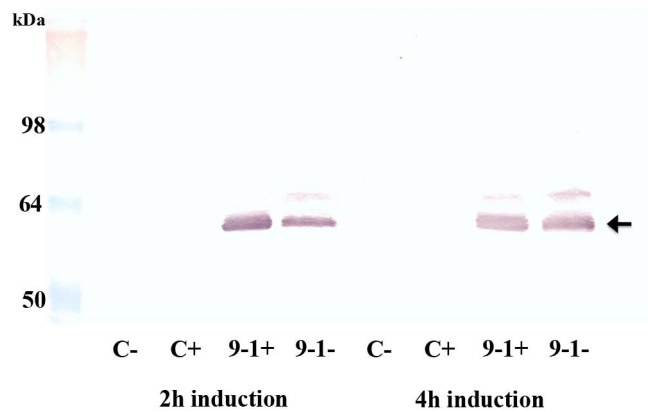


Figure 6.2.1c Full-length PrMPK9-1 recombinant protein expression can be detected with the anti-6xHis antibody. Expression was induced for 2 hours (**2h**) or 4 hours (**4h**) with 1mM IPTG. The gel shows expression of PrMPK9-1 recombinant protein (~57kDa, ~56kDa plus 6xHis-tag, arrowed) after both 2 and 4 hours in samples that were induced with 1mM IPTG (**9-1+**), but not in controls, containing empty vector (**C+/C-**). The blot also suggests that expression is 'leaky', as protein expression can be detected in un-induced samples (**9-1-**).

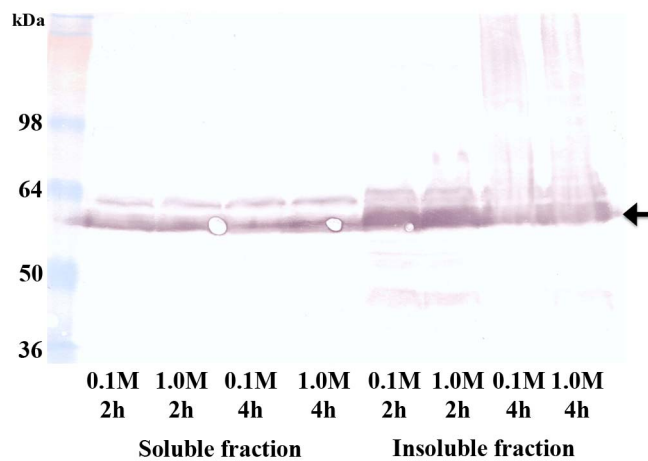


Figure 6.2.1d Full-length PrMPK9-1 recombinant protein is expressed in the soluble and insoluble cell fractions. Protein extracts were separated into the soluble and insoluble fractions and detected with the anti-6xHis antibody. The protein is present at a higher level in the insoluble fraction, although there is a lower level of protein in the soluble fraction. Length of expression (**2h/4h**) and concentration of IPTG used for expression induction (**0.1M/1.0M**) are shown.

In order to purify the PrMPK9-1 recombinant protein and remove endogenous *E. coli* proteins, Ni-NTA (nickel-nitrilotriacetic acid) Agarose resin was used. The Ni-NTA Agarose resin allows high capacity binding of 6xHis-tagged proteins, in this case PrMPK9-1, with minimal non-specific binding. The purified His-tagged PrMPK9-1 is then eluted from the resin with imidazole, which competes for binding sites on the resin.

A ~750µl sample of recombinant protein from the soluble fraction, which had been induced for 4 hours with 1mM IPTG, was incubated with 100µl of Ni-NTA Agarose resin containing 20mM imidazole. The resin was then washed with increasing concentrations of imidazole, at lower levels to wash out endogenous proteins with histidine residues that interact with the resin and then at a high level to elute the recombinant protein from the resin. 30µl of each fraction was separated on a 12% SDS-PAGE gel and either transferred to nitrocellulose filter and probed with an anti-6xHis antibody, or Coomassie Blue stained (data not shown), to see in which fraction the protein was eluted.

Figure 6.2.1e shows that the majority of the protein was eluted in the 100mM imidazole fraction. Because the protein was eluted at a low concentration of imidazole (<100mM) the purification procedure was repeated using an intermediate wash step of 60mM imidazole.

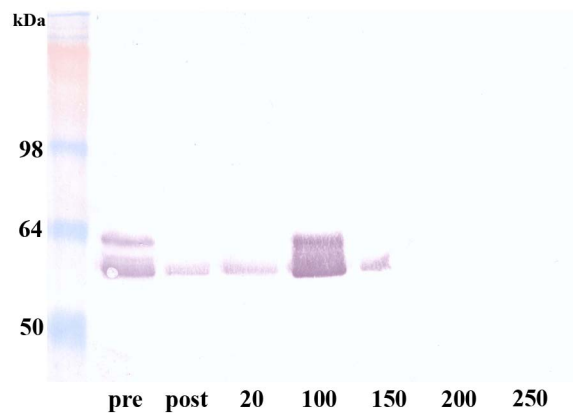


Figure 6.2.1e Purification of the PrMPK9-1 recombinant protein with Ni-NTA Agarose resin. Endogenous *E. coli* proteins were washed from the beads by increasing the imidazole concentration. Higher levels of imidazole out-compete the His-tagged proteins for binding sites and the proteins are eluted. The blot shows the majority of the His-tagged protein binds to the Ni-NTA Agarose resin, by comparing the protein sample before binding to the resin (**pre**) and the supernatant removed from the beads after binding (**post**). The majority of the recombinant protein is eluted in the 100mM imidazole fraction. Numbers represent imidazole concentration in each wash. Loadings: 10 μ l of pre and post, 30 μ l of imidazole fractions.

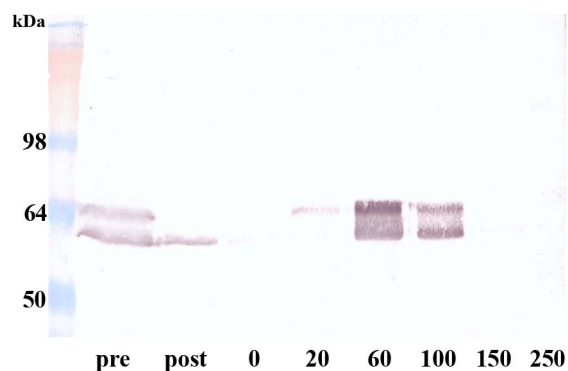


Figure 6.2.1f Purification of the PrMPK9-1 recombinant protein with Ni-NTA Agarose resin. The majority of the recombinant protein is eluted in the 60mM imidazole fraction, and a substantial amount is not eluted until the 100mM fraction. Loadings: 10 μ l of pre and post, 30 μ l of imidazole fractions. **pre**: before binding to the resin. **post**: supernatant removed from the beads after binding. Numbers represent imidazole concentration in each wash.

Figure 6.2.1f shows that the majority of PrMPK9-1 protein was eluted from the resin in only 60mM imidazole, although a significant amount is not eluted until the 100mM fraction. Although the protein is eluted from the resin in a low concentration of imidazole, the Coomassie Blue stained gel (data not shown) indicates that the majority of endogenous protein was not present in the 60mM imidazole fraction, suggesting the PrMPK9-1 protein in this fraction was reasonably pure.

6.2.2 Detection of recombinant PrMPK9-1 protein with the anti-AtMPK3 antibody

Earlier evidence suggested that it was possible to detect p56 with an anti-AtMPK3 antibody (Li *et al.*, 2007, see Chapter 4). As the current findings suggested p56 was not a AtMPK3 orthologue, western blot analysis was carried out to see if the recombinant PrMPK9-1 protein could be detected by the anti-AtMPK3 antibody, as would be expected if *PrMPK9-1* is a candidate for encoding p56. Purified PrMPK9-1 recombinant protein was separated on a 12% SDS-PAGE gel, transferred to nitrocellulose filter, and probed with the anti-AtMPK3 antibody. For detection an anti-rabbit IgG alkaline phosphatase conjugated antibody was used. Figure 6.2.2a shows that the anti-AtMPK3 antibody can detect a protein of ~57kDa, that corresponds to the PrMPK9-1 recombinant protein.

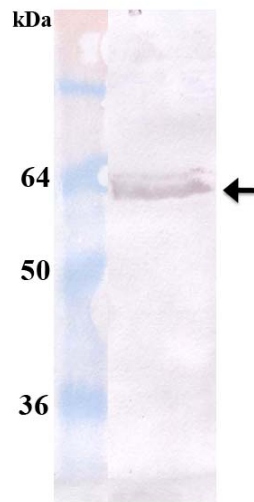


Figure 6.2.2a The anti-AtMPK3 antibody cross-reacts with the PrMPK9-1 recombinant protein. The anti-AtMPK3 antibody can detect a protein of ~57kDa (arrowed), that corresponds to the PrMPK9-1 recombinant protein.

6.2.3 Production of an anti-PrMPK9-1 antibody

6.2.3.1 Production of an anti-PrMPK9-1 peptide antibody

In order to confirm that p56 was encoded by PrMPK9-1, attempts were made to raise an antibody against PrMPK9-1, to determine if this antibody could cross-react with p56. Due to the ease of making anti-peptide antibodies (compared to antibodies raised against a recombinant protein) attempts were made to raise an antibody against a specific PrMPK9-1 peptide. As the core MAPK catalytic domains show high homology, it was decided to select a region from the C-terminus of the protein, as this region is generally most specific to each individual MAPK. A C-terminal sequence of PrMPK9-1 was selected and sent to Sigma-Genosys Ltd. where it was analysed for the most suitable peptide to use for antibody production. The sequence was run through various programs to determine the antigenicity, solubility and aggregation potential of the peptide and whether there was likely to be any difficulty generating and purifying the peptide for conjugation and injection.

A 15 amino acid sequence was selected (GEPIDEQSEVDDLSQ), which represented amino acids 472-486 of PrMPK9-1, and was subsequently chosen for peptide production. This peptide was then used to raise a polyclonal antibody in two rabbits. Immunisations were administered on day 1, 14, 28, 42, 56 and 70, and bleeds were taken on days 49 and 63, with a terminal bleed of the animal after 77 days.

As part of the antibody production service, Sigma-Genosys carried out an Enzyme-Linked Immuno Sorbent Assay (ELISA) to detect the presence of specific antibody in the first bleed

sample. The ELISA carried out on the first bleed showed that there was no response compared to the pre-immune serum. Because of this, ELISA was also carried out on the second bleed. The ELISA results suggested that there may be a very slight response to the immunisation, but it was too low to be suitable in any application.

6.2.3.2 Construction of a PrMPK9-1 recombinant protein for antibody production

Although it may be possible to raise an antibody against the 15 amino acid peptide selected above, this attempt failed. Therefore, an attempt was made to raise an antibody against a partial C-terminal PrMPK9-1 recombinant protein (PrMPK9-1C). The *A. thaliana* and *P. rhoeas* MAPK sequences were aligned in order to determine a specific region in PrMPK9-1 suitable for raising an antibody. PrMPK9-1 diverged most from the other MAPKs in the C-terminal region (terminal 103 amino acids), and therefore this region was selected for antibody production.

Primers were designed to amplify a 309bp 3' region of *PrMPK9-1* (103 amino acids, corresponding to amino acids 391-493; PrMPK9-1C_5'NdeI and PrMPK9-1_3'XhoI, PrMPK9-1C). The primers also contained *NdeI* and *XhoI* restriction sites, respectively, to allow directional ligation of the sequence into the pET21-b expression vector. The fragment was amplified from hydrated pollen cDNA, using proofreading polymerase (KOD Hot Start DNA Polymerase). The *PrMPK9-1* amplification product was ligated into the pDrive cloning vector, cloned, and sequenced to verify the sequence. *PrMPK9-1* was digested from the pDrive cloning vector using the *NdeI* and *XhoI* restriction sites, and ligated into the pET-21b expression vector (also digested with *NdeI* and *XhoI*). The PrMPK9-1-pET-21b construct was

cloned, and sequenced to verify the sequence. For protein expression, purified plasmid DNA containing the PrMPK9-1-pET-21b construct was used to transform *E. coli* BL21 competent cells.

In initial expression experiments, protein expression was induced for 4 hours with 1mM IPTG. Proteins were extracted in a TRIS-NaCl buffer and separated into the soluble and insoluble fractions. 5 μ l of sample was run on a 15% SDS-PAGE gel and stained with Coomassie Blue stain. Figure 6.2.3.2a shows that there was a large quantity of the PrMPK9-1C protein in the soluble fraction after 4 hours of induction with 1mM IPTG. A very small amount of protein was detected in the insoluble fraction, but there was no protein in the control samples (*E. coli* containing empty pET-21b vector).

In order to remove endogenous *E. coli* proteins, the PrMPK9-1C recombinant protein was purified using Ni-NTA Agarose resin (as described in 6.2.1). 12 μ l of each imidazole fraction was separated on an 18% SDS-PAGE gel and stained with Coomassie Blue stain. Figure 6.2.3.2b shows that the majority of the endogenous *E. coli* protein is eluted with 50mM imidazole, without severe loss of PrMPK9-1C binding.

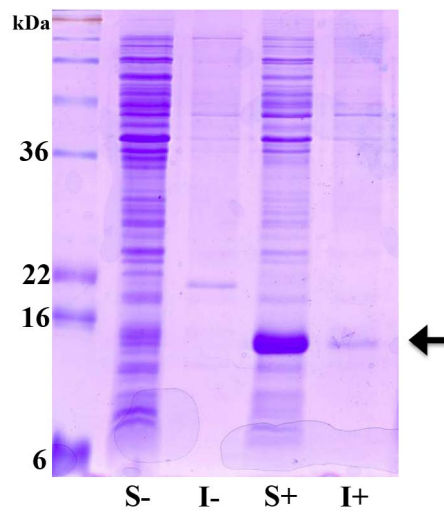


Figure 6.2.3.2a Expression of the PrMPK9-1C recombinant protein. PrMPK9-1C recombinant protein is present in the soluble fraction (S+) after 4 hours of induction with 1mM IPTG. There is a small amount of protein in the insoluble fraction (I+). There was no detection of the protein in the control samples (containing empty vector) (not shown) and un-induced samples (-).

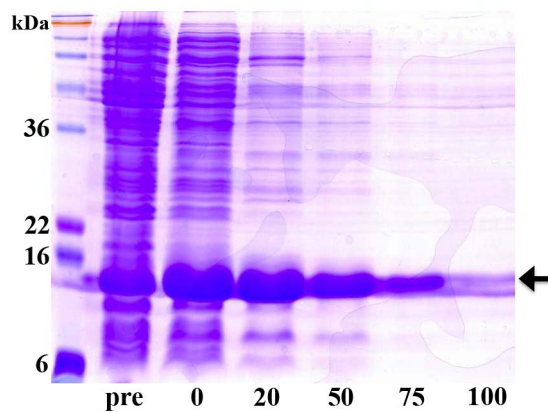


Figure 6.2.3.2b Purification of the PrMPK9-1C recombinant protein with Ni-NTA Agarose resin. The blot shows the proteins still bound to the beads after washing with imidazole i.e. 20mM shows resin that was washed with 20mM imidazole, and then proteins were eluted by adding 250mM imidazole, and separated on the SDS-PAGE gel. The majority of the endogenous *E. coli* protein is eluted with 50mM imidazole, without severe loss of PrMPK9-1C binding. 30 μ l of each fraction was loaded. Numbers represent concentration of imidazole. **pre**: sample before binding.

In order to produce enough recombinant protein for antibody production (0.5-1.5mg of 0.5-1mg/ml protein was required) expression was carried out on a larger scale. For antibody production the antigen (PrMPK9-1C) samples could only contain a maximum 200mM imidazole (without NaCl) or 300mM NaCl (without imidazole) if the antigen concentration was ~1mg/ml. As the PrMPK9-1C sample contained 300mM NaCl and 250mM imidazole it required further purification. To remove imidazole and NaCl the recombinant protein was passed over a PD-10 desalting column. This was used as an alternative to dialysis, as the dialysis membrane generally available has a molecular weight cut off of 12-14kDa. As the PrMPK9-1C recombinant protein was ~11kDa this method of purification was not suitable. ~800µl of purified PrMPK9-1C protein (obtained from ~100ml of *E. coli* culture) was made up to a total volume of 2.5ml with 1x PBS (as recommended by the manufacturer's instructions) and passed over the de-salting column. The recombinant protein was eluted in 3.5ml 1x PBS. 20µl samples from Ni-NTA purified protein, pre-desalting (after dilution into 2.5ml) and after de-salting (in 3.5ml) were separated on an 18% SDS-PAGE gel and stained with Coomassie Blue stain. Figure 6.2.3.2c suggests that de-salting was successful and no protein was lost in the process.

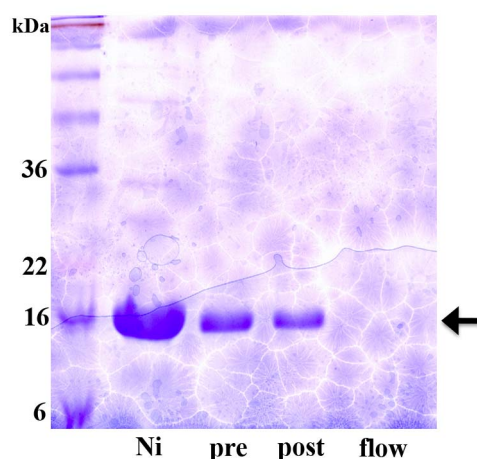


Figure 6.2.3.2c Purification of PrMPK9-1C using the PD-10 desalting columns. The gel shows Ni-NTA purified recombinant protein (**Ni**, arrowed), and protein before desalting (in 2.5ml) (**pre**) and after desalting (in 3.5ml) (**post**). The gel represents a 1/1, 1/3.3, and 1/4.7 dilution of each sample, respectively, compared to the Ni-NTA purified sample. The gel shows that the PrMPK9-1C protein was eluted in the correct fraction (and did not pass directly through the column, shown by the column flow through (**flow**)) and suggests no protein was lost in the process.

Once de-salted, the recombinant protein was reduced in volume (to increase the concentration) using a freeze dryer and the final protein concentration was determined. 0.5-1.5mg of the antigen was required in at 0.5-1mg/ml. The final PrMPK9-1C sample contained ~1.1mg recombinant protein in ~1.7ml buffer (~0.63mg/ml). This protein was dispatched to Biogenes GmbH and used for the generation of rabbit polyclonal antiserum in two animals. Immunisations were administered on day 1, 7, 14 and 28, and bleeds were taken on day 28 with a terminal bleed of the animal after 97 days.

To test the antigenicity of the anti-PrMPK9-1 antisera, pre-immune sera (taken before immunisation) and anti-PrMPK9-1 antisera were used in western blot analyses on PrMPK9-1C recombinant protein, which was used as an antigen. ~15ug unpurified PrMPK9-1C recombinant protein was separated on an 18% SDS-PAGE gel and transferred to nitrocellulose membrane. The membrane was probed with either pre-immune sera or anti-PrMPK9-1 antisera from one of the two rabbits at a titre of 1:1000. Antibodies from both rabbits detected a protein of ~11kDa (corresponding to PrMPK9-1C), which was not detected by the pre-immune sera (Figure 6.2.3.2d).

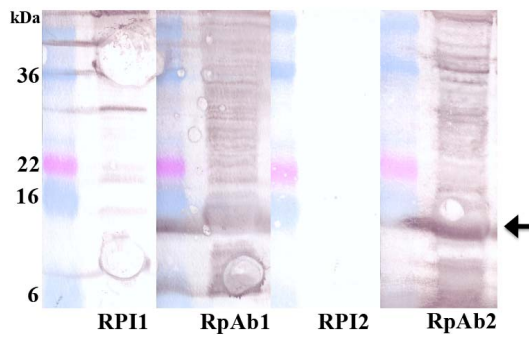


Figure 6.2.3.2d The anti-PrMPK9-1 antibody detects recombinant PrMPK9-1C. Pre-immune sera and anti-PrMPK9-1 antiserum was tested to see if it cross-reacted with PrMPK9-1C recombinant protein, used as an antigen. The anti-PrMPK9-1 antisera from both rabbits could detect a ~11kDa protein that corresponded to PrMPK9-1C (**RpAb1** and **RpAb2**, arrowed). This ~11kDa protein was not detected by either pre-immune sera (**RPI1** and **RPI2**).

Initial western blotting experiment suggested the anti-PrMPK9-1 antisera detected the PrMPK9-1C recombinant protein. To confirm this, the antibody was purified by passing through an Immobilised *E. coli* Lysate column, which removes antibodies that were raised against contaminating *E. coli* proteins present in the recombinant protein sample used as an immunogen. The purified antisera were also tested at a range of titres on purified PrMPK9-1C recombinant protein at various concentrations. Approximately 1000ng, 200ng, 100ng and 20ng purified PrMPK9-1C recombinant protein was separated on 18% SDS-PAGE gels and transferred nitrocellulose filters. The primary antisera were initially tested at titres of 1:1000 and 1:5000. An anti-rabbit IgG alkaline phosphatase conjugated antibody was used for detection.

Figure 6.2.3.2e shows the purified anti-PrMPK9-1 antiserum detects a protein of ~11kDa, but no band of this size is detected by the pre-immune serum. The western blot also showed there was little background detection, although a protein of ~30kDa was also detected. These results suggested that antiserum from both animals contained anti-PrMPK9-1 antibodies that recognise the recombinant protein used to immunise the animal.

To confirm the anti-PrMPK9-1 antibody detected the PrMPK9-1 protein, western blotting was carried out on the full length PrMPK9-1 recombinant protein. ~15ug PrMPK9-1 recombinant protein (and control) were separated on a 12% SDS-PAGE gel, transferred to nitrocellulose filter and probed with the anti-PrMPK9-1 antibody. For detection an anti-rabbit IgG alkaline phosphatase conjugated antibody was used. Figure 6.2.3.2f shows that the antibody detects a band of ~57kDa, corresponding to the full-length PrMPK9-1 recombinant protein.

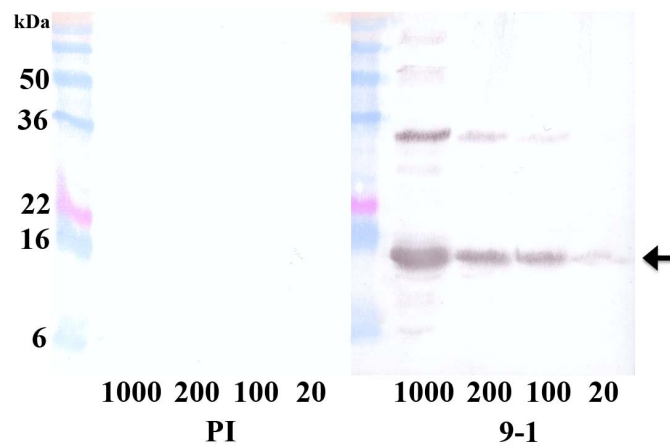


Figure 6.2.3.2e The purified anti-PrMPK9-1 antisera can detect PrMPK9-1C recombinant protein. PrMPK9-1 antisera (**PrMPK9-1**) can detect a ~12kDa protein (corresponding to PrMPK9-1C, arrowed) in 1000ng (**1000**), 200ng (**200**), 100ng (**100**) and 20ng (**20**) of PrMPK9-1C recombinant protein. The pre-immune serum (**PI**) does not detect this protein. A protein of ~30kDa is also detected. Detection of the ~35kDa protein is likely to represent antibody raised against *E. coli* protein (from the original sample sent to raise the anti-PrMPK9-1 antibody against) detecting *E. coli* proteins in the PrMPK9-1C recombinant protein sample.

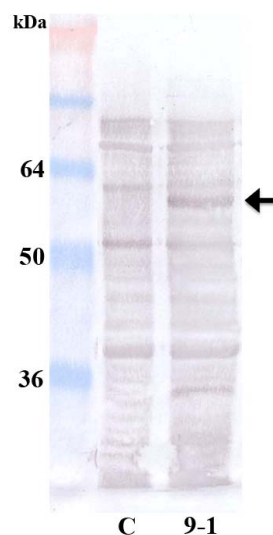


Figure 6.2.3.2f Detection of the full-length PrMPK9-1 recombinant protein with the anti-PrMPK9-1 antibody. The anti-PrMPK9-1 antibody can detect the full-length PrMPK9-1 recombinant protein (**9-1**, ~57kDa, arrowed), but does not detect this protein in a control sample (which does not express the recombinant protein, **C**).

6.2.4 The anti-PrMPK9-1 antibody can detect a ~56kDa protein in pollen

Once it had been shown the anti-PrMPK9-1 antibody could detect PrMPK9-1, western blotting was carried out to see if the anti-PrMPK9-1 antibody could detect proteins in *P. rhoeas* pollen. Calyculin A is a serine/threonine protein phosphatase inhibitor that can be used to prevent dephosphorylation of MAPKs (Honkanen *et al.*, 1994). Calyculin A can therefore be used to increase levels of phosphorylated phospho-proteins above their basal level (such as p56) in the absence of a stimulus (for example, an incompatible SI reaction). Pollen was hydrated, grown and either treated with calyculin A (final concentration of 0.25 μ M), or GM as a control. 250ng of calyculin A-treated or untreated pollen protein was separated on a 12% SDS-PAGE gel, transferred to nitrocellulose membrane and probed with either an anti-pTepY antibody (which specifically detects dually phosphorylated MAPKs in the T-X-Y domain), the anti-PrMPK9-1 antibody, or pre-immune sera.

Western blotting showed (Figure 6.2.4a) that the anti-pTXpY could detect a ~56kDa protein corresponding to p56 (Rudd *et al.*, 2003) in calyculin A treated pollen, but not in untreated pollen. The anti-PrMPK9-1 antibody was also shown to cross-react with a protein of ~56kDa and this was independent of protein phosphorylation by calyculin A, as would be expected. This ~56kDa protein could not be detected by the pre-immune sera.

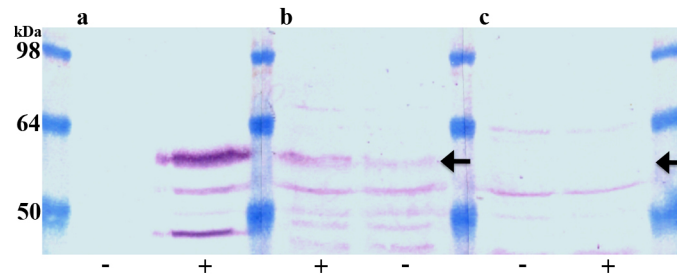


Figure 6.2.4a The anti-PrMPK9-1 antibody detects a ~56kDa protein in *Papaver rhoeas* pollen. (a) Detection of activated p56 in pollen extracts following addition of calyculin A (+) using an anti-pTXpY antibody. The protein is not detected in the absence of calyculin A (-); (b) The anti-PrMPK9-1 antibody appears to identify the same band. As would be expected, this detection is not dependent on p56 activation; (c) The p56 band is not detected by pre-immune serum.

6.2.5 The anti-PrMPK9-1 antibody cross-reacts with a 56kDa phospho-protein

Approximately 150mg of pollen was hydrated, grown, and treated for 10 minutes with calyculin A (final concentration of 0.25 μ M) to prevent dephosphorylation of proteins. Pollen proteins were extracted and their concentration was determined. An \sim 500 μ l extract of \sim 14 μ g/ μ l was obtained. The sample contained a large number of small phosphorylated proteins so, in order to reduce saturation of the PhosphoProtein purification column by these proteins, the pollen protein extract was 'washed' using an Amicon[®] Ultra-4 Centrifugal Filter Unit, which has a molecular cut off point of 10kDa. The pollen extract was diluted in 3ml of lysis buffer and added to the Amicon[®] Ultra-4 Centrifugal Filter Unit. A series of spins were carried out and the column was washed several times to help remove small proteins from the sample. The protein extract was concentrated and its concentration was determined. An \sim 500 μ l extract of \sim 7 μ g/ μ l was obtained (\sim 3.5mg in total).

To extract the phosphorylated proteins the sample was diluted in 25ml of lysis buffer and passed through a phospho-column to enrich for phospho-proteins. The dilution step was to ensure the sample was at \sim 0.1mg/ml to allow the phosphate groups to be easily accessible during purification. The column was washed to remove un-phosphorylated proteins and the phospho-proteins were eluted from the column in 5 fractions of 500 μ l. The protein concentration of each fraction was determined and showed the majority of the proteins were eluted in fraction 3 (\sim 500 μ l of 111 μ g/ml).

To determine if any of the phospho-proteins could cross-react with the anti-PrMPK9-1 antibody 30 μ l of fraction 3 (\sim 3.3 μ g) and 30 μ l of calyculin treated pollen (\sim 90 μ g) were run on

an SDS-PAGE gel, transferred to nitrocellulose membrane and probed with the anti-PrMPK9-1 antibody. For detection, an anti-rabbit IgG HRP conjugated antibody was used. Results showed (Figure 6.2.5a) that a protein of ~56kDa, eluted from the phospho-column, can be detected by the anti-PrMPK9-1 antibody. Although the protein loading may not be relative, the western blot may suggest that the other bands detected in calyculin A treated pollen are no longer present after purification by the phospho-column.

The membrane in Figure 6.2.5a was washed in urea to remove the bound antibody, and the membrane was re-probed with the anti-pTXpY antibody to determine if this phospho-protein was a MAPK. Figure 6.2.5b shows a similar pattern of detection in the purified sample to that seen in calyculin A treated pollen as would be expected if the MAPKs present had been phosphorylated. The anti-pTXpY antibody cross-reacts with the ~56kDa band in fraction 3, as expected, and also with three other proteins. These results suggest that an ~56kDa protein can be phosphorylated, can cross-react with the anti-PrMPK9-1 antibody, and also cross-reacts with the anti-pTXpY antibody that specifically detects the activated activation motif of MAPKs.

To confirm the above result the western blotting was repeated, but in the reverse order. Samples were run as before, but were probed first with the anti-pTXpY antibody. The membrane was then treated with urea to remove the bound antibody, and re-probed with the anti-PrMPK9-1 antibody. This showed detection of the same proteins seen in Figure 6.2.5a and Figure 6.2.5b (data not shown).

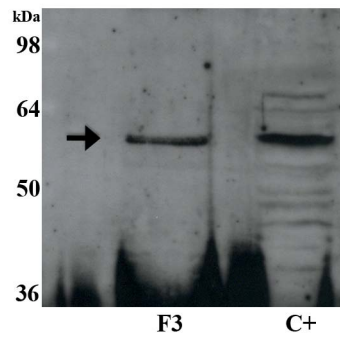


Figure 6.2.5a A ~56kDa phospho-protein cross-reacts with the anti-PrMPK9-1 antibody. Western blot of phospho-proteins eluted from the phospho-protein purification column in fraction 3 (F3) and calyculin A treated pollen (C+) and probed with the anti-PrMPK9-1 antibody. A protein of ~56kDa is eluted from the column and detected by the antibody. The membrane was exposed for 4 minutes.

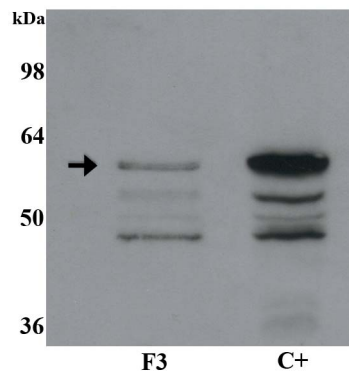


Figure 6.2.5b A ~56kDa phospho-protein can be detected by the anti-pTXpY antibody that specifically detects activated MAPKs. The membrane probed with anti-PrMPK9-1 antibody (Figure 6.2.5a) was treated with urea to remove the bound antibody, and the membrane was re-probed to see if the anti-pTEpY antibody could detect the same ~56kDa protein. A protein of ~56kDa is detected by the antibody in both fraction 3 from the phospho-volumn (F3) and also as previously demonstrated in calyculin A treated pollen (C+). The antibody also detects three other phosphorylated proteins. The membrane was exposed for 3 minutes.

6.2.6 PinPoint™ purification of the anti-PrMPK9-1 antibody

In order to further reduce non-specific binding of the anti-PrMPK9-1 antibody, and to allow the antibody to be used more efficiently for immuno-precipitation experiments, the antibody was purified using the PinPoint™ Xa Protein Purification System. This system allows the production of a biotinylated fusion protein in *E. coli* that can then be affinity purified using avidin resin. The region corresponding to the C-terminal region used to raise the anti-PrMPK9-1 antibody (PrMPK9-1C) was selected to be tagged and bound to the resin so the anti-PrMPK9-1 antibody could then be purified by affinity purification through the column.

Primers were designed to amplify the same C-terminal region of PrMPK9-1 used for antibody production (PrMPK9-1CPP), and *HindIII* and *NotI* restriction sites were incorporated upstream and downstream respectively, to allow ligation into the Xa3 PinPoint™ expression vector (PrMPK9-1PP5'*HindIII* and PrMPK9-1PP3'*NotI*). The PrMPK9-1CPP sequence was amplified from hydrated pollen cDNA by PCR using a proofreading polymerase (KOD Hot Start DNA Polymerase, Novagen). The resultant PCR product was cloned, and sequenced. The 309bp sequence was identical to the *PrMPK9-1* sequence previously cloned. The PrMPK9-1CPP fragment was digested from the pDrive cloning vector using the *HindIII* and *NotI* restriction sites and ligated into the PinPoint™ Xa3 expression vector, which had been cut with *HindIII* and *NotI*. *E. coli* DH5 α was transformed with the Xa3-PrMPK9-1CPP construct and purified plasmid DNA was sequenced to confirm the construct was correct and in-frame. Purified plasmid DNA was then used to transform *E. coli* JM109 competent cells for expression of the recombinant protein.

Test expression was carried out in the presence of 2 μ M biotin and 100 μ M ampicillin, for selection. Expression of the recombinant protein was induced with 1mM IPTG for 3 hours. Control vectors were also induced or un-induced by IPTG, which contained an empty Xa3 expression vector. Proteins were extracted from a 1ml sample, which were re-suspended in 100 μ l TRIS-NaCl buffer. 20 μ l of each sample was separated on an 18% SDS-PAGE gel and analysed by Coomassie blue staining (Figure 6.2.6a).

The Coomassie stained gel showed expression of a protein that migrated to \sim 30kDa. The predicted recombinant protein was \sim 24kDa (PrMPK9-1C \sim 11kDa, biotin tag \sim 13kDa). This expression could not be seen in control vectors, and expression seemed to be independent of induction with 1mM IPTG.

To confirm this recombinant protein was PrMPK9-1C, and that it had been biotinylated, 7.5 μ l of the above samples were separated on an 18% SDS-PAGE gel, transferred to nitrocellulose membrane, and probed with either the anti-PrMPK9-1 antibody (Figure 6.2.6b) or a NeutrAvidin protein (conjugated to HRP) which specifically binds to biotin (Figure 6.2.6c).

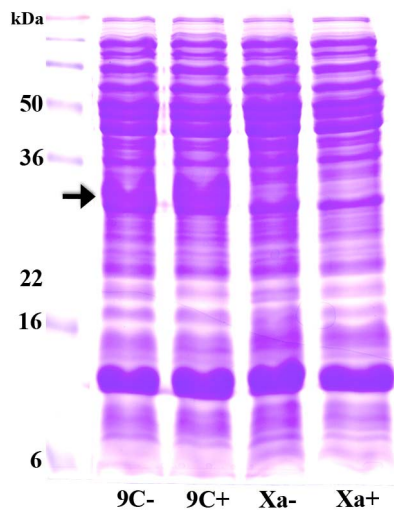


Figure 6.2.6a Expression of the PrMPK9-1CPP recombinant protein. The PrMPK9-1C Xa3 construct can express the recombinant protein (**9C+**, arrowed). The predicted size of the biotin-tagged protein is ~24kDa (PrMPK9-1C ~11kDa, biotin tag ~13kDa). Expression of this protein is not seen in control vectors that do not contain the construct. Expression seems to be independent of induction with 1mM IPTG (**9C-**). **Xa-**: un-induced control Xa3 vector; **Xa+**: induced control Xa3 vector.

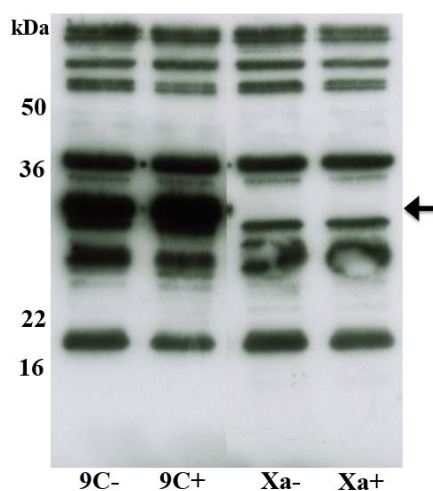


Figure 6.2.6b PrMPK9-1CPP cross-reacts with the anti-PrMPK9-1 antibody. Recombinant PrMPK9-1CPP (9C) and an empty control vector (Xa) were expressed and probed with the anti-PrMPK9-1 antibody. The western blot shows detection of PrMPK9-1CPP recombinant protein (arrowed) in cells that contain the Xa3-PrMPK9-1CPP construct, but not in control vectors. There is a small increase in expression in PrMPK9-1 in the IPTG induced sample (+) compared to the un-induced sample (-). The membrane was exposed for 10 seconds.

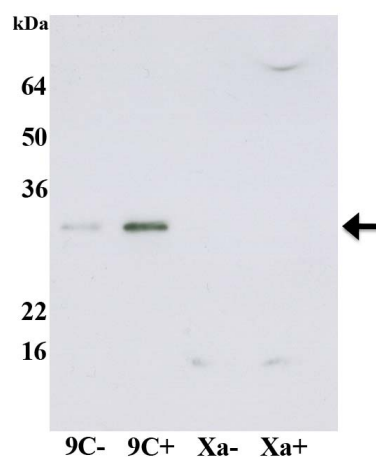


Figure 6.2.6c PrMPK9-1CPP cross-reacts with the NeutrAvidin Protein (conjugated to HRP). Recombinant PrMPK9-1CPP (9C) and an empty control vector (Xa) were expressed and probed with the NeutrAvidin Protein. The western blot shows detection of PrMPK9-1CPP recombinant protein (arrowed) in cells that contain the Xa3-PrMPK9-1CPP construct, but not in control vectors. There is an increase in biotinylation of PrMPK9-1CPP in the IPTG induced sample (+) compared to the un-induced sample (-). The membrane was exposed for 1 minute.

Figure 6.2.6b shows that the anti-PrMPK9-1 antibody can detect the ~30kDa protein that was identified in Figure 6.2.6a, confirming this protein is PrMPK9-1CPP. Induction with IPTG seemed to show a small increase in expression levels, and there was no expression of this protein in control samples. Figure 6.2.6c confirms that the PrMPK9-1CPP is biotinylated, as the NeutrAvidin protein can detect the same ~30kDa protein. Again, this shows an increase in expression after induction with IPTG, and there is no biotinylation of proteins in control samples. This data provided good evidence that the Xa3-PrMPK9-1CPP construct was being expressed and that the protein was successfully biotinylated. This allowed large-scale expression to be carried out to express enough recombinant protein to proceed with construction of the affinity purification column to purify the anti-PrMPK9-1 antibody.

TetraLink™ Tetrameric Avidin Resin will bind and immobilise biotinylated proteins from a complex mixture of proteins (Cress *et al.*, 1993). The biotin-avidin interaction binds with very high affinity (essentially irreversible), which provides stability of the complex under a wide variety of wash conditions. This allows multiple affinity purification of proteins, in this case the anti-PrMPK9 antibody, using the same resin. The manufacturer's instructions suggested that ~330ml of original culture could be bound to ~1ml of TetraLink™ Tetrameric Avidin Resin. Protein extraction showed that 100ml of culture provided ~2.4ml of cell lysate and therefore at least 8ml of lysate would be required to bind to 1ml of resin.

Protein expression was scaled up to provide 25ml of cell lysate. 12ml of cell lysate was added to 1ml TetraLink™ Tetrameric Avidin Resin and incubated at 4°C overnight to bind the biotin-tagged antibody to the avidin resin. The excess lysate was removed from the beads and the resin was then used to make a column using disposable plastic columns. To help ensure

the avidin resin was saturated, an additional 4ml of cell lysate containing biotinylated PrMPK9-1CPP was passed over the resin. The column was washed and prepared for affinity purification of the anti-PrMPK9-1 antibody.

5ml of antibody was affinity purified using the column. To find out which fraction the antibody was eluted in the protein concentration of each fraction was determined. The results suggested that the majority of the antibody was eluted in the third fraction (~244µg total at 0.348µg/µl), with the majority of the remaining antibody found in fractions 2 and 4 (each contained around a third of the protein found in fraction 3).

6.2.6.1 PinPoint™ purified anti-PrMPK9-1 antibody can detect PrMPK9-1C recombinant protein

To determine if the affinity purified anti-PrMPK9-1 antibody could cross-react with the PrMPK9-1C recombinant protein western blotting was carried out. 200ng, 20ng, 2ng and 0.2ng of purified PrMPK9-1C recombinant protein was separated on an 18% SDS-PAGE gel, transferred to nitrocellulose membrane and probed with either the PinPoint™ affinity purified anti-PrMPK9-1 antibody at a titre of 1:1000, or the original anti-PrMPK9-1 antibody (purified using the Immobilised *E. coli* Lysate Kit) for comparison. For detection an anti-rabbit IgG alkaline phosphatase-conjugated antibody was used.

Figure 6.2.6.1a shows that the PinPoint™ affinity purified anti-PrMPK9-1 could detect the purified PrMPK9-1C recombinant protein at a similar level to the original anti-PrMPK9-1 antibody.

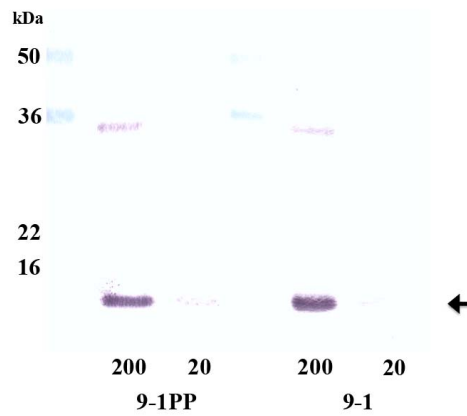


Figure 6.2.6.1a PrMPK9-1C recombinant protein cross-reacts with PinPoint™ affinity purified anti-PrMPK9-1 antibody. 200ng (**200**) and 20ng (**20**) purified PrMPK9-1C recombinant protein probed with PinPoint™ affinity purified anti-PrMPK9-1 (**9-1PP**, 1:1000, left) and anti-PrMPK9-1 antibody (purified using the Immobilised *E. coli* Lysate Kit) (**9-1**, 1:1000, right).

6.2.7 The PinPoint™ purified anti-PrMPK9-1 antibody can detect a ~56kDa protein from *P. rhoeas* pollen.

To test how clean the PinPoint™ purified anti-PrMPK9-1 antibody was on a pollen protein extract western blotting was carried out. ~100µg of pollen protein was separated on a 12% SDS-PAGE gel, transferred to nitrocellulose membrane and probed with either the original purified anti-PrMPK9-1 antibody or the PinPoint™ purified anti-PrMPK9-1 antibody (both antibodies were used at a titre of 1:1000). For detection, an anti-rabbit IgG HRP conjugated antibody was used. Figure 6.2.7a shows that the purified antibody is more specific and considerably reduces non-specific background binding.

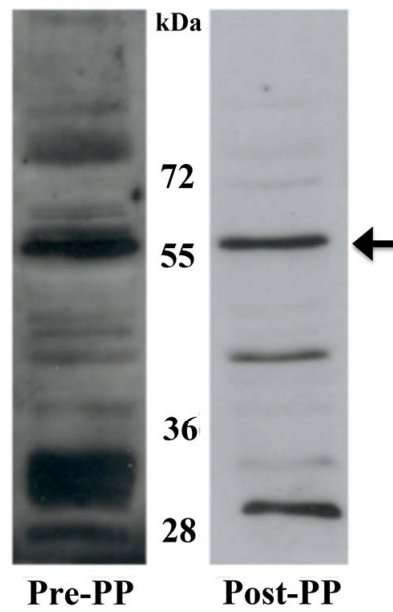


Figure 6.2.7a PinPoint purified anti-PrMPK9-1 antibody compared to un-purified anti-PrMPK9-1 antibody. Un-purified (**Pre-PP**, left) and Pin Point purified (**Post-PP**, right) anti-PrMPK9-1 antibody used to detect pollen proteins. Both antibodies were used at a titre of 1:1000, and membranes were exposed to film for 1 minute for detection. The purified antibody severely reduces background detection. The antibody detects a protein of ~56kDa thought to correspond to p56 (arrowed).

6.2.8 Detection of p56 during compatible and incompatible SI reactions

Previous experiments had shown the anti-PrMPK9-1 and anti-pTXpY antibodies detected a band of ~56kDa in calyculin A treated pollen. Experiments were carried out to determine if the anti-pTEpY and anti-PrMPK9-1 antibodies were detecting the same protein band and also if this could be shown in pollen undergoing an incompatible SI reaction compared to a control sample. ~4mg of pollen was hydrated for each treatment, grown and treated with either recombinant S-proteins to initiate an incompatible SI response (for 10 minutes, as this is when we see peak activation of p56), or with GM as a control. Pollen proteins were extracted and 40µl were run on each of two 12% SDS-PAGE gels. One gel was Coomassie Blue stained so that protein loading could be compared and the other gel was transferred to a nitrocellulose membrane and probed with the anti-pTXpY antibody. For detection an anti-rabbit IgG HRP conjugated antibody was used. Figure 6.2.8a shows that the protein loading was relatively equal between treated and untreated samples. The western blotting (Figure 6.2.8a) showed that after 10 minutes of an incompatible reaction there is increased phosphorylation of p56 (~56kDa). To determine if this protein could be detected by the PinPoint™ purified anti-PrMPK9-1 antibody, the membrane was stripped with urea to remove antibody binding and re-probed with the anti-PrMPK9-1 antibody. For detection an anti-rabbit IgG HRP conjugated antibody was used. Figure 6.2.8a shows that a protein, at exactly the same position as the one detected by the anti-pTXpY antibody (~56kDa), cross-reacted with the anti-PrMPK9-1 antibody. In addition a protein of ~72kDa was detected in the SI treated samples. These results suggest the anti-pTXpT and anti-PrMPK9-1 antibodies cross-react with the same protein.

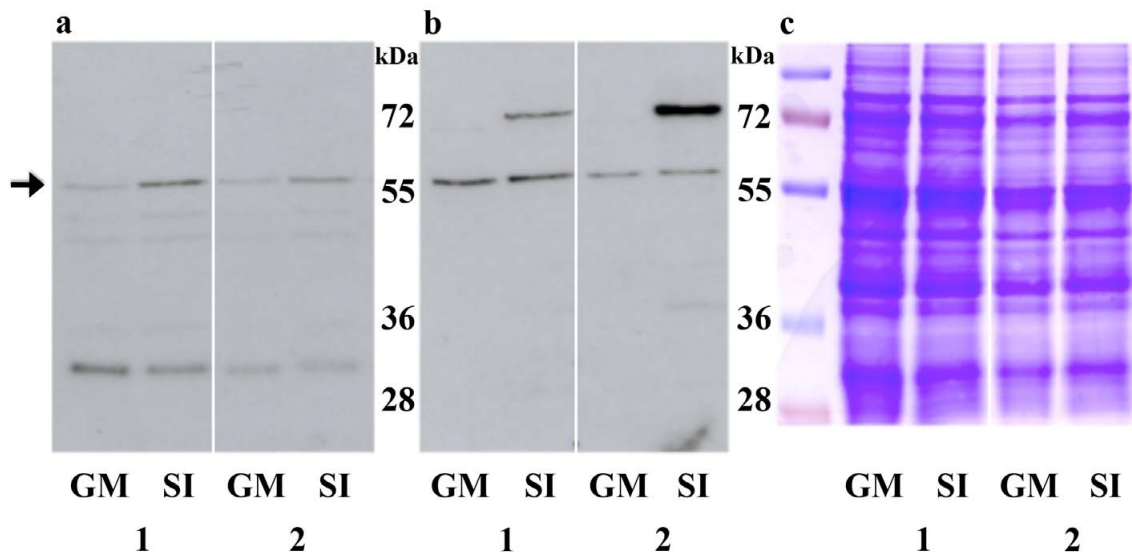


Figure 6.2.8a The anti-PrMPK9-1 and anti-pTXpY antibodies detect the same ~56kDa protein band in an incompatible SI reaction. (a) Western blot showing detection of a ~56kDa protein (p56, arrowed), with the anti-pTXpY antibody (exposure 40 minutes). In untreated pollen (GM) p56 shows a basal level of phosphorylation. After 10 minutes of an incompatible SI reaction (SI) there is increased phosphorylation of p56. (b) The membrane used for probing with the anti-pTXpY antibody 9-1 (a) was stripped with urea to remove the antibody and re-probed with the anti-PrMPK9-1 antibody (exposure 3 minutes). The anti-PrMPK9-1 antibody detects a band of exactly the same size as the anti-pTXpY antibody, which has been shown to detect p56. (c) Coomassie stained gel showing equal loading between untreated (GM) and incompatible SI treated (SI) pollen. 1 and 2 represent two replicates of the experiment.

6.2.8.1 The anti-PrMPK9-1 antibody can detect proteins present in recombinant S-protein samples used to initiate SI *in vitro*.

It was thought that the ~72kDa protein (and also the fainter bands at ~36kDa and ~28kDa) on the western blot above, using the anti-PrMPK9-1 antibody (Figure 6.2.8a), could be due to contamination from the recombinant S-proteins used to initiate the incompatible SI reaction, as this band was not detected in previous experiments on pollen proteins. ~250 μ g of recombinant S₁ and S₈ proteins, used in the incompatible SI reaction above, were run on a 12% SDS-PAGE gel, transferred to nitrocellulose membrane and probed with the anti-PrMPK9-1 antibody. For detection an anti-rabbit HRP-conjugated antibody was used. The results showed that a protein of ~72kDa was detected in both recombinant S₁ and S₈ protein samples (Figure 6.2.8.1a). The ~36kDa and the ~28kDa proteins were detected in the S₁ and S₈ recombinant protein samples, respectively. This suggested that the other proteins detected in Figure 6.2.8a were the result of contamination from the S-proteins used to initiate the SI reaction.

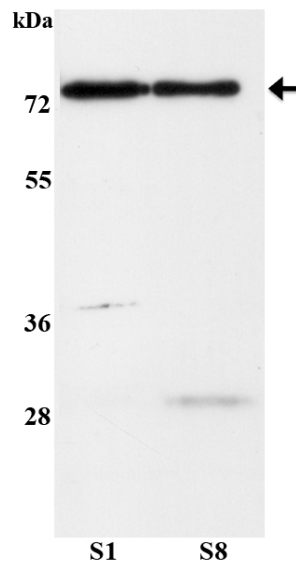


Figure 6.2.8.1a Recombinant S-proteins used to stimulate an incompatible SI reaction are detected by anti-PrMPK9-1 antibody. ~250 μ g of recombinant S₁ (**S1**) and S₈ (**S8**) were run on an SDS-PAGE gel and probed with the anti-PrMPK9-1 antibody. The anti-PrMPK9-1 antibody cross-reacts with a ~72kDa protein (as seen in Figure 6.2.8a). The fainter bands seen in Figure 6.2.8a can also be seen at ~36kDa and ~28kDa in S₁ (**S1**) and S₈ (**S8**) samples, respectively. The membrane was exposed for 3 minutes.

6.2.9 Immuno-precipitation experiments using the anti-PrMPK9-1 antibody

6.2.9.1 Immuno-precipitation using Protein A sepharose beads

Initial attempts at immuno-precipitation utilised Protein A sepharose beads. Protein A binds to the fragment crystallizable (Fc) region of antibodies through interaction with the heavy chain and can therefore be used to isolate and purify antibodies from mixtures of proteins (Langone, 1982). As Protein A binds to the Fc region, it still allows antigen binding in the fragment antigen binding (Fab) region.

2250 μ g of Calyculin A treated or untreated pollen was incubated with the anti-PrMPK9-1 antibody to allow binding of proteins recognised by the anti-PrMPK9-1 antibody. 25 μ l of Protein A sepharose beads were then added to the protein/antibody mixture to purify the antibody. The binding capacity of the beads is \sim 20mg IgG/ml beads. Therefore, as the anti-PrMPK9-1 antibody is \sim 20 μ g/ μ l, and 25 μ l of beads are used, a total of \sim 500 μ g antibody is bound. The beads were washed to remove unbound proteins, the immuno-precipitated proteins were eluted from the beads by boiling and 30 μ l were separated on a 12% SDS-PAGE gel. The gel was transferred to nitrocellulose filter and probed with the anti-pTXpY antibody to detect phosphorylated MAPK proteins present. For detection an anti-rabbit alkaline phosphatase conjugated antibody was used.

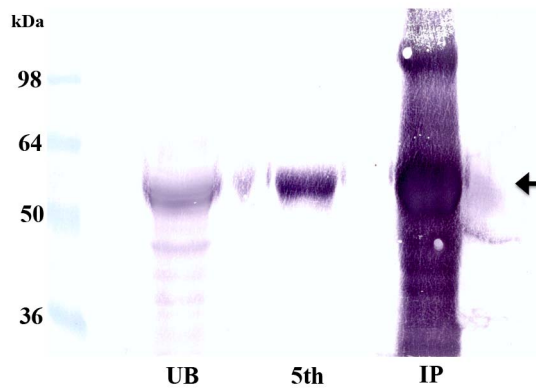


Figure 6.2.9.1a Proteins immuno-precipitated with the anti-PrMPK9-1 antibody and detected with the anti-pTepY antibody. The western blot shows unbound proteins (**UB**), proteins eluted in the 5th wash (**5th**) and immuno-precipitated proteins (**IP**) immuno-precipitated with the anti-PrMPK9-1 antibody and detected with the anti-pTXpY (which has been previously been shown to detect p56). In all samples a band of ~55kDa is detected (arrowed). This band most likely represents detection of the antibody heavy chain, used for immuno-precipitation, by the anti-rabbit IgG alkaline phosphatase conjugated antibody used for detection.

Figure 6.2.9.1a shows that a band of ~55kDa is detected in the immuno-precipitated sample. As this band is prominent and also detected in the unbound and 5th wash fractions, it was thought that this may represent contamination from the antibody heavy chain. As the anti-PrMPK9-1 and anti-pTXpY antibodies are both raised in rabbit, the anti-rabbit IgG alkaline phosphatase conjugated antibody used for detection is likely to not only bind to the anti-pTXpY antibody, but also the heavy chain (~55kDa) and light chain (~28kDa) of the anti-PrMPK9-1 antibody that have separated on the gel.

To attempt to overcome the problem of contamination by the antibody heavy chain a light chain-specific secondary antibody was obtained. The immuno-precipitation experiments were repeated as above, but for detection an anti-rabbit IgG light chain-specific HRP conjugated antibody was used. For comparison the immuno-precipitation was also carried out using the pre-immune sera.

Previous experiments had shown that a protein corresponding to p56 could be detected in calyculin A treated pollen (Figure 6.2.5a/b). Figure 6.2.9.1b shows the ~55kDa protein was detected in samples immuno-precipitated with the anti-PrMPK9-1 antibody and the pre-immune sera. Previous experiments had shown the ~56kDa protein detected by the anti-PrMPK9-1 antibody could not be detected in pollen by the pre-immune sera, suggesting the protein seen in the immuno-precipitated samples could not represent this protein. Although a light chain-specific antibody was used it seems there was still detection of the anti-PrMPK9-1 antibody heavy chain, as seen in Figure 6.2.9.1a. The presence of the ~55kDa protein, which is unlikely to represent p56 as it is detected by the pre-immune sera, makes it impossible to visualise proteins in the region of ~55kDa due to the quantity of this protein.

The immuno-precipitation experiments were repeated using the anti-pTEpY antibody for immuno-precipitation and the anti-PrMPK9-1 antibody (or pre-immune sera) for detection, to see if the reverse situation could reduce contamination. Figure 6.2.9.1c suggests that there was still detection of the antibody heavy chain (~55kDa). The ~55kDa band was detected by both the anti-PrMPK9-1 antibody and the pre-immune sera, suggesting that this band is not specifically detected by the anti-PrMPK9-1 antibody.

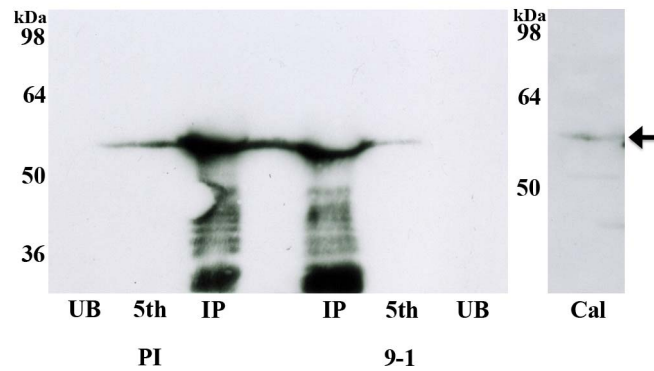


Figure 6.2.9.1b Proteins immuno-precipitated with the anti-PrMPK9-1 antibody and detected with a light-chain-specific secondary antibody. The western blot shows unbound proteins (**UB**), proteins eluted in the 5th wash (**5th**) and immuno-precipitated proteins (**IP**) immuno-precipitated with the anti-PrMPK9-1 antibody (**9-1**) or pre-immune sera (**PI**), and detected with the anti-pTXpY antibody, using an anti-rabbit IgG light-chain-specific secondary antibody for ECL (film exposed for 1 minute). Detection of a ~56kDa corresponding to p56 is shown in the calyculin a treated sample (**Cal**, film exposed for 10 minutes). In the immuno-precipitated samples (**IP**) there is detection of a ~55kDa protein which corresponds to the antibody heavy chain.

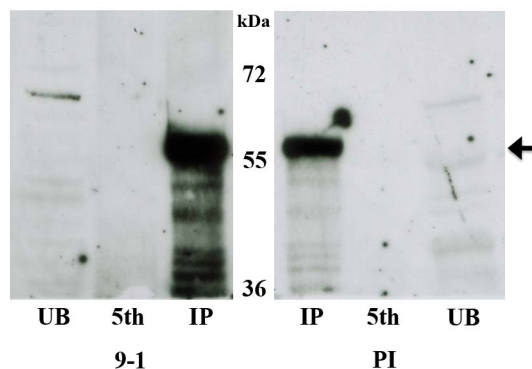


Figure 6.2.9.1c Proteins immuno-precipitated with the anti-pTXpY antibody and detected with the anti-PrMPK9-1 antibody. The western blot shows unbound proteins (**UB**), proteins eluted in the 5th wash (**5th**) and immuno-precipitated proteins (**IP**), immuno-precipitated with the anti-PrMPK9-1 antibody and detected with the anti-pTEpY. A protein band of ~55kDa is detected by both the anti-PrMPK9-1 antibody (**9-1**) and pre-immune sera (**PI**) (arrowed), which is likely to correspond to the anti-pTEpY antibody heavy chain.

6.2.9.2 Immuno-precipitation of radio-labelled proteins

Because it was not possible to use immuno-precipitation with the Protein A sepharose beads due to contamination from the antibody heavy chain, alternative approaches were investigated. In order to circumvent detection using antibodies, a radio-labelling approach was utilised. Rudd (1997) had previously shown it was possible to use ^{32}P - γATP to look at protein kinase activity in endogenous pollen proteins. ^{32}P - γATP introduced in the cell is used as a substrate by MAPKs (and MAPKKs) to phosphorylate proteins, which incorporates ^{32}P to the phosphorylated site. This radio-labelling allows visualisation by phosphor-imaging and therefore negates the use of antibodies. Attempts were made to radio-label phosphorylated proteins by treating pollen with calyculin A in the presence of ^{32}P - γATP . Proteins could then be immuno-precipitated with the anti-PrMPK9-1 antibody and labelled proteins could be detected by phosphor-imaging. It was known that a protein corresponding to p56 could be phosphorylated by calyculin A and, as p56 is likely to be encoded by PrMPK9-1, it was proposed p56 could be detected by this method.

Pollen was hydrated, grown and treated with either calyculin A for 10 minutes, or with GM as a negative control. $\sim 480\mu\text{g}$ of pollen (in $60\mu\text{l}$) was labelled with ^{32}P - γATP , and then immuno-precipitated using the anti-PrMPK9-1 antibody as described above (6.2.9.1). The unbound fraction, the fifth wash and the immuno-precipitated samples were separated on a 12% SDS-PAGE gel. The gel was washed in 40% methanol and 10% HAc to fix the proteins and dried in a vacuum drier. The gel was then exposed to a phosphor-screen. Figure 6.2.9.2a shows that it was not possible to detect any phosphorylated proteins in the immuno-precipitated sample.

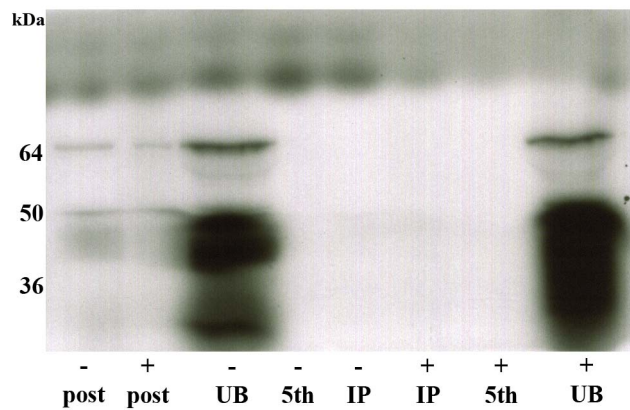


Figure 6.2.9.2a Phosphor-image of ^{32}P labelled proteins immuno-precipitated using the anti-PrMPK9-1 antibody. The phosphor-image shows unbound proteins (**UB**), proteins eluted in the 5th wash (**5th**) and immuno-precipitated proteins (**IP**) that have been calyculin A treated (+) or untreated (-) in the presence of ^{32}P - γATP and immuno-precipitated with the anti-PrMPK9-1 antibody. To show the radio-labelling was successful a sample after radio-labelling is shown (**post**). No proteins can be detected in the immuno-precipitated samples. The gel was exposed for 2 days.

6.2.9.3 Immuno-precipitation using affinity-purified, biotinylated anti-PrMPK9-1 antibody

As previous attempts failed to detect immuno-precipitated proteins by using Protein A sepharose beads or by radio-labelling of proteins prior to immuno-precipitation, an alternative method was required. Methodology that involved irreversible binding of the antibody to some conjugate, while allowing reversible affinity purification of proteins bound to the antibody, were investigated. Previous experiments had used the biotin-avidin affinity purification technology to purify the anti-PrMPK9-1 antibody. The biotin-avidin interaction binds with very high affinity (essentially irreversible), which provides stability of the complex under a wide variety of wash conditions. It was proposed that the anti-PrMPK9-1 antibody could be biotinylated and then bound to avidin resin. This anti-PrMPK9-1 antibody-avidin complex should then allow for immuno-precipitation experiments to be carried out (by binding of proteins to the anti-PrMPK9-1 antibody) and as the antibody-avidin is stable under a variety of wash conditions, should allow for elution of proteins from the antibody-avidin complex without contamination from any antibody.

In order to biotinylate the anti-PrMPK9-1 antibody using the EZ-Link[®] Sulfo-NHS-LC-Biotinylation Kit, 0.5-2ml of 1-10mg of antibody was required in a 1x PBS buffer. 25ml of anti-PrMPK9-1 antibody was purified over the PinPoint[™] purification column described earlier (6.2.6) in 5ml aliquots, to yield ~3940g of protein in ~10.5ml of TRIS-NaCl buffer. To concentrate the antibody and to change the TRIS-NaCl buffer to PBS buffer an Amicon[®] Ultra-4 Centrifugal Filter Unit was used. The antibody was added to the column in a number of aliquots and concentrated down to ~500µl. 1x PBS was added in 1ml aliquots and spun

through the column to change the buffer. 1746 μ g of antibody was recovered in 1710 μ l 1xPBS, giving a final concentration of 1.02mg/ml.

Using the EZ-Link[®] Sulfo-NHS-LC-Biotinylation Kit, 23.29 μ l of Biotin Solution was required to biotinylate the 1746 μ g of 1.02mg/ml antibody, according to the manufacturer's instructions. The biotinylation reaction was carried out and incorporation of biotin was calculated using the HABA calculator provided by the manufacturer (<http://www.piercenet.com/haba/habacalc.cfm>) using the cuvette format. This calculated that 9.12 moles of biotin were incorporated per IgG molecule. To check that biotinylation was successful, 25 μ l of antibody before and after biotinylation were separated on a 12% SDS-PAGE gel, transferred to nitrocellulose membrane, and probed with either NeutrAvidin protein (conjugated to HRP), which specifically detects biotinylation, or an anti-rabbit IgG (conjugated to HRP), which binds to the antibody heavy chain (~55kDa). Figure 6.2.9.3a shows that before biotinylation it was not possible to detect the antibody heavy chain, but after biotinylation it is possible to detect incorporation, suggesting biotinylation was successful. This figure also shows the anti-rabbit IgG detects the same amount of antibody present before and after biotinylation, irrelevant of the biotinylation state.

The biotinylated antibody was then bound to TetraLink[™] TetramericAvidin Resin. To test that the biotinylated antibody had bound to the avidin resin, antibody before binding, the unbound fraction removed from the resin, and the resin with bound antibody, were separated on a 12% SDS-PAGE gel, transferred to nitrocellulose membrane and probed with either NeutrAvidin protein (conjugated to HRP) or anti-rabbit IgG (conjugated to HRP). Figure 6.2.9.3b shows that virtually all the biotinylated antibody was bound to the avidin resin, as no

biotinylated antibody was present in the unbound fraction removed from the resin after binding. The western blot with the anti-rabbit IgG antibody suggested the majority of the antibody was incorporated onto the beads. As there is some detection of antibody heavy chain in the fraction removed from the resin after binding, this antibody is most likely represents antibody that was not biotinylated.

To confirm that the antibody bound to the avidin resin could detected PrMPK9-1, western blotting was carried out on recombinant PrMPK9-1C protein. PrMPK9-1C recombinant protein was separated on an 18% SDS-PAGE gel, transferred to nitrocellulose membrane and probed with anti-PrMPK9-1 antibody before biotinylation, pre-binding to the avidin resin, and with the fraction removed from the resin after binding. For detection, an anti-rabbit HRP-conjugated antibody was used. Figure 6.2.9.3c shows that anti-PrMPK9-1 antibody before biotinylation and pre-binding to the avidin resin show similar levels of detection of the PrMPK9-1C recombinant protein. However, detection using anti-PrMPK9-1 antibody, from the fraction removed from the resin after binding, showed much lower levels of detection of the PrMPK9-1C recombinant protein. This fraction is likely to contain un-biotinylated antibody, but shows that the majority of the antibody has bound to the avidin resin.

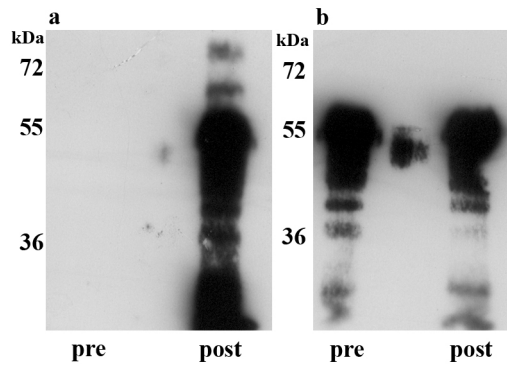


Figure 6.2.9.3a Biotinylation of anti-PrMPK9-1. (a) Detection of anti-PrMPK9-1 heavy chain (~55kDa) with the NeutrAvidin protein (conjugated to HRP), which only detects biotinylated protein. Before biotinylation (**pre**) there is no biotinylation of antibody heavy chain. The blot shows that biotinylation of the antibody was successful (**post**). (b) Detection of the antibody before (**pre**) and after (**post**) biotinylation with the anti-rabbit IgG antibody. This shows that similar levels of antibody have been loaded. The membrane was exposed to film for 3 seconds.

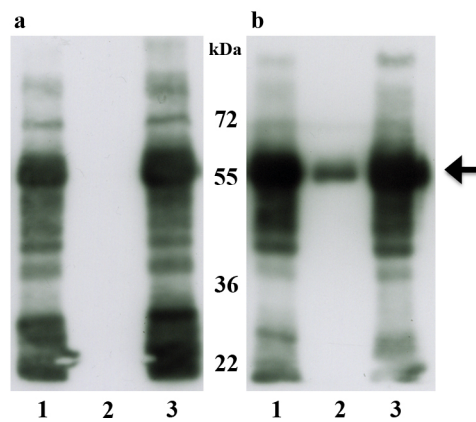


Figure 6.2.9.3b Anti-PrMPK9-1 antibody binds to the avidin resin. Detection of anti-PrMPK9-1 antibody heavy chain (~55kDa, arrowed) before binding to the avidin resin (**1**), in the fraction removed from the resin after binding (**2**), and bound to the resin (**3**). Detection with the NeutrAvidin Protein (conjugated to HRP) (**a**), which binds to biotinylated proteins and anti-rabbit IgG (conjugated to HRP) (**b**), which binds to antibody heavy chain. Loadings: 1 = 5 μ l, 2 and 3 = 12.5 μ l (due to 1 in 2.5 dilution during binding to the resin). Membrane was exposed for 2 seconds.

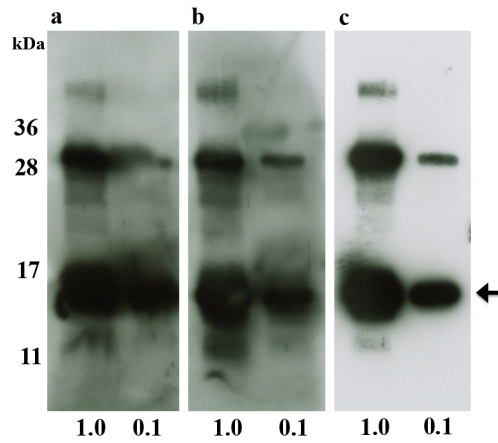


Figure 6.2.9.3c Anti-PrMPK9-1 successfully binds to the avidin resin. Detection of recombinant PrMPK9-1C (arrowed ~11kDa) with anti-PrMPK9-1 antibody before biotinylation (**a**, 1:1000 titre), before binding to the avidin resin (**b**, 1:1000 titre), and from the fraction removed from the resin after binding (**c**, 1:400 titre due to 1 in 2.5 dilution during binding to the resin). 1mg (**1**) and 0.1mg (**0.1**) recombinant PrMPK9-1C protein loaded. Membranes a and b were exposed for 3 seconds and membrane c for 30 seconds. By 30 seconds membranes a and b had saturated the film, showing a much lower concentration of antibody in the fraction removed from the resin after binding (**c**).

To determine how effectively the PrMPK9-1-avidin resin could immuno-precipitate PrMPK9-1, immuno-precipitation experiments were carried out using pollen extracts from calyculin A treated or untreated pollen. 50mg of pollen was hydrated, grown and treated with either calyculin A (0.25 μ M final concentration) or a GM control. Proteins were extracted by sonication and protein concentration was determined. 2mg of pollen extract was added to 100 μ l PrMPK9-1-avidin resin and incubated to allow proteins to bind the resin. Figure 6.2.9.3d shows a Coomassie Blue stained gel illustrating protein input was equal between the calyculin A treated and the untreated extracts. The resin was washed with buffer to remove unbound proteins and then changing the pH using citric acid eluted the bound proteins. The total elution had a volume of 140 μ l. 30 μ l of the unbound fraction and 30 μ l of the immuno-precipitated proteins were run on a 12% SDS-PAGE gel and transferred to a nitrocellulose membrane. The membrane was probed with the anti-pTEpY antibody to detect any activated MAPKs. For detection, an anti-rabbit HRP-conjugated antibody was used.

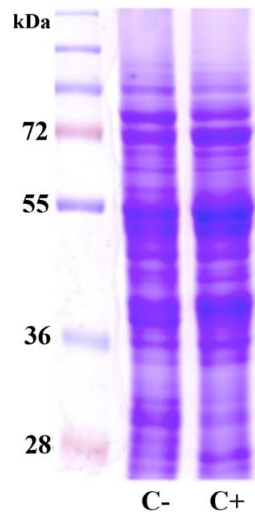


Figure 6.2.9.3d Calyculin A treated and untreated pollen protein input for immuno-precipitation experiments. Equivalent amounts of calyculin A treated (C+) and untreated (C-) pollen proteins used for immuno-precipitation. As extracts were at different concentrations equal amounts of protein had to be used to make immuno-precipitation experiments comparable. C- = 2.4 μ l protein and C+ = 10 μ l protein, equivalent to ~40 μ g protein.

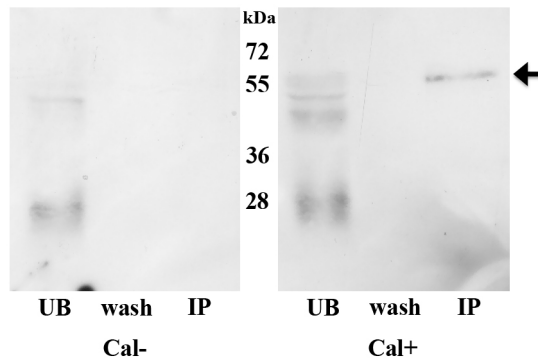


Figure 6.2.9.3e Immuno-precipitation of calyculin A treated and untreated pollen with the anti-PrMPK9-1 antibody, detected by western blotting with the anti-pTXpY antibody. Two protein bands are detected after a 40-minute exposure in the calyculin A treated pollen (CalA+), but not in the untreated pollen (CalA-). The band (arrowed) corresponds to the position of p56 (~56kDa). UB: un-bound fraction (this represents proteins that did not bind to the anti-PrMPK9-1 resin) IP: immuno-precipitated proteins.

The western blot (Figure 6.2.9.3e) shows that the calyculin A-treated pollen contained a single protein of ~56kDa that was immuno-precipitated by the anti-PrMPK9-1 antibody and subsequently detected by the anti-pTXpY antibody, which recognizes dually phosphorylated MAPKs. No proteins were detected in the untreated sample.

To determine the identity of the protein in the calyculin A treated pollen sample, a band corresponding to this protein was sent for analysis by FT-ICR MS. A 12% SDS-PAGE gel was run containing 45µl of the immuno-precipitated proteins. The proteins were stained with Coomassie Blue stain for visualization, and a plug corresponding to the protein band was excised, trypsin digested and sent for analysis by FT-ICR MS. It was possible to see the ~56kDa protein band on the Coomassie Blue stained gel (data not shown). The MS data was compared to the 'Plant' database, with the relevant modifications accounted for. The ~56kDa protein band showed very significant peptide matches with PrMPK9-1 (Table 6.2.9.3a).

Reference Scan(s), File	Peptide	P (pro) P (pep)	Score XC
PrMPK9-1		0.0000034749641138	24.05772
	K.GSYGVVASAVDHTGK.V	0.0002051724056350	0.83117
	R.YQILEVIGK.G	0.0000034749641138	0.84930
	K.VDPLALNLLER.L	0.0000747725806030	1.13475
	K.VDPLALNLLER.L	0.0000915136846175	1.15432

Table 6.2.9.3a PrMPK9-1 peptides identified from the ~56kDa protein band. The peptide probabilities show that all the peptides present in PrMPK9-1 are highly significant matches. Probabilities (**P (pro)/P (pep)**) of less than 0.001 are considered significant.

6.2.10 Immuno-localisation of PrMPK9-1

To determine the localisation of PrMPK9-1, immuno-localisation was carried out in normal growing pollen tubes. Pollen was hydrated and grown, fixed and probed with the PinPoint™ purified anti-PrMPK9-1 antibody. For visualization of the anti-PrMPK9-1 primary antibody an anti-rabbit IgG-FITC antibody was used. The results are shown in Figure 6.2.10a. The immuno-localisation suggests that PrMPK9-1 is distributed throughout the pollen tube. DAPI staining allowed visualization of the nucleus. This suggested that PrMPK9-1 was located in both the nucleus and cytoplasm.

Preliminary experiments were also carried out to determine if the localisation of PrMPK9-1 changed during an incompatible SI response. Pollen was hydrated and grown as before but treated with S-proteins for 10 minutes to mimic an incompatible SI response, before fixing. The results suggested that there was no change in the distribution of PrMPK9-1 (data not shown).

Due to time constraints it was not possible to carry out certain controls for the immuno-localisation experiments. For example, this would include carrying out the immuno-localisation using the pre-immune serum in place of the anti-PrMPK9-1 antibody to determine if the signal seen is above background levels and to show that the protein detected in the immuno-localisation experiments, cannot be detected by the pre-immune serum. In addition, immuno-localisation should be carried out using only the secondary antibody (the anti-rabbit IgG-FITC antibody), which would also determine background fluorescence. These will be required to confirm the immuno-localisation results.

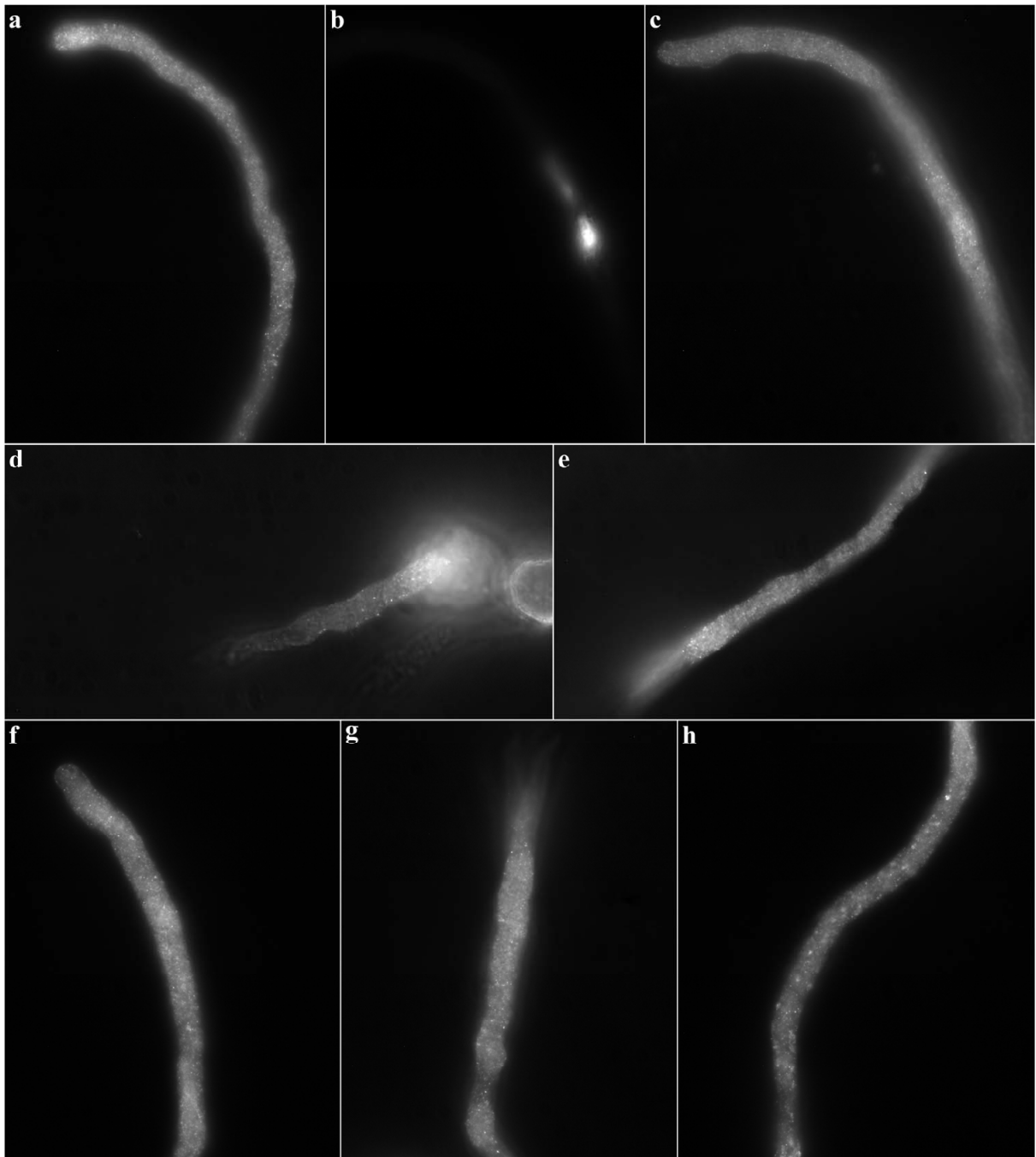


Figure 6.2.10a Immunolocalisation of PrMPK9-1. (b) A DAPI stain of the pollen tube nucleus. (a) PrMPK9-1 localisation in the same pollen tube shown in plate b. PrMPK9-1 signal, as represented by the punctate foci, suggests that the PrMPK9-1 protein is present in both the cytoplasm and the nucleus. (c-h) PrMPK9-1 signal in a number of pollen tubes shows similar localisation to that shown in plate a.

6.3 DISCUSSION

6.3.1 The anti-AtMPK3 antibody can detect recombinant PrMPK9-1

Earlier results (Li et al., 2007) had shown that the anti-AtMPK3 antibody bound specifically to p56, which led to investigations to determine if p56 was an AtMPK3 orthologue. A *PrMPK3* gene has been cloned which is predicated to encode a ~43kDa protein, and is therefore unlikely to encode p56. Bioinformatics and proteomics analysis have now suggested that *PrMPK9-1* is a strong candidate to encode p56. In order to further characterise PrMPK9-1 a full-length recombinant protein was expressed in *E. coli*. It has been shown that the anti-AtMPK3 antibody can cross-react with this PrMPK9-1 recombinant protein, which helps to confirm the claim that *PrMPK9-1* is a very strong candidate for encoding p56. Alignments of the PrMPK9-1 protein were made with the region of AtMPK3 used to raise the anti-AtMPK3 antibody. Analysis showed that there are no obvious regions of homology between the region used for antibody production and PrMPK9-1. Although epitopes can range from around 5 to 12 amino acids it is difficult to determine which region of PrMPK9-1 the anti-AtMPK3 antibody identifies.

6.3.2 Production of an anti-PrMPK9-1 antibody

An antibody was raised against PrMPK9-1 and it was shown that this antibody could be used to identify a protein corresponding to p56. Due to ease, initial attempts were made to raise an antibody against a specific C-terminal peptide of PrMPK9-1. This region was selected due to its specificity to PrMPK9-1 and because it passed various selection criteria, suggesting it was

a suitable antigen. ELISA experiments and western blotting experiments (data not shown) suggested the antisera raised against this peptide were not antigenic. ELISA results suggested that there was a slight response to the antigen but that it was not considered strong enough to be used for any practical application. Because the peptide selected passed various selection criteria it is difficult to suggest why this peptide was not a suitable antigen.

Because it was not possible to raise an antibody against a peptide an antibody was raised against a larger C-terminal PrMPK9-1 recombinant protein. This region was specific to PrMPK9-1 and it was proposed that a larger region of the protein would be more likely to be antigenic. This peptide resulted in the production of antisera that could detect the PrMPK9-1 protein.

In order to increase specificity and reduce background the anti-PrMPK9-1 antibody was purified. Although the recombinant protein sample sent to raise the antibody against was nearly pure, it was likely that the majority of this non-specific binding was due to proteins raised against *E. coli* proteins present in the recombinant protein sample. The antibody was purified using the PinPoint™ Xa Protein Purification System. Western blotting experiments showed that the purification severely reduced background and increased specificity of the antisera. This purification of the antibody allowed for better specificity during western blotting and immuno-localisation experiments.

6.3.3 Detection of pollen proteins using the anti-PrMPK9-1 antibody

Initial experiments were carried out to determine if the anti-PrMPK9-1 antibody could detect any pollen proteins, especially in the region of p56. These experiments showed that it was possible for the antibody to detect a band of ~56kDa that corresponded to p56 (shown by detection with the anti-pTXpY antibody). To enrich for phospho-proteins and to determine if the anti-PrMPK9-1 antibody could detect a ~56kDa protein that can be phosphorylated (as would be expected if it detects a MAPK), western blotting experiments were carried out on calyculin A treated pollen extracts purified using a phospho-column. As the anti-PrMPK9-1 antibody cross-reacted with a phospho-protein at exactly the same position as p56 it provided good evidence that the anti-PrMPK9-1 and anti-pTXpY antibodies were detecting the same protein.

Previous experiments had been carried out on calyculin A treated pollen, which can be used to phosphorylate proteins with a basal level of activity in the absence of a stimulus. To provide more evidence that the two antibodies were detecting p56, western blotting was carried out on pollen that had undergone an incompatible SI reaction. This confirmed that both antibodies were detecting a protein corresponding to p56 in an incompatible SI reaction. In these western blot experiments there was detection of a large protein of ~72kDa, and two fainter proteins of ~36kDa and ~28kDa, which had not been detected in previous immuno-blotting experiments. As the only difference between this and previous experiments was the addition of recombinant S-proteins (to initiate an incompatible SI reaction) it was argued they may be contaminating the samples. Evidence showed that the S-proteins did in fact contain proteins that cross-reacted with the anti-PrMPK9-1 antibody. It is likely that the recombinant S-protein

samples were not pure and contained endogenous *E. coli* proteins and these proteins were detected by the PrMPK9-1 antisera. It was not determined if this cross-reactivity was due to *E. coli* antibodies still present in the purified antisera, or if antibodies specific to PrMPK9-1 were able to detect *E. coli* proteins.

6.3.4 Immuno-precipitation of p56 with the anti-PrMPK9-1 antibody

Initial attempts to immuno-precipitate p56 with the anti-PrMPK9-1 antibody were carried out using protein A sepharose resin. However, it was not possible to visualise proteins in the ~55kDa region on western blots due to the presence of a large protein band of ~55kDa being detected. Both the antibody used for immuno-precipitation (anti-PrMPK9-1), and the antibody used for western blot analysis (anti-pTXpY), were raised in the same animal. For western blotting an anti-rabbit IgG secondary antibody was used that cross-reacted with the anti-pTXpY antibody. During the boiling step, prior to separation of immuno-precipitated proteins on SDS-PAGE gels, it is likely that the anti-PrMPK9-1 antibody was dissociated from the protein A-sepharose resin and was also separated on the gel. This meant that, as an anti-rabbit IgG secondary antibody was used for detection, there was likely to be detection of the anti-PrMPK9-1 antibody proteins as well as any immuno-precipitated proteins. Even though experiments were not carried out to directly determine that it was the antibody heavy chain that was being detected, results showed that as a band of ~55kDa was detected by both the pre-immune sera and the anti-PrMPK9-1 antibody (and it had already been shown the pre-immune sera did not cross-react with a ~56kDa protein in pollen). This implied that even if the antibody heavy chain was not responsible for the contamination this method of immuno-precipitation was not suitable.

To circumvent using detection with antibodies, radio-labelling of proteins was carried out. Although this method of detection is relatively sensitive it was not possible to visualise any phosphorylated proteins immuno-precipitated with the anti-PrMPK9-1 antibody. This radio-labelling method has been used previously in poppy pollen to investigate the phosphorylation of p26.1 and p68 in incompatible SI reactions (Rudd, 1997) and to demonstrate the ability of p56 to phosphorylate substrates (Rudd *et al.*, 2003). This technique has also been used to show *in vitro* phosphorylation of a MAPK by its upstream MAPKK (Kiegerl *et al.*, 2000). However, this technique has never been used to study the activation of p56 directly. Proteins were extracted from pollen that had been treated with calyculin A for 10 minutes. It may be by this time that the majority of p56 proteins in the extract have been phosphorylated and therefore will not incorporate radio-labelled phosphorous into p56, and therefore cannot be visualised. To overcome this problem the experiment was repeated but the extract was not stimulated with calyculin A until after the addition of ^{32}P - γ ATP (data not shown). As the incubation time with ^{32}P - γ ATP was 10 minutes it was argued the majority of p56 activated in this time would have radio-labelled phosphorous incorporated. Results showed it was still not possible to detect p56.

In order to remove contamination by the antibody heavy chain, irreversible binding of biotinylated antibody to avidin resin was utilised. As the avidin-biotin binding is so strong and remains so under a variety of wash conditions, it allowed immuno-precipitation to be carried out without contamination from the antibody heavy chain. The anti-PrMPK9-1 antibody was biotinylated and bound to avidin resin. This complex could then be used for immuno-precipitation experiments. Preliminary experiments showed that it was possible to use this technique to immuno-precipitate a ~56kDa protein, that can then be specifically

detected with the anti-pTXpY antibody, without contamination from antibody heavy chain. FT-ICR MS analysis of this protein confirmed that the immuno-precipitated protein was PrMPK9-1. In order to confirm that PrMPK9-1 corresponds to p56 additional experiments will have to be carried out. The above immuno-precipitation experiments need to be repeated with pollen that has undergone a compatible or incompatible SI reaction, as an incompatible SI reaction is the only known condition under which p56 is activated. As p56 is not activated in a compatible SI reaction (beyond its basal level of activation) western-blotting experiments should reveal a change in phosphorylation of this protein, which can be detected with the anti-pTXpY antibody.

In the future, this immuno-precipitation method should allow co-immuno-precipitation experiments to identify proteins that interact with PrMPK9-1. This should give an insight into the role PrMPK9-1 plays in signal transduction pathways and help to clarify if it plays a role in incompatible SI reactions.

6.3.5 Immuno-localisation

Immuno-localisation experiments suggest that PrMPK9-1 is localised throughout the pollen tube in both the cytoplasm and the nucleus. These experiments need to be repeated, and with the relevant controls as described above, in order to confirm this finding. However, the pattern of expression seen here is similar to that seen by Coronado *et al.* (2002; 2007). In mature pollen an anti-ERK1/2 antibody was used to look at ERK1/2 (MAPK) orthologues, and showed that they localised in the cytoplasm and nucleus (Coronado *et al.*, 2002). However, in these immuno-localisation experiments it was not determined which MAPKs

were detected by the ERK1/2 antibody. Coronado *et al.* (2007) also used an anti-Ntf4 antibody to look at the localisation of Ntf4 in tobacco pollen grains. It was shown that Ntf4 was localised in both vegetative and the generative nuclei, and also in the cytoplasm, in mature pollen. Although Ntf4 is not an orthologue of PrMPK9-1 these experiments are the only evidence of MAPK localisation in pollen.

Preliminary experiments suggested there was no difference in the distribution of PrMPK9-1 after an incompatible SI reaction. Further experiments over a larger time scale may help to confirm this finding. In addition, the anti-pTXpY antibody could be used in immunolocalisation and co-immunolocalisation experiments to determine the localisation of activated PrMPK9-1 during an incompatible SI reaction.

6.3.6 Summary

In summary, this chapter provides convincing evidence that PrMPK9-1 encodes p56, although this evidence is not conclusive. The anti-PrMPK9-1 antibody can detect a ~56kDa protein in pollen. It is also known that the ~56kDa protein, detected by the anti-PrMPK9-1 antibody, can be phosphorylated. In addition to this immunoprecipitation experiments show that the anti-PrMPK9-1 antibody can purify PrMPK9-1, and the anti-pTXpY antibody, that only detects dually phosphorylated MAPKs, specifically detects this protein.

CHAPTER 7

**Preliminary studies to define a role for MPK9 in *Arabidopsis*
*thaliana***

CHAPTER 7 - PRELIMINARY STUDIES TO DEFINE A ROLE FOR *MPK9* IN *ARABIDOPSIS THALIANA*

7.1 INTRODUCTION

Reverse genetics is an important tool in the study of gene function whereby a gene is mutated and its effects on phenotype are investigated. Originally many mutant genes were identified by random spontaneous mutation. Random mutation of genes can be induced using chemicals or gamma radiation. An alternative to these methods is based on the insertion of foreign DNA into a gene of interest. In *Arabidopsis*, and other species, this utilises the T-DNA elements from *Agrobacterium tumefaciens*. *Agrobacterium tumefaciens* causes crown gall in many species of plants by the transfer of a Ti plasmid, which contains genes on the T-DNA region that allow production of a unique food source for the bacteria, into plant cells where it semi-randomly incorporates the T-DNA into the plant's genome allowing expression of the genes. This T-DNA insertion of *Agrobacterium* has been exploited in biotechnology allowing the insertion of modified T-DNA elements into the plant germline DNA. Modified Ti plasmids that have the tumour-promoting genes removed can be used as a vector to transfer genes of interest into the plants genome using *Agrobacterium* (for a review see Perinov and Sundaresan, 2000; Krysan *et al.*, 1999). The SALK Institute for Biological Sciences has created thousands of *Arabidopsis* T-DNA insertion lines, which have been sequenced and stored in the T-DNA Express database (<http://signal.salk.edu/cgi-bin/tdnaexpress>, SIGnAL).

To date it is not possible to transform *P. rhoeas* via these traditional transformation processes. In order to determine if any of the *Arabidopsis thaliana* MAPKs (with particular emphasis on

AtMPK9) had any role in pollen growth or development several T-DNA insertion lines were obtained to see if this data could shed light on the potential roles of these MAPKs in poppy. To check for MAPK insertion lines the T-DNA Express database from SIGnAL was used. Lines were available as heterozygous knockout lines for *AtMPK9* (SALK064439, Δ9), *AtMPK20* (SALK148463, Δ20) and *AtMPK19* (SALK075214, Δ19) and as homozygous knockout lines for *AtMPK8* (SALK037501, Δ8) and *MPK17* (SALK020801, Δ17). No line is currently available for *AtMPK15*.

This chapter is concerned with the phenotypic analysis of the above T-DNA insertion lines. Plants were grown to see if there were any differences in pollen related phenotypes compared to wild-type *Arabidopsis thaliana* ecotype Col-0 plants. Three criteria were investigated: i) Alexander's stain used to look at the viability of the pollen. Alexander's stain (Alexander, 1969) can be used to determine viable and non-viable pollen in a number of species. Alexander's stain contains acid fuchsin, which stains the pollen protoplasm a red-pink, and malachite green, which stains the exine walls of aborted pollen green (Figure 7.1a). ii) Pollen growth was investigated *in vivo* using aniline blue staining of the pollen growing through the stigma. Aniline blue staining detects callose structures and can be used to detect pollen tube growth, as callose is deposited in pollen cell walls and in pollen tubes during growth (Hauser and Morrison, 1964) (Figure 7.1b). iii) Effects on fertility were analysed using seed counts and by measuring silique length.



Figure 7.1a Alexander's stain showing viable and non-viable pollen grains. Alexander's stain contains acid fuchsin, which stains the pollen protoplasm red-pink in viable pollen (left) and malachite green, which stains the exine walls of non-viable pollen green (right).

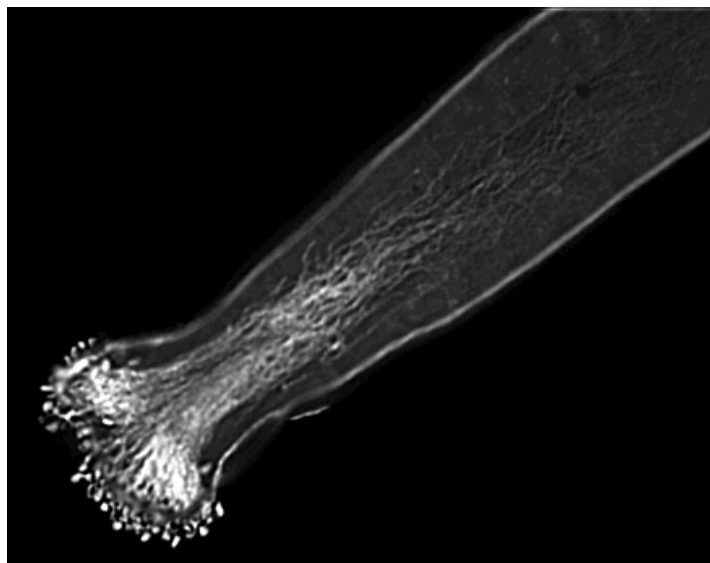


Figure 7.1b Aniline blue staining of growing pollen tubes. The aniline blue stain detects callose, which is deposited in growing pollen tubes and in pollen cell walls.

7.2 RESULTS

7.2.1 Determination of MAPK homozygous T-DNA knockout lines

Apart from an *AtMPK15*-deficient line, the T-DNA insertion lines obtained represented of all the highly pollen expressed p56 candidate genes from Affymetrix chip data (see Chapter 4). The T-DNA Expresses website (<http://signal.salk.edu/cgi-bin/tdnaexpress>) was used to predict the probable site of the insertion for each line and primers were designed to amplify a region of ~400bp around this (~200bp upstream and downstream of the insert). Each primer set was tested to see if it would amplify the wild-type gene of interest by PCR. Amplification products were cloned and sequenced to confirm the amplification product was from the correct gene. To confirm the position of the insert one of the gene specific primers (either the 5' or 3' primer depending upon the orientation of the insert) was used in combination with a left border primer (Lba1) found on the T-DNA insertion. Amplification products were cloned and sequenced to determine the position of the insert. If no amplification product was obtained new primers were designed to clone the gene/insert of interest and the process was repeated. All genes and insert were successfully cloned apart from the *AtMPK19* T-DNA knockout line. Table 7.2.1a shows the primers used to sequence the gene and insert of each T-DNA insertion line.

T-DNA	5' gene primer	3' gene primer	5' insert primer	3' insert primer	Position
Δ8	MPK8TDNAu/s	MPK8TDNAd/s	MPK8TDNAu/s	LbaI	1096bp
Δ9	MPK9TDNAu/s	MPK9TDNAd/s	MPK9TDNAu/s	LbaI	196bp
Δ17	MPK17TDNAu/s	MPK17TDNAd/s2	MPK17TDNAu/s	LbaI	744bp
Δ20	MPK20TDNAu/s2	MPK20TDNAd/s	MPK20TDNAu/s2	LbaI	425bp

Table 7.2.1a Primers used to amplify gene and insert sequences from MAPK T-DNA knockout lines.

Combinations of primer used to clone the gene and insert for each of the lines is shown, along with the predicted position of the insert. The insert position shows the position in genomic DNA from the gene start codon.

Before any phenotypic analysis could be carried out seeds were grown and genotyped to obtain homozygous plants for all the T-DNA insertion lines. In addition, expression analysis was carried out to confirm the mRNA was being knocked down. Total mRNA from each knockout line and from wild-type plants was extracted and total cDNA was synthesised. PCR amplification was used, with the primers listed in Table 7.2.1a, to show that the mRNA was present in wild-type plants and absent in the respective knockout line (Figure 7.2.1a). As a control GAPD was amplified from wild-type cDNA and each knockout line.

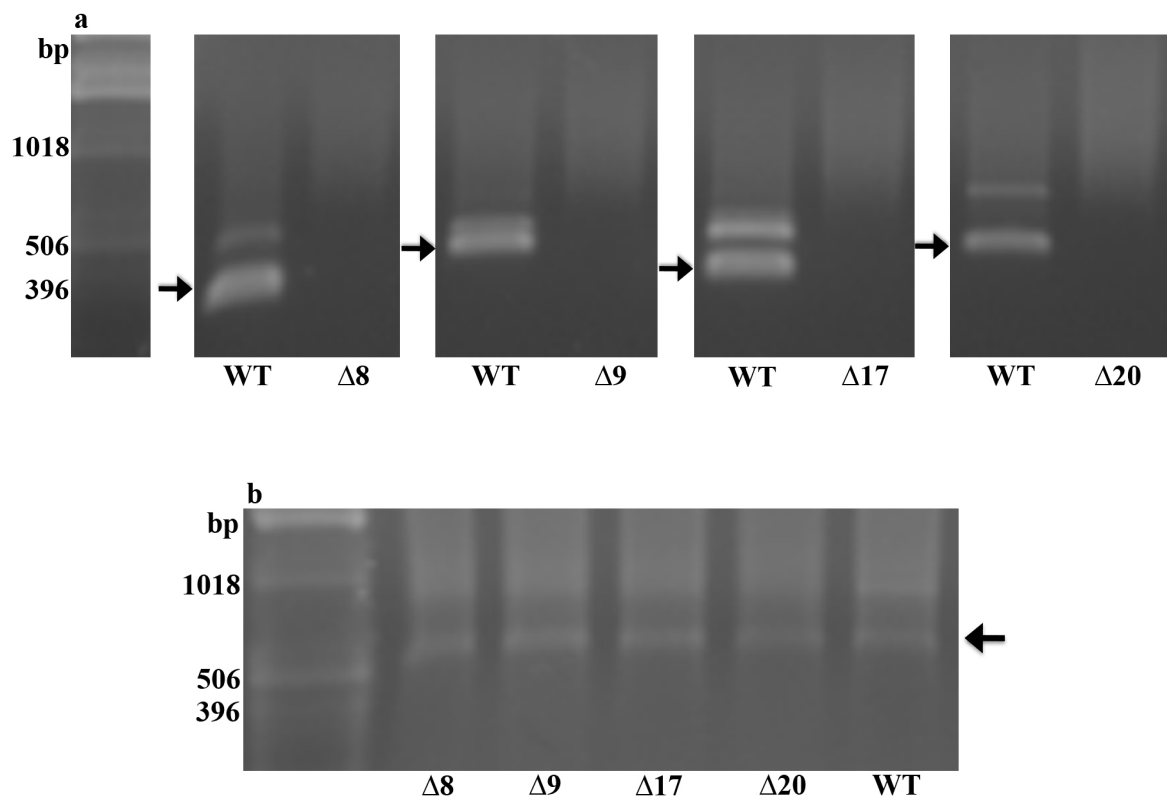


Figure 7.2.1a Expression analysis of mRNA in the MAPK T-DNA knockout lines. Expression of *AtMPK8*, *AtMPK9*, *AtMPK17* and *AtMPK20* in wild-type plants and in each of the respective T-DNA knockout lines (arrowed) showing mRNA expression is abolished in the knockout lines (a). Expression of GAPD mRNA in each of the four lines ($\Delta 8$, $\Delta 9$, $\Delta 17$, $\Delta 20$) and wild-type plants (WT) was used as a control (b). The gene sequences are predicted to be as follows, MPK8: 304bp; MPK9: 434bp; MPK17: 333bp; 20: 431bp. The upper bands most likely represent genomic contamination (predicted product sizes: MPK8: 507bp; MPK9: 526bp; MPK17: 574bp; MPK20: 757bp)

7.2.2 Phenotypic analysis of T-DNA insertion lines

The main purpose of the phenotypic analysis was to investigate pollen related defects. However initial analysis of all the T-DNA insertion lines suggested that none of the lines showed any defects in their vegetative phenotypes.

7.2.2.1 Pollen viability test using Alexander's stain

To determine if there was any difference in pollen viability between wild-type plants and the MAPK knockout T-DNA lines Alexander's stain was used. Plants were grown for each line (WT, $\Delta 8$, $\Delta 9$, $\Delta 17$, $\Delta 20$) and flowers were harvested from the main inflorescence about 3-5 days after the first flowers had opened. A number of anthers were picked from each plant, from a number of plants, and also plants grown at different times for analysis. A total of 1,500 pollen grains were counted for each line and the number of viable versus non-viable pollen grains was determined. To determine if there was a significant difference between wild-type and the T-DNA knockout lines a Chi-squared test was used. Table 7.2.2.1a shows the results.

The Chi-squared test suggested there were no significant differences in pollen viability between wild-type plants and any of the T-DNA knockout lines.

Line	Viable pollen	Non-viable pollen	Chi-squared
WT	1491	9	1.000
$\Delta 8$	1490	10	0.738
$\Delta 9$	1494	6	0.316
$\Delta 17$	1489	11	0.504
$\Delta 20$	1488	12	0.316

Table 7.2.2.1a Pollen viability in the MAPK T-DNA knockout lines. The table shows the number of viable and non-viable pollen grains from a total of 1500 pollen grains counted. Pollen for each line was counted from multiple plants from plants sown at, at least two different time points. The table also shows the Chi-squared test compared to wild-type pollen. This suggests there was no difference between knockout lines and wild-type plants.

7.2.2.2 *In vivo* pollen growth using aniline blue staining

To determine if there was any difference in pollen growth between wild-type plants and the MAPK T-DNA insert lines aniline blue staining was used. Plants were grown for each line ($\Delta 8$, $\Delta 9$, $\Delta 17$, $\Delta 20$) and wild-type plants. Wild-type plants were pollinated with wild-type pollen or pollen from one of the knockout lines. Pollen growth down the stigma was investigated after 2, 4, 6 and 12 hours after pollination. To establish if there was any difference in pollen viability in the knockout lines compared to wild-type plants a T-test was carried out. Table 7.2.2.2a shows the results.

The T-test showed that there was no significant difference in pollen tube growth between wild-type plants and any of the T-DNA knockout lines.

		$\Delta 8$	$\Delta 9$	$\Delta 17$	$\Delta 20$	WT
2h	Mean	5.971	6.371	6.057	5.943	5.975
	St Dev	0.734	1.184	0.461	0.692	0.822
	St Error	0.278	0.448	0.174	0.262	0.291
	T-Test	0.993	0.475	0.813	0.936	1.000
4h	Mean	11.229	11.800	11.386	11.157	11.110
	St Dev	0.953	1.207	0.782	0.776	1.748
	St Error	0.360	0.456	0.296	0.293	0.553
	T-Test	0.860	0.352	0.667	0.941	1.000
6h	Mean	14.643	15.586	13.929	14.471	14.425
	St Dev	0.900	1.525	1.291	0.920	2.170
	St Error	0.340	0.576	0.488	0.348	0.767
	T-Test	0.801	0.250	0.596	0.957	1.000
12h	Mean	20.957	20.229	20.071	19.471	19.625
	St Dev	3.206	2.202	1.884	2.547	2.615
	St Error	1.212	0.832	0.712	0.278	0.755
	T-Test	0.373	0.600	0.673	0.902	1.000

Table 7.2.2.2a Pollen growth rates in the MAPK T-DNA knockout lines. The T-test results suggest there were no differences in pollen tube growth rates between wild-type plants and any of the T-DNA insertion lines. **St Dev**: standard deviation; **St Error**: standard error.

7.2.2.3 Effects on fertility

To investigate any difference in fertility seed counts and silique length measures were used. The silique lengths were measured and seeds counted from mature siliques. At least 50 plants were analysed for each line grown and from plants grown from at least two different time points. To establish any differences between wild-type and knockout lines a T-test was carried out. Table 7.2.2.3a shows the results.

The T-test showed that there was no significant difference in seed number or silique length between wild-type plants and any of the T-DNA knockout lines.

	Seed count					Silique length				
	$\Delta 8$	$\Delta 9$	$\Delta 17$	$\Delta 20$	WT	$\Delta 8$	$\Delta 9$	$\Delta 17$	$\Delta 20$	WT
Mean	1.681	1.700	1.659	1.708	1.674	68.600	67.860	67.880	68.120	70.140
St. Dev	0.069	0.078	0.070	0.085	0.093	4.571	6.559	6.083	5.637	5.876
St. Error	0.010	0.011	0.010	0.012	0.013	0.646	0.928	0.860	0.797	0.831
T-test	0.670	0.132	0.363	0.059	1.000	0.147	0.070	0.062	0.083	1.000

Table 7.2.2.3a Fertility in the MAPK T-DNA knockout lines. The T-test results show there were no differences in both number of seeds and silique length between wild-type plants and any of the T-DNA insertion lines. **St Dev**: standard deviation; **St Error**: standard error.

7.2.3 Construction of double T-DNA knockout lines

Because there was little evidence of pollen related defects in single knockout lines an attempt was made to construct double knockout lines in case of redundancy between genes. Each of the single T-DNA knockout lines ($\Delta 8$, $\Delta 17$, $\Delta 20$) were crossed with the MPK9 T-DNA knockout line, in both orientations, with plants being both pollen donors and pollen recipient. The position of the genes on the *A. thaliana* chromosomes (*AtMPK8* on chromosome 1, *AtMPK17* and *AtMPK20* at either end of the arms of chromosome 2, and *AtMPK9* on chromosome 3) meant that the genes were not linked which aided crossing. Plants from the original cross were genotyped to determine which plants were heterozygous for each T-DNA and these plants were then self-fertilised to create homozygous plants for both T-DNA insert. These plants were self-fertilised for at least one additional generation to confirm both knockouts were inherited (and all progeny contained both T-DNA insertions). Once $\Delta 9 \times \Delta 8$, $\Delta 9 \times \Delta 17$ and $\Delta 9 \times \Delta 20$ homozygous double T-DNA knockout lines were obtained, phenotypic analysis was carried out to determine if any of these plants had any pollen defective phenotypes. None of the lines demonstrated any defects in their vegetative phenotypes.

7.2.3.1 Pollen viability test using Alexander's stain

Alexander's staining was carried out as described above. The results are shown in table 7.2.3.1a.

Line	Viable pollen	Non-viable pollen	Chi-squared
WT	1490	10	1.000
$\Delta 9x\Delta 8$	1487	13	0.341
$\Delta 9x\Delta 17$	1492	8	0.526
$\Delta 9x\Delta 20$	1491	9	0.751

Table 7.2.3.1a Pollen viability in the MAPK double T-DNA knockout lines. The table shows the number of viable and non-viable pollen grains from a total of 1500 pollen grains counted. Pollen for each line was counted from multiple plants from plants sown at, at least two different time points. The table also shows the Chi-squared test compared to wild-type pollen. This suggests there was no difference between knockout lines and wild-type plants.

None of the double T-DNA knockout lines showed any differences in pollen viability compared to wild type plants.

7.2.3.2 *In vivo* pollen growth using aniline blue staining

Aniline blue staining was carried out for the double T-DNA knockout lines as described above. The results and T-test results are shown in table 7.2.3.2a. The T-test suggested there were no differences between T-DNA knockout lines and wild type plants.

		$\Delta 9x\Delta 8$	$\Delta 9x\Delta 17$	$\Delta 9x\Delta 20$	WT
2h	Mean	5.956	6.043	6.271	5.980
	St Dev	0.714	0.700	0.550	0.700
	St Error	0.238	0.264	0.208	0.222
	T-Test	0.941	0.858	0.373	1.000
4h	Mean	11.500	11.250	11.688	11.182
	St Dev	0.872	0.843	0.897	1.365
	St Error	0.330	0.298	0.317	0.412
	T-Test	0.592	0.902	0.375	1.000
6h	Mean	15.214	15.229	14.825	14.822
	St Dev	1.353	0.986	0.848	1.436
	St Error	0.512	0.373	0.300	0.479
	T-Test	0.587	0.533	0.996	1.000
12h	Mean	21.157	20.686	19.988	19.718
	St Dev	1.539	2.155	2.068	2.869
	St Error	0.582	0.815	0.731	0.865
	T-Test	0.243	0.457	0.824	1.000

Table 7.2.3.2a Pollen growth rates in the MAPK double T-DNA knockout lines. The T-test results suggest there were no differences in pollen tube growth rates between wild-type plants and any of the T-DNA insertion lines. **St Dev**: standard deviation; **St Error**: standard error.

7.2.3.3 Effects on fertility

Differences in fertility were investigated in the double T-DNA knockout lines via seed counts and silique length, as described above. The results are shown in Table 7.2.3.3a.

	Seed count				Silique length			
	$\Delta 9x\Delta 8$	$\Delta 9x\Delta 17$	$\Delta 9x\Delta 20$	WT	$\Delta 9x\Delta 8$	$\Delta 9x\Delta 17$	$\Delta 9x\Delta 20$	WT
Mean	70.380	68.120	69.980	70.180	1.683	1.666	1.660	1.667
St. Dev	5.739	5.298	2.737	5.837	0.057	0.075	0.062	0.093
St. Error	0.812	0.749	0.387	0.825	0.008	0.011	0.009	0.013
T-test	0.863	0.068	0.827	1.000	0.303	0.953	0.660	1.000

Table 7.2.3.3a Fertility in the MAPK double T-DNA knockout lines. The T-test results show there were no differences in both number of seeds and silique length between wild-type plants and any of the T-DNA insertion lines. **St Dev**: standard deviation; **St Error**: standard error.

The results suggested that there were no differences between wild type plants and any of the double T-DNA knockout lines.

7.3 DISCUSSION

This chapter describes the use of *Arabidopsis thaliana* T-DNA insertion lines to look at the role of MAPKs in pollen development. T-DNA knockout lines of *AtMPK8*, *AtMPK9*, *AtMPK17* and *AtMPK20* were obtained and phenotypic analysis suggested there were no differences in pollen related phenotypes when compared to wild-type plants. It is known in *A. thaliana* that there is redundancy between members of the MAPK family, notably *AtMPK3* and *AtMPK6* (Mishra *et al.*, 2006). Therefore to overcome this problem attempts were made to construct double T-DNA insertion lines between *AtMPK9* deficient lines and the other T-DNA knockout lines ($\Delta 8 \times \Delta 9$, $\Delta 9 \times \Delta 17$, $\Delta 9 \times \Delta 20$). The results suggested that there were no pollen or vegetative defects in any of the double T-DNA insertion knockout lines compared to wild-type plants. Preliminary experiments to determine pollen related phenotypes for the remaining crosses ($\Delta 8 \times \Delta 17$, $\Delta 8 \times \Delta 20$, $\Delta 17 \times \Delta 20$) again suggested there was no difference between wild-type and knockout plants, although this remains to be confirmed.

It may be that these genes no longer function or function in very specific cells or after certain stimuli, which makes it hard to study them. It has been shown that some MAPKs display functional redundancy, but this redundancy is only in certain responses or developmental processes (for example there is not complete redundancy in embryo development (Bush and Krysan, 2007)). It may be that some, or all, of the MAPK studied show some redundancy. In order to overcome this it may be possible to construct triple knockouts or use another

approach such as RNAi. Because MAPKs show high homology to each other it may be difficult to target specific MAPKs by RNAi without effecting the expression of closely related MAPKs, or to find regions conserved between the MAPKs of interest. The question of how redundant MAPK members are remains to be determined. As MAPKs are involved in a large number of developmental processes it is likely that knocking a substantial number of MAPKs out will result in severe deficiencies or lethality due to effects on a number of these processes. This in turn makes it difficult to determine which MAPK are playing roles in specific processes, due to the redundancy. To circumvent this it may be possible to use triple T-DNA knockout lines, but this is dependant on the availability of these lines. For example *AtMPK9*, *AtMPK8* and *AtMPK15* all cluster in a closely related group and may show redundancy, but to date there is no T-DNA insertion line available for *AtMPK15*.

CHAPTER 8

General Discussion

CHAPTER 8 - GENERAL DISCUSSION

The self-incompatibility response in *Papaver rhoeas* presents a model system to examine cell signalling in plants. The development of an *in vitro* bioassay (Franklin-Tong *et al.*, 1988) and work over the last 20 years has allowed major advances in our understanding of the processes that take place during an incompatible SI reaction in *P. rhoeas*. Although research has identified the male and female determinants of self-incompatibility and several other components required to inhibit and terminate pollen tube growth, knowledge of the mechanisms involved in transducing signals between these components remains fairly limited, both in *Brassica* SSI and *P. rhoeas* GSI. One of the major components of cell signalling pathways are mitogen-activated protein kinases (MAPKs), which are involved in the transduction of extracellular signals from various stimuli into the cell, where they trigger various cellular responses. Evidence has shown that a MAPK, p56, is involved in the self-incompatibility response in *P. rhoeas* and data suggests it is involved in signalling to programmed cell death (Rudd *et al.*, 2003; Li *et al.*, 2007).

The previous chapters describe attempts to clone and characterise p56. Preliminary experiments suggested that an *MPK3*-like gene might encode p56, as an anti-AtMPK3 antibody specifically cross-reacted with a protein corresponding to p56 from pollen extracts (Li *et al.*, 2007). A *MPK3*-like gene was cloned from *P. rhoeas* and, due to the predicted molecular weight of the PrMPK3 protein, was unlikely to encode p56 (Chapter 3). Investigations to identify new candidates utilised both bioinformatics and proteomics approaches (Chapter 4). Several candidate genes were identified and attempts were made to clone these genes from *P. rhoeas* pollen. A strong candidate gene was identified, which has

homology to *AtMPK9* and is a member of the T-D-Y class of MAPKs and has been designated *PrMPK9-1* (Chapter 5). *PrMPK9-1* is expressed in pollen and is predicted to encode a protein with a molecular weight of 56kDa, which corresponds to the molecular weight of p56. In addition, FT-ICR MS analysis of p56 suggested that it showed homology to the protein encoded by *PrMPK9-1*.

To confirm that *PrMPK9-1* encodes p56, an antibody was raised against C-terminal recombinant PrMPK9-1 protein. This was used in immuno-blotting experiments to show that it could detect a protein corresponding to p56 (Chapter 6). The anti-PrMPK9-1 antibody could detect a protein of the same size as the one detected by the anti-pTXpY antibody (which detects dually phosphorylated MAPKs and which had previously been shown to detect p56) from a pollen protein extract. Further experiments using a phospho-column suggested that the 56kDa protein detected by the anti-PrMPK9-1 antibody could be phosphorylated, providing further evidence that *PrMPK9-1* encodes p56. Finally, immuno-precipitation experiments provided the most convincing evidence that the anti-PrMPK9-1 antibody detects the same 56kDa protein as the anti-pTXpY antibody. Proteins were extracted from calyculin A-treated or untreated pollen and immuno-precipitation was carried out using the anti-PrMPK9-1 antibody. Calyculin A is a phosphatase inhibitor that prevents dephosphorylation of MAPKs. Immuno-precipitated proteins were analysed in immuno-blotting experiments using the anti-pTXpY antibody and revealed that the 56kDa protein could be detected in calyculin A-treated samples, but not in the untreated samples. This data suggests that the 56kDa protein detected by the anti-pTXpY antibody is the same protein that is detected by the anti-PrMPK9-1 antibody. In addition, the 56kDa immuno-precipitated protein was shown to contain peptides found in the PrMPK9-1 predicted protein.

Although the findings provide strong evidence that p56 is encoded by *PrMPK9-1*, this remains to be confirmed. To date, immuno-precipitation of the 56kDa protein with anti-PrMPK9-1 antibody and detection after western blotting with the anti-pTXpY antibody, has been carried out with pollen that has undergone treatment with calyculin A. To confirm that this is the same protein that is activated during an incompatible SI reaction the immuno-precipitation needs to be repeated with protein extracts from pollen that has undergone an incompatible SI reaction and compared with compatible pollen as a control. This would help to confirm that the 56kDa protein detected is in fact p56. Preliminary experiments suggest that a 56kDa protein from pollen that has undergone an incompatible SI reaction can be immuno-precipitated by the anti-PrMPK9-1 antibody and detected by the anti-pTXpY antibody in immuno-blotting experiments (data not shown) and this activation is not seen in unchallenged pollen. Further experiments are needed to confirm this result.

Reverse genetics is an important tool in the investigation of gene function and will be important in determining whether *PrMPK9-1* encodes p56 and elucidating its role in SI. Unfortunately, the traditional *Agrobacterium*-mediated transformation method cannot always be used for the fast and efficient transformation of non-model plant species including *Papaver rhoeas*. Because of this, the role of the *PrMPK9-1* orthologue in *Arabidopsis thaliana*, *AtMPK9*, was investigated. In *A. thaliana*, *AtMPK9* is specifically expressed in pollen, shown from Affymetrix chip data, but to date there is no known function for *AtMPK9*. A T-DNA insertion knockout line was obtained for *AtMPK9* and its pollen phenotype was investigated, both in terms of pollen growth and development. Results suggested that there was no obvious difference in pollen or vegetative phenotype when compared to wild-type plants. In case of redundancy, the *AtMPK9*-deficient plants were crossed with *AtMPK8*, *AtMPK17* and

AtMPK20 T-DNA insertion knockout lines. These three genes are T-D-Y MAPKs and closely related to *AtMPK9*, all showing expression in pollen. Like *AtMPK9*, these genes have no known function. Like the single *AtMPK9* T-DNA insertion line, the double T-DNA knockout lines showed no obvious difference in pollen or vegetative phenotype, when compared to wild-type plants.

There are several possible reasons as to why there were no obvious differences in the T-DNA knockout lines when compared to wild-type plants. It may be that *AtMPK9* is expressed in specific cells or tissues or that it is only activated under certain conditions or in response to certain stimuli. In terms of self-incompatibility, it is proposed that *A. thaliana* used to possess the SSI mechanisms seen in other *Brassica* family members, but has lost this mechanism and is now self-compatible (Charlesworth and Vekemans, 2005). Whether this gene has an alternative function, or no longer functions, in *A. thaliana* remains to be determined. It may also be that the genes studied show functional redundancy. Because there is little work carried out on the T-D-Y group of MAPK in dicotyledonous plants it is difficult to know if these genes/proteins show functional redundancy, or even if this redundancy is shown with MAPKs from other groups. One potential solution to study these genes is to use RNAi lines to knock down several genes. Again it is difficult to determine how many or which genes will need to be knocked down in order to study their function.

As traditional *Agrobacterium*-mediated transformation methods cannot always be used for transformation of non-model plant species, viral induced gene silencing (VIGS) has been developed in a number of plant species in order to overcome this problem. VIGS utilises the plant's natural ability to suppress the accumulation of foreign RNAs by an RNA-mediated

defence mechanism against plant viruses. VIGS most likely acts by post-transcriptional gene silencing (PTGS) or a similar method. The virus vectors can be modified to incorporate host sequences, that when expressed in the plant causes suppression of the host's RNA. It is believed that VIGS may be used in order to knock down genes in *Papaver rhoeas*. The method has already been successfully used in the closely related *Papaver somniferum* and *Eschscholzia californica* basal eudicots (Hileman et al., 2005, Wege et al., 2007), and therefore suggests this methodology is transferable to *P. rhoeas*. Preliminary experiments have begun to set up VIGS in *P. rhoeas* (data not shown).

Antisense oligonucleotide silencing has been used successfully in *Papaver rhoeas* to knock down/out the male component of SI to confirm its role in *P. rhoeas* self-incompatibility (Wheeler *et al.*, 2009) and this approach could also be utilised to study the role of *PrMPK9-1* in SI.

Recent work has shown that it is possible to introduce a *P. rhoeas*-like SI into *A. thaliana* (de Graaf, unpublished). In these experiments *PrpS* was introduced into *A. thaliana* plants driven by a pollen specific promoter (*ntp303-PrpS₁-GFP*). The GFP-tagged PrpS₁ was expressed in pollen and further experiments showed that it was possible to inhibit pollen tube growth after treatment with 'incompatible' S-proteins, when compared to treatment with 'compatible' S-proteins in which the pollen grew normally. This suggests that it is possible to make *A. thaliana* exhibit *P. rhoeas*-like SI and that the male and female components are sufficient to induce this type of SI in *A. thaliana*. This result is quite extraordinary when the evolutionary distance between the two species is considered and suggests that *A. thaliana* still has the components needed to induce pollen tube growth inhibition. It is interesting that these

components should still result in cessation of pollen tube growth as not only is there the evolutionary difference between the two species but, as mentioned before, *A. thaliana* is a member of the *Brassicaceae* family whose members show *Brassica* SSI, and although *A. thaliana* is now self-compatible it is thought that *A. thaliana* once showed SSI but has lost this ability (Charlesworth and Vekemans, 2005).

To date it is not known which mechanisms are involved in this pollen tube growth inhibition, whether these are the same as in *P. rhoeas* and whether this process includes a programmed cell death-like pathway. Further experiments will be required to determine how this process works but it is likely to play a major role in the future analysis of the *P. rhoeas* SI reaction. Once this pathway is further investigated it may be possible to study the role of p56. Work described in this thesis suggested that there was no obvious role for the PrMPK9-1 orthologue, AtMPK9, (and AtMPK8, AtMPK17 and AtMPK20) in pollen growth and development in *A. thaliana* plants. It was suggested that this might be due to the function of AtMPK9 in specific cells or in response to certain stimuli. Whether AtMPK9 is involved in this *P. rhoeas*-like SI remains to be determined. However, this is all dependent upon the plants showing a similar MAPK activation pathway and which markers can be used to show that AtMPK9 is involved (i.e. does removing AtMPK9 result in the loss of a programmed cell death like process?). If so it may be possible to complement *AtMPK9* deficient *P. rhoeas* SI-like lines with *PrMPK9-1* in order to restore the original function of AtMPK9. However these experiments could become extremely complex if there is redundancy between the MAPKs involved.

So what role is p56 (PrMPK9-1?) likely to have in *P. rhoeas* self-incompatibility? Because of its timing in the self-incompatibility response, showing peak activation after 10 minutes, p56 is unlikely to be involved in the initial pollen tube growth inhibition events that take place within a few minutes of an incompatible response. However, p56 has been shown to be required for PCD in an incompatible reaction and this activation is upstream of the caspase-3-like activity (Li *et al.*, 2007). MAPKs are known to trigger PCD in plants in response to various stresses and stimuli, including biotic stresses (Yang *et al.*, 2001; Zhang and Klessig, 2001; Ren *et al.*, 2002; Ligterink *et al.*, 1997; Kroj *et al.*, 2003). The SI response could be considered analogous with these abiotic stress responses, whereby the plant differentiates between self and non-self, and may show similarities in the MAPK signalling pathways.

MAPKs have been shown to be involved in pollen development (Heberle-Bors *et al.*, 2001) and are required for tip growth (Samaj *et al.*, 2002). It is known that, although p56 appears to be the only MAPK that is specifically activated by SI, other MAPK are present and are activated in pollen. Work carried out to study the role of p56 in SI included using the MAPK inhibitor apigenin and the MEK inhibitors U0126 and PD98059 and suggested that knocking out MAPK activity resulted in pollen tube growth inhibition, while retaining pollen viability (Li *et al.*, 2007). Because apigenin is a general MAPK inhibitor and U0126/PD98059 prevent MAPKK activity, it is difficult to determine which MAPKs these drugs are inhibiting. It may be that p56 has a role in pollen tube growth, and it does show a basal level of activity in growing pollen, however it is likely that other pollen-expressed MAPKs (e.g. PrMPKB) play more major roles in pollen tube growth.

Experiments showed that changes to the actin cytoskeleton play an important role in SI in *P. rhoeas* and it is known that MAPKs are involved in actin dynamics (Thomas *et al.*, 2006; Samaj *et al.*, 2002). In alfalfa, SIMK has been shown to play a role in the formation of root hairs by signalling from the actin cytoskeleton to the tip growth machinery and its activation requires vesicle trafficking and an intact actin cytoskeleton (Samaj *et al.*, 2002). Evidence suggests that SIMK is not only associated with the actin cytoskeleton, but changing actin dynamics directly affects its activity. Like root hairs, pollen shows a similar tip growth pattern that involves vesicle trafficking and an intact actin cytoskeleton (see Samaj *et al.*, 2006 for a review). It is likely therefore that MAPKs and actin interactions are involved in pollen tube growth, but whether this includes p56 and whether similar signalling events take place in an incompatible SI reaction, potentially resulting in PCD, remain to be determined.

It is proposed that SIPK, when activated, can phosphorylate the actin binding protein profilin and a MEK2-SIPK-profilin cascade plays a role in the reorganisation of the actin cytoskeleton during pollen germination and growth (Limmongkon *et al.*, 2004). Evidence suggests that PrABP80 and profilin (another ABP) have a role in Ca²⁺-dependent F-actin depolymerisation during an incompatible SI reaction (Huang *et al.*, 2004), but again, it has not been determined if this involves MAPK activity. It is likely that the role of actin and MAPK phosphorylation can not only regulate components of the actin cytoskeleton, but disturbances of the actin cytoskeleton are also sensed by MAPKs.

It is known that changes in actin dynamics using the drugs latrunculin B and jasplakinolide (which inhibit and promote actin polymerisation, respectively) can induce PCD (Thomas *et al.*, 2006). However, preliminary experiments show that latrunculin B and jasplakinolide do

not activate p56, suggesting that there may not be a direct link between actin dynamics and p56 (Li and Franklin-Tong, unpublished).

In dicotyledonous plants the only published work on a T-D-Y MAPK is on *Arabidopsis thaliana* *AtMPK18*, which mediates cortical microtubule functions (Walia *et al.*, 2009). In *P. rhoeas* SI, changes in microtubule dynamics do not trigger PCD, but evidence suggests there may be a role for microtubule depolymerisation in mediating PCD. In addition, MAP65-1a is a microtubule-associated protein that is phosphorylated by the MAPK NTF6 in tobacco, showing that MAPKs may regulate microtubules via microtubule-associated proteins (Sasabe *et al.*, 2006).

Evidence has shown that ROS and NO are found in growing pollen tubes and are involved in the hypersensitive response (HR) and PCD (Prado *et al.*, 2004; Potocky *et al.*, 2007; Neill *et al.*, 2002; Zaninotto *et al.*, 2006) and it is known that ROS can activate MAPKs (Ahlfors *et al.*, 2004; Kumar and Klessig, 2000; Samuel *et al.*, 2000). Recent data using live-cell imaging suggests that SI induces relatively rapid and transient increases in ROS and NO (Franklin-Tong *et al.*, unpublished). How ROS are involved in SI is not yet known, but it has been shown that SI can cause the rapid disruption of mitochondria, where ROS are produced (Thomas and Franklin-Tong, 2004). In addition, it is thought in yeast that the actin cytoskeleton could regulate ROS release from mitochondria (Gourlay *et al.*, 2004).

Evidence shows that there is a large amount of interaction between actin, microtubules, MAPKs and ROS (and NO), and all of these components have been shown to be involved in PCD. Actin, microtubules and MAPKs (and potentially ROS) are involved in an incompatible

SI response in *P. rhoeas* and it is likely that signalling between these components provide the link between pollen tube growth inhibition and pollen tube PCD.

It will be interesting to determine what interacts with PrMPK9-1. Upstream there is likely to be a MAPKK and a MAPKKK that are involved with the signal transduction pathway to activate PrMPK9-1. In *A. thaliana*, work was carried out to determine which MAPKKs were responsible for activating specific MAPKs, but these results did not determine which MAPKKs could interact and phosphorylate AtMPK9 (Lee *et al.*, 2008a). Hopefully, co-immuno-precipitation using the anti-PrMPK9-1 antibody and SDS-PAGE could help identify proteins that interact both upstream and downstream of PrMPK9-1. In addition, yeast two-hybrid experiments could be used to determine proteins that interact with PrMPK9-1 (e.g. other kinases or regulators such as phosphatases). For example PrMPK9-1 could be used as a 'bait' protein to screen a *P. rhoeas* pollen-specific 'prey' library to determine if PrMPK9-1 interacts with pollen-specific 'prey' proteins. Positive protein-protein interactions can be determined by reporter gene expression, which is driven by the protein-protein interaction, and interacting 'prey' proteins can be identified by DNA sequencing.

This work represents another step forward in disentangling the numerous signalling events that take place during an incompatible SI reaction in *P. rhoeas*. The results described here suggest a novel role for MAPK signalling in the self-incompatibility response, for a previously uncharacterised MAPK orthologue. Future work will help to confirm the role of p56 in SI and shed light on the signalling networks that take place in order to successfully inhibit incompatible pollen in the *Papaver rhoeas* SI response.

References

References

- Agrawal, G. K., Agrawal, S. K., Shibato, J., Iwahashi, H. and Rakwal, R.** (2003a). Novel rice MAP kinases OsMSRMK3 and OsWJUMK1 involved in encountering diverse environmental stresses and developmental regulation. *Biochemical and Biophysical Research Communications*. **300 (3)**: 775-783.
- Agrawal, G. K., Rakwal, R. and Iwahashi, H.** (2002). Isolation of novel rice (*Oryza sativa* L.) multiple stress responsive MAP kinase gene, OsMSRMK2, whose mRNA accumulates rapidly in response to environmental cues. *Biochemical and Biophysical Research Communications*. **294 (5)**: 1009-1016.
- Agrawal, G. K., Tamogami, S., Iwahashi, H., Agrawal, V. P. and Rakwal, R.** (2003b). Transient regulation of jasmonic acid-inducible rice MAP kinase gene (OsBWMK1) by diverse biotic and abiotic stresses. *Plant Physiology and Biochemistry*. **41 (4)**: 355-361.
- Ahlfors, R., Macioszek, V., Rudd, J., Brosche, M., Schlichting, R., Scheel, D. and Kangasjarvi, J.** (2004). Stress hormone-independent activation and nuclear translocation of mitogen-activated protein kinases in *Arabidopsis thaliana* during ozone exposure. *Plant Journal*. **40 (4)**: 512-522.
- Albach, D. C., Meudt, H. M. and Oxelman, B.** (2005). Piecing together the "new" Plantaginaceae. *American Journal of Botany*. **92 (2)**: 297-315.
- Alexander, M. P.** (1969). Differential Staining of Aborted and Nonaborted Pollen. *Stain Technology*. **44 (3)**: 117-&.
- Altschul, S. F., Gish, W., Miller, W., Myers, E. W. and Lipman, D. J.** (1990). Basic Local Alignment Search Tool. *Journal of Molecular Biology*. **215 (3)**: 403-410.

Altschul, S. F., Madden, T. L., Schaffer, A. A., Zhang, J. H., Zhang, Z., Miller, W. and Lipman, D. J. (1997). Gapped BLAST and PSI-BLAST: a new generation of protein database search programs. *Nucleic Acids Research*. **25 (17)**: 3389-3402.

Anderson, M. A., Cornish, E. C., Mau, S. L., Williams, E. G., Hoggart, R., Atkinson, A., Bonig, I., Grego, B., Simpson, R., Roche, P. J., Haley, J. D., Penschow, J. D., Niall, H. D., Tregear, G. W., Coghlan, J. P., Crawford, R. J. and Clarke, A. E. (1986). Cloning of cDNA for a Styler Glycoprotein Associated with Expression of Self-Incompatibility in *Nicotiana glauca*. *Nature*. **321 (6065)**: 38-44.

Andreasson, E., Jenkins, T., Brodersen, P., Thorgrimsen, S., Petersen, N. H. T., Zhu, S. J., Qiu, J. L., Micheelsen, P., Rocher, A., Petersen, M., Newman, M. A., Nielsen, H. B., Hirt, H., Somssich, I., Mattsson, O. and Mundy, J. (2005). The MAP kinase substrate MKS1 is a regulator of plant defense responses. *Embo Journal*. **24 (14)**: 2579-2589.

Asai, T., Tena, G., Plotnikova, J., Willmann, M. R., Chiu, W. L., Gomez-Gomez, L., Boller, T., Ausubel, F. M. and Sheen, J. (2002). MAP kinase signalling cascade in *Arabidopsis* innate immunity. *Nature*. **415 (6875)**: 977-983.

Balbi, V. and Devoto, A. (2008). Jasmonate signalling network in *Arabidopsis thaliana*: crucial regulatory nodes and new physiological scenarios. *New Phytologist*. **177 (2)**: 301-318.

Bardel, J., Louwagie, M., Jaquinod, M., Jourdain, A., Luche, S., Rabilloud, T., Macherel, D., Garin, J. and Bourguignon, J. (2002). A survey of the plant mitochondrial proteome in relation to development. *Proteomics*. **2 (7)**: 880-898.

Bardwell, L. and Thorner, J. (1996). A conserved motif at the amino termini of MEKs might mediate high-affinity interaction with the cognate MAPKs. *Trends in Biochemical Sciences*. **21 (10)**: 373-374.

Benson, D. A., Karsch-Mizrachi, I., Lipman, D. J., Ostell, J. and Wheeler, D. L. (2007). GenBank. *Nucleic Acids Research*. **35**: D21-D25.

Bergmann, D. C., Lukowitz, W. and Somerville, C. R. (2004). Stomatal development and pattern controlled by a MAPKK kinase. *Science*. **304 (5676)**: 1494-1497.

Bögre, L., Calderini, O., Binarova, P., Mattauch, M., Till, S., Kiegerl, S., Jonak, C., Pollaschek, C., Barker, P., Huskisson, N. S., Hirt, H. and Heberle-Bors, E. (1999). A MAP kinase is activated late in plant mitosis and becomes localized to the plane of cell division. *Plant Cell*. **11 (1)**: 101-113.

Bonneau, L., Ge, Y., Drury, G. E. and Gallois, P. (2008). What happened to plant caspases? *Journal of Experimental Botany*. **59 (3)**: 491-499.

Bosch, M., Franklin-Tong, V.E. (2008). Self-incompatibility in Papaver: signalling to trigger PCD in incompatible pollen. *Journal of Experimental Botany*. **59 (3)**: 481-490.

Bower, M. S., Matias, D. D., FernandesCarvalho, E., Mazzurco, M., Gu, T. S., Rothstein, S. J. and Goring, D. R. (1996). Two members of the thioredoxin-h family interact with the kinase domain of a Brassica S locus receptor kinase. *Plant Cell*. **8 (9)**: 1641-1650.

Brader, G., Djamei, A., Teige, M., Palva, E. T. and Hirt, H. (2007). The MAP kinase kinase MKK2 affects disease resistance in Arabidopsis. *Molecular Plant-Microbe Interactions*. **20 (5)**: 589-596.

Brewbaker, J. L. and Kwack, B. H. (1963). Essential Role of Calcium Ion in Pollen Germination and Pollen Tube Growth. *American Journal of Botany*. **50 (9)**: 859-&.

Brodersen, P., Petersen, M., Nielsen, H. B., Zhu, S. J., Newman, M. A., Shokat, K. M., Rietz, S., Parker, J. and Mundy, J. (2006). Arabidopsis MAP kinase 4 regulates salicylic acid- and jasmonic acid/ethylene-dependent responses via EDS1 and PAD4. *Plant Journal*. **47 (4)**: 532-546.

Brugiere, S., Kowalski, S., Ferro, M., Seigneurin-Berny, D., Miras, S., Salvi, D., Ravel, S., d'Herin, P., Garin, J., Bourguignon, J., Joyard, J. and Rolland, N. (2004). The

hydrophobic proteome of mitochondrial membranes from Arabidopsis cell suspensions. *Phytochemistry*. **65** (12): 1693-1707.

Bush, S. M. and Krysan, P. J. (2007). Mutational evidence that the Arabidopsis MAP kinase MPK6 is involved in anther, inflorescence, and embryo development. *Journal of Experimental Botany*. **58** (8): 2181-2191.

Cabrillac, D., Cock, J. M., Dumas, C. and Gaude, T. (2001). The S-locus receptor kinase is inhibited by thioredoxins and activated by pollen coat proteins. *Nature*. **410** (6825): 220-223.

Calderini, O., Glab, N., Bergounioux, C., Heberle-Bors, E. and Wilson, C. (2001). A novel tobacco mitogen-activated protein (MAP) kinase kinase, NtMEK1, activates the cell cycle-regulated p43(Ntf6) MAP kinase. *Journal of Biological Chemistry*. **276** (21): 18139-18145.

Cardinale, F., Meskiene, I., Ouaked, F. and Hirt, H. (2002). Convergence and divergence of stress-induced mitogen-activated protein kinase signaling pathways at the level of two distinct mitogen-activated protein kinase kinases. *Plant Cell*. **14** (3): 703-711.

Carter, C., Pan, S. Q., Jan, Z. H., Avila, E. L., Girke, T. and Raikhel, N. V. (2004). The vegetative vacuole proteome of Arabidopsis thaliana reveals predicted and unexpected proteins. *Plant Cell*. **16** (12): 3285-3303.

Champion, A., Picaud, A. and Henry, Y. (2004). Reassessing the MAP3K and MAP4K relationships. *Trends in Plant Science*. **9** (3): 123-129.

Charlesworth, D. and Vekemans, X. (2005). How and when did Arabidopsis thaliana become highly self-fertilising. *Bioessays*. **27** (5): 472-476.

Cheong, Y. H., Moon, B. C., Kim, J. K., Kim, C. Y., Kim, M. C., Kim, I. H., Park, C. Y., Kim, J. C., Park, B. O., Koo, S. C., Yoon, H. W., Chung, W. S., Lim, C. O., Lee, S. Y. and Cho, M. J. (2003). BWMK1, a rice mitogen-activated protein kinase, locates in the

nucleus and mediates pathogenesis-related gene expression by activation of a transcription factor. *Plant Physiology*. **132** (4): 1961-1972.

Chinchilla, D., Zipfel, C., Robatzek, S., Kemmerling, B., Nurnberger, T., Jones, J. D. G., Felix, G. and Boller, T. (2007). A flagellin-induced complex of the receptor FLS2 and BAK1 initiates plant defence. *Nature*. **448**: 497-U12.

Cho, S. K., Larue, C. T., Chevalier, D., Wang, H. C., Jinn, T. L., Zhang, S. Q. and Walker, J. C. (2008). Regulation of floral organ abscission in *Arabidopsis thaliana*. *Proceedings of the National Academy of Sciences of the United States of America*. **105** (40): 15629-15634.

Comisaro, M. B. and Marshall, A. G. (1974). Fourier-Transform Ion-Cyclotron Resonance Spectroscopy. *Chemical Physics Letters*. **25** (2): 282-283.

Cooperman, B. S., Baykov, A. A. and Lahti, R. (1992). Evolutionary Conservation of the Active-site of Soluble Inorganic Pyrophosphatase. *Trends in Biochemical Sciences*. **17** (7): 262-266.

Coronado, M. J., Gonzalez-Melendi, P., Segui, J. M., Ramirez, C., Barany, I., Testillano, P. S. and Risueno, M. C. (2002). MAPKs entry into the nucleus at specific interchromatin domains in plant differentiation and proliferation processes. *Journal of Structural Biology*. **140** (1-3): 200-213.

Coronado, M. J., Testillano, P. S., Willson, C., Vicente, O., Helbere-Bors, E. and Risueno, M. C. (2007). In situ molecular identification of the Ntf4 MAPK expression sites in maturing and germinating pollen. *Biology of the Cell*. **99** (4): 209-221.

Cress, D. (1993). A one-step, nondenaturing purification method for recombinant proteins produced in *E. coli*. *Promega Notes Magazine*. **42**: 2-7.

Cruz-Garcia, F., Hancock, C. N., Kim, D. and McClure, B. (2005). Styolar glycoproteins bind to S-RNase in vitro. *Plant Journal*. **42 (3)**: 295-304.

Dai, S., Li, L., Chen, T., Chong, K., Xue, Y. and Wang, T. (2006a). Proteomic analyses of *Oryza sativa* mature pollen reveal novel proteins associated with pollen germination and tube growth. *Proteomics*. **6 (8)**: 2504-2529.

Dai, Y., Wang, H. Z., Li, B. H., Huang, J., Liu, X. F., Zhou, Y. H., Mou, Z. L. and Li, J. Y. (2006b). Increased expression of MAP KINASE KINASE7 causes deficiency in polar auxin transport and leads to plant architectural abnormality in *Arabidopsis*. *Plant Cell*. **18 (2)**: 308-320.

de Graaf, B. H. J., Rudd, J. J., Wheeler, M. J., Perry, R. M., Bell, E. M., Osman, K., Franklin, F. C. H. and Franklin-Tong, V. E. (2006). Self-incompatibility in *Papaver* targets soluble inorganic pyrophosphatases in pollen. *Nature*. **444 (7118)**: 490-493.

Dickinson, H. (1995). Dry Stigmas, Water and Self-Incompatibility in Brassica. *Sexual Plant Reproduction*. **8 (1)**: 1-10.

Djamei, A., Pitzschke, A., Nakagami, H., Rajh, I. and Hirt, H. (2007). Trojan horse strategy in *Agrobacterium* transformation: Abusing MAPK defense signaling. *Science*. **318**: 453-456.

Döczi, R., Brader, G., Pettko-Szandtner, A., Rajh, I., Djamei, A., Pitzschke, A., Teige, M. and Hirt, H. (2007). The *Arabidopsis* Mitogen-Activated Protein Kinase Kinase MKK3 Is Upstream of Group C Mitogen-Activated Protein Kinases and Participates in Pathogen Signaling. *Plant Cell*. **19 (10)**: 3266-3279.

Droillard, M. J., Boudsocq, M., Barbier-Brygoo, H. and Lauriere, C. (2004). Involvement of MPK4 in osmotic stress response pathways in cell suspensions and plantlets of *Arabidopsis thaliana*: activation by hypoosmolarity and negative role in hyperosmolarity tolerance. *Febs Letters*. **574 (1-3)**: 42-48.

Droillard, M. J., Boudsocq, M., Barbler-Brygoo, H. and Lauriere, C. (2002). Different protein kinase families are activated by osmotic stresses in *Arabidopsis thaliana* cell suspensions - Involvement of the MAP kinases AtMPK3 and AtMPK6. *Febs Letters*. **527 (1-3)**: 43-50.

Dujardin, P., Rojasbeltran, J., Gebhardt, C. and Brasseur, R. (1995). Molecular-cloning and Characterization of a Soluble Inorganic Pyrophosphatase in Potato. *Plant Physiology*. **109 (3)**: 853-860.

Ehrhardt, D. W. and Shaw, S. L. (2006). Microtubule dynamics and organization in the plant cortical array. *Annual Review of Plant Biology*. **57**: 859-875.

Eisenberg, E. and Levanon, E. Y. (2003). Human housekeeping genes are compact. *Trends in Genetics*. **19 (7)**: 362-365.

Elion, E. A. (2006). Detection of protein-protein interactions by coprecipitation. *Curr Protoc Mol Biol*. **Chapter 20** Unit 20.5.

Entani, T., Iwano, M., Shiba, H., Che, F. S., Isogai, A. and Takayama, S. (2003). Comparative analysis of the self-incompatibility (S-) locus region of *Prunus mume*: identification of a pollen-expressed F-box gene with allelic diversity. *Genes to Cells*. **8 (3)**: 203-213.

Feilner, T., Hultschig, C., Lee, J., Meyer, S., Immink, R. G. H., Koenig, A., Possling, A., Seitz, H., Beveridge, A., Scheel, D., Cahill, D. J., Lehrach, H., Kreutzberger, J. and Kersten, B. (2005). High throughput identification of potential *Arabidopsis* mitogen-activated protein kinases substrates. *Molecular & Cellular Proteomics*. **4 (10)**: 1558-1568.

Feiz, L., Irshad, M., Pont-Lezica, R. F., Canut, H. and Jamet, E. (2006). Evaluation of cell wall preparations for proteomics: a new procedure for purifying cell walls from *Arabidopsis* hypocotyls. *Plant Methods*. **2**: 10.

Felix, G., Duran, J. D., Volko, S. and Boller, T. (1999). Plants have a sensitive perception system for the most conserved domain of bacterial flagellin. *Plant Journal*. **18 (3)**: 265-276.

Foote, H. C. C., Ride, J. P., Franklin-Tong, V. E., Walker, E. A., Lawrence, M. J. and Franklin, F. C. H. (1994). Cloning and Expression of a Distinctive Class of Self-incompatibility (S) Gene from *Papaver rhoeas* L.. *Proceedings of the National Academy of Sciences of the United States of America*. **91 (6)**: 2265-2269.

Franklin-Tong, V. E., Drobak, B. K., Allan, A. C., Watkins, P. A. C. and Trewavas, A. J. (1996). Growth of pollen tubes of *Papaver rhoeas* is regulated by a slow-moving calcium wave propagated by inositol 1,4,5-trisphosphate. *Plant Cell*. **8 (8)**: 1305-1321.

Franklin-Tong, V. E., Hackett, G. and Hepler, P. K. (1997). Ratio-imaging of Ca-i(2+) in the self-incompatibility response in pollen tubes of *Papaver rhoeas*. *Plant Journal*. **12 (6)**: 1375-1386.

Franklin-Tong, V. E., Holdaway-Clarke, T. L., Straatman, K. R., Kunke, J. G. and Hepler, P. K. (2002). Involvement of extracellular calcium influx in the self-incompatibility response of *Papaver rhoeas*. *Plant Journal*. **29 (3)**: 333-345.

Franklin-Tong, V. E., Lawrence, M. J. and Franklin, F. C. H. (1988). An *in vitro* Bioassay for the Stigmatic Product of the Self-incompatibility Gene in *Papaver rhoeas* L. *New Phytologist*. **110 (1)**: 109-118.

Franklin-Tong, V. E., Ride, J. P. and Franklin, F. C. H. (1995). Recombinant Stigmatic Self-incompatibility-(S-) Protein Elicits a Ca²⁺ Transient in Pollen of *Papaver rhoeas*. *Plant Journal*. **8 (2)**: 299-307.

Franklin-Tong, V. E., Ride, J. P., Read, N. D., Trewavas, A. J. and Franklin, F. C. H. (1993). The self-incompatibility response in *Papaver rhoeas* is mediated by cytosolic free calcium. *Plant Journal*. **4 (1)**: 163-177.

Freier, S. M., Kierzek, R., Jaeger, J. A., Sugimoto, N., Caruthers, M. H., Neilson, T. and Turner, D. H. (1986). Improved Free-energy Parameters for Predictions of RNA Duplex Stability. *Proceedings of the National Academy of Sciences of the United States of America*. **83 (24)**: 9373-9377.

Fu, S. F., Chou, W. C., Huang, D. D. and Huang, H. J. (2002). Transcriptional regulation of a rice mitogen-activated protein kinase gene, OsMAPK4, in response to environmental stresses. *Plant and Cell Physiology*. **43 (8)**: 958-963.

Ganders, F. R. (1979). The Biology of Heterostyly. *New Zealand Journal of Botany*. **17 (4)**: 607-635.

Garrington, T. P. and Johnson, G. L. (1999). Organization and regulation of mitogen-activated protein kinase signaling pathways. *Current Opinion in Cell Biology*. **11 (2)**: 211-218.

Geitmann, A. (1999). **Cell death of self-incompatible pollen tubes: necrosis or apoptosis?** Fertilization in higher plants: molecular and cytological aspects. M. Cresti, G. Cai and A. Moscatelli. Berlin, Springer-Verlag.

Geitmann, A., Snowman, B. N., Emons, A. M. C. and Franklin-Tong, V. E. (2000). Alterations in the actin cytoskeleton of pollen tubes are induced by the self-incompatibility reaction in *Papaver rhoeas*. *Plant Cell*. **12 (7)**: 1239-1251.

Giranton, J. L., Dumas, C., Cock, J. M. and Gaude, T. (2000). The integral membrane S-locus receptor kinase of Brassica has serine/threonine kinase activity in a membranous environment and spontaneously forms oligomers in planta. *Proceedings of the National Academy of Sciences of the United States of America*. **97 (7)**: 3759-3764.

Glazebrook, J. and Ausubel, F. M. (1994). Isolation of Phytoalexin-deficient Mutants of *Arabidopsis thaliana* and Characterization of their Interactions with Bacterial Pathogens.

Proceedings of the National Academy of Sciences of the United States of America. **91 (19):** 8955-8959.

Goldraij, A., Kondo, K., Lee, C. B., Hancock, C. N., Sivaguru, M., Vazquez-Santana, S., Kim, S., Phillips, T. E., Cruz-Garcia, F. and McClure, B. (2006). Compartmentalization of S-RNase and HT-B degradation in self-incompatible *Nicotiana*. *Nature.* **439 (7078):** 805-810.

Golz, J. F., Clarke, A. E. and Newbigin, E. (2000). Mutational approaches to the study of self-incompatibility: Revisiting the pollen-part mutants. *Annals of Botany.* **85** 95-103.

Golz, J. F., Su, V., Clarke, A. E. and Newbigin, E. (1999). A molecular description of mutations affecting the pollen component of the *Nicotiana glauca* S locus. *Genetics.* **152 (3):** 1123-1135.

Gomez, S. M., Nishio, J. N., Faull, K. F. and Whitelegge, J. P. (2002). The chloroplast grana proteome defined by intact mass measurements from liquid chromatography mass spectrometry. *Molecular & Cellular Proteomics.* **1 (1):** 46-59.

Gomez-Gomez, L., Felix, G. and Boller, T. (1999). A single locus determines sensitivity to bacterial flagellin in *Arabidopsis thaliana*. *Plant Journal.* **18 (3):** 277-284.

Gourlay, C. W., Carpp, L. N., Timpson, P., Winder, S. J. and Ayscough, K. R. (2004). A role for the actin cytoskeleton in cell death and aging in yeast. *Journal of Cell Biology.* **164 (6):** 803-809.

Green, D. R. and Reed, J. C. (1998). Mitochondria and apoptosis. *Science.* **281 (5381):** 1309-1312.

Gu, T. S., Mazzurco, M., Sulaman, W., Matias, D. D. and Goring, D. R. (1998). Binding of an arm repeat protein to the kinase domain of the S-locus receptor kinase. *Proceedings of the National Academy of Sciences of the United States of America.* **95 (1):** 382-387.

Gudesblat, G. E., Iusem, N. D. and Morris, P. C. (2007). Guard cell-specific inhibition of Arabidopsis MPK3 expression causes abnormal stomatal responses to abscisic acid and hydrogen peroxide. *New Phytologist*. **173 (4)**: 713-721.

Gupta, R., Huang, Y. F., Kieber, J. and Luan, S. (1998). Identification of a dual-specificity protein phosphatase that inactivates a MAP kinase from Arabidopsis. *Plant Journal*. **16 (5)**: 581-589.

Haffani, Y. Z., Gaude, T., Cock, J. M. and Goring, D. R. (2004). Antisense suppression of thioredoxin h mRNA in Brassica napus cv. Westar pistils causes a low level constitutive pollen rejection response. *Plant Molecular Biology*. **55 (5)**: 619-630.

Hahn, A. and Harter, K. (2009). Mitogen-Activated Protein Kinase Cascades and Ethylene: Signaling, Biosynthesis, or Both? *Plant Physiology*. **149 (3)**: 1207-1210.

Hamel, L. P., Nicole, M. C., Sritubtim, S., Morency, M. J., Ellis, M., Ehlting, J., Beaudoin, N., Barbazuk, B., Klessig, D., Lee, J., Martin, G., Mundy, J., Ohashi, Y., Scheel, D., Sheen, J., Xing, T., Zhang, S. Q., Seguin, A. and Ellis, B. E. (2006). Ancient signals: comparative genomics of plant MAPK and MAPKK gene families. *Trends in Plant Science*. **11 (4)**: 192-198.

Hancock, C. N., Kent, L. and McClure, B. A. (2005). The stylar 120 kDa glycoprotein is required for S-specific pollen rejection in Nicotiana. *Plant Journal*. **43 (5)**: 716-723.

Hauser, E. J. P. and Morrison, J. H. (1964). Cytochemical Reduction of Nitro Blue Tetrazolium as Index of Pollen Viability. *American Journal of Botany*. **51 (7)**: 748-&.

He, C. Z., Fong, S. H. T., Yang, D. C. and Wang, G. L. (1999). BWMK1, a novel MAP kinase induced by fungal infection and mechanical wounding in rice. *Molecular Plant-Microbe Interactions*. **12 (12)**: 1064-1073.

- Hearn, M. J., Franklin, F. C. H. and Ride, J. P.** (1996). Identification of a membrane glycoprotein in pollen of *Papaver rhoeas* which binds stigmatic self-incompatibility (S-) proteins. *Plant Journal*. **9 (4)**: 467-475.
- Heberle-Bors, E., Voronin, V., Touraev, A., Testillano, P. S., Risueno, M. C. and Wilson, C.** (2001). MAP kinase signaling during pollen development. *Sexual Plant Reproduction*. **14 (1-2)**: 15-19.
- Hetherington, A. M. and Brownlee, C.** (2004). The generation of Ca²⁺ signals in plants. *Annual Review of Plant Biology*. **55**: 401-427.
- Higgins, J. D., Armstrong, S. J., Franklin, F. C. H. and Jones, G. H.** (2004). The Arabidopsis MutS homolog AtMSH4 functions at an early step in recombination: evidence for two classes of recombination in Arabidopsis. *Genes & Development*. **18 (20)**: 2557-2570.
- Hileman, L. C., Drea, S., de Martino, G., Litt, A. and Irish, V. F.** (2005). Virus-induced gene silencing is an effective tool for assaying gene function in the basal eudicot species *Papaver somniferum* (opium poppy). *Plant Journal*. **44 (2)**: 334-341.
- Hirt, H.** (2000). MAP kinases in plant signal transduction. *Results Probl Cell Differ*. **27**: 1-9.
- Hiscock, S. J. and Allen, A. M.** (2008). Diverse cell signalling pathways regulate pollen-stigma interactions: the search for consensus. *New Phytologist*. **179 (2)**: 286-317.
- Hiscock, S. J. and McInnis, S. M.** (2003). The diversity of self-incompatibility systems in flowering plants. *Plant Biology*. **5 (1)**: 23-32
- Holmes-Davis, R., Tanaka, C. K., Vensel, W. H., Hurkman, W. J. and McCormick, S.** (2005). Proteome mapping of mature pollen of *Arabidopsis thaliana*. *Proteomics*. **5 (18)**: 4864-4884.

- Honkanan, R. E., Codispoti, B. A., Tse, K. and Boynton, A. L.** (1994). Characterization of Natural Toxins with Inhibitory Activity Against Serine Threonine Protein Phosphatases. *Toxicon*. **32 (3)**: 339-350.
- Hoyos, M. E. and Zhang, S. Q.** (2000). Calcium-independent activation of salicylic acid-induced protein kinase and a 40-kilodalton protein kinase by hyperosmotic stress. *Plant Physiology*. **122 (4)**: 1355-1363.
- Hruz, T., Laule, O., Szabo, G., Wessendorp, F., Bleuler, S., Oertle, L., Widmayer, P., Gruissem, W. and Zimmermann, P.** (2008). Genevestigator V3: A Reference Expression Database for the Meta-Analysis of Transcriptomes. *Advances in Bioinformatics*. 420747.
- Hua, Z. H. and Kao, T. H.** (2006). Identification and characterization of components of a putative Petunia S-locus F-box-containing E3 ligase complex involved in S-RNase-based self-incompatibility. *Plant Cell*. **18 (10)**: 2531-2553.
- Huang, H. J., Fu, S. F., Tai, Y. H., Chou, W. C. and Huang, D. D.** (2002). Expression of *Oryza sativa* MAP kinase gene is developmentally regulated and stress-responsive. *Physiologia Plantarum*. **114 (4)**: 572-580.
- Huang, J., Zhao, L., Yang, Q. Y. and Xue, Y. B.** (2006). AhSSK1, a novel SKP1-like protein that interacts with the S-locus F-box protein SLF. *Plant Journal*. **46 (5)**: 780-793.
- Huang, S., Lee, H. S., Karunanandaa, B. and Kao, T. H.** (1994). Ribonuclease-Activity of *Petunia inflata* S-Proteins is Essential for Rejection of Self-Pollen. *Plant Cell*. **6 (7)**: 1021-1028.
- Huang, S. J., Blanchoin, L., Chaudhry, F., Franklin-Tong, V. E. and Staiger, C. J.** (2004). A gelsolin-like protein from *Papaver rhoeas* pollen (PrABP80) stimulates calcium-regulated severing and depolymerization of actin filaments. *Journal of Biological Chemistry*. **279 (22)**: 23364-23375.

Hunter, P. (2009). Me, myself and I. The genetics and molecular biology behind self-incompatibility and the avoidance of inbreeding in plants. *EMBO reports*. **10 (12)**: 1297-300.

Ichimura, K., Casais, C., Peck, S. C., Shinozaki, K. and Shirasu, K. (2006). MEKK1 is required for MPK4 activation and regulates tissue-specific and temperature-dependent cell death in Arabidopsis. *Journal of Biological Chemistry*. **281 (48)**: 36969-36976.

Ichimura, K., Mizoguchi, T., Irie, K., Morris, P., Giraudat, J., Matsumoto, K. and Shinozaki, K. (1998). Isolation of ATMEKK1 (a MAP kinase kinase Kinase) - Interacting proteins and analysis of a MAP kinase cascade in Arabidopsis. *Biochemical and Biophysical Research Communications*. **253 (2)**: 532-543.

Ichimura, K., Shinozaki, K., Tena, G., Sheen, J., Henry, Y., Champion, A., Kreis, M., Zhang, S. Q., Hirt, H., Wilson, C., Heberle-Bors, E., Ellis, B. E., Morris, P. C., Innes, R. W., Ecker, J. R., Scheel, D., Klessig, D. F., Machida, Y., Mundy, J., Ohashi, Y., Walker, J. C. and Grp, M. (2002). Mitogen-activated protein kinase cascades in plants: a new nomenclature. *Trends in Plant Science*. **7 (7)**: 301-308.

Igic, B. and Kohn, J. R. (2006) The distribution of plant mating systems: Study bias against obligately outcrossing species. *Evolution*. **60**: 1098-1103.

Innes, R. W. (2001). Mapping out the roles of MAP kinases in plant defense. *Trends in Plant Science*. **6 (9)**: 392-394.

Ioerger, T. R., Gohlke, J. R., Xu, B. and Kao, T. H. (1991). Primary Structural Features of the Self-Incompatibility Protein in Solanaceae. *Sexual Plant Reproduction*. **4 (2)**: 81-87.

Ishimizu, T., Shinkawa, T., Sakiyama, F. and Norioka, S. (1998). Primary structural features of rosaceous S-RNases associated with gametophytic self-incompatibility. *Plant Molecular Biology*. **37 (6)**: 931-941.

Iwano, M., Entani, T., Shiba, H., Kakita, M., Nagai, T., Mizuno, H., Miyawaki, A., Shoji, T., Kubo, K., Isogai, A. and Takayama, S. (2009). Fine-Tuning of the Cytoplasmic Ca²⁺ Concentration Is Essential for Pollen Tube Growth. *Plant Physiol.* **150** (3): 1322-1334.

Jeong, M. J., Lee, S. K., Kim, B. G., Kwon, T. R., Cho, W. S., Park, Y. T., Lee, J. O., Kwon, H. B., Byun, M. O. and Park, S. C. (2006). A rice (*Oryza sativa* L.) MAP kinase gene, OsMAPK44, is involved in response to abiotic stresses. *Plant Cell Tissue and Organ Culture.* **85** (2): 151-160.

Jiang, L. X., Yang, S. L., Xie, L. F., Puah, C. S., Zhang, X. Q., Yang, W. C., Sundaresan, V. and Ye, D. (2005). VANGUARD1 encodes a pectin methylesterase that enhances pollen tube growth in the Arabidopsis style and transmitting tract. *Plant Cell.* **17** (2): 584-596.

Jonak, C., Okresz, L., Bogre, L. and Hirt, H. (2002). Complexity, cross talk and integration of plant MAP kinase signalling. *Current Opinion in Plant Biology.* **5** (5): 415-424.

Jones, J. D. G. and Dangl, J. L. (2006). The plant immune system. *Nature.* **444**: 323-329.

Joo, S., Liu, Y., Lueth, A. and Zhang, S. Q. (2008). MAPK phosphorylation-induced stabilization of ACS6 protein is mediated by the non-catalytic C-terminal domain, which also contains the cis-determinant for rapid degradation by the 26S proteasome pathway. *Plant Journal.* **54** (1): 129-140.

Jordan, N. D., Franklin, F. C. H. and Franklin-Tong, V. E. (2000). Evidence for DNA fragmentation triggered in the self-incompatibility response in pollen of *Papaver rhoeas*. *Plant Journal.* **23** (4): 471-479.

Jordan, N. D., Kakeda, K., Conner, A., Ride, J. P., Franklin-Tong, V. E. and Franklin, F. C. H. (1999). S-protein mutants indicate a functional role for SBP in the self-incompatibility reaction of *Papaver rhoeas*. *Plant Journal.* **20** (1): 119-125.

Kaboord, B. and Perr, M. (2008). Isolation of proteins and protein complexes by immunoprecipitation. *Methods in Molecular Biology*. 349-364.

Kachroo, A., Schopfer, C. R., Nasrallah, M. E. and Nasrallah, J. B. (2001). Allele-specific receptor-ligand interactions in Brassica self-incompatibility. *Science*. **293 (5536)**: 1824-1826.

Kakeda, K., Jordan, N. D., Conner, A., Ride, J. P., Franklin-Tong, V. E. and Franklin, F. C. H. (1998). Identification of residues in a hydrophilic loop of the Papaver rhoeas S protein that play a crucial role in recognition of incompatible pollen. *Plant Cell*. **10 (10)**: 1723-1731.

Kakita, M., Murase, K., Iwano, M., Matsumoto, T., Watanabe, M., Shiba, H., Isogai, A. and Takayama, S. (2007). Two distinct forms of M-locus protein kinase localize to the plasma membrane and interact directly with S-Locus receptor kinase to transduce self-incompatibility signaling in Brassica rapa. *Plant Cell*. **19 (12)**: 3961-3973.

Kandoth, P. K., Ranf, S., Pancholi, S. S., Jayanty, S., Walla, M. D., Miller, W., Howe, G. A., Lincoln, D. E. and Stratmann, J. W. (2007). Tomato MAPKs LeMPK1, LeMPK2, and LeMPK3 function in the systemin-mediated defense response against herbivorous insects. *Proceedings of the National Academy of Sciences of the United States of America*. **104 (29)**: 12205-12210.

Keyse, S. M. (2000). Protein phosphatases and the regulation of mitogen-activated protein kinase signalling. *Current Opinion in Cell Biology*. **12 (2)**: 186-192.

Kieber, J. J., Rothenberg, M., Roman, G., Feldmann, K. A. and Ecker, J. R. (1993). Ctr1, a Negative Regulator of the Ethylene Response Pathway in Arabidopsis, Encodes a Member of the Raf Family of Protein-kinases. *Cell*. **72 (3)**: 427-441.

Kiegerl, S., Cardinale, F., Siligan, C., Gross, A., Baudouin, E., Liwosz, A., Eklof, S., Till, S., Bogre, L., Hirt, H. and Meskiene, I. (2000). SIMKK, a mitogen-activated protein kinase

(MAPK) kinase, is a specific activator of the salt stress-induced MAPK, SIMK. *Plant Cell*. **12** (11): 2247-2258.

Kondo, K., Yamamoto, M., Itahashi, R., Sato, T., Egashira, H., Hattori, T. and Kowyama, Y. (2002a). Insights into the evolution of self-compatibility in *Lycopersicon* from a study of stilar factors. *Plant Journal*. **30** (2): 143-153.

Kondo, K., Yamamoto, M., Matton, D. P., Sato, T., Hirai, M., Norioka, S., Hattori, T. and Kowyama, Y. (2002b). Cultivated tomato has defects in both S-RNase and HT genes required for stilar function of self-incompatibility. *Plant Journal*. **29** (5): 627-636.

Koo, S. C., Yoon, H. W., Kim, C. Y., Moon, B. C., Cheong, Y. H., Han, H. J., Lee, S. M., Kang, K. Y., Kim, M. C., Lee, S. Y., Chung, W. S. and Cho, M. J. (2007). Alternative splicing of the OsBWMK1 gene generates three transcript variants showing differential subcellular localizations. *Biochemical and Biophysical Research Communications*. **360** (1): 188-193.

Kovtun, Y., Chiu, W. L., Tena, G. and Sheen, J. (2000). Functional analysis of oxidative stress-activated mitogen-activated protein kinase cascade in plants. *Proceedings of the National Academy of Sciences of the United States of America*. **97** (6): 2940-2945.

Kovtun, Y., Chiu, W. L., Zeng, W. K. and Sheen, J. (1998). Suppression of auxin signal transduction by a MAPK cascade in higher plants. *Nature*. **395** (6703): 716-720.

Kroj, T., Rudd, J. J., Nurnberger, T., Gabler, Y., Lee, J. and Scheel, D. (2003). Mitogen-activated protein kinases play an essential role in oxidative burst-independent expression of pathogenesis-related genes in parsley. *Journal of Biological Chemistry*. **278** (4): 2256-2264.

Krysan, P. J., Jester, P. J., Gottwald, J. R. and Sussman, M. R. (2002). An Arabidopsis mitogen-activated protein kinase kinase gene family encodes essential positive regulators of cytokinesis. *Plant Cell*. **14** (5): 1109-1120.

- Krysan, P. J., Young, J. C. and Sussman, M. R.** (1999). T-DNA as an insertional mutagen in Arabidopsis. *Plant Cell*. **11 (12)**: 2283-2290.
- Kumar, D. and Klessig, D. F.** (2000). Differential induction of tobacco MAP kinases by the defense signals nitric oxide, salicylic acid, ethylene, and jasmonic acid. *Molecular Plant-Microbe Interactions*. **13 (3)**: 347-351.
- Kurup, S., Ride, J. P., Jordan, N., Fletcher, G., Franklin-Tong, V. E. and Franklin, F. C. H.** (1998). Identification and cloning of related self-incompatibility S-genes in *Papaver rhoeas* and *Papaver nudicaule*. *Sexual Plant Reproduction*. **11 (4)**: 192-198.
- Lai, Z., Ma, W. S., Han, B., Liang, L. Z., Zhang, Y. S., Hong, G. F. and Xue, Y. B.** (2002). An F-box gene linked to the self-incompatibility (S) locus of *Antirrhinum* is expressed specifically in pollen and tapetum. *Plant Molecular Biology*. **50 (1)**: 29-42.
- Lampard, G. R., MacAlister, C. A. and Bergmann, D. C.** (2008). Arabidopsis Stomatal Initiation Is Controlled by MAPK-Mediated Regulation of the bHLH SPEECHLESS. *Science*. **322 (5904)**: 1113-1116.
- Lane, M. D. and Lawrence, M. J.** (1993). The Population-genetics of the Self-incompatibility Polymorphism in *Papaver rhoeas*. 7. The Number of S-alleles in the Species. *Heredity*. **71**: 596-602.
- Langone, J. J.** (1982). Applications of Immobilized Protein-A in Immunochemical Techniques. *Journal of Immunological Methods*. **55 (3)**: 277-296.
- Larkin, M. A., Blackshields, G., Brown, N. P., Chenna, R., McGettigan, P. A., McWilliam, H., Valentin, F., Wallace, I. M., Wilm, A., Lopez, R., Thompson, J. D., Gibson, T. J. and Higgins, D. G.** (2007). Clustal W and clustal X version 2.0. *Bioinformatics*. **23**: 2947-2948.

Lawrence, M. J. (2000). Population genetics of the homomorphic self-incompatibility polymorphisms in flowering plants. *Annals of Botany*. **85**: 221-226.

Lawrence, M. J., Afzal, M. and Kenrick, J. (1978). Genetic-control of Self-incompatibility in *Papaver rhoeas*. *Heredity*. **40 (Apr)**: 239-253.

Lee, H. S., Huang, S. S. and Kao, T. H. (1994). S-Proteins Control Rejection of Incompatible Pollen in *Petunia inflata*. *Nature*. **367 (6463)**: 560-563.

Lee, J. S. and Ellis, B. E. (2007). Arabidopsis MAPK phosphatase 2 (MKP2) positively regulates oxidative stress tolerance and inactivates the MPK3 and MPK6 MAPKs. *Journal of Biological Chemistry*. **282 (34)**: 25020-25029.

Lee, J. S., Huh, K. W., Bhargava, A. and Ellis, B. E. (2008a). Comprehensive analysis of protein-protein interactions between Arabidopsis MAPKs and MAPK kinases helps define potential MAPK signalling modules. *Plant Signal Behav.* **3 (12)**: 1037-41.

Lee, J. S., Wang, S., Sritubtim, S., Chen, J. G. and Ellis, B. E. (2009). Arabidopsis mitogen-activated protein kinase MPK12 interacts with the MAPK phosphatase IBR5 and regulates auxin signaling. *Plant Journal*. **57 (6)**: 975-985.

Lee, M. O., Cho, K., Kim, S. H., Jeong, S. H., Kim, J. A., Jung, Y. H., Shim, J., Shibato, J., Rakwal, R., Tamogami, S., Kubo, A., Agrawal, G. K. and Jwa, N. S. (2008b). Novel rice OsSIPK is a multiple stress responsive MAPK family member showing rhythmic expression at mRNA level. *Planta*. **227 (5)**: 981-990.

Leung, J., Orfanidi, S., Cheddor, F., Meszaros, T., Bolte, S., Mizoguchi, T., Shinozaki, K., Giraudat, J. and Bogre, L. (2006). Antagonistic interaction between MAP kinase and protein phosphatase 2C in stress recovery. *Plant Science*. **171 (5)**: 596-606.

Levchenko, A., Bruck, J. and Sternberg, P. W. (2000). Scaffold proteins may biphasically affect the levels of mitogen-activated protein kinase signaling and reduce its threshold

properties. *Proceedings of the National Academy of Sciences of the United States of America*. **97 (11)**: 5818-5823.

Lewis, M. W., Leslie, M. E. and Liljegren, S. J. (2006). Plant separation: 50 ways to leave your mother. *Current Opinion in Plant Biology*. **9 (1)**: 59-65.

Li, S. T., Samaj, J. and Franklin-Tong, V. E. (2007). A mitogen-activated protein kinase signals to programmed cell death induced by self-incompatibility in Papaver pollen. *Plant Physiology*. **145 (1)**: 236-245.

Ligterink, W., Kroj, T., zurNieden, U., Hirt, H. and Scheel, D. (1997). Receptor-mediated activation of a MAP kinase in pathogen defense of plants. *Science*. **276 (5321)**: 2054-2057.

Lim, P. O., Kim, H. J. and Nam, H. G. (2007). Leaf senescence. *Annual Review of Plant Biology*. **58**: 115-136.

Limmongkon, A., Giuliani, C., Valenta, R., Mittermann, I., Heberle-Bors, E. and Wilson, C. (2004). MAP kinase phosphorylation of plant profilin. *Biochemical and Biophysical Research Communications*. **324 (1)**: 382-386.

Lind, J. L., Bacic, A., Clarke, A. E. and Anderson, M. A. (1994). A Style-specific Hydroxyproline-rich Glycoprotein with Properties of both Extensins and Arabinogalactan Proteins. *Plant Journal*. **6 (4)**: 491-502.

Lind, J. L., Bonig, I., Clarke, A. E. and Anderson, M. A. (1996). A style-specific 120-kDa glycoprotein enters pollen tubes of *Nicotiana glauca* in vivo. *Sexual Plant Reproduction*. **9 (2)**: 75-86.

Liu, P., Sherman-Broyles, S., Nasrallah, M. E. and Nasrallah, J. B. (2007). A cryptic modifier causing transient self-incompatibility in *Arabidopsis thaliana*. *Current Biology*. **17 (8)**: 734-740.

- Liu, Q. P. and Xue, Q. Z.** (2007). Computational identification and phylogenetic analysis of the MAPK gene family in *Oryza sativa*. *Plant Physiology and Biochemistry*. **45 (1)**: 6-14.
- Liu, Y. D. and Zhang, S. Q.** (2004). Phosphorylation of 1-aminocyclopropane-1-carboxylic acid synthase by MPK6, a stress-responsive mitogen-activated protein kinase, induces ethylene biosynthesis in *Arabidopsis*. *Plant Cell*. **16 (12)**: 3386-3399.
- Lorenzo, O., Chico, J. M., Sanchez-Serrano, J. J. and Solano, R.** (2004). Jasmonate-insensitive1 encodes a MYC transcription factor essential to discriminate between different jasmonate-regulated defense responses in *Arabidopsis*. *Plant Cell*. **16 (7)**: 1938-1950.
- Lukowitz, W., Roeder, A., Parmenter, D. and Somerville, C.** (2004). A MAPKK kinase gene regulates extra-embryonic cell fate in *Arabidopsis*. *Cell*. **116 (1)**: 109-119.
- Luu, D. T., Qin, X. K., Morse, D. and Cappadocia, M.** (2000). S-RNase uptake by compatible pollen tubes in gametophytic self-incompatibility. *Nature*. **407 (6804)**: 649-651.
- Lydyard, P. M., Whelan, A. and Fanger, M. W.** (2004). Instant Notes in Immunology. BIOS Scientific Publishers, London. 2nd Edition.
- Marshall, A. G., Hendrickson, C. L. and Jackson, G. S.** (1998). Fourier transform ion cyclotron resonance mass spectrometry: A primer. *Mass Spectrometry Reviews*. **17 (1)**: 1-35.
- Matsuoka, D., Nanmori, T., Sato, K., Fukami, Y., Kikkawa, U. and Yasuda, T.** (2002). Activation of AtMEK1, an *Arabidopsis* mitogen-activated protein kinase kinase, in vitro and in vivo: analysis of active mutants expressed in *E-coli* and generation of the active form in stress response in seedlings. *Plant Journal*. **29 (5)**: 637-647.
- McClure, B., Mou, B. Q., Canevascini, S. and Bernatzky, R.** (1999). A small asparagine-rich protein required for S-allele-specific pollen rejection in *Nicotiana*. *Proceedings of the National Academy of Sciences of the United States of America*. **96 (23)**: 13548-13553.

- McClure, B. A., Gray, J. E., Anderson, M. A. and Clarke, A. E.** (1990). Self-incompatibility in *Nicotiana alata* Involves Degradation of Pollen Ribosomal-RNA. *Nature*. **347 (6295)**: 757-760.
- McClure, B. A., Haring, V., Ebert, P. R., Anderson, M. A., Simpson, R. J., Sakiyama, F. and Clarke, A. E.** (1989). Style Self-incompatibility Gene-products of *Nicotiana alata* are Ribonucleases. *Nature*. **342 (6252)**: 955-957.
- McCubbin, A. G. and Kao, T. H.** (2000). Molecular recognition and response in pollen and pistil interactions. *Annual Review of Cell and Developmental Biology*. **16** 333-364.
- McCurdy, D. W., Kovar, D. R. and Staiger, C. J.** (2001). Actin and actin-binding proteins in higher plants. *Protoplasma*. **215 (1-4)**: 89-104.
- Meimoun, P., Ambard-Bretteville, F., Francs-Small, C. C. D., Valot, B. and Vidal, J.** (2007). Analysis of plant phosphoproteins. *Analytical Biochemistry*. **371**: 238-246.
- Melikant, B., Giuliani, C., Halbmayr-Watzina, S., Limmongkon, A., Heberle-Bors, E. and Wilson, C.** (2004). The Arabidopsis thaliana MEK AtMKK6 activates the MAP kinase AtMPK13. *Febs Letters*. **576 (1-2)**: 5-8.
- Mészáros, T., Helfer, A., Hatzimasoura, E., Magyar, Z., Serazetdinova, L., Rios, G., Bardoczy, V., Teige, M., Koncz, C., Peck, S. and Bogre, L.** (2006). The Arabidopsis MAP kinase kinase MKK1 participates in defence responses to the bacterial elicitor flagellin. *Plant Journal*. **48 (4)**: 485-498.
- Miles, G. P., Samuel, M. A., Zhang, Y. L. and Ellis, B. E.** (2005). RNA interference-based (RNAi) suppression of AtMPK6, an Arabidopsis mitogen-activated protein kinase, results in hypersensitivity to ozone and misregulation of AtMPK3. *Environmental Pollution*. **138 (2)**: 230-237.

Millar, A. H., Heazlewood, J. L., Kristensen, B. K., Braun, H. P. and Moller, I. M. (2005). The plant mitochondrial proteome. *Trends in Plant Science*. **10 (1)**: 36-43.

Mishra, N. S., Tuteja, R. and Tuteja, N. (2006). Signaling through MAP kinase networks in plants. *Archives of Biochemistry and Biophysics*. **452 (1)**: 55-68.

Monroe-Augustus, M., Zolman, B. K. and Bartel, B. (2003). IBR5, a dual-specificity phosphatase-like protein modulating auxin and abscisic acid responsiveness in Arabidopsis. *Plant Cell*. **15 (12)**: 2979-2991.

Moon, H., Lee, B., Choi, G., Shin, S., Prasad, D. T., Lee, O., Kwak, S. S., Kim, D. H., Nam, J., Bahk, J., Hong, J. C., Lee, S. Y., Cho, M. J., Lim, C. O. and Yun, D. J. (2003). NDP kinase 2 interacts with two oxidative stress-activated MAPKs to regulate cellular redox state and enhances multiple stress tolerance in transgenic plants. *Proceedings of the National Academy of Sciences of the United States of America*. **100 (1)**: 358-363.

Murase, K., Shiba, H., Iwano, M., Che, F. S., Watanabe, M., Isogai, A. and Takayama, S. (2004). A membrane-anchored protein kinase involved in Brassica self-incompatibility signaling. *Science*. **303 (5663)**: 1516-1519.

Murfett, J., Atherton, T. L., Mou, B., Gasser, C. S. and McClure, B. A. (1994). S-RNase Expressed in Transgenic Nicotiana Causes S-allele-specific Pollen Rejection. *Nature*. **367 (6463)**: 563-566.

Naithani, S., Chookajorn, T., Ripoll, D. R. and Nasrallah, J. B. (2007). Structural modules for receptor dimerization in the S-locus receptor kinase extracellular domain. *Proceedings of the National Academy of Sciences of the United States of America*. **104 (29)**: 12211-12216.

Nakagami, H., Soukupova, H., Schikora, A., Zarsky, V. and Hirt, H. (2006). A mitogen-activated protein kinase kinase kinase mediates reactive oxygen species homeostasis in Arabidopsis. *Journal of Biological Chemistry*. **281 (50)**: 38697-38704.

Naoi, K. and Hashimoto, T. (2004). A semidominant mutation in an Arabidopsis mitogen-activated protein kinase phosphatase-like gene compromises cortical microtubule organization. *Plant Cell*. **16 (7)**: 1841-1853.

Nasrallah, M. E., Liu, P. and Nasrallah, J. B. (2002). Generation of self-incompatible Arabidopsis thaliana by transfer of two S locus genes from A-lyrata. *Science*. **297 (5579)**: 247-249.

Neill, S. J., Desikan, R., Clarke, A., Hurst, R. D. and Hancock, J. T. (2002). Hydrogen peroxide and nitric oxide as signalling molecules in plants. *Journal of Experimental Botany*. **53 (372)**: 1237-1247.

Nicole, M. C., Hamel, L. P., Morency, M. J., Beaudoin, N., Ellis, B. E. and Seguin, A. (2006). MAP-ping genomic organization and organ-specific expression profiles of poplar MAP kinases and MAP kinase kinases. *Bmc Genomics*. **7**.

Nishihama, R., Ishikawa, M., Araki, S., Soyano, T., Asada, T. and Machida, Y. (2001). The NPK1 mitogen-activated protein kinase kinase kinase is a regulator of cell-plate formation in plant cytokinesis. *Genes & Development*. **15 (3)**: 352-363.

Nishihama, R., Soyano, T., Ishikawa, M., Araki, S., Tanaka, H., Asada, T., Irie, K., Ito, M., Terada, M., Banno, H., Yamazaki, Y. and Machida, Y. (2002). Expansion of the cell plate in plant cytokinesis requires a kinesin-like protein/MAPKKK complex. *Cell*. **109 (1)**: 87-99.

Noir, S., Brautigam, A., Colby, T., Schmidt, J. and Panstruga, R. (2005). A reference map of the Arabidopsis thaliana mature pollen proteome. *Biochemical and Biophysical Research Communications*. **337 (4)**: 1257-1266.

Nuhse, T. S., Bottrill, A. R., Jones, A. M. E. and Peck, S. C. (2007). Quantitative phosphoproteomic analysis of plasma membrane proteins reveals regulatory mechanisms of plant innate immune responses. *Plant Journal*. **51 (5)**: 931-940.

O'Brien, M., Kapfer, C., Major, G., Laurin, M., Bertrand, C., Kondo, K., Kowyama, Y. and Matton, D. P. (2002). Molecular analysis of the stylar-expressed *Solanum chacoense* small asparagine-rich protein family related to the HT modifier of gametophytic self-incompatibility in *Nicotiana*. *Plant Journal*. **32 (6)**: 985-996.

O'Brien, M., Major, G., Chantha, S. C. and Matton, D. P. (2004). Isolation of S-RNase binding proteins from *Solanum chacoense*: identification of an SBP1 (RING finger protein) orthologue. *Sexual Plant Reproduction*. **17 (2)**: 81-87.

Ortiz-Masia, D., Perez-Amador, M. A., Carbonell, J. and Marcote, M. J. (2007). Diverse stress signals activate the C1 subgroup MAP kinases of *Arabidopsis*. *Febs Letters*. **581 (9)**: 1834-1840.

Ouaked, F., Rozhon, W., Lecourieux, D. and Hirt, H. (2003). A MAPK pathway mediates ethylene signaling in plants. *Embo Journal*. **22 (6)**: 1282-1288.

Parinov, S. and Sundaresan, V. (2000). Functional genomics in *Arabidopsis*: large-scale insertional mutagenesis complements the genome sequencing project. *Current Opinion in Biotechnology*. **11 (2)**: 157-161.

Pearson, G., Robinson, F., Gibson, T. B., Xu, B. E., Karandikar, M., Berman, K. and Cobb, M. H. (2001). Mitogen-activated protein (MAP) kinase pathways: Regulation and physiological functions. *Endocrine Reviews*. **22 (2)**: 153-183.

Pendle, A. F., Clark, G. P., Boon, R., Lewandowska, D., Lam, Y. W., Andersen, J., Mann, M., Lamond, A. I., Brown, J. W. S. and Shaw, P. J. (2005). Proteomic analysis of the *Arabidopsis* nucleolus suggests novel nucleolar functions. *Molecular Biology of the Cell*. **16 (1)**: 260-269.

Petersen, M., Brodersen, P., Naested, H., Andreasson, E., Lindhart, U., Johansen, B., Nielsen, H. B., Lacy, M., Austin, M. J., Parker, J. E., Sharma, S. B., Klessig, D. F.,

Martienssen, R., Mattsson, O., Jensen, A. B. and Mundy, J. (2000). Arabidopsis MAP kinase 4 negatively regulates systemic acquired resistance. *Cell*. **103 (7)**: 1111-1120.

Pierson, E. S., Miller, D. D., Callahan, D. A., vanAken, J., Hackett, G. and Hepler, P. K. (1996). Tip-localized calcium entry fluctuates during pollen tube growth. *Developmental Biology*. **174 (1)**: 160-173.

Popescu, S. C., Popescu, G. V., Bachan, S., Zhang, Z. M., Gerstein, M., Snyder, M. and Dinesh-Kumar, S. P. (2009). MAPK target networks in Arabidopsis thaliana revealed using functional protein microarrays. *Genes & Development*. **23 (1)**: 80-92.

Potocky, M., Jones, M. A., Bezvoda, R., Smirnov, N. and Zarsky, V. (2007). Reactive oxygen species produced by NADPH oxidase are involved in pollen tube growth. *New Phytologist*. **174 (4)**: 742-751.

Poulter, N. S., Vatovec, S. and Franklin-Tong, V. E. (2008). Microtubules are a target for self-incompatibility signaling in Papaver pollen. *Plant Physiology*. **146 (3)**: 1358-1367.

Prado, A. M., Porterfield, D. M. and Feijo, J. A. (2004). Nitric oxide is involved in growth regulation and re-orientation of pollen tubes. *Development*. **131 (11)**: 2707-2714.

Préstamo, G., Testillano, P. S., Vicente, O., Gonzalez-Melendi, P., Coronado, M. J., Wilson, C., Heberle-Bors, E. and Risueno, M. C. (1999). Ultrastructural distribution of a MAP kinase and transcripts in quiescent and cycling plant cells and pollen grains. *Journal of Cell Science*. **112 (7)**: 1065-1076.

Qiao, H., Wang, F., Zhao, L., Zhou, J. L., Lai, Z., Zhang, Y. S., Robbins, T. P. and Xue, Y. B. (2004a). The F-Box protein AhSLF-S-2 controls the pollen function of S-RNase-based self-incompatibility. *Plant Cell*. **16 (9)**: 2307-2322.

Qiao, H., Wang, H. Y., Zhao, L., Zhou, J. L., Huang, J., Zhang, Y. S. and Xue, Y. B. (2004b). The F-box protein AhSLF-S-2 physically interacts with S-RNases that may be

inhibited by the ubiquitin/26S proteasome pathway of protein degradation during compatible pollination in *antirrhinum*. *Plant Cell*. **16** (3): 582-595.

Qiu, J. L., Zhou, L., Yun, B. W., Nielsen, H. B., Fiil, B. K., Petersen, K., MacKinlay, J., Loake, G. J., Mundy, J. and Morris, P. C. (2008). Arabidopsis mitogen-activated protein kinase kinases MKK1 and MKK2 have overlapping functions in defense signaling mediated by MEKK1, MPK4, and MKS1. *Plant Physiology*. **148** (1): 212-222.

Quettier, A. L., Bertrand, C., Habricot, Y., Miginiac, E., Agnes, C., Jeannette, E. and Maldiney, R. (2006). The *pht1-3* mutation in a putative dual-specificity protein tyrosine phosphatase gene provokes hypersensitive responses to abscisic acid in *Arabidopsis thaliana*. *Plant Journal*. **47** (5): 711-719.

Reape, T. J., Molony, E. M. and McCabe, P. F. (2008). Programmed cell death in plants: distinguishing between different modes. *Journal of Experimental Botany*. **59** (3): 435-444.

Ren, D. T., Liu, Y. D., Yang, K. Y., Han, L., Mao, G. H., Glazebrook, J. and Zhang, S. Q. (2008). A fungal-responsive MAPK cascade regulates phytoalexin biosynthesis in *Arabidopsis*. *Proceedings of the National Academy of Sciences of the United States of America*. **105** (14): 5638-5643.

Ren, D. T., Yang, H. P. and Zhang, S. Q. (2002). Cell death mediated by MAPK is associated with hydrogen peroxide production in *Arabidopsis*. *Journal of Biological Chemistry*. **277** (1): 559-565.

Rentel, M. C., Lecourieux, D., Ouaked, F., Usher, S. L., Petersen, L., Okamoto, H., Knight, H., Peck, S. C., Grierson, C. S., Hirt, H. and Knight, M. R. (2004). OXI1 kinase is necessary for oxidative burst-mediated signalling in *Arabidopsis*. *Nature*. **427** (6977): 858-861.

Reyna, N. S. and Yang, Y. N. (2006). Molecular analysis of the rice MAP kinase gene family in relation to Magnaporthe grisea infection. *Molecular Plant-Microbe Interactions*. **19** (5): 530-540.

Rojas-Beltran, J. A., Dubois, F., Mortiaux, F., Portetelle, D., Gebhardt, C., Sangwan, R. S. and du Jardin, P. (1999). Identification of cytosolic Mg²⁺-dependent soluble inorganic pyrophosphatases in potato and phylogenetic analysis. *Plant Molecular Biology*. **39** (3): 449-461.

Rudd, J. J. (1997). Identification and characterisation of changes in pollen protein phosphorylation associated with the self-incompatibility (SI) response of *Papaver rhoeas* L. University of Birmingham. PhD.

Rudd, J. J., Franklin, F. C. H. and FranklinTong, V. E. (1997). Ca²⁺-independent phosphorylation of a 68 kDa pollen protein is stimulated by the self-incompatibility response in *Papaver rhoeas*. *Plant Journal*. **12** (3): 507-514.

Rudd, J. J., Franklin, F. C. H., Lord, J. M. and FranklinTong, V. E. (1996). Increased phosphorylation of a 26-kD pollen protein is induced by the self-incompatibility response in *Papaver rhoeas*. *Plant Cell*. **8** (4): 713-724.

Rudd, J. J. and Franklin-Tong, V. E. (2003). Signals and targets of the self-incompatibility response in pollen of *Papaver rhoeas*. *Journal of Experimental Botany*. **54** (380): 141-148.

Rudd, J. J., Osman, K., Franklin, F. C. H. and Franklin-Tong, V. E. (2003). Activation of a putative MAP kinase in pollen is stimulated by the self-incompatibility (SI) response. *Febs Letters*. **547** (1-3): 223-227.

Salvi, D., Rolland, N., Joyard, J. and Ferro, M. (2008). Purification and proteomic analysis of chloroplasts and their sub-organellar compartments. *Methods in Molecular Biology*. 19-36.

Samaj, J., Muller, J., Beck, M., Bohm, N. and Menzel, D. (2006). Vesicular trafficking, cytoskeleton and signalling in root hairs and pollen tubes. *Trends in Plant Science*. **11 (12)**: 594-600.

Samaj, J., Ovecka, M., Hlavacka, A., Lecourieux, F., Meskiene, I., Lichtscheidl, I., Lenart, P., Salaj, J., Volkmann, D., Bogre, L., Baluska, F. and Hirt, H. (2002). Involvement of the mitogen-activated protein kinase SIMK in regulation of root hair tip growth. *Embo Journal*. **21 (13)**: 3296-3306.

Samuel, M. A., Miles, G. P. and Ellis, B. E. (2000). Ozone treatment rapidly activates MAP kinase signalling in plants. *Plant Journal*. **22 (4)**: 367-376.

Samuel, M. A., Mudgil, Y., Salt, J. N., Delmas, F., Ramachandran, S., Chilelli, A. and Goring, D. R. (2008). Interactions between the s- domain receptor kinases and AtPUB-ARM E3 ubiquitin ligases suggest a conserved signaling pathway in arabidopsis. *Plant Physiology*. **147 (4)**: 2084-2095.

Sasabe, M., Soyano, T., Takahashi, Y., Sonobe, S., Igarashi, H., Itoh, T. J., Hidaka, M. and Machida, Y. (2006). Phosphorylation of NtMAP65-1 by a MAP kinase down-regulates its activity of microtubule bundling and stimulates progression of cytokinesis of tobacco cells. *Genes & Development*. **20 (8)**: 1004-1014.

Sassa, H., Nishio, T., Kowyama, Y., Hirano, H., Koba, T. and Ikehashi, H. (1996). Self incompatibility (S) alleles of the Rosaceae encode members of a distinct class of the T-2/S ribonuclease superfamily. *Molecular & General Genetics*. **250 (5)**: 547-557.

Schopfer, C. R., Nasrallah, M. E. and Nasrallah, J. B. (1999). The male determinant of self-incompatibility in Brassica. *Science*. **286 (5445)**: 1697-1700.

Schweighofer, A., Kazanaviciute, V., Scheikl, E., Teige, M., Doczi, R., Hirt, H., Schwanninger, M., Kant, M., Schuurink, R., Mauch, F., Buchala, A., Cardinale, F. and Meskiene, I. (2007). The PP2C-type phosphatase AP2C1, which negatively regulates MPK4

and MPK6, modulates innate immunity, jasmonic acid, and ethylene levels in Arabidopsis. *Plant Cell*. **19** (7): 2213-2224.

Shiba, H., Takayama, S., Iwano, M., Shimosato, H., Funato, M., Nakagawa, T., Che, F. S., Suzuki, G., Watanabe, M., Hinata, K. and Isogai, A. (2001). A pollen coat protein, SP11/SCR, determines the pollen S-specificity in the self-incompatibility of Brassica species. *Plant Physiology*. **125** (4): 2095-2103.

Shimosato, H., Yokota, N., Shiba, H., Iwano, M., Entani, T., Che, F. S., Watanabe, M., Isogai, A. and Takayama, S. (2007). Characterization of the SP11/SCR high-affinity binding site involved in self/nonself recognition in Brassica self-incompatibility. *Plant Cell*. **19** (1): 107-117.

Sijacic, P., Wang, X., Skirpan, A. L., Wang, Y., Dowd, P. E., McCubbin, A. G., Huang, S. and Kao, T. H. (2004). Identification of the pollen determinant of S-RNase-mediated self-incompatibility. *Nature*. **429** (6989): 302-305.

Sims, T. L. and Ordanic, M. (2001). Identification of a S-ribonuclease-binding protein in *Petunia hybrida*. *Plant Molecular Biology*. **47** (6): 771-783.

Singh, A., Ai, Y. and Kao, T. H. (1991). Characterization of Ribonuclease-activity of 3 S-allele-associated Proteins of *Petunia inflata*. *Plant Physiology*. **96** (1): 61-68.

Sirover, M. A. (1999). New insights into an old protein: the functional diversity of mammalian glyceraldehyde-3-phosphate dehydrogenase. *Biochimica Et Biophysica Acta-Protein Structure and Molecular Enzymology*. **1432** (2): 159-184.

Smith, L. G. and Oppenheimer, D. G. (2005). Spatial control of cell expansion by the plant cytoskeleton. *Annual Review of Cell and Developmental Biology*. **21** 271-295.

- Snowman, B. N., Kovar, D. R., Shevchenko, G., Franklin-Tong, V. E. and Staiger, C. J.** (2002). Signal-mediated depolymerization of actin in pollen during the self-incompatibility response. *Plant Cell*. **14 (10)**: 2613-2626.
- Song, F. M. and Goodman, R. M.** (2002). OsBIMK1, a rice MAP kinase gene involved in disease resistance responses. *Planta*. **215 (6)**: 997-1005.
- Soyano, T., Nishihama, R., Morikiyo, K., Ishikawa, M. and Machida, Y.** (2003). NQK1/NtMEK1 is a MAPKK that acts in the NPK1 MAPKKK-mediated MAPK cascade and is required for plant cytokinesis. *Genes & Development*. **17 (8)**: 1055-1067.
- Staiger, C. J.** (2000). Signaling to the actin cytoskeleton in plants. *Annual Review of Plant Physiology and Plant Molecular Biology*. **51**: 257-288.
- Stein, J. C., Dixit, R., Nasrallah, M. E. and Nasrallah, J. B.** (1996). SRK, the stigma-specific S locus receptor kinase of Brassica, is targeted to the plasma membrane in transgenic tobacco. *Plant Cell*. **8 (3)**: 429-445.
- Stein, J. C., Howlett, B., Boyes, D. C., Nasrallah, M. E. and Nasrallah, J. B.** (1991). Molecular-Cloning of a Putative Receptor Protein-Kinase Gene Encoded at the Self-Incompatibility Locus of Brassica oleracea. *Proceedings of the National Academy of Sciences of the United States of America*. **88 (19)**: 8816-8820.
- Stone, S. L., Anderson, E. M., Mullen, R. T. and Goring, D. R.** (2003). ARC1 is an E3 ubiquitin ligase and promotes the ubiquitination of proteins during the rejection of self-incompatible Brassica pollen. *Plant Cell*. **15 (4)**: 885-898.
- Straatman, K. R., Dove, S. K., Holdaway-Clarke, T., Hepler, P. K., Kunkel, J. G. and Franklin-Tong, V. E.** (2001). Calcium signalling in pollen of *Papaver rhoeas* undergoing the self-incompatibility (SI) response. *Sexual Plant Reproduction*. **14 (1-2)**: 105-110.

Suarez-Rodriguez, M. C., Adams-Phillips, L., Liu, Y. D., Wang, H. C., Su, S. H., Jester, P. J., Zhang, S. Q., Bent, A. F. and Krysan, P. J. (2007). MEKK1 is required for flg22-induced MPK4 activation in Arabidopsis plants. *Plant Physiology*. **143** (2): 661-669.

Suzuki, G., Kai, N., Hirose, T., Fukui, K., Nishio, T., Takayama, S., Isogai, A., Watanabe, M. and Hinata, K. (1999). Genomic organization of the S locus: Identification and characterization of genes in SLG/SRK region of S-9 haplotype of Brassica campestris (syn. rapa). *Genetics*. **153** (1): 391-400.

Takahashi, F., Yoshida, R., Ichimura, K., Mizoguchi, T., Seo, S., Yonezawa, M., Maruyama, K., Yamaguchi-Shinozaki, K. and Shinozaki, K. (2007). The mitogen-activated protein kinase cascade MKK3-MPK6 is an important part of the jasmonate signal transduction pathway in Arabidopsis. *Plant Cell*. **19** (3): 805-818.

Takahashi, K., Isobe, M. and Muto, S. (1998). Mastoparan induces an increase in cytosolic calcium ion concentration and subsequent activation of protein kinases in tobacco suspension culture cells. *Biochimica Et Biophysica Acta-Molecular Cell Research*. **1401** (3): 339-346.

Takasaki, T., Hatakeyama, K., Suzuki, G., Watanabe, M., Isogai, A. and Hinata, K. (2000). The S receptor kinase determines self-incompatibility in Brassica stigma. *Nature*. **403** (6772): 913-916.

Takayama, S. and Isogai, A. (2005). Self-incompatibility in plants. *Annual Review of Plant Biology*. **56**: 467-489.

Takayama, S., Shiba, H., Iwano, M., Shimosato, H., Che, F. S., Kai, N., Watanabe, M., Suzuki, G., Hinata, K. and Isogai, A. (2000). The pollen determinant of self-incompatibility in Brassica campestris. *Proceedings of the National Academy of Sciences of the United States of America*. **97** (4): 1920-1925.

Tanoue, T. J. and Nishida, E. (2003). Molecular recognitions in the MAP kinase cascades. *Cellular Signalling*. **15** (5): 455-462.

- Teige, M., Scheikl, E., Eulgem, T., Doczi, F., Ichimura, K., Shinozaki, K., Dangl, J. L. and Hirt, H.** (2004). The MKK2 pathway mediates cold and salt stress signaling in Arabidopsis. *Molecular Cell*. **15 (1)**: 141-152.
- Terpe, K.** (2006). Overview of bacterial expression systems for heterologous protein production: from molecular and biochemical fundamentals to commercial systems. *Applied Microbiology and Biotechnology*. **72 (2)**: 211-222.
- Thomas, S. G. and Franklin-Tong, V. E.** (2004). Self-incompatibility triggers programmed cell death in Papaver pollen. *Nature*. **429 (6989)**: 305-309.
- Thomas, S. G., Huang, S. J., Li, S. T., Staiger, C. J. and Franklin-Tong, V. E.** (2006). Actin depolymerization is sufficient to induce programmed cell death in self-incompatible pollen. *Journal of Cell Biology*. **174 (2)**: 221-229.
- Trieu, E. P., Gross, J. K. and Targoff, I. N.** (2009). Immunoprecipitation-western blot for proteins of low abundance. *Methods Mol Biol*. **536**: 259-75.
- Ulm, R., Ichimura, K., Mizoguchi, T., Peck, S. C., Zhu, T., Wang, X., Shinozaki, K. and Paszkowski, J.** (2002). Distinct regulation of salinity and genotoxic stress responses by Arabidopsis MAP kinase phosphatase 1. *Embo Journal*. **21 (23)**: 6483-6493.
- Ulm, R., Revenkova, E., di Sansebastiano, G. P., Bechtold, N. and Paszkowski, J.** (2001). Mitogen-activated protein kinase phosphatase is required for genotoxic stress relief in Arabidopsis. *Genes & Development*. **15 (6)**: 699-709.
- Ushijima, K., Sassa, H., Dandekar, A. M., Gradziel, T. M., Tao, R. and Hirano, H.** (2003). Structural and transcriptional analysis of the self-incompatibility locus of almond: Identification of a pollen-expressed F-box gene with haplotype-specific polymorphism. *Plant Cell*. **15 (3)**: 771-781.

Visser, K., Heimovaara-Dijkstra, S., Kijne, J. W. and Wang, M. (1998). Molecular cloning and characterization of an inorganic pyrophosphatase from barley. *Plant Molecular Biology*. **37 (1)**: 131-140.

Walia, A., Lee, J. S., Wasteneys, G. and Ellis, B. (2009). Arabidopsis mitogen-activated protein kinase MPK18 mediates cortical microtubule functions in plant cells. *The Plant Journal*.

Walker, E. A., Ride, J. P., Kurup, S., Franklin-Tong, V. E., Lawrence, M. J. and Franklin, F. C. H. (1996). Molecular analysis of two functional homologues of the S-3 allele of the *Papaver rhoeas* self-incompatibility gene isolated from different populations. *Plant Molecular Biology*. **30 (5)**: 983-994.

Wang, A. M., Doyle, M. V. and Mark, D. F. (1989). Quantitation of Messenger-RNA by the Polymerase Chain-reaction. *Proceedings of the National Academy of Sciences of the United States of America*. **86 (24)**: 9717-9721.

Wang, H. C., Ngwenyama, N., Liu, Y. D., Walker, J. C. and Zhang, S. Q. (2007). Stomatal development and patterning are regulated by environmentally responsive mitogen-activated protein kinases in Arabidopsis. *Plant Cell*. **19 (1)**: 63-73.

Wang, H.-Z., Zhou, X.-f., Song, Z.-X., Liu, W.-G. and Zeng, X.-L. (2003). Degenerate PCR and its application in gene cloning. *Yichuan*. **25 (2)**: 201-204.

Wang, Y., Tsukamoto, T., Yi, K. W., Wang, X., Huang, S. S., McCubbin, A. G. and Kao, T. H. (2004). Chromosome walking in the *Petunia inflata* self-incompatibility (S-) locus and gene identification in an 881-kb contig containing S-2-RNase. *Plant Molecular Biology*. **54 (5)**: 727-742.

Wege, S., Scholz, A., Gleissberg, S. and Becker, A. (2007). Highly efficient virus-induced gene silencing (VIGS) in california poppy (*Eschscholzia californica*): An evaluation of VIGS

as a strategy to obtain functional data from non-model plants. *Annals of Botany*. **100 (3)**: 641-649.

Weller, S. G. (2009). The different forms of flowers - what have we learned since Darwin? *Botanical Journal of the Linnean Society*. **160 (3)**: 249-261.

Wen, J. Q., Oono, K. and Imai, R. (2002). Two novel mitogen-activated protein signaling components, OsMEK1 and OsMAP1, are involved in a moderate low-temperature signaling pathway in rice. *Plant Physiology*. **129 (4)**: 1880-1891.

Wheeler, M. J., Armstrong, S. A., Franklin-Tong, V. E. and Franklin, F. C. H. (2003). Genomic organization of the *Papaver rhoeas* self-incompatibility S-1 locus. *Journal of Experimental Botany*. **54 (380)**: 131-139.

Wheeler, M. J., de Graaf, B. H. J., Hadjiosif, N., Perry, R. M., Poulter, N. S., Osman, K., Vatovec, S., Harper, A., Franklin, F. C. H. and Franklin-Tong, V. E. (2009). Identification of the pollen self-incompatibility determinant in *Papaver rhoeas*. *Nature*. **459 (7249)**: 992-995.

Whitmarsh, A. J. and Davis, R. J. (1998). Structural organization of MAP-kinase signaling modules by scaffold proteins in yeast and mammals. *Trends in Biochemical Sciences*. **23 (12)**: 481-485.

Whittaker, S. (2001). The characterisation of protein kinases in pollen of *Papaver rhoeas*. University of Birmingham. PhD.

Widmann, C., Gibson, S., Jarpe, M. B. and Johnson, G. L. (1999). Mitogen-activated protein kinase: Conservation of a three-kinase module from yeast to human. *Physiological Reviews*. **79 (1)**: 143-180.

Wright, S. (1939). The distribution of self-sterility alleles in populations. *Genetics*. **24 (4)**: 538-552.

- Xing, Y., Jia, W. S. and Zhang, J. H.** (2008). AtMKK1 mediates ABA-induced CAT1 expression and H₂O₂ production via AtMPK6-coupled signaling in Arabidopsis. *Plant Journal*. **54** (3): 440-451.
- Xu, J., Li, Y., Wang, Y., Liu, H. X., Lei, L., Yang, H. L., Liu, G. Q. and Ren, D. T.** (2008). Activation of MAPK kinase 9 induces ethylene and camalexin biosynthesis and enhances sensitivity to salt stress in Arabidopsis. *Journal of Biological Chemistry*. **283** (40): 26996-27006.
- Xue, Y. B., Carpenter, R., Dickinson, H. G. and Coen, E. S.** (1996). Origin of allelic diversity in antirrhinum S locus RNases. *Plant Cell*. **8** (5): 805-814.
- Yang, K. Y., Liu, Y. D. and Zhang, S. Q.** (2001). Activation of a mitogen-activated protein kinase pathway is involved in disease resistance in tobacco. *Proceedings of the National Academy of Sciences of the United States of America*. **98** (2): 741-746.
- Yoo, S. D., Cho, Y. H., Tena, G., Xiong, Y. and Sheen, J.** (2008). Dual control of nuclear EIN3 by bifurcate MAPK cascades in C₂H₄ signalling. *Nature*. **451** (7180): 789-U1.
- Yuan, B., Shen, X., Li, X., Xu, C. and Wang, S. P.** (2007). Mitogen-activated protein kinase OsMPK6 negatively regulates rice disease resistance to bacterial pathogens. *Planta*. **226** (4): 953-960.
- Zaninotto, F., La Camera, S., Polverari, A. and Delledonne, M.** (2006). Cross talk between reactive nitrogen and oxygen species during the hypersensitive disease resistance response. *Plant Physiology*. **141** (2): 379-383.
- Zhang, S. Q. and Klessig, D. F.** (2001). MAPK cascades in plant defense signaling. *Trends in Plant Science*. **6** (11): 520-527.

Zhou, C. J., Cai, Z. H., Guo, Y. F. and Gan, S. S. (2009). An Arabidopsis Mitogen-Activated Protein Kinase Cascade, MKK9-MPK6, Plays a Role in Leaf Senescence. *Plant Physiology*. **150 (1)**: 167-177.

Zipfel, C., Robatzek, S., Navarro, L., Oakeley, E. J., Jones, J. D. G., Felix, G. and Boller, T. (2004). Bacterial disease resistance in Arabidopsis through flagellin perception. *Nature*. **428 (6984)**: 764-767.

Zou, J. J., Song, L. F., Zhang, W. Z., Wang, Y., Ruan, S. L. and Wu, W. H. (2009). Comparative Proteomic Analysis of Arabidopsis Mature Pollen and Germinated Pollen. *Journal of Integrative Plant Biology*. **51 (5)**: 438-455.

Appendix

Appendix

ii.i) Primers

Original name	Sequence	Thesis name
GAPD-N	5'-CTTGAAGGGTGGTGCCAAGAAGG-3'	GAPDN
GAPD-C	5'-CCTGTTGTGCGCCAACGAAGTCAG-3'	GAPDC
PapaverGAPD5'	5'-GAAGGGTGGTGCCAAGAAGGTTATC-3'	PrGAPD5'
PapaverGAPD3'	5'-GCCTTCTTCTCAAGTCTCACAGTAAG-3'	PrGAPD3'
PrGAPD5'RACE3	5'-GACAGTTGGTGGTGCAACTAGCG-3'	PrGAPD-5R1
PrGAPD5'RACE2	5'-GTGTATTCAATTCTCGTTGACACC-3'	PrGAPD-5R2
PrGAPD5'RACE1	5'-CGACTTGATCGTCCATGTTGCC-3'	PrGAPD-5R3
PrGAPDCu/s	5'-CCACTTCTCGCTTTTCTCTCTGC-3'	PrGAPDCu/s
PrGAPDCd/s	5'-CCTATAAACCAAGCTCAGAGCGC-3'	PrGAPDCd/s
AtMAPK3_5'	5'-CCACCACCACTAAGAAGACAGTTC-3'	AtMPK3_5'
AtMAPK3_3'	5'-CTGTCGGTGTGCCAAGCAACTCTG-3'	AtMPK3_3'
BMAPK3hom3'C	5'-ATCATCTCTTTAATXTGYTCTTCTCC-3'	MPK3A_3'
BMAPK3hom3'T	5'-ATCATCTCTTTAATXTGYTCTTCTTC-3'	MPK3B_3'
BMAPK3hom5'A	5'-GATTTCCGGCGGTTCAAACCTCAYGGXGGACAAT-3'	MPK3A_5'
BMAPK3hom5'G	5'-GATTTCCGGCGGTTCAAACCTCAYGGXGGACAGT-3'	MPK3B_5'
MAPK3hom3'spe1	5'-CATNTCYTTWATYTGTYTCYTC-3'	MPK3 spe1_3'
MAPK3hom3'degl	5'-CATNNTCYTTDATYTGTYTCYTC-3'	MPK3 deg1_3'
MAPK3hom5'degl	5'-ATGGAYACNGAYYTNCAICARAT-3'	MPK3 deg1_5'
MAPK3hom5'spe1	5'-ATGGAYACBGATCTTCAICARAT-3'	MPK3 spe1_5'
MAPK3hom5'spe2	5'-GGTTGYATNTWYATGGARCTNATG-3'	MPK3 spe2_5'
MAPK3homdegA3'	5'-TTXACRTGXGWRAXARYTTXGC-3'	MPK3deg2_3'
MAPK3homdegA5'	5'-GGXTTYACXCAYAAYGARGA-3'	MPK3deg2_5'
PrMPK35'RACEcont	5'-CTCCGATTATGCCCATCGGTCCG-3'	PrMPK5'Rcont
PrMPK3_5'	5'-GTGATTTTGGTTTGGCTCGCCC-3'	PrMPK3_5'
PrMPK3_3'RACE	5'-CCGATGAACCAGTTTGTTCAGTC-3'	PrMPK3_3'R
PrMPK3_5'RACE1	5'-GAATCTGGTACAAGAAATACTGGCTG-3'	PrMPK3_5'R1A
PrMPK3_5'RACE2	5'-CGGTCATAAATTCATTTTCCGAAGTAGG-3'	PrMPK3_5'R2A
PrMPK3_5'RACE3	5'-GCAGTATAATCTGAAGAATTGAGC-3'	PrMPK3_5'R3A
PrMPK35'RACE3	5'-GGTCACTGTCCATGAGTTCAGTG-3'	PrMPK3_5'R3B
PrMPK35'RACE2	5'-CCTGGTATTGGTGGTGAATGAC-3'	PrMPK3_5'R2B
PrMPK35'RACE1	5'-CCAATAACATTCTCATGGTCCAAATCG-3'	PrMPK3_5'R1B
PrMPK3A5'	5'-CCTCCGATTATGCCCATCGGTCCG-3'	PrMPK3_5'A
PrMPK3A3'	5'-GGTCACTGTCCATGAGTTCAGTG-3'	PrMPK3_3'A
PrMPK3C3'	5'-CAAACAAAACAGATTTACCTATGCAAG-3'	PrMPK3_3'C
PrMPK3C5'	5'-GTACATCAGCTGCGGTTACTTAC-3'	PrMPK3_5'C
PrMPK3liked/s1	5'-GAATGAATCATTTGCACCACATG-3'	PrMPK3d/s1
PrMPK3liked/s2	5'-GATGGTGTTCCTTCAACTGGTTGC-3'	PrMPK3d/s2
PrMPK3likeu/s1	5'-GTCTAAAGAGAGACTGTGAAGAG-3'	PrMPK3u/s1
JPrMPK3_5'int	5'-GTCCCTCCGATTATGCCCATCGG-3'	PrMPK3-5'
JPrMPK3_3'int	5'-GGCGAGGATGTGGTGGTAGC-3'	PrMPK3-3'
TDYdeg5'1	5'-CAAGARGTTRTTGGVAAAGGMAG-3'	TDYdeg5'1
TDYdeg3'1	5'-TAYTTAGAGWARAANGADCCAC-3'	TDYdeg3'1
TDYdeg5'2	5'-AAACCNAAGAACATHYTVGC-3'	TDYdeg5'2
TDYdeg3'2	5'-GAGGATGATAYTCHARWATCTC-3'	TDYdeg3'2
PrMPK20_3RACEA	5'-GTTACTAAGGACGACATTAAGGAGCC-3'	PrMPK20-3R1
PrMPK20_3RACEB	5'-CCATACTTTAAAAGCTTGTCAAGGG-3'	PrMPK20-3R2
PrMPK20_5RACE1	5'-CTTTCTCTCCTGTATGAGTGTCAATG-3'	PrMPK20-5R1
PrMPK20_5RACE2	5'-CACGCAGTATCCTTGCAGCATCC-3'	PrMPK20-5R2

PrMPK20_5RACE3	5'-CTTGAGGGTGGCAACATGATGTGC-3'	PrMPK20-5R3
PrMPK20gen5'	5'-CTTCTTTGCAGAGTACCACGGAG-3'	PrMPK20gen5'
PrMPK20gen3'	5'-GAAACTCCTTCAAGTACTACTCCCG-3'	PrMPK20gen3'
PrMPK20gen5'int	5'-CCGAAGGATAGACCAACTGCAGAAG-3'	PrMPK20gen5'int
PrMPK20gen3'int	5'-GTTCCCTCTCTGCCCTTGACAAGC-3'	PrMPK20gen3'int
JPrMPK20_5'int	5'-AAGCTATGGTGTGTGTGCTCAGC-3'	PrMPK20-5'
JPrMPK20_3'int	5'-GGCTGCTTCTTCTCATGCTGG-3'	PrMPK20-3'
AtMPK9-5'	5'-CACACATTCAAGCGAAAAGGTTGCC-3'	MPK9-5'1
AtMPK9_5'A	5'-CCTTCACGCCGTGAGTTCAGAGAC-3'	MPK9-5'2
AtMPK9_5'B	5'-CCAAGTTATCAAGGCGAACGATGATC-3'	MPK9-5'3
MPK9OP_5'1	5'-GGTTGCCATTAAGAARATCAATG-3'	MPK9-5'4
MPK9OP_5'2	5'-GATCAAGCTTCTCAGKYTGCTCCG-3'	MPK9-5'5
AtMPK9-3'	5'-CATATTGCCGAGATATCTCCTCGCC-3'	MPK9-3'1
AtMPK9-3'2	5'-CTGATGCTGGCACTTTTCAGCAAGC-3'	MPK9-3'2
AtMPK9_3'A	5'-GTGTTGGCGTTGAAGAGGTGAGCC-3'	MPK9-3'3
AtMPK9_3'B	5'-GGAGGGCTTTCGAGGGTCTGAC-3'	MPK9-3'4
MPK9OP_3'1	5'-GCAAATTGTCTCTTAAAGCGATCAAC-3'	MPK9-3'5
MPK9OP_3'2	5'-GGTACATGAAGCTAGTCTGYTCTCC-3'	MPK9-3'6
AtMPK8-5'	5'-GAGTTGCGATCAAGAAGATCAACG-3'	MPK8-5'1
AtMPK8_5'A	5'-CGGAGTATGGAGAAGCTAACAGG-3'	MPK8-5'2
AtMPK8-3'	5'-GAAGGCGGAGAGCCAAAGGATCAG-3'	MPK8-3'1
AtMPK8-3'2	5'-GCATTTAGAACCGCTGATGCTTGC-3'	MPK8-3'2
AtMPK8_3'A	5'-CACCATTTGGAGCAGGAACTCTC-3'	MPK8-3'3
AtMPK17-5'	5'-GGTGAAGCAAGTCAATATCAGATCC-3'	MPK17-5'1
AtMPK17_5'A	5'-CGACCTCACTCCTCAGCATCATC-3'	MPK17-5'2
AtMPK17_5'B	5'-CATGCTTCTCCTTGTGCGCAAG-3'	MPK17-5'3
MPK17AO5'1	5'-GTGGAGATCAAGCAYATYATGC-3'	MPK17-5'4
MPK17AO5'2	5'-GTTCTTAAGGTAAAYGAYGACC-3'	MPK17-5'5
AtMPK17-3'	5'-GCGCCACAGGATCGATATTGGG-3'	MPK17-3'1
AtMPK17-3'2	5'-CCTTCTGTGATGATAAGCCAGTTGC-3'	MPK17-3'2
AtMPK17_3'A	5'-CTTCGTCTTCTGATGAGCACACCCG-3'	MPK17-3'3
AtMPK17_3'B	5'-CCGGAGTTGCTGCTTTGTCTAC-3'	MPK17-3'4
MPK17AO3'1	5'-CGAGTCGGGCAAACSTYGTGTTG-3'	MPK17-3'5
MPK17AO3'2	5'-GAAGTGACTTTCTCTGMWGTGG-3'	MPK17-3'6
AtMPK19-5'	5'-GCTATGGAGTTGTATGTGCAGC-3'	MPK19-5'1
MPK18-19_5'	5'-GCATTATGCTGCCCKCCTTCTAAG-3'	MPK19-5'2
AtMPK19-3'	5'-GCCAACAGTCTTTCAGAAAGACGC-3'	MPK19-3'1
AtMPK19-3'2	5'-GGGTTTGGGTTTCAGCTCAGCTGG-3'	MPK19-3'2
MPK18-19_3'	5'-CTCTCTAGAGGTATGACYGGCCC-3'	MPK193'3
AtMPK20-5'	5'-GCTATAGACACTCTTACGGGTGAG-3'	MPK20-5'1
AtMPK20-3'	5'-GAAGGTGCCCTAGCAGATCAGTC-3'	MPK20-3'1
AtMPK20-3'2	5'-CTTCCGGTGAGCAGAACCACCAGG-3'	MPK20-3'2
PrMPK93'RACE_3	5'-GAGAGATACTCGAGTACCATCCGC-3'	PrMPK9-3R1
PrMPK93'RACE_2	5'-GTATCTTCGTGGTGCAGATCAGGC-3'	PrMPK9-3R2
PrMPK95RACE_3	5'-CTAAGAAGCTGGAACAGAAAGAACTG-3'	PrMPK9-5R1
PrMPK95RACE_2	5'-GTTTCGCGAGTAAGATCGTCATTCAC-3'	PrMPK9-5R2
PrMPK95RACE_1	5'-GCTTTATTTCAACAACATCTGGATGC-3'	PrMPK9-5R3
PrMPK9A5'NdeI	5'-ATTCATATGGGGGGAGGAGGAACACTCGTG-3'	PrMPK9A5'NdeI
PrMPK9A3'NotI	5'-AATGCGGCCGCAAGTCTTAGCTTAGTAG-3'	PrMPK9A3'NotI
PrMPK9Agen5'	5'-CTGCCATTAATTTTCATGTGTTGGGG-3'	PrMPK92gen5'
PrMPK9Agen3'	5'-GAAAAAACCTGAAAACATCAGTGG-3'	PrMPK92gen3'
PrMPK8_3RACE3	5'-GATGTACGAGAATTAATTTACCG-3'	PrMPK8-3R1
PrMPK8_3RACE2	5'-GGAGTATCATCCCCAAATGCTTC-3'	PrMPK8-3R2
PrMPK8_5RACE3	5'-GTTTCAGGAGTAAGATCATCATTTGCC-3'	PrMPK8-5R1
PrMPK8_5RACE2	5'-GATCTGATTCCATCAACTCAAATACG-3'	PrMPK8-5R2
PrMPK8_5RACE1	5'-AAATATCTTTAAATTCTCTCCTAGATC-3'	PrMPK8-5R3
MPK9Bgen5'	5'-GAATCAAGGAAACAAGAAGAGAAGAAG-3'	PrMPK91gen5'
PrMPK8gen3'	5'-GTAGTTATCTGCCGACTTTCTGG-3'	PrMPK8gen3'

MPKB5'int	5'-TTTGTATCAGATACTCCGTGGATTG-3'	PrMPKB-5'1
MAPKBd/s	5'-GTGGTTGATGATGAACACCAAATC-3'	PrMPKB-3'1
JPrMPKB_5'int	5'-GCGACCCTAAGCCATGGTGGC-3'	PrMPKB-5'2
JPrMPKB_3'int	5'-GGTGCACATGATCTCGACCGGG-3'	PrMPKB-3'2
MPKC5'int	5'-GGATTGGCTCGCACCTGTAGC-3'	PrMPKC-5'1
MAPKCd/s	5'-CGAGAACAGGATCATAATTACCC-3'	PrMPKC-3'1
JPrMPKC_5'int	5'-GTGGCAAACGGTGTGAGATTG-3'	PrMPKC-5'2
JPrMPKC_3'int	5'-GGGAAGATGGGTTTTCGCCC-3'	PrMPKC-3'2
PrMPK9B5'NdeI	5'-ATTCATATGGGCGAGACGGAATTTTTCAC-3'	PrMPK9-1_5'NdeI
PrMPK9B3'XhoI	5'-AATCTCGAGGGAACCTAGTTGAGAAATCTTC-3'	PrMPK9-1_3'XhoI
PrMPK9B5'intNdeI	5'-ATTCATATGGGTGAGAAAAGCACTCCTCC-3'	PrMPK9-1C_5'NdeI
MPK9BPP5'HindIII	5'-ATTAAGCTTGGTGAGAAAAGCACTCCTCC-3'	PrMPK9-1PP5'HindIII
MPK9BPP3'NotI	5'-AATGCGCCGCTCAGGAACCTAGTTGAGAAATCTT-3'	PrMPK9-1PP3'NotI
MPK8T-DNAu/s	5'-CTTGGTACTCCACCTCCTGAGTC-3'	MPK8TDNAu/s
MPK8T-DNAd/s	5'-CATGATCTTTAACTAACTTCTTCTCTC-3'	MPK8TDNAd/s
MPK9TDNAu/s	5'-GCACTGGAGACTGAGTTCTTTAC-3'	MPK9TDNAu/s
MPK9TDNAd/s	5'-CACTGAGTATGGTGATGCTAATCG-3'	MPK9TDNAd/s
MPK17T-DNAu/s2	5'-GACTACGTTGCTACAAGATGGTAC-3'	MPK17TDNAu/s2
MPK17T-DNAd/s	5'-CAAACGCTGAAGTAACCTCAGCG-3'	MPK17TDNAd/s
MPK20TDNAu/s2	5'-CTGGAGATGGAGTTCTTTTCTGAC-3'	MPK20TDNAu/s2

For mixed base sites: N = A, G, C, T; V = G, A, C; D = G, A, T; B = G, T, C; H = A, T, C; W = A, T; M = A, C; R = A, G; K = G, T; S = G, C; Y = C, T.

iii.i) Leaf mRNA and genomic sequences of *PrMPK3*. Start and stop codons are shown in green and red, respectively. In the genomic DNA sequence exons are indicated in grey.

>PrMPK3 leaf mRNA

```

GGGGGGGGGGGGGGGGTGGTATACAATTTGTCTAAAGAGAGACTGTGAAGAGATAATTTTGTGGTTTTCATCTT
CAATAGCTTTAATGCGAGATATTCCTCAAAAACCCAGATAACGCTAATAACCCACCAGCTGATTTTCCAGCAATTT
TAACTCATGGAGGTCGATTTGTTCAGTATAATATCTTTGGTAATTTGTTTGAGATCACTATCAAATATCGTCCCTC
CGATTATGCCCATCGGTCGTGGTGCTTATGGAATCGTATGTTCTGTGTTGAATTCAGAGACAAATGAAATGGTTG
CGATTAAGAAGATTGCTAATGCATTTGACAATTACATGGATGCTAAAAGAACTCTAAGAGAGATTAAGTTCTTTC
AGCATTGGACCATGAGAATGTTATTGGTATTAGAGATGTCATTCCACCACCAATACCAGGAGCATTTTCTGATG
TTTATATAGCCACTGAACTCATGGACAGTGACCTCCATCAAATAAATTCGCTCTAACCAAGGTTTATCGGAGGAAC
ACAGCCAGTATTTCTTGTACCAGATTTCTTCGTGGTTTGAAGTATATTCATTCGCCAATGTTATTCATAGGGATT
TAAAACCGAGCAACCTTTTGTAAATGCAAACCTGTGACTTAAAGATTTGTGATTTTGGTTTGGCTCGCCCTACTT
CGGAAAATGAATTTATGACCGAGTATGTTGTCAC TAGATGGTATAGAGCACCAGAGTTGTTGCTCAATTCCTCAG
ATTATACTGCTGCAATTGATGTGTGGTCAGTGGGATGTATCTTTATGGAGCTGATGAATAGGAGACCACATTTTG
CGGGTAGGGATCATGTACATCAGCTGCGGTTACTTACTGAGCTCCTCGGCACACCTACTGAAGCTGATCTAGGTT
TTGTTCCGGAGTGATGATGCAAGAAGGTATCTCCAACAGCTACCACCACATCCTCGCCAACCTTTTGAATGGTTT
TCCCACACGTTAACCCTGTTGCCATTGATCTCATTGAAAAAATGTTGACATTTGACCCTACAAGAAGAATCACAG
TTGAAGAAGCTTTGGCTCATCCTTACCTGAAAGGTTGCACGATATAGCCGATGAACCAGTTTGTTCAGTCCCTT
TCTCTTTTGAATTTGAACAACAAGTCCCTCACAGAAGAGCAGATAAAGGAGATGATATACAGAGAATCCGTGGCAT
TTAATCCAGAGTACTTGCATAGCTAAATCTGTTTTGTTTGGAGCATTGTTAATGACTATTAATTCATGTGGTGCA
AATGATTCATTGATATATAATATGCAACCAGTTGAAGAAAACACCATCAAATGAAGTATCTAAACGAATTTTCT
ATTTCCATTGATTTCTTTTCTGTAAGATCTTTTAGATGAGATCCTCTTTGGTGATCGGGAACCTTCTGATAGTTG
ATTTTATTATGACATTTTGTGATGTTGATGTAATACTGGCTGCCTGAGCCTGTTACCTAGAGTAAATATGTTTCA
TTGTATTCCCTTTGATTCTTAAATAAATTTCTCTGGCAAAAAAAAAAAAAAAAAAAAAAAAAAAAAAAAAAAAAA

```

>PrMPK3 genomic DNA

```

ATGCGAGATATTCCTCAAAAACCCAGATAACGCTAATAACCCACCAGCTGATTTTCCAGCAATTTTAACTCATGGA
GGTTCGATTTGTTTCAGTATAATATCTTCGGTAATTTGTTTGGAGATCACTATCAAATATCGTCCCTCCGATTATGCC
ATCGGTCGTGGTGCTTATGGAATCGTATGTAATTTTTCATATCTTGATTAGCACC AATGATTCTGTGATATTC
TCTTTTTTTTTTTTTGTTTAAATTGAGTTGACTTTAATAATTTAATTTTGTGGTTTTAGTTCTGTGTTGA
ATTTCAGAGACAAATGAAATGGTTGCGATTAAGAAGATTGCTAATGCATTTGACAATTACATGGATGCTAAAAGAA
CTCTAAGAGAGATTAAGTTCTTTCAGCATTTGGACCATGAGAAATGATGCTATTAATCTTAACTTCTTTTTTTT
TTTTTTTTTAATCAAACCTTGGTATGTTATTTTTCTCTGCTGATTTTGAATGNGTGGAGATAAATTTGTTAATTTAC
TAAGAATTTGAGCTTATCTTTAGCTTCAATAATTTATTGTTATAACAATTACNTATTTTAAATTTTGTGG
ATGAAGTAAACACAAATCTGAAATGGGGTTTTGAAGAAGTCAATTTTGGTCTCTGGTTTTATAATCTGTTGTGTT
CCATTTGTATCTGTGCGGTGGACTTGGGTAGGACTTCAGCGAGGAAACACTATCTATTCGCAATTCCTAATTTGGC
GCACAAAAATTTGCACAATTTAAACTGGGCATTACTTTTCTCAAGAAATCAAGTGAACCTCAAATTTGTAATAGAG
GCAACTAGATTGAACTCAAATTTGCAATGGAGGCAACTAGATTTTTCTGTTCCATCAACATAGGTGTTTTTTGTT
TACCGTACAAGAACATAATCTATTTCTCATATTTGGATTCTACAATTTGAGTGCACTTTTTTCAGCATTAATGACAA
GTGTGAATTTAGAACTTTTCTTGGGAAATAACTTTCTTTGTAGTTTCTGTATCTGAGTAGACAGCAATGAGCTCC
CTGCAAACTGAATTTTCTTCTTGGTTTTGGTATATGAAATGAGATGCTTGTGGACAACTCACATCAAATAAAG
GGCTAAGCTGAACATTTTCTTCTACATGCGGATGCTTGTGCAATTTAACTAGGGTTGAATTTTGTGTATGTTAAA
CAGGTTATTGGTATTAGAGATGTCATTCACCACCAATACCAGGAGCATTTTCTGATGTTTATATAGCCACTGAA
CTCATGGACAGTGACCTCCATCAAATAAATTCGCTCTAACCAAGGTTTATCGGAGGAACACAGCCAGGTAAC TGAC
AGCTTCTATCCCCTTTTATAATAATAAAAAACCTATGACTTTTTTGAACCTGTTTTGGTAGTTAATAGGCTAATA
CCTAATATTTGTTTCTTCTTCGATTTGTTGTGTCAGTATTTCTTGTACCAGATTCCTTCGTGGTTTGAAGTGTATTC
ATTCCGCCAATGTTATTCATAGGGATTTAAAACCGAGCAACCTTTTGTCAAATGCAAACCTGTGACTTAAAGATTT
GTGGTTTTGGTTTGGCTCGCCCTACTTCGAAAAATGAATTTATGACCGAGTATGTTGTCACTAGATGGTATAGAG
CACCAGATGTTGTGACTCAATTTCTCAGATTATACTAGGATGCAATGATGTGTGGTCAGTGGGATGTATCTTTATGG
AGCTGATGAATAGGACCACTATTTGCGGGTAGGCTCATGTACATCAGCTGCGGTTACTTACTGAGGTAAGAT
GATAAGTTGTACCATATGAACTTGTAGTTTCAGGGTCAATCAATTTCTTTTGGTGTTCACAAAGGGTATCTTA
CACATGGTTATTGACACTGTAGCTCCTCGGCACACCTACTGAAGCTGATCTAGGTTTTTGTTCGGAGTGATGATGC
AAGAAGGTATCTCCAACAGCTACCACCACATCCTCGCCAACCTTTTGAATGGTTTTCCACACGTTAACCCCTGT
TGCCATTGATCTCATTTGAAAAAATGTTGACATTTGACCTTACAAGAAGAATCACAGGTACATTTATTCATGCCTC

```

AGTCATCCATTTTTACCAGTGTTATCTTTCAACCCTGAACACAATATTCAGTATATGACTTCCTTATTGCCTGTG
TATGTATGTATATTTAAGATTGACTAGTTTCGTCCTTAATATCACCTCTCTCTTCCCTACTAGAACTCCCTAAGAT
TCTTCCCAATTGTTAGTATATTTATCGAGCCTTATTATTATAGTCATTATTATTTTCCAAATAAACTCTTATCTA
TATTTGGATTGGGTAATCATGATCCCTCACTCAGTTTAAAGCCACAGCTACGAGTTTGGTCCCTGAAAAAAGATT
TTTCTCTCTTATTAGACCAGCTATTTTGCTAATACGTCCTATTTAACTGGGAGAGTTCTAAAGTGAACCTATTGAT
GTCCATGGGACTGATTGGATATGTAACCTATATATATATATATAGAACTCTGNTCCCATAGGGTAATCTGTCTTA
GGAAGAGACAGAATTAGAAAATCTGTGGTCTAAGTGGGAAGCACTCCTAAACTCTAACCATTTGATCAGTTAAAAAT
TTAAAAAATCNAATTTTTTNCCCCGGCTTAAAACCATATAAGGGACNATNGCTGTNCNGTNTGACAGAATGGNTC
AANCTGGAGTTAAGTGTCCCTGTTGAACCTGTGGNTGTGAAACACAATCGAGANAAAATTACGGCATATTTAAGG
TGCAGGCTGTGCTTGAGGTATTTTGGTAAGAGCGTGCAGACTTGGAATATTCTCGACGCCATNATCTTCTTTTT
AGCAGCCATTTGAAGCTTTCAATGGATTTTTTTTTTTTTTTTTTCTTTTTTCTCAGTCTACCATGTTTGGGCCCCA
TTTGATATATGATCAAACAATTGTGATTGTGGTCCCTGTGGAGGTTAAATGCCAAATGATGCCACACTATTTCCC
AACAGAAGCACTTGGTCTTCTTGTACAACCTATCTTTTATGTCATACCGTGCATCATGTCATACTTAAGTCTTATG
GAAAACCCCTTTCTGGTTTCAACTTGGGGCACTTCTTAATTTTCATTATGAATATTGAAAATGTATTTTCATGGAT
GCAGTTGAAGAAGCTTTGGCTCATCCTTACCTTGAAAGGTTGCACGATATAGCCGATGAACCAGTTTGTTTCAGTC
CCTTTCTCTTTTGAATTTGAACAACAAGTCCTCACAGAAGAGCAGATAAAGGAGATGATATACAGAGAATCCGTG
GCATTTAATCCAGAGTACTTGCATAGGTA

iv.i Sequest search raw data. 'Arabidopsis/Brassica' database.

Reference Scan(s)	Peptide	MH+	z	P (pro) P (pep)	Score XC	Coverage DeltaCn	MW Sp	Accession RSp	Peptide (Hits) Ions	Count
SL1 gi 23296853 gb AAN13187.1 putative mitogen-activated protein kinase [Arabidopsis thaliana]				1	18.15		66190.5	23296853	2 (1 1 0 0 0)	
1411	K.INDVFEHVSDATR.I	1502.72340	3	1	2.98	0.21	374.9	1	16/48	5
1629	K.LEFDFER.K	955.45197	2	1	0.99	0.43	99.8	2	5/12	2
gi 7106542 dbj BAA92222.1 ATMPK8 [Arabidopsis thaliana] [MASS=61513]				1	18.15		61475.4	7106542	2 (1 1 0 0 0)	
1411	K.INDVFEHVSDATR.I	1502.72340	3	1	2.98	0.21	374.9	1	16/48	5
1629	K.LEFDFER.K	955.45197	2	1	0.99	0.43	99.8	2	5/12	2
gi 53850802 gb AAU95462.1 mitogen-activated protein kinase 9 [Brassica napus]				1	10.15		57391.5	53850802	1 (1 0 0 0 0)	
1411	K.INDVFEHVSDATR.I	1502.72340	3	1	2.98	0.21	374.9	1	16/48	5
gi 18401750 ref NP_566595.1 mitogen-activated protein kinase, putative / MAPK, putative (MPK9) [Ar				1	10.15		58358.1	18401750	1 (1 0 0 0 0)	
1411	K.INDVFEHVSDATR.I	1502.72340	3	1	2.98	0.21	374.9	1	16/48	5
gi 9294059 dbj BAB02016.1 MAP kinase [Arabidopsis thaliana]				1	10.15		70727.0	9294059	1 (1 0 0 0 0)	
1411	K.INDVFEHVSDATR.I	1502.72340	3	1	2.98	0.21	374.9	1	16/48	5
gi 1255448 dbj BAA09057.1 mitogen-activated protein kinase [Arabidopsis thaliana]				1	10.06		65939.5	1255448	1 (1 0 0 0 0)	
1301	K.FNDIKSCK.G	1012.47683	2	1	1.12	0.10	61.3	1	6/14	2
gi 20466652 gb AAM20643.1 MAP kinase, putative [Arabidopsis thaliana]				1	8.06		108091.7	20466652	1 (0 1 0 0 0)	
2333	K.NWVVKVCDFLSR.M	1580.78899	2	1	1.15	0.10	14.4	20	3/24	9
gi 12324206 gb AAG52072.1 putative MAP kinase; 28156-31112 [Arabidopsis thaliana]				1	8.12		65210.6	12324206	1 (0 1 0 0 0)	
1411	K.INDVFDHISDATR.I	1502.72340	3	1	2.36	0.47	207.6	2	12/48	1
gi 18410420 ref NP_565070.1 mitogen-activated protein kinase, putative / MAPK, putative (MPK15) [A				1	8.12		49394.9	18410420	1 (0 1 0 0 0)	
1411	K.INDVFDHISDATR.I	1502.72340	3	1	2.36	0.47	207.6	2	12/48	1
SL2 gi 9294059 dbj BAB02016.1 MAP kinase [Arabidopsis thaliana]				1	28.13		70727.0	9294059	5 (3 2 0 0 0)	
1055	K.GSYGVVASAIDTHSGEK.V	1677.80785	3	1	2.59	0.38	150.1	1	12/64	1
1158	R.NGTSQTGYSAR.S	1141.52324	2	1	1.58	0.14	16.3	31	3/20	2
1273	R.LLAFDPK.D	803.46617	2	1	2.18	0.00	322.0	1	8/12	12
1278	R.LLAFDPK.D	803.46617	2	1	2.28	0.14	405.2	1	9/12	12
1289	R.LLAFDPK.D	803.46617	2	1	1.83	0.00	335.1	1	8/12	12
gi 18401750 ref NP_566595.1 mitogen-activated protein kinase, putative / MAPK, putative (MPK9) [Ar				1	28.13		58358.1	18401750	5 (3 2 0 0 0)	
1055	K.GSYGVVASAIDTHSGEK.V	1677.80785	3	1	2.59	0.38	150.1	1	12/64	1
1158	R.NGTSQTGYSAR.S	1141.52324	2	1	1.58	0.14	16.3	31	3/20	2
1273	R.LLAFDPK.D	803.46617	2	1	2.18	0.00	322.0	1	8/12	12
1278	R.LLAFDPK.D	803.46617	2	1	2.28	0.14	405.2	1	9/12	12
1289	R.LLAFDPK.D	803.46617	2	1	1.83	0.00	335.1	1	8/12	12
gi 23296853 gb AAN13187.1 putative mitogen-activated protein kinase [Arabidopsis thaliana]				1	18.11		66190.5	23296853	6 (2 3 1 0 0)	
1273	R.LLAFDPK.D	803.46617	2	1	2.18	0.00	322.0	1	8/12	12
1278	R.LLAFDPK.D	803.46617	2	1	2.28	0.14	405.2	1	9/12	12
1289	R.LLAFDPK.D	803.46617	2	1	1.83	0.00	335.1	1	8/12	12
1480	K.LEFDFER.K	955.45197	2	1	0.98	0.42	91.7	2	5/12	2
1755	K.LEFDFER.K	955.45197	2	1	1.61	0.18	195.8	1	7/12	2
2011	K.LEFDFER.K	955.45197	2	1	1.43	0.22	54.1	10	4/12	2
gi 42572471 ref NP_974331.1 mitogen-activated protein kinase, putative / MAPK, putative (MPK9) [Ar				1	18.11		48366.7	42572471	4 (2 2 0 0 0)	

1158		R.NGTSQTGYSAR.S	1141.52324	2	1	1.58	0.14	16.3	31	3/20	2
1273		R.LLAFDPK.D	803.46617	2	1	2.18	0.00	322.0	1	8/12	12
1278		R.LLAFDPK.D	803.46617	2	1	2.28	0.14	405.2	1	9/12	12
1289		R.LLAFDPK.D	803.46617	2	1	1.83	0.00	335.1	1	8/12	12
gi 7106542 dbj BAA92222.1 ATMPK8 [Arabidopsis thaliana] [MASS=61513]											
116		K.LEFDFER.K	955.45197	2	1	0.99	0.30	30.3	4	4/12	2
285		K.LEFDFER.K	955.45197	2	1	0.88	0.42	59.2	4	4/12	2
1273		R.LLAFDPK.D	803.46617	2	1	2.18	0.00	322.0	1	8/12	12
1278		R.LLAFDPK.D	803.46617	2	1	2.28	0.14	405.2	1	9/12	12
1289		R.LLAFDPK.D	803.46617	2	1	1.83	0.00	335.1	1	8/12	12
1480		K.LEFDFER.K	955.45197	2	1	0.98	0.42	91.7	2	5/12	2
1755		K.LEFDFER.K	955.45197	2	1	1.61	0.18	195.8	1	7/12	2
2011		K.LEFDFER.K	955.45197	2	1	1.43	0.22	54.1	10	4/12	2
gi 7106544 dbj BAA92223.1 ATMPK9 [Arabidopsis thaliana]											
1273		R.LLAFDPK.D	803.46617	2	1	2.18	0.00	322.0	1	8/12	12
1278		R.LLAFDPK.D	803.46617	2	1	2.28	0.14	405.2	1	9/12	12
1289		R.LLAFDPK.D	803.46617	2	1	1.83	0.00	335.1	1	8/12	12
gi 15231915 ref NP_188090.1 mitogen-activated protein kinase, putative / MAPK, putative (MPK19) [A]											
1273		R.LLAFDPK.D	803.46617	2	1	2.18	0.00	322.0	1	8/12	12
1278		R.LLAFDPK.D	803.46617	2	1	2.28	0.14	405.2	1	9/12	12
1289		R.LLAFDPK.D	803.46617	2	1	1.83	0.00	335.1	1	8/12	12
gi 25408817 pir D84859 probable MAP kinase [imported] - Arabidopsis thaliana											
1273		R.LLAFDPK.D	803.46617	2	1	2.18	0.00	322.0	1	8/12	12
1278		R.LLAFDPK.D	803.46617	2	1	2.28	0.14	405.2	1	9/12	12
1289		R.LLAFDPK.D	803.46617	2	1	1.83	0.00	335.1	1	8/12	12
gi 9294393 dbj BAB02403.1 mitogen-activated protein kinase [Arabidopsis thaliana]											
1273		R.LLAFDPK.D	803.46617	2	1	2.18	0.00	322.0	1	8/12	12
1278		R.LLAFDPK.D	803.46617	2	1	2.28	0.14	405.2	1	9/12	12
1289		R.LLAFDPK.D	803.46617	2	1	1.83	0.00	335.1	1	8/12	12
gi 24030176 gb AAN41270.1 putative MAP kinase ATMPK9 [Arabidopsis thaliana]											
1273		R.LLAFDPK.D	803.46617	2	1	2.18	0.00	322.0	1	8/12	12
1278		R.LLAFDPK.D	803.46617	2	1	2.28	0.14	405.2	1	9/12	12
1289		R.LLAFDPK.D	803.46617	2	1	1.83	0.00	335.1	1	8/12	12
gi 53850802 gb AAU95462.1 mitogen-activated protein kinase 9 [Brassica napus]											
1273		R.LLAFDPK.D	803.46617	2	1	2.18	0.00	322.0	1	8/12	12
1278		R.LLAFDPK.D	803.46617	2	1	2.28	0.14	405.2	1	9/12	12
1289		R.LLAFDPK.D	803.46617	2	1	1.83	0.00	335.1	1	8/12	12
gi 3785991 gb AAC67338.1 putative MAP kinase [Arabidopsis thaliana]											
1273		R.LIAFDPK.D	803.46617	2	1	2.18	0.11	322.0	1	8/12	3
1278		R.LIAFDPK.D	803.46617	2	1	2.28	0.00	405.2	1	9/12	3
1289		R.LIAFDPK.D	803.46617	2	1	1.83	0.13	335.1	1	8/12	3
gi 18410420 ref NP_565070.1 mitogen-activated protein kinase, putative / MAPK, putative (MPK15) [A]											
1273		R.LIAFDPK.D	803.46617	2	1	2.18	0.11	322.0	1	8/12	3
1278		R.LIAFDPK.D	803.46617	2	1	2.28	0.00	405.2	1	9/12	3
1289		R.LIAFDPK.D	803.46617	2	1	1.83	0.13	335.1	1	8/12	3
gi 12324206 gb AAG52072.1 putative MAP kinase; 28156-31112 [Arabidopsis thaliana]											
1273		R.LIAFDPK.D	803.46617	2	1	2.18	0.11	322.0	1	8/12	3
1278		R.LIAFDPK.D	803.46617	2	1	2.28	0.00	405.2	1	9/12	3

iv.i Sequest search raw data. 'Plant' database.

Reference Scan(s), File Old	Peptide	MH+	DeltaM	z	Type	P (pro) P (pep)	Score XC	Coverage DeltaCn	MW Sp	Accession RSp	Peptide (Hits) Ions	Count
MPK8_ORYSA Mitogen-activated protein kinase 8 (MAP kinase 8) (OsWJUMK1) (Wound- and JA-uninducible MAP kinase 1)						1.00000	14.06		65137.52	108860806.0	3 (0 1 2 0 0)	
444,	-IHNIFEHLSDAAR.-	1522.776123047	-0.01973	2	CID	1.00000	0.90	0.06	86.26	9.0	45413	7
445,	-IHNIFEHLSDAAR.-	1522.776123047	-0.01973	2	CID	1.00000	1.27	0.13	94.94	6.0	45413	7
2394,	-VSTVQYGVSR.-	1095.579345703	-0.01082	2	CID	0.99952	0.73	0.10	73.92	80.0	43252	3
putative mitogen activated protein kinase [Oryza sativa (japonica cultivar-group)]						1.00000	10.06		48729.50	55297327.0	2 (1 1 0 0 0)	
444,	-IHNIFEHISDAAR.-	1522.776123047	-0.01973	2	CID	1.00000	0.90	0.02	86.26	9.0	45413	2
445,	-IHNIFEHISDAAR.-	1522.776123047	-0.01973	2	CID	1.00000	1.27	0.00	94.94	6.0	45413	2
MAPK [Zea mays]						1.00000	8.07		16255.59	39599008.0	1 (0 1 0 0 0)	
4832,	-KKIANVFDNRVDALR.-	1758.997314453	-0.00178	2	CID	1.00000	1.37	0.07	42.42	108.0	46874	
SL1						1.00000	10.10		68352.18		1 (1 0 0 0 0)	
Populus trichocarpus MPK9-2	.RTNHNHNDHINNINKTTSSN	4175.002929688	-0.06373	6	CID	1.00000	1.95	0.17	354.71	2.0	38/370	
2098,	VSSSGCPQSSVNVKEGIK.-					1.00000	10.09		70726.97	9294059.0	1 (1 0 0 0 0)	
MAP kinase [Arabidopsis thaliana]						1.00000	1.88	0.05	331.49	1.0	11994	1
1095,	K.GSYGVVASAIDTHSGEK.V	1677.807861328	0.00444	2	CID	1.00000	10.07		57391.54	53850802.0	1 (1 0 0 0 0)	
mitogen-activated protein kinase 9 [Brassica napus]						1.00000	1.37	0.10	151.20	4.0	14946	4
763,	-QFAHLEEHYGK.-	1358.648803711	0.00547	3	CID	1.00000	10.06		57017.39		1 (1 0 0 0 0)	
Populus trichocarpus MPK17						1.00000	1.26	0.02	236.31	7.0	13485	
721,	-YIHTGNVFHR.-	1243.633056641	-0.00830	3	CID	1.00000	10.05		64628.35	75322461.0	1 (1 0 0 0 0)	
MPK7_ORYSA Mitogen-activated protein kinase 7 (MAP kinase 7) (OsMAPK6) (MAP kinase 6)						1.00000	1.02	0.01	134.94	16.0	44044	2
736,	-QFAILEENGGK.-	1205.616088867	-0.01265	2	CID	1.00000	8.09		67030.27		1 (0 1 0 0 0)	
Populus trichocarpus MPK9-1						1.00000	1.79	0.16	258.75	3.0	11994	
1095,	-GSYGVVGS AIDTHTGK.-	1677.807861328	0.00444	2	CID	1.00000	8.06		42353.83	457406.0	1 (0 1 0 0 0)	
MAP kinase [Arabidopsis thaliana]						1.00000	1.16	0.12	170.23	2.0	41852	99
1395,	-ICDFGLAR.-	951.4716796875	0.00078	2	CID	0.99578	8.05		151082.20	15231270.0	1 (0 1 0 0 0)	
SL2						0.99578	8.05		151082.20	15231270.0	1 (0 1 0 0 0)	
MAPKKK7; ATP binding / kinase/ protein kinase/ protein serine/threonine kinase/ protein-tyrosine kinase [Arabidopsis thaliana]						0.99578	1.00	0.11	29.67	142.0	44652	1
2093,	-GKENGSLDTTTR.-	1278.628417969	0.01885	2	CID	0.99993	10.05		64628.35	75322461.0	1 (1 0 0 0 0)	
MPK7_ORYSA Mitogen-activated protein kinase 7 (MAP kinase 7) (OsMAPK6) (MAP kinase 6)						0.99993	1.04	0.05	54.87	160.0	43983	2
753,	-QFAILEENGGK.-	1205.616088867	-0.01692	2	CID	1.00000	10.11		61475.37	7106542.0	2 (2 0 0 0 0)	
SL3						1.00000	1.46	0.08	188.00	1.0	13/48	16
ATMPK8 [Arabidopsis thaliana]	K.INDVFEHVSDATR.I	1502.723388672	0.00568	3	CID	1.00000	2.23	0.02	208.79	1.0	45597	16
1437,	K.INDVFEHVSDATR.I	1502.723388672	0.00859	2	CID	1.00000	10.10		67030.27		2 (1 1 0 0 0)	
1454,						1.00000	1.89	0.09	62.42	12.0	11871	
Populus trichocarpus MPK9-1						1.00000	1.91	0.36	151.38	2.0	11963	
1100,	-GSYGVVGS AIDTHTGK.-	1677.807861328	0.01067	2	CID	1.00000	8.11		70726.97	9294059.0	2 (1 1 0 0 0)	
1117,	-GSYGVVGS AIDTHTGK.-	1677.807861328	0.00603	2	CID	1.00000	1.73	0.34	140.46	1.0	11933	1
MAP kinase [Arabidopsis thaliana]						1.00000	2.22	0.14	237.04	1.0	11994	1
1100,	K.GSYGVVASAIDTHSGEK.V	1677.807861328	0.01067	2	CID	1.00000	8.11		49394.88	18410420.0	2 (0 2 0 0 0)	
1117,	K.GSYGVVASAIDTHSGEK.V	1677.807861328	0.00603	2	CID	1.00000	8.11		49394.88	18410420.0	2 (0 2 0 0 0)	
ATMPK15; MAP kinase/ kinase [Arabidopsis thaliana]						1.00000	8.11		49394.88	18410420.0	2 (0 2 0 0 0)	

1437,	-.INDVFDHISDATR.-	1502.723388672	0.00568	3	CID	1.00000	1.34	0.16	131.60	3.0	17838	1
1454,	-.INDVFDHISDATR.-	1502.723388672	0.00859	2	CID	1.00000	2.19	0.32	116.45	4.0	45536	1
putative mitogen-activated protein kinase [Oryza sativa (japonica cultivar-group)]						1.00000	8.05		66317.93	47900280.0	1 (0 1 0 0 0)	
1371,	-.GEKSSPQLR.-	1001.537414551	-0.00868	2	CID	1.00000	1.04	0.09	74.41	56.0	42522	3

iv.ii sequest search values (Bioworks, Xcalibur[®])

Scan(s):	Displays the scan number; double clicking the scan number displays the scan data for the peptide.
Peptide:	Displays the peptide sequences.
MH+:	Displays the molecular weight of the peptides.
z:	Displays the charge state of the peptide.
Type:	Displays the activation type.
P (pep):	Displays the probability value for the peptide only if the unified search file was loaded.
Sf:	Displays the final score (Sf) that indicates how good the peptide match is; its S is calculated using the XCorr, ΔCn , Sp, and RSp values, the peptide mass, the charge state, and the number of matched peptides for the search.
XC:	Displays the cross-correlation value between the observed peptide fragment mass spectrum and the one theoretically predicted. For more information on XC, see An Approach to Correlate Tandem Mass Spectral Data of Peptides with Amino Acid Sequences in a Protein Database; Eng, J.K., McCormick, A.L., and Yates, J.R., III; (1994) J. Am. Soc. Mass Spectrometry 5, 976-989.
ΔCn :	Displays the change in cross-correlation between the first and the n th peptide match, where n is the peptide hit number for which ΔCn is calculated. The equation used to calculate Cn for the nth hit is $\Delta Cn = (XC_{corr1} - XC_{corn}) / XC_{corr1}$, where XC_{corr1} is the XCorr of the first hit and XC_{corn} is the XCorr of the nth hit. For example, to calculate ΔCn for a fourth hit, you would use the XCorr value for the first hit and the XCorr value for the fourth hit in the equation.
Sp:	Displays the percent of peptide fragment ions in an MS/MS spectrum that match with the experimental data; Sp is a preliminary score.
RSp:	Displays the ranking of the particular match during the preliminary scoring (Sp).
Ions:	Displays the ion value for the peptide calculated by dividing the number of matched ions by the total number of ions value; or how many of the experimental ions matched with the theoretical ions.

Count: Displays number of duplicate entries found for each .dta file.

v.i) Pollen mRNA and genomic sequence of PrMPK20. Start and stop codons are shown in green and red, respectively. In the genomic DNA sequence exons are indicated in grey.

>PrMPK20 pollen mRNA

```

GGGGGGGGGGGGGGGGTTATCTGGTCTAGACCGAAATTTAAAAGCTGTAAAGTTTGCCTTTTTGTTCAGTTG
ATTCTAAGCTAATTCTATTGCAACAATTTGAAGGAATTCCTTGTACTTATTGTCATTAATTATTATCGGCAATC
GAAGTAGCAAGATTTTTTTGTTTTTGTATCCTCAGTAGATGTGTTATCACTTTAGGAAGTGATTTGTCCGTGGCCT
CTAAACTTGGCTGATGTTACTGCATTCGAATGAATGGAGGACATTAAGCATGGCAGGATTGTGTCTGTTCAAAGA
TAAGTGAGAGAAAGCAAAAAAAAAAGCATTAGAGGATTTATTGCGACAAATATCTTGTTCAGACATTTCTGT
GCGTATTTGGTAGTCTTGCAGTAGAATAACATAAGTCCTTTCAGAAATAAAGGAACGCTGTAGGATTTCTCCG
GTTCACTTTAGTTGGTCTGTTTTCTGCTGTTGCTTCATTTCTCTCCCTTTTAAGAAATCATAATCCAGTTTTT
TCTTCTTTCAGAGTACCACGGAGATGATTTCTTCACTGATTATGGTGATGCCAACAGATAACAAGATAACAAGAG
GTTGTAGGTAAAGGAAGCTATGGTGTGTTGTGCTCAGCTATTGACACTCATAACAGGAGAGAAAGTGGCAATAAAG
AAGATACATGATATTTTTGAGCATATCTCGGATGCTGCAAGGATACGCGTGAAATAAAGCTTCTCAGGCTCCTA
CGGCATCTGACATTGTCGAAATAAAGCACATCATGTTGCCACCCTCAAGAAGGGATTTAAGGATATTTATGTC
GTATTCGAACTTATGGAGTCAGATCTTCATCAAGTCATTAAGCTAATGATGACTTGACCAAAGACCCTATCAG
TTTTTTCTTTATCAGCTTCTGCGCGCATTTGAAGTATATCCACACAGCAAATGTATTTTCATCGGGATTTAAAACCA
AAGAATATATTTGGCAAATGCGAATTTGAAACTTAAAATATGTGACTTCGGCCTTGCAAGAGTGGCATTCAATGAT
ACCCCAACAACGATATTTGGACGGATTATGTTGCTACGAGATGGTATAGAGCTCCGGAAGTGTGTGGATCGTTT
TTCTCTAAGTATACTCCAGCGATAGATATTTGGAGTATCGGTTGCATATTTGCCGAAGTATTAACAGGGAAGCCT
CTATTTCTGGTAAAAATGTTGTTTCATCAGCTGGATTTGATGACTGACCTGCTTGGTACGCCGTCTGTTGGTATACC
ATTTCTCGGTCGCAATGAGAAAGCCAGGAAATACCTTACCAGCATGAGGAAGAAGCAGCCGGTCTGTTTCGCA
CAGAAGTTCGCCAAGTCCAGATCCATTTGCTGTCAAACCTTTTAGAAAGGCTCTTAGCGTTTGATCCGAAGGATAGA
CCAAGTGCAGGAGAGGCATTGGCTGATCCATACTTTAAAAGCTTGTCAAGGGCAGAGAGGGAACCATCTTGCCAG
CCAATCACCAAGCTAGAGTTTGAGTTTGAGAGGCGGCGGGTTACTAAGGACGACATTAAGGAGCTTATTTTTAGG
GAGATACTAGAATATCATCCACAGCTGCTCAAAGACTACATCAGTGGAGCTGAAAGAACAACTTTCTATACCCT
AGTGCTGTTGATCAGTTCCGGAAGCAGTTTGCACACCTCGAGGATAATGGTGGTAAAAGTGGCCCTGTCAATCCA
CTCGAGAGGAAGCATGTTCACTGCCAAGATCTACCATTGTCCATTCAAATACCATCCCTCCCAAGGAGCAGCCT
GATCTATCCAGAGAGCGGCAAATTCAGATACTGGTTATTACAAGAATCCGAGAGATGCAAATGGAATTTCAAGGA
AGCTTGCCAGGATTCAACCAGTAGCACAACAACGAACTCCATGGCTAAACCTGGAAAAGTTCGGGGACCTGTT
GTGCCATATGAGAACACTAGCGGTATTAGAGATGCGTATGATCCAAGAACGTACATCAGGAATGCAGTTCTTCCCT
CCTCAGCCTATCCCTTCTCCCTACGGTATCCGCAGAACTAATGTGATGGTTAATCAAGAAAAATCAGGAAGTGAA
ATTGAGAGAGATTTATCACTAGCCAGACAATCGCAGCTTTCACAATGCAACATGATGGCCAAATTTGGCCCCAGAT
GTAGCAATTGACATAAACTCTTCCAGTTTTTATCTAGCACGTGCAGGTGTGACATCAAAGATAGATCAGACTGAT
AATAATAATCAAATTTGCGATTGATACGAATCTGCTACAAGCAAAGTCCCAGTTTGGTGAAATGGGTGTTGCTGCT
GCTGCAGCTGCGGCTGCTCGTAGAAAAGGTAAGCACGGTTTACGTACGGTATGCTTAGGATGTACTAGGAGAAGTTG
TTTATAGGAGGAAAGAAAATCAAAAACGGGAGTAGTACTTGAAGGAGTTTCTACTTTGTACAACAGAGAAGAAGGT
TAAGTTTACTTGAACAAGAGAGATAAAGTGTAGGAAGAAGTGCCAATGATGATGGTTTTGTAAACGTTTCTTGTG
GTAAGATTCAGCTCCATGCATGTTTGTGATGGTGGTTTTCTATGTTTGTCTCACTGTAAAAGCAGAATAAACTAAT
TGATCTCAGTAAAAATTATACGGTTTTATAT

```

>PrMPK20 genomic DNA

```

ATG GATTTCTTCACTGATTATGGTGATGCCAACAGATAACAAGATAACAAGAGTTGTAGGTAAAGGAAGCTATGGT
GTTGTGTGCTCAGCTATTGACACTCATAACAGGAGAGAAAGTGGCAATAAAGAAGATACATGATATTTTTGAGCAT
ATCTCGGATGCTGCAAGGATACTGCGTGAAATAAAGCTTCTCAGGCTCCTACGGCATCTGACATTTGTCGAAATA
AAGCACATCATGTTGCCACCCTCAAGAAGGGATTTAAGGATATTTATGTCGTATTCGAACCTATGGAGTCAGAT
CTTCATCAAGTCATTAAGCTAATGATGACTTGACCAAAGACCCTATCAGTTTTTTCTTTATCAGCTTCTGCGC
GCATTGAAGTATATCCACACAGGTA AAACTTCTCTGCGATGCCAGTTTACCATCAAATCTTATGTGATACCA
ATAACGGGATAGCTTCTGTTTGAATATAGGGGTTGGGGTGTATATGCTAGGAAAGTTTGATTACCTTGTCTTA
ATGGACATGCTGTCTAGTTTGTACGACTGTACAAAATTTGACCCAAGTCTTCTTTCTGATATTTAAGCTAATTTG
CTGCAGCAAATGATTTTCATCGGGATTTAAAACCAAAGAATATATTTGGCAAATGCGAATTTGAAACTTAAAATAT
GTGACTTCGGCTTGCAGAGTGGCATTCAATGATACCCCAACAACGATATTTGGACGGTATGTTATTCAAACCT
TACAGTATTGTGTTAGTCTATTTTAGTATTTTACCCTTCCCTTGNTTTTCTAANCATGGGTTTTATGTCATTTTAT
GTTGCAGGATTATGTTGCTACGAGATGGTATAGAGCTCCGGAAGTGTGTGGATCGTTTTTTCTCTAAGGTTAGTTT
AGTTTAGCCTGGATAAATCTTATTTTTGTATCAGCAGTCCCTTGTGGCTGCTAATGAGTACCCTTTATGGATGAGT
GAGTCTTCGGTAATTTGTTGCTTTGTAAAAAACTGTTCTAGAAGTCTTGACTACATGAAAACCTGTTTTTAAA

```

TTAGTCGGAAATCTGTTCTGAATGCTTTTAAAGTAGTAAACCAGTAGTTCCTAGACTAAAAAAGTGCTTGTTCCAGG
ATGGGATGTGCACCTCCCCCAAGCTGAAATGTCCTGCAATTCAGGTAACGCGTTGGGTCTGATATCTAGTCAT
CTGGGCTACTTTAAGCTAGAGTTAACAGTTTGTGTTTTTTCAGTAACTTCGATGTTGAATGCCTGATGTATTCTATA
CTTCTGTACAACAGTATACTCCAGCGATAGATATTTGGAGTATCGGTTGCATATTTGCCGAAGTATTAACAGGGA
AGCCTCTATTTCTGGTAAAAATGTTGTTTCATCAGCTGGATTTGATGACTGACCTGCTTGGTACGCCGTCGTTGG
ATACCATTTCTCGGGTATGCTATGTTTATTTCTTTCTCTTAGTTTACTGTTTGAGTTGTACACTTGTACTCTT
TTCTTAGTGATAATTTTGATGTCAATACCTTTGTGTTCTATGTGCAGGTCCGCAATGAGAAAGCCAGGAAATACC
TTACCAGCATGAGGAAGAAGCAGCCGGTGTGCTTCGCACAGAAGTTCCCGAATGCAGATCCATTTGCTGTCAAAC
TTTTAGAAAAGGCTCTTAGCGTTTATCCGAAGGATAGACCAACTGCCGAAGAGGTAACATGGATTATTTTTGCA
CTTTTCAGTTTCGACAATCTCATAGAGATAATTATAAAATTTAAGCTTACATTTAAAGACATCTGGCTTTTGTGTC
TAGCTTTGTTGTTGGTGTCCAGAATCTCATATCTTGACAGTTCTGTTTCTTGTATATTGTCTGAATACCCTTTT
TTGGTCAGGCATTGGCTGATCCATACTTTAAAAGCTTGTAAGGGCAGAGAGGGAACCATTTGCCAGCCAATCA
CCAAGCTAGAGTTTGAATTTGAGAGGCGCGGGTTACTAAGGACGACATTAAGGAGCTTATTTTTAGGGAGATAC
TAGAATATCATCCACAGCTGCTCAAAGACTACATCAGTGGAGCTGAAAGAACAAACTTTCTATACCCTAGGTATT
ACTTGCTACTTATCTAGTTTTTACTCCCTTGTATCTCTGGGTGCTAGTTTACTGATTTTTGCTTTATCTATTTTTA
TGCAGTGTCTGTTGATCAGTTCCCGAAGCAGTTTGCACACCTCGAGGATAATGGTGGTAAAAGTGCCCCGTGCTATT
CCACTCGAGAGGAAGCATGTTTCACTGCCAAGGTATGTTGCTCACTACATTACATGTGCATGGTTCAAGTCACTT
TTCTTTTGTAGCGTCTCCTCTATGGGCTTTGCAAGTTATGAAATAAATGTTTCATACATGTGGNATCAGTGGA
TGTATCCATTTCTTTTCCGCTGTTAATTAGCGCTGGGAGGAATGTGTATTTTTAGACATATTGGAACCTGNTTT
CTTGCCGATTGGTTACCTAATTTTCGTCGTATTGAGCGGAAGTGNNTTATAAATGGAAGTGTGATATGCTTAGC
AGAAACAGTTAGTCCAACCTTTCTCTCTGAACAATTTGTAGGAAGTATCAATTAGTTCGGTTAGTTAATTATG
TCTTTGAAATTTGGAACCTCGCTGAAAGTCTCTTGGTGCATTTCGAAAGAAAAGTGAACGCTACAGCATTTTGG
CATATAATTTGCCTGTGTAACCTCAAGAATGCATCATTTTGTGTAATGCATGACATTAATGGAATGTGAATGCA
TTTTAATTGCAATATGAGGCCATGGCGCCCCATTTTAAATCGTGTTCCTAGTCCGTGCGAAAATTTATCTAGTTTTAA
ATGCCTCGTGGTGGCGGCCCTTCTTGAAAGCGGTAGGCTTCTGACGGCATCACGTAGGATATAAGTGTCCATGTT
GTTCTTAATATGTCTGTCCATTACTGAAAGGATGGACAAAGAGTAGTGTTCATCACATTAAGAAGTTCATTAAC
AATGTGAATTTATGACGTAGTAAAACTCAAGTCAAAGTAACTGCTTGACTGGTCTTGTTTTAGGTGCTAATGTA
TTTTACATGTATTGGGCAGATCTACCATTGTCCATTCAAATACCATCCCCTCCAGGAGCAGCCTGATCTATCC
AGAGAGCGGCAAATTCAGATACTGGTTATTACAAGAATCCGAGAGATGCAAATGGAATTTTCAGGAAGCTTGTCC
AGGATTC AACAGTAGCACAAACGAACTCCATGGGTATGTGAAGTCTCTTTGAGTCACTGAGTATGATTTTTT
CTAGTATACGCATGTTCAAAGAAAACATGAGTTTTCAATTAATGACAGTCTGATGCGTAATACTAGTTCTGAGTT
AGTCCAGCGAGCTTGTGCTCCTCTTTGTTGTTTGAATGCGTTGAATTTGCTCCAGTTATCTGTATGTAGTGG
ATTGCTGAACTATTTGTGTGTGTGTAAGCTAAACCTGGAAAAGTTGCGGGACCTGTTGTGCCATATGAGAACACTA
GCGGTATTAGAGATGCGTATGATCCAAGAACGTACATCAGGAATGCAGTTCTTCTCCTCAGCCTATCCCTTCTC
CCTACGGTATCCGCAGAACTAATGTGATGGTTAATCAAGAAAAATCAGGAAGTGAATTTGAGAGAGATTTATCAC
TAGCCAGACAATCGCAGCTTTCACAATGCAACATGATGGCCAAATTTGGCCCCAGATGTAGCAATTGACATAAACT
CTTCCCAGTTTTATCTAGCACGTGCAGGTGTGACATCAAAGATAGATCAGACTGATAATAATAATCAAATTTGCGA
TTGATACGAATCTGCTACAAGCAAAGTCCCAGTTTGGTGAATGGGTGTTGCTGCTGCTGCAGCTGCGGCTGCTC
GTAGAAAAGGTAAGCACGGTTCAGTACGGTATGTCTAGGATGTAC **TAG**

v.ii Pollen mRNA sequence of PrMPK9-2. Start and stop codons are shown in green and red, respectively.

>MPK9-2 pollen mRNA

```
GGGGGGGGGGGGGGGCAACAAAGNTGATAGAAAATTGGAATTAACGGCTTGAGTNGAAGCTATCAGATCATCTAA
GGGACCGAGCAAGAGAACCTTGGGCTTGAGCAAATAGGTCTGGAGTTTATNCCATTGACAGAGGTGACCGGAGGA
TCAGTTGATTTGTGAGACTCCAGCAAATTTGGAGTCTCAACTTTGGGCTGCCATTAATTTTCATGTGTTGGGGAAAC
GAAGTGTTAATAGGGCTGGCAATGGCGGGAGTGGATCTGATCTAGTTTATTGAGGGAGTGTACATATGGGGGA
GGAGGAACTACTCGTGGATGGGGTTCGTCGTTGGTTTCAACGTCGATCGTCTTCTTCAACATCTTCTCTCCACG
TCTCATCGCAAACCTGAACTCAGATGACAACAAGAATGATGACAACGAAGAAACCGGACAAATAACATTACCGGCA
ACAGTTCAGAAAGATGAACAACAACAGGAGGAACTCACTATAAATTGAAGACTTTGACCTTTCTGGTTTGAAG
TCCATCAAAGTCCCTAAACGACAAAACCTGGGTCACCACTTTTGACTCTCAAATAAAGAAAGGCACGGTGGACACA
GAGTTCTTACCGAGTATGGTGAGGCAAGTCGCTACCAAATCCAGGAAGTCATTGGAAAAGGAAGTTATGGCATT
GTTGGGCTCGACGTCGACACCCACACTGGTGAGAAGGTAGCAATTAAGAAGATAAATGATGTATTTGGACATGTT
TCTGATGCTATGCGCATTCTAAGGGAAATCAAGCTTCTTCGGCTGCTACGGCATCCAGATGTTGTTGAAATAAAG
CATATAATGCTTCTCCATCTCGAAGAGAAATCAAAGATATTTATGTTGTATTTGAGTTGATGGAGTCTGACCTC
CACCAAGTAATTAAGTGAATGACGATCTTACTCGCGAACACCATCAGTTCTTTCTGTTCAGCTTCTTAGAGCA
TTAAAATATATACATACAGCAAATGTGTTTTCATCGTGATATAAAGCCAAAAAACATTTCTGTGAACCGGATTGC
AAGCTGAAGATTTGTGATTTTCGGGCTTGCTCGTGTGTCATTTAATGATGCCCATCAGCTATATTTCTGGACAGAT
TATGTGGCAACCCGATGGTATCGTGCTCCTGAACTGTGCGGCTCCTTTTTCTCAAATACACCCCTGCCGATTGAC
ATTTGGAGCATAGGATGCATATTTGCAGAAATGCTTTCAGGGAAGCCACTGTTTCCCGGAAAGAATGTGGTGCAT
CAATTGGATCTTATGACCGATCTGCTTGGTACACCTTCAACTGAATCCATTACAAGAATTCGAAACGAAAAGGCT
AGAAGATATCTAAGTAATATGAGGAAGAAAACACCAGTCCCTTTCTCGCAGAAGTTTCTTGATGCAGATCCGCTG
GCTCTTCAATTACTTGAGCGGTTACTTGCTTTTGATCCGAAAGATCGTCCATCAGCTGAAGATGACTAACTGAC
CCGTACTTTTCGTGGTTTGTCAACTGCGGACCGTGAATCATCAGCACAACCCATTTTCGAAGCTTGAGTTTCAATTT
GAGAAAAGGAAATTAGCAAAAAGAGGATGTTAGGGAGTTGATCTATCGAGAGATACTCGAGTACCATCCGCAGATG
TTGCAGGAGTATCTTCGTGGTGCAGATCAGGCTAGCTTCATGTACCCTAGTGGAGTTGATAGGTTTAAAAGACAA
TTTGCACATCTCGAGGAAAATTTATGGCAGAGGAGAAAAGGGCACCCACCATTGCATAGAAAGCATGACTCCTTG
CCAAGAGAGCGGGTCTGTGCACCCAAAGACGAACTGCATACCTAAAAAATGGGTTTCGAAAAGCATGGTGCAGCT
TTAGTTCATCAACTATCGAAAATCTCCCTAGGTCACATCTAGAAATGGATGCGTCGCTGATACAGAATGGCCCA
AGCAAGGGAAATTACAGTCTAACAGCTTGTAAAGAGTGCAGCATCAGTGGCTCACAATGTGTAGTTGTTAAA
GGAATGAAAAGATTCGGAGGAAGAACCGATTATGGAGCAGAATGGTGGGTTGTGGATGATTTGTCTACTAAGCTA
AGAGCACTTTAAAGTTTTGATACAAAATGGGTAGCTTCCACTGATAGTTTTTCAGGGTTTTTTCTTTACTTATGTCTG
TATCCATGTCTATTCTGTGTAATTGCCGTGCTCTGTGCTATCTTGATTCATGATGCCTATTTTGTGTTGTATATT
GTTCTTGTTTTTTGCAGCAACAGAAAATAGCAGAAATCTTTACCTTTTTTCATTGGTTGCCGCAGCATTGCCAG
TGCACTTGGCCTAAAAAAAAAAAAAAAAAAAAAAAAAAAAA
```

v.iii Pollen mRNA sequence of PrMPK9-1. Start and stop codons are shown in green and red, respectively.

>PrMPK9-1 Pollen mRNA

```
GGGGGGGGGGGGGGTGTCTTCTCATTTTTTTTCAACATTCTTGTACCCAAAAGAGCAACTAGTAGTAGTGGATT
TTAAAGAGATTGTTTTAAAATTTATTTGAATCAAGGAAACAAGAAGAGAAGAAGAAAATTGCCATTTTTCTGATT
CGAAGAGAATATCGGCGAGACGGAATTTTTCCACCGAGTATGGTGAGGCGAGTCGGTACCAAATTTAGAGGTTAT
TGGCAAAGGAAGTTATGGTGTGTTGCATCTGCTGTTGACACCCATACTGGAGAGAAGGTAGCAATTAAGAAGAT
TAATGATGTTTTTGGAGCATGTCTCTGATGCTACACGTATTCTAAGAGAAAATTAACCTCCTTAGGCTGCTACGCCA
TCCGGATGTTGTAGAGATTAACACATTATGCTTCCCTCCATCTAGGAGAGAATTTAAAGATATTTATGTCGTATT
TGAGTTGATGGAATCAGATCTTCACCAAGTAATTAAGGCAAATGATGATCTTACTCCTGAACATTATCAGTTTTT
CTTGATCAACTTCTTCGTTCTTTAAAATATATACATTTCAGCCAATGTGTTCCATCGGGATTTAAAGCCGAAAAA
CATTCTTGCTAATGCGGACTGCAACTGAAGATTTGTGACTTTGGGCTTGCTCGTGTATCATTTAATGATGCCCC
ATCAGCTATTTTCTGGACTGATTATGTGGCAACGAGATGGTATCGGGCACCTGAACTTTGCGGCTCTTTTTTCTC
CAAATACACTCCCGCAATCGATATCTGGAGTATAGGATGCATATTTGCAGAAGCTTACAGGCAAGCCATTGTT
TCCTGGGAAGAATGTTGTGCATCAATGGATCTCATGACTGATTTGCTTGGTACACCTTCCACTGAATCCGTTGC
GCGGATTCGAAATGAAAAGGCTAGAAGATATTTAAGTGGGATGTGGAAGAAACCTCCAGTTCCTTTACGCAGAA
GTTCCCTAAAAGTGGATCCTTTGGCTCTCAATCTTCTTGAACGACTGCTTGCTTTTGATCCCAAAGACCGTCCATC
TGCTGAAGAAGCATTAGCTGATCCATATTTTCATGGTTTGGCAAATGTGGACCGCGAACCATCAACGCAACCCAT
CTCAAAATTTGAGTTTGAATTTGAAAGGAGGAAAATGTCAAAGGAAGATGTACGAGAATTAATTTACCGAGAGAT
ATTGGAGTATCATCCCCAAATGCTTCAGGAATACCTGAATGGTGCAGATCAAACCTAGCTTCCGTGACCCAAGTGG
AGTTGATCGATTCAAACGACAGTTTGCTCATTGGAGGAGCATTATGGTAAAAGCGGTGAGAAAAGCACTCCTCC
ACTTCAGAGACAGCATGCGTCTTTACCTAGGGAGAGGGTCTGCGCACCTAAGGAAGAGTCTGCTGATCAACACGA
TAATAGTGAAAACCGGAGTGCAGCTTCTGTTGTTTATAAAAACCCCTTCAGAGCCCAACAAAAGCAAATAGCGCTAC
ACGCAGCCTTATGAAGAGTGAGAGCATCAGTGTCTCCCAATGTGTCGTGTAACGGGAAAAAGAATTTAACGGG
AGAACCAATTGATGAACAGAGTGAGGTTGATGATTTATCTCAGAAGATTTCTCAACTAGGTTCCATGATTATACCA
GAAAGTCGGCAGATAACTACAATTCCTTCATCCATTTTTTTTTCCGCTAACATGTGTGTATCAATGTCAATCAC
CTCTCTGAATATCGAGTTTCAAAGAAAACCTGAATTAGGTTTCTTGTAGTAGTATGCTGGCTGCATAATTTTTGC
TGCAGAAAATGATTTGTTATTTATCAGTTGTATTATTACAATTTACATAAAATGAATGAAGAGATGGTAAAACA
AAAAAAGAAAAAAAAAAAAAAAAAAAAAAAAAAAA
```

v.iv Leaf mRNA and genomic sequence of PrGAPD-C. Start and stop codons are shown in green and red, respectively.

>PrGAPD-C leaf mRNA

```
AATTCCTTACTTCTTTTCATTTTATACCCTTCAATTTCTTATCATCTTCATGGCTCCAGCAAAGATCAAGATCGG
AATCAACGGGTTCGGAAGAATCGGAAGATTGGTTGCTAGAGTTGCCCTACAGAGAGATGATGTTGAACTTGTTGC
TGTTAACGACCCATTCATCACTACTGACTACATGACATACATGTTCAAGTATGACACTGTTACGGTCAATGGAA
GCACCATGAACTCAAGGTTAAGGACACCAAGACCCCTCCTCTTCGGTGAGAAGGAAGTTGCAGTCTTCGGTTGCAG
AAACCCCGAGGAGATCCCATGGGCTGAGACTGGAGCTGAATACATTTGTTGAGTCAACTGGAGTGTTCAGTACAA
GGACAAAGCTGCTGCTCATTTGAAGGGTGGAGCCAAGAAGGTTATCATTTCTGCTCCCAGCAAGGACGCACCCAT
GTTTGTGTTGGTGTCAACGAGAAGGAATACACCTCAGACATTAACATTCCTTTCAAACGCTAGTTGCACCACCAA
CTGTCTTGCTCCCTTGCCAAGGTCATCAATGACAGATTTGGCATTGTTGAGGGTCTCATGACCCTGTCCACGC
AATGACTGCTACACAAAAGACTGTTGATGGTCCATCCAGCAAGGACTGGAGAGGTGGAAGGGCTGCTTCATTCAA
CATCATTCCCTAGCAGCACTGGTGCAGCTAAGGCTGTCCGTAAGTTCTCCCAGCATTAAATGGAATAATTGACCGG
TATGGCTTTCCGTGTTCCAACCGTCGATGTTTCAGTGGTTGATCTTACTGTGAGACTTGAGAAGAAGGCAACTTA
TGAAGAGATTAAGGCTGCCATCAAGGAGGAGTCCGAGGGTAAGATGAAAGGAATCTTGGGATACGTTGATGAAGA
TTTGGTCTCTACTGACTTTTTGGGTGACAACAGGTCAGCATTTTCGACGCCAAGGCCGGAATTGCTCTTAATGA
CAACTTCGTCAAGCTTGTGTCATGGTATGACAACGAATGGGGTTACAGTTCCCGTGTATTGACTTGATCGTCCA
CGTTGCCAACACTCAGTAAAGCTCTGCTTCGGAACCTCAGTTGAACCAAGGATGGTGTCCAGCAAAATTTTCAGT
CTTGAGTTTTAGTTTAGTGTGTCCCTCTCAGTGTGGGTGCTTGATGGAAGGGAGGATATGTTGGAATAATAAC
GAAGTTAGCTTTT
```

>PrGAPD-C gDNA

```
ATGGGTAATTCGCTCTTCCCTCAACCTCATCATTTGTTGCTTCTCGTTTTAATTTAATCTTGTTTTGCTTTGATTTCA
CTCTAAATCTGACTATTTCTTATGATTTTCTTCTTCTTCTTGTGCTTTTCAGCTCCAGCAAAGATCAAGATCGGAA
TCAACGGTATTAGATCCTACCTGTTTCTTCTTCTTCTGATCTTTATTTGTGTGTTGGATGTTTTGGTCTGATCT
GGTTTTGGTTGATATTTAGGGTTCGGAAGAATCGGAAGATTGGTTGCTAGAGTTGCCCTACAGAGAGATGATGT
TGAACCTGTTGCTGTTAACGACCCATTCATCACTACTGATTACATGGTATAATGATTTTTACCCTTGGTATATC
GATGATTTCTATGTTTGTGTTTGCAGATCTACTTGGAGAGTTGTCAGTCCATATGCTTTGTAGATCTATTTTTATC
TGTAATTTTTTTTTAGCTCCTCAGGCTTTGGTAGAATTGATTTTACAGTTAAATCTTGTACTGTGATGGGATTA
TTTTTTTTCGATTTGATTTTATGATTTTATTTCTTAAAGTCTACGAGTCTAATCTTTATGAATTATGATCG
TGGTGTATCGATCTGTTATCAAACTAAGTGTCAATTTAATGTTTCATCGGAACTTTTAGATTTAGTTGTAATCAT
CTGGGAGTGTCTCCTAAAAGTTTTTTTTTCTGACAGTTAAATGTATGATTTAAAATTTGTGCGAATATTGTATTGA
TTTGTCCAAATTTGAAGTTATGATTAATTTCTTCTTAAATCTCATTTTATAAGTAAGCATGCTTGAGATTAATAT
TATTATGGATCGTCCATAATGATTTGTTAATGATGGTTTCTGTATTTGTAGACATACATGTTCAAGTATGACAC
TGTTACGGTCAATGGAAGCACCATGAACTCAAGGTTAAGGACACCAAGACCCCTCCTCTTCGGTGAGAAGGAAGT
TGCAGTCTTCGGTTCAGAAAACCCCGAGGAGATCCCATGGGCTGAGACTGGAGCTGAATACATTTGTTGAGTCAAC
TGGAGTGTTCAGTACAAAGGACAAAGCTGCTGCTCATTTGAAGGTTTGTATGATGCTAGATTTCTTTGTACATAATG
AGCATATTTGAAATTCAGTGACAAGTCAATCTACTGCCAGTTTAGGTGTCAATCAGAATGGTTTTGTACAAATGT
GCATAGACTTCAGTTGCGATAAATTTGTCATCTCTGTTATCTGAAATTCAGTCCACCGTACTTTCTTGTGGTTTTGGG
AGTAAGTTTGATCTGATTCATACATTTGAACTTGAATTTGCTACTAAAGAATACAAGAAGATTTGTTCTTATCTAT
TAAACATACATTTAACAAGTCTTATGCGAGGGTTTTATGGCCATAAAGTATAAGCTTTTTCATTAATTTGGTTATTGAT
ATACCTTGCATTTAACAATTTGTTGCTTGTGATCTAGGGTGGAGCCAAGAAGGTTATCATTTCTGCTCCCAGCA
AGGACGCACCCATGTTTGTGTTGGTGTCAACGAGAAGGAATACACCTCCGACATTAACATTTTCAAACGCTA
GTTGCACCACCAACTGCTTGTCTCCCTTGCCAAGGTTTTGTTTGTGCTTGTGATTATCTATTTTATCAAGTTGCG
GTGCCATCTTTGTTTTTATTATCGGTGCCATCTTTGTTTTTATTATCGGTCAAGTGTTCCTTATGTTTTTTCATA
ATGTTCTGCAGGTCATCAATGACAGATTTGGCATTGTTGAGGGTCTCATGACCCTGTCCACGCAATGACTGGTT
AGTATTGCTCTGTGATGTTTGTGTTGAATGAATTTGAGGATTTATGGATTATGATCTTATGTTTACTCATTTC
ATGTTACTCACTCATGTGTTTCCGTTCCAGCTACACAAAAGACTGTTGATGGTCCATCCAGCAAGGACTGGAGAG
GTGGAAGGGCTGCTTCATTCAACATCATTCCTAGCAGCACTGGTGCAGCTAAGGTACCTCACTGGATAGTTTCTT
GACACTTGAGTACTGGCTGATTTTGCAAATCCAATCATGAGTCCCTGATTTTTTTTCTTCTTGTGATATTGTGTAG
GCTGTCCGTAAGTTCTCCCAGCACTTAATGGAAAATTTGACCGGTATGGCTTTCCGTGTTCCCACCGTCGATGTT
TCAGTGGTTGATCTTACTGTGAGACTTGAGAAGAAGGCAACTTATGAAGAGATTAAGCTGCCATCAAGTACGAA
TTAAGTTTTAGTTACTTACCAATTCAGTTTTATAAATTTGTTGCTGGGTATGTTATATGAGCTATATCTAAATTT
ACGGCTTTGTTTCTGCTCAGGGAGGAGTCCGAGGGTAAGATGAAAGGAATCTTGGGATACGTTGATGAAGATTTG
```

GTCTCTACTGACTTTTTGGGTGACAACAGGTATGAGTTGCTGTCTTGCTGATACTTTTAGTGGATCATTTTTTTG
TTATTTCTTGCACTGCATGCAGTTGTGTTATATGTATTATTTCTGACTTGTGTGTACCAACTCAGGTCAAGCATT
TTCGACGCCAAGGCCGAATTGCTCTTAATGACAACCTCGTCAAGCTTGTGTCATGGTATGACAACGAATGGGGT
TACAGTCCCCTGTTATTGACTTGATCGTCCACGTTGCCAACACTCAGTAA